2016

Investigation of Plasma Electrolytic Oxidation (PEO) Coated Bores in Internal Combustion Engines

Vladislav Leshchinsky
University of Windsor

Investigation of Plasma Electrolytic Oxidation (PEO) Coated Bores in Internal Combustion Engines

By

Vladislav Leshchinsky

A Thesis
Submitted to the Faculty of Graduate Studies
through the Department of Mechanical, Automotive, and Materials Engineering
in Partial Fulfillment of the Requirements for
the Degree of Master of Applied Science
at the University of Windsor

Windsor, Ontario, Canada

2016

Investigation of Plasma Electrolytic Oxidation (PEO) Coated Bores in Internal Combustion Engines

by

Vladislav Leshchinsky

APPROVED BY:

_____

Dr. J. Johrendt, Outside Program Reader
Mechanical, Automotive, and Materials Engineering

_____

Dr. D. Green, Internal Program Reader
Mechanical, Automotive, and Materials Engineering

_____

Dr. X. Nie, Advisor
Mechanical, Automotive, and Materials Engineering

_____

Dr. J. Tjong, Co-Advisor
Ford Motor Company of Canada

August 2, 2016

DECLARATION OF CO-AUTHORSHIP

I hereby declare that this thesis incorporates material that is a result of joint research conducted by the Powertrain Engineering Research and Development Center (PERDC) of Ford Motor Company and the Mechanical, Automotive, and Materials Engineering (MAME) department of the University of Windsor, under the supervision of Dr. J. Tjong and Dr. X. Nie, respectively. The collaborated work is covered in Chapters 3, 4, and 5 of this thesis. The primary contributions made in this thesis through methodology, experimental procedure, data analysis, and discussions were performed by the author.

I am aware of the University of Windsor Senate Policy on Authorship and I certify that I have properly acknowledged the contribution of other researchers to my thesis, and have obtained written permission from each of the co-author(s) to include the above material(s) in my thesis.

I certify that, with the above qualification, this thesis, and the research to which it refers, is the product of my own work.

I declare that, to the best of my knowledge, my thesis does not infringe upon anyone's copyright nor violate any proprietary rights and that any ideas, techniques, quotations, or any other material from the work of other people included in my thesis, published or otherwise, are fully acknowledged in accordance with the standard referencing practices. Furthermore, to the extent that I have included copyrighted material that surpasses the bounds of fair dealing within the meaning of the Canada Copyright Act, I certify that I have obtained written permission from the copyright owner(s) to include such material(s) in my thesis.

I declare that this is a true copy of my thesis, including any final revisions, as approved by my thesis committee and the Graduate Studies office, and that this thesis has not been submitted for a higher degree to any other University or Institution.

ABSTRACT

With increasing fuel economy and emission restrictions being placed onto the automotive industry, there is always a need for innovation and research in striving to reduce energy loss and make internal combustion engines more efficient. An area of potential improvement is through the reduction of frictional parasitic losses in tribological systems. This study investigates the feasibility of use for low-friction Plasma Electrolytic Oxidation (PEO) coatings on cylinder bores in order to reduce the frictional coefficients along the piston ring and cylinder bore sliding surface. For PEO coatings, wear is a limiting factor and this study aims at understanding the main influencing factors for wear on PEO in cylinder bores. Through fired-engine dynamometer testing, it was determined that large piston-to-bore clearance distances, increased oil retention, and a small dispersed surface porosity morphology created a tribological environment which produced improved wear resistance of PEO coatings in cylinder bores.

ACKNOWLEDGEMENTS

I would like to thank my advisor, Dr. X. Nie, and co-advisor, Dr. J. Tjong, for their guidance, supervision, and support throughout this project and for providing me with the opportunity to work on this research.

Additionally, I would like to thank all members of the Powertrain Engineering Research and Development Center (PERDC) at the Ford Motor Company of Canada for providing the resources, expertise, and skill in accomplishing this research.

Special thanks to Nick DiLaudo of PERDC and Guang Wang from the Surface Coatings Research Group at the University of Windsor for the endless support they provided.

Finally, I would like to extend my appreciation to my committee memebers, Dr. J. Johrendt and Dr. D. Green, for their review, feedback, and advice regarding this study.

TABLE OF CONTENTS

DECLARATION OF CO-AUTHORSHIP iii
ABSTRACT iv
ACKNOWLEDGEMENTS v
LIST OF FIGURES x
LIST OF TABLES xvi
LIST OF ABBREVIATIONS xviii
ORGANIZATION OF THESIS 1
1. INTRODUCTION 2
1.1. BACKGROUND 3
1.2. PISTON RING-CYLINDER LOSSES 5
1.3. OBJECTIVES 7
2. LITERATURE REVIEW 8
2.1. PLASMA TRANSFERRED WIRE ARC 10
2.1.1. TRIBOLOGY OF PTWA COATINGS 12
2.1.2. PTWA COATED BORES 14
2.2. PEO COATINGS 16
2.2.1. PEO COATING PROCESS 17
2.2.2. TRIBOLOGY OF PEO COATINGS 19
2.2.3. PEO COATED BORES 24
2.3. HONING 25
2.3.1. HONING PROCESS 29
2.4. PISTON RINGS 33
2.4.1. PHYSICAL VAPOR DEPOSITION (PVD) 36
2.4.2. DIAMOND-LIKE CARBON COATINGS 39

2.5. LITERATURE STATEMENT 43
3. INVESTIGATION METHODOLOGY 44
3.1. CONTROLLING PARAMETERS 44
3.1.1. SLIDING SURFACE PROFILE 45
3.1.2. BORE SIZE 47
3.1.3. PISTON RINGS 48
3.1.4. COATING TYPE 51
4. EXPERIMENTAL PROCEDURE 53
4.1. PRE-TREATMENT 53
4.2. PEO COATING DEPOSITION 54
4.3. FINAL SURFACE PROFILE MODIFICATION 56
4.4. ENGINE ASSEMBLY 56
4.5. DYNAMOMETER 58
4.5.1. DYNAMOMETER CHECKS 61
4.6. TEARDOWN ANALYSIS 65
5. EXPERIMENTAL RESULTS 71
5.1. TRIAL 1 – ENGINE 2599 71
5.1.1. PRE-TEST PARAMETER SELECTION 71
5.1.2. DYNAMOMETER TEST 75
5.1.3. TEARDOWN ANALYSIS 78
5.2. TRIAL 2 – ENGINE 2633 84
5.2.1. PRE-TEST PARAMETER SELECTION 84
5.2.2. DYNAMOMETER TEST 88
5.2.3. TEARDOWN ANALYSIS 92
5.3. TRIAL 3 – ENGINE 2595 105

5.3.1. PRE-TEST PARAMETER SELECTION 105
5.3.2. DYNAMOMETER TEST 107
5.3.3. TEARDOWN ANALYSIS 113
5.4. TRIAL 4 – ENGINE 2595R 120
5.4.1. PRE-TEST PARAMETER SELECTION 121
5.4.2. DYNAMOMETER TEST 124
5.4.3. TEARDOWN ANALYSIS 126
6. DISCUSSION 138
6.1. SUMMARY 138
6.2. COATING TYPE 140
6.2.1. ENGINE TRIAL 2 140
6.3. CLEARANCE 142
6.3.1. ENGINE TRIAL 1 143
6.3.2. ENGINE TRIALS 2 & 3 143
6.3.3. ENGINE TRIAL 4 144
6.4. SURFACE PROFILE 145
6.4.1. ENGINE TRIAL 2 145
6.4.2. ENGINE TRIAL 3 145
6.4.3. ENGINE TRIAL 4 146
6.5. PISTON RINGS 146
7. RECOMMENDATIONS 148
7.1. COATING TYPE 148
7.2. CLEARANCE 148
7.3. SURFACE PROFILE 149
7.4. PISTON RINGS 149

7.5. RECOMMENDED FUTURE WORK 150
7.5.1. DECK PLATE 150
7.5.2. PISTON RINGS 151
7.5.3. HONING 151
8. CONCLUSIONS 152
REFERENCES 155
BIBLIOGRAPHY 159
APPENDICIES 161
APPENDIX A 161
VITA AUCTORIS 182

LIST OF FIGURES

Figure 1: Vehicle Energy Map of Parasitic Losses - Full Cycle [21] 4
Figure 2: Energy Losses in an Internal Combustion Engine [22] 4
Figure 3: Stribeck Curve - Coefficient of Friction vs. f(Viscosity, Velocity, Force) [10] 6
Figure 4: Stribeck Curve Lubrication Regions [10] 6
Figure 5: PTWA Spray Head Schematic [5] 10
Figure 6: PTWA - Pre-treatment - Mechanical Roughening by "Dove-tail" Machining – Cross-sectional view [5] 12
Figure 7: PTWA - Wire Feedstock – SUNA Wires - Oil Retention Comparison [5] 13
Figure 8: PTWA - Tribology Test - Cameron Plint TE77 - COF vs. Frequency vs. Lubricant Temperature [8] 14
Figure 9: PTWA - Morphology Variation in Cylinder Bore [8] 15
Figure 10: PTWA - Morphology & Thickness Variation in Cylinder Bore [8] 16
Figure 11: PTWA - Thickness Variation in Cylinder Bores with Varying Current [8] ... 16
Figure 12: PEO Deposition System – Schematic [14] 17
Figure 13: Current vs. Voltage Plot of (a) Surface Dissolution and (b) Oxide Film Formation [3] 19
Figure 14: PEO - Current Frequency Variation Comparison – Cross-sectional View [2] 21
Figure 15: PEO - Unipolar Current Mode Microstructure – Top Surface View [1] 22
Figure 16: PEO - Bipolar Current Waveform – Schematic [2] 23
Figure 17: PEO - Bipolar Current Mode Microstructure – Top Surface View [1] 23
Figure 18: Surface Profile - Cross-Section – Schematic 26
Figure 19: Profilometric Measurement - Schematic [36] 26
Figure 20: Surface Profile to Material Ratio Schematic [31] 27
Figure 21: Material Ratio Curve [9] 27
Figure 22: Honing Operation - Schematic [25] 29
Figure 23: Honing Angle Measurements – Schematic [28] 30
Figure 24: Evaporation PVD - Filament - Schematic [15] 37
Figure 25: Evaporation PVD - Electron Beam - Schematic [15] 38
Figure 26: Sputtering PVD - General Technique – Schematic [12] 39

Figure 27: DLC Piston Ring Comparison - Coefficient of Friction [11] 42
Figure 28: DLC Piston Ring Comparison - Relative Scuffing Resistance [11] 42
Figure 29: DLC Piston Ring Comparison - Durability (Scuffing) [7] 43
Figure 30: Controlling Parameters and Subset Variables 45
Figure 31: Piston Ring Gap Feature - Schematic 50
Figure 32: PEO Coating - Type A – Morphology – Top Surface View 52
Figure 33: PEO Coating - Type B – Morphology – Top Surface View 52
Figure 34: Cylinder Bore Processing Procedure Prior to Engine Trial 54
Figure 35: PEO Cylinder Bore Coating System - Schematic 55
Figure 36: Dynamometer 18 Hour Break-In Curve 59
Figure 37: Measurement of Depression via Wear at TDC - Setup 67
Figure 38: Cylinder Bore - Measurement Location Terminology 70
Figure 39: Dynamometer 1 - Engine 2599 - Surface Profile Values – Before Dynamometer 72
Figure 40: Dynamometer 1 - Engine 2599 - Bore Straightness - Before Dynamometer Test 73
Figure 41: Dynamometer 1 - Engine 2599 - Crankcase Pressure vs. Engine Hours 76
Figure 42: Dynamometer 1 - Engine 2599 - Borescope - 9.5 Test Hours 77
Figure 43: Dynamometer 1 - Engine 2599 - Dynamometer Check Results 78
Figure 44: Dynamometer 1 - Engine 2599 - Teardown - Cylinders 78
Figure 45: Longitudinal Cross-Section - Cylinder 2 - Compression Volume Region vs. Piston Stroke Region - Coating Thickness 80
Figure 46: Cylinder 2 - Compression Volume - Coating Thickness - EDS Point Analysis 80
Figure 47: Cylinder 2 - Piston Stroke Volume - Coating Thickness - EDS Point Analysis 81
Figure 48: Cylinder 2 - Horizontal Cross-Section - Stroke Profile 81
Figure 49: Dynamometer 1 - Engine 2599 – Teardown - Piston Skirts - Major Thrust Side 82
Figure 50: Dynamometer 1 - Engine 2599 – Teardown - Piston Skirts - Minor Thrust Side 82

Figure 51: Cylinder 2 - Upper Compression Ring - SEM & EDS 83
Figure 52: Cylinder 2 - Lower Compression Ring - SEM & EDS 84
Figure 53: Dynamometer 2 - Engine 2633 - Surface Profile Values – Before Dynamometer 85
Figure 54: Dynamometer 2 - Engine 2633 - Bore Straightness - Before Dynamometer Test 87
Figure 55: Dynamometer 2 - Engine 2633 - Borescope - 4.5 Test Hours 90
Figure 56: Dynamometer 2 - Engine 2633 - Borescope - 9.5 Test Hours 91
Figure 57: Dynamometer 2 - Engine 2633 - Dynamometer Check Results 92
Figure 58: Dynamometer 2 - Engine 2633 - Teardown - Cylinders 1 & 2 93
Figure 59: Dynamometer 2 - Engine 2633 - Cylinder 1 - Back – Piston Ring Travel Schematic 93
Figure 60: Dynamometer 2 - Engine 2633 - Bore Dimensional Comparison - Before & After Dynamometer – Cylinder 1 95
Figure 61: Dynamometer 2 - Engine 2633 - Bore Dimensional Comparison - Before & After Dynamometer - Cylinder 2 95
Figure 62: Dynamometer 2 - Engine 2633 - Surface Profile - Statistical Comparison - Before & After Dynamometer 96
Figure 63: Dynamometer 2 - Engine 2633 - Teardown - Piston Skirts - Cylinders 1 & 2 96
Figure 64: Dynamometer 2 - Engine 2633 - Teardown - Upper Compression Rings - Cylinders 1 & 2 97
Figure 65: Dynamometer 2 - Engine 2633 - Teardown - Lower Compression Rings - Cylinder 1 & 2 97
Figure 66: Dynamometer 2 - Engine 2633 - Teardown - Lower Compression Ring Groove – Cylinder 1 - EDS Analysis 97
Figure 67: Dynamometer 2 - Engine 2633 - Teardown - Cylinders 3 & 4 98
Figure 68: Dynamometer 2 - Engine 2633 - Wear Pattern - Large (Cyld. 3) vs. Small (Cyld. 4) Bore Size 99
Figure 69: Dynamometer 2 - Engine 2633 - Bore Dimensional Comparison - Before & After Dynamometer - Cylinder 3 100

Figure 70: Dynamometer 2 - Engine 2633 - Bore Dimensional Comparison - Before & After Dynamometer - Cylinder 4 100
Figure 71: Dynamometer 2 - Engine 2633 - Teardown - Piston Skirts - Cylinders 3 & 4 101
Figure 72: Dynamometer 2 - Engine 2633 - Teardown - Upper Compression Ring - Cylinder 3 – SEM - x70 Mag. vs. x280 Mag. 102
Figure 73: Dynamometer 2 - Engine 2633 - Teardown - Upper Compression Ring - Cylinder 3 - EDS Point Analysis 102
Figure 74: Dynamometer 2 - Engine 2633 - Teardown - Lower Compression Ring - Cylinder 3 – SEM - x70 Mag. vs. x280 Mag. 103
Figure 75: Dynamometer 2 - Engine 2633 - Teardown - Lower Compression Ring - Cylinder 3 - EDS Point Analysis 103
Figure 76: Dynamometer 2 - Engine 2633 - Teardown - Upper Compression Ring – Cylinder 4 - SEM 104
Figure 77: Dynamometer 2 - Engine 2633 - Teardown - Lower Compression Ring - Cylinder 4 - EDS Point Analysis 104
Figure 78: Dynamometer 3 - Engine 2595 - Surface Profile Values – Before Dynamometer 106
Figure 79: Dynamometer 3 - Engine 2595 - Borescope - 4.5 Test Hours 109
Figure 80: Dynamometer 3 - Engine 2595 - Borescope - 9.5 Test Hours 110
Figure 81: Dynamometer 3 - Engine 2595 - Borescope - 13.5 Test Hours 111
Figure 82: Dynamometer 3 - Engine 2595 - Borescope - 18 Test Hours 112
Figure 83: Dynamometer 3 - Engine 2595 - Dynamometer Check Results 113
Figure 84: Dynamometer 3 - Engine 2595 - Teardown - Cylinders 114
Figure 85: Dynamometer 3 - Engine 2595 - Surface Profile - Statistical Comparison - Before & After Dynamometer 115
Figure 86: Dynamometer 3 - Engine 2595 - Profilometry - Ring Flutter - Cylinder 1... 115
Figure 87: Dynamometer 3 - Engine 2595 - Profilometry - Ring Flutter - Cylinder 2... 116
Figure 88: Dynamometer 3 - Engine 2595 - Profilometry - Ring Flutter - Cylinder 3... 116
Figure 89: Dynamometer 3 - Engine 2595 - Profilometry - Ring Flutter - Cylinder 4... 117

Figure 90: Dynamometer 3 - Engine 2595 - Teardown - Piston Skirts - Major Thrust Side 117
Figure 91: Dynamometer 3 - Engine 2595 - Teardown - Piston Skirts - Minor Thrust Side 118
Figure 92: Dynamometer 3 - Engine 2595 - Upper Compression Rings - SEM & EDS - Debris 118
Figure 93: Dynamometer 3 - Engine 2595 - Lower Compressing Ring - Groove - SEM & EDS - Debris 119
Figure 94: Dynamometer 3 - Engine 2595 - Teardown - Piston Rings - Lower Compression Rings - Wear - Cylinder 2 120
Figure 95: Dynamometer 3 - Engine 2595 - Teardown - Lower Compression Rings - Wear Height 120
Figure 96: Dynamometer 4 - Engine 2595R - Surface Profile Values – Before Dynamometer 121
Figure 97: Dynamometer 4 - Engine 2595R - Bore Straightness – Before Dynamometer Test 123
Figure 98: Dynamometer 4 - Engine 2595R - Borescope - 4.5 Test Hours 125
Figure 99: Dynamometer 4 - Engine 2595R - Dynamometer Check Results 126
Figure 100: Dynamometer 4 - Engine 2595R - Teardown - Cylinders 127
Figure 101: Dynamometer 4 - Engine 2595R - Journal Bearing - Cylinder 4 128
Figure 102: Dynamometer 4 - Engine 2595R - Teardown - Cylinders – Wear Marks – Minor Thrust Side 129
Figure 103: Dynamometer 4 - Engine 2595R - Teardown - Cylinders – Wear Marks – Major Thrust Side 129
Figure 104: Dynamometer 4 - Engine 2595R - Bore Dimensional Comparison - Before & After Dynamometer - Cylinder 1 131
Figure 105: Dynamometer 4 - Engine 2595R - Bore Dimensional Comparison - Before & After Dynamometer - Cylinder 2 131
Figure 106: Dynamometer 4 - Engine 2595R - Bore Dimensional Comparison - Before & After Dynamometer - Cylinder 3 132

Figure 107: Dynamometer 4 - Engine 2595R - Bore Dimensional Comparison - Before & After Dynamometer - Cylinder 4 132
Figure 108: Dynamometer 4 - Engine 2595R - Teardown - Piston Skirts - Piston 1 133
Figure 109: Dynamometer 4 - Engine 2595R - Teardown - Piston Skirts - Piston 2 134
Figure 110: Dynamometer 4 - Engine 2595R - Teardown - Piston Skirts - Piston 3 134
Figure 111: Dynamometer 4 - Engine 2595R - Teardown - Piston Skirts - Piston 4 134
Figure 112: Dynamometer 4 - Engine 2595R - Upper Compression Ring - Cylinder 1 - SEM & EDS 135
Figure 113: Dynamometer 4 - Engine 2595R - Upper Compression Rings - Cylinder 2-4 135
Figure 114: Dynamometer 4 - Engine 2595R - Lower Compression Rings - Cylinder 1 & 2 - SEM & EDS 136
Figure 115: Dynamometer 4 - Engine 2595R - Lower Compression Rings - Cylinder 3 & 4 - SEM & EDS 137
Figure 116: Summary - Controlling Parameters & Results 139
Figure 117: Discussion - Ring Flutter Wear – Comparison Between Engine Trials 2 & 3 144

LIST OF TABLES

Table 1: Production Bore Coatings by Manufacturers [24] 9
Table 2: Surface Parameter Equations [31] 26
Table 3: Production Piston Ring - Characteristics 49
Table 4: Experimental Piston Ring - Characteristics 49
Table 5: Nippon Piston Ring Co. - Piston Ring Closed Gap Specifications for Cylinder Bore Size 75 - 89 mm 51
Table 6: A356 Mechanical Properties [37] 53
Table 7: Equipment Specifications 64
Table 8: Dynamometer 1 - Engine 2599 - Diameter, Coating Type, and Coating Thickness 73
Table 9: Dynamometer 1 - Engine 2599 - Clearance Stack-Up 74
Table 10: Dynamometer 1 - Engine 2599 - Piston Ring Selection 74
Table 11: Dynamometer 1 - Engine 2599 - Maximum Values of Surface Depression via Wear at TDC 79
Table 12: Dynamometer 2 - Engine 2633 - Diameter, Coating Type, and Coating Thickness 86
Table 13: Dynamometer 2 - Engine 2633 - Clearance Stack-Up 87
Table 14: Dynamometer 2 - Engine 2633 - Piston Ring Selection 88
Table 15: Dynamometer 2 - Engine 2633 - Maximum Values of Surface Depression via Wear at TDC – Cylinder 1 & 2 94
Table 16: Dynamometer 2 - Engine 2633 - Maximum Values of Surface Depression via Wear at TDC – Cylinder 3 & 4 99
Table 17: Dynamometer 2 - Engine 2633 - Bore Dimension Statistical Summary - Before & After Dynamometer - All Cylinders 101
Table 18: Dynamometer 3 - Engine 2595 - Diameter, Coating Type, and Coating Thickness 106
Table 19: Dynamometer 3 - Engine 2595 - Clearance 107
Table 20: Dynamometer 3 - Engine 2595 - Piston Ring Selection 107
Table 21: Dynamometer 3 - Engine 2595 - Maximum Values of Surface Depression via Wear at TDC 114

Table 22: Dynamometer 4 - Engine 2595R - Diameter, Coating Type, and Coating Thickness 122
Table 23: Dynamometer 4 - Engine 2595R - Clearance 123
Table 24: Dynamometer 4 - Engine 2595R - Piston Ring Selection 124
Table 25: Dynamometer 4 - Engine 2595R - Maximum Values of Surface Depression via Wear at TDC 130
Table 26: Dynamometer 4 - Engine 2595R - Surface Profile - Statistical Comparison - Before & After Dynamometer 130
Table 27: Dynamometer 4 - Engine 2595R - Bore Dimension Statistical Comparison - All Cylinders 133
Table 28: Dynamometer 2 - Engine 2633 - Coating & Dynamometer Checks 140
Table 29: Wear Rate - Comparison - Depression by Wear at TDC 143
Table 30: Recommendations - Surface Profile Parameters 149

LIST OF ABBREVIATIONS

PEO	Plasma Electrolytic Oxidation
MAO	Micro-arc Oxidation
PTWA	Plasma Transferred Wire Arc
DLC	Diamond-like Carbon
PVD	Physical Vapor Deposition
CVD	Chemical Vapor Deposition
TDC	Top Dead Center
BDC	Bottom Dead Center
Ra	Average Surface Roughness
Rvk	Average Surface Valleys
Rpk	Average Surface Peaks
MR1	Surface Peak Material Ratio
MR2	Surface Valley Material Ratio
GTDI	Gasoline Turbo Direct Injection
EPA	Environmental Protection Agency
SEM	Scanning Electron Microscopy
EDS	Energy Dispersive Spectroscopy
CMM	Coordinate Measurement Machine

ORGANIZATION OF THESIS

Chapter 1 – Introduction: an introduction to coating technology and its application in various industries is made with particular emphasis on the automotive sector. The driving force for this study is provided by discussing new industry restrictions and explains how coating technology can assist in achieving those goals with particular focus on powertrain tribological systems.

Chapter 2 – Literature Review: a literature review of coating packages related to Ford Motor Company powertrain systems is provided. Coating packages discussed are Plasma Transferred Wire Arc (PTWA), Diamond-Like Carbon (DLC), and Plasma Electrolytic Oxidation (PEO). Their composition, deposition methods, and processing techniques are discussed within this chapter. Additionally, the critical surface processing technique of honing is also reviewed.

Chapter 3 – Investigation Methodology: the methodology behind this study is provided by discussing the independent variables that were controlled during the investigation.

Chapter 4 – Experimental Procedure: the experimental procedure is outlined with detailed descriptions of processes and equipment used. Additionally, investigation deliverables are given in the form of post-test analysis tests and dynamometer checks.

Chapter 5 – Experimental Results: detailed results of four separate fired-engine tests are provided and the reasoning behind each modification to controlling parameters.

Chapter 6 – Discussion of Results: results from all dynamometer tests, including their post-test analysis results are compared and discussed. Reasoning for wear and test outcome is discussed.

Chapter 7 – Recommendations: future study recommendations are made which include recommendations for additional controlling parameters as well as additional studies to conduct in order to better understand various phenomena and test results.

Chapter 8 – Conclusions: A concise explanation of the significant results obtained from this study is provided.

CHAPTER 1

1. INTRODUCTION

Coating technology has been and continues to be developed, with the introduction and research of new coating deposition processes and advanced materials for increased tribological performance and corrosion resistance. These improved parameters can have many beneficial implications such as enhanced durability, increased efficiency, greater cost-savings, and reduced emissions in whichever systems they are used. Furthermore, as these coating performance parameters continue to be enhanced, their integration into mechanical systems becomes more widespread. Wherever there is a tribological impact, thin films and coatings have the potential to provide a wide array of benefits, and it is the goal of researchers and industry professionals alike to maximize that potential.

Wherever there are surfaces in contact and relative motion, the application of thin films and coatings have the potential to be advantageous in cost, durability, and performance. The possible areas of implementation are not only limited to the commonly discussed automotive industry but expand to also include the medical, architectural, marine, and civil sectors, just to name a few.

The automotive industry in particular has a great history of research, development, and implementation of coating technologies due to a combination of the competitive nature of the sector and their extensive use of mechanical, and subsequently, tribological systems in their vehicles. Coatings can be implemented in countless contact and sliding interfaces within the powertrain and drivetrain systems alone.

With ever increasing regulations on emission and fuel economy standards set for vehicles, thin film and coatings are a potentially useful tool in helping to achieve those goals not only in order to meet government regulations but to also increase performance and provide an industrial competitive advantage.

Utilizing coating technology in vehicles is not a new concept. Different types of coatings are used on various parts of a vehicle and their success in those areas for corrosion

prevention or friction reduction have provided the foundation and continued interest for research, development, and integration of thin films and coatings.

The current initiative for the use of coatings in tribo-systems within powertrain components is driven by the increasing environmental standards set for cars and light trucks. The following fuel economy standards and emission standards have been set by the United States Environmental Protection Agency (EPA):

- Fuel Economy for passenger cars and light trucks [18]
  - 35.5 MPG by 2016
  - 54.5 MPG by 2025
- Emissions for passenger cars [19]
  - 213 grams of CO_2/mile by 2017
  - 144 grams of CO_2/mile by 2025

As a sign of how stringent the EPA standards have become can be shown by referring to the 2008 fuel economy standards of 24.1 MPG for passenger cars [20]. For this reason, significant investment has been made into technologies that have the potential to limit energy loss in vehicle powertrain systems, such as coatings for friction reduction, which in turn could assist in helping to achieve the new environmental standards.

1.1. BACKGROUND

Reducing energy losses in various vehicle systems is the way by which fuel economy and emission goals will be achieved. Overall, it is widely understood that a vehicle is very inefficient in converting the potential energy available from the combustible fuel into actual movement.

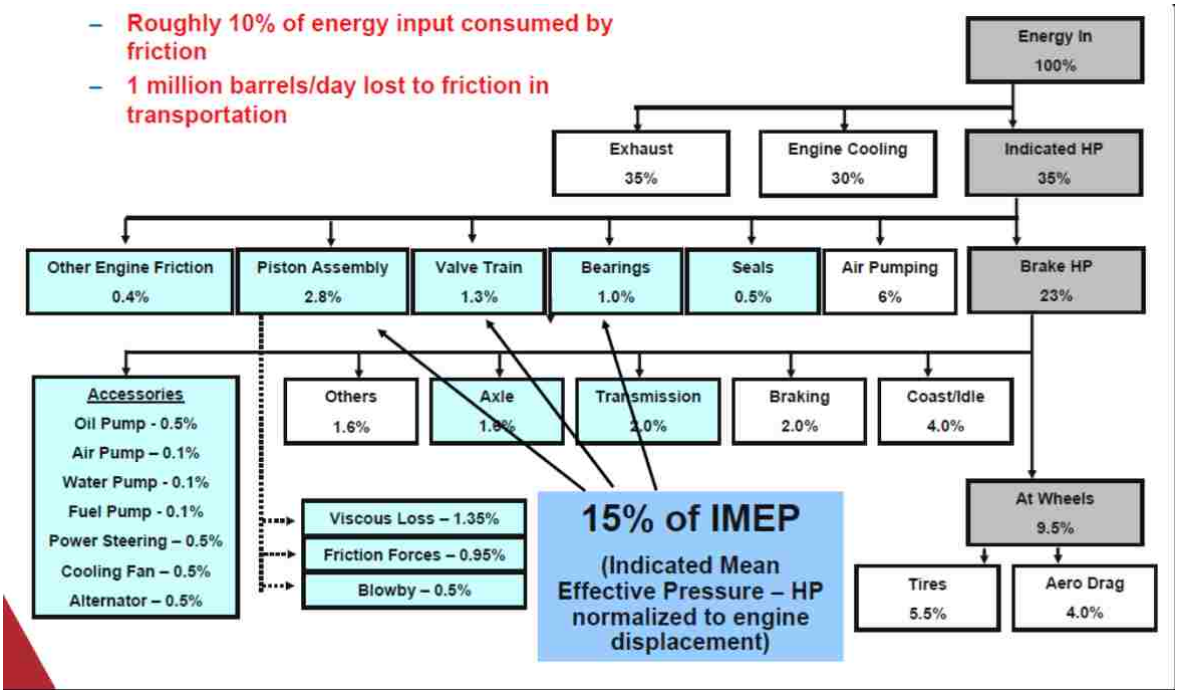

Figure 1: Vehicle Energy Map of Parasitic Losses - Full Cycle [21]

Based on research conducted by Argonne National Laboratories in 2006, they stated that "More energy is lost to friction than delivered to the wheel" [21]. This statement shows how significant the energy losses in a vehicle are – otherwise known as parasitic losses, as shown in Figure 1. Focusing on the powertrain component, the energy losses can be broken down further to display that 13% of internal combustion engine energy losses are a result of friction [22] as displayed in Figure 2

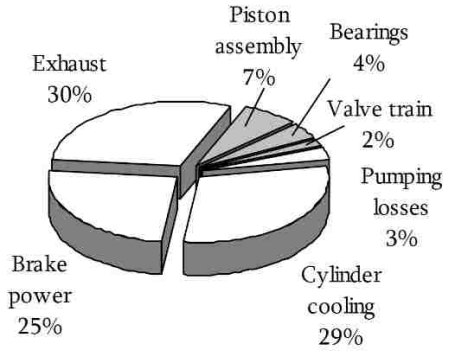

Figure 2: Energy Losses in an Internal Combustion Engine [22]

Therefore, the study of these frictional losses can play a large role in understanding and improving powertrain efficiency. The topic of tribology is defined as being the study of interacting surfaces in relative motion, and therefore has a strong and direct link to coatings. For this reason, many aspects applicable to tribology directly translate to coating technology, and often times help in improving performance features of coatings. Studies done on asperity contact, solid lubricants, and liquid lubrication are only some of the tribological factors studied that are extremely pertinent to vehicle powertrain coating applications. Furthermore, deposition techniques are also a major consideration when taking steps towards applying a coating. The deposition process significantly affects the factors that make coatings appealing in mechanical systems, including but not limited to microstructure, composition, surface topography, and cost-savings. Consequently, tribological advancements in terms of materials and lubrication have simultaneously been developed alongside deposition processes to be able to improve coating technology as a whole package.

1.2. PISTON RING-CYLINDER LOSSES

A mechanical system of particular interest for the implementation of coating technology is in the heart of the engine; the piston ring-cylinder bore arrangement. It has been reported that the parasitic losses due to the friction between piston rings and cylinder walls can amount to 20% of the total mechanical losses due to friction in an internal combustion engine [4]. Therefore, the research and implementation of low-friction coatings in this tribological system has the potential to provide progress in increasing fuel-economy, improving durability, and reducing emissions.

The friction in this interface is highly dependent on material properties, composition, and topography, as well as temperature, pressure, and sliding velocity. Furthermore, as the study of tribology suggests, friction coefficient and wear are dynamic characteristics, meaning that they change with changing conditions. Below is a figure representing a general curve for coefficient of friction in a sliding interface under lubricated conditions. Figure 3 displays a dynamic profile of coefficient of friction with respect to a function of viscosity, velocity, and force.

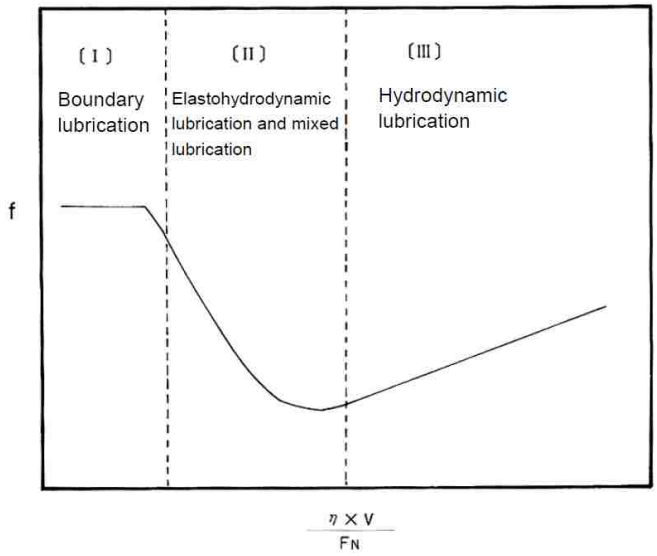

Figure 3: Stribeck Curve - Coefficient of Friction vs. f(Viscosity, Velocity, Force) [10]

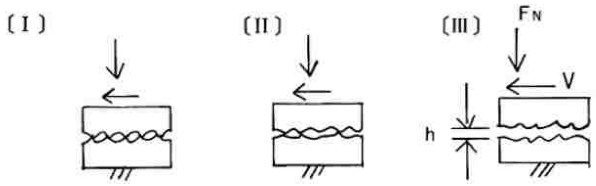

Figure 4: Stribeck Curve Lubrication Regions [10]

Figure 3 and Figure 4 display the three general lubrication regions that occur throughout the Stribeck curve. It is important to note that the oil film thickness, displayed by "h", increases as the curve extends through each region. The oil film thickness directly contributes to the drop in coefficient of friction due to the reduced contact of opposing surface asperities.

Moreover, all lubrication regions of the Stribeck curve are important for the analysis and study of piston ring tribological effects on the cylinder wall. Although it may be instinctive to assume that hydrodynamic lubrication effects dominate the entire piston ring-cylinder system due to the very high sliding speeds endured during engine operation, areas in which the piston reaches top dead center (TDC) and bottom dead center (BDC) experience a high friction-low oil film thickness lubrication region in the Stribeck curve, referred to as the boundary lubrication region. This is due to the piston reaching a momentary zero velocity

at its highest and lowest positions in the cylinder, along with the decreased sliding speeds during acceleration and deceleration near those points. For this reason, it is important to study and understand the wear and subsequent durability of the interface surfaces at worst case conditions of boundary lubrication, where there is substantial surface asperity contact, to represent top dead center (TDC) and bottom dead center (BDC) cylinder regions, cold starts, and oil-deprived engine operation.

1.3. OBJECTIVES

It was the goal of this study to investigate the potential use of Plasma Electrolytic Oxidization (PEO) coatings on linerless aluminum cylinder bores for the purposes of improved tribological properties between the piston ring and cylinder wall sliding system in order to address the industrial strategy of reductions in weight and frictional parasitic losses of internal combustion engines. More specifically, the study had the following objectives:

1. To perform a literature study to gain knowledge and information about several parameters which affect the cylinder bore to piston ring tribological system:
    a. A current low-friction cylinder bore coating in production by the Ford Motor Company – Plasma Transferred Wire Arc;
    b. Purpose and application of hard coatings on piston rings, along with their desired properties;
    c. Diamond-like Carbon piston ring coatings, their deposition techniques and functionality; and
    d. Honing procedures, benefits, and emerging honing technologies.
2. To conduct fired-engine tests of engines with PEO coated cylinder bores on a dynamometer:
    a. Varying only four different independent variables of bore size, coating type, surface profile, and piston rings; and
    b. Analyzing the effects of variables on the wear behavior of piston ring-cylinder wall systems and providing recommendations on optimal operating ranges for each independent variable for the purpose of improving coating wear resistance.

CHAPTER 2

2. LITERATURE REVIEW

Powertrain and metallurgy have advanced enough to allow for use of hypoeutectic aluminum engine blocks in gasoline engines which provide a relatively large weight savings over the much older option of cast iron engine blocks. Additionally, aluminum in general has much better thermal diffusivity properties than cast iron to allow for greater heat dissipation, therefore cooling the block more efficiently [35]. However, the hypoeutectic aluminum alloy used in engine blocks lacks greatly in tribological performance, specifically in the piston ring-cylinder bore arrangement. Two commonly used hypoeutectic aluminum alloys in engine blocks are A380 and A356. These hardness values, combined with the lack of solid lubricants create a tribo-system that experiences significant friction and wear. For this reason, cylinder bore inserts were introduced as a solution to this problem.

Cylinder bore inserts, otherwise known as cylinder liners, maintain most of the weight savings that come from having a hypoeutectic aluminum engine block while simultaneously allowing for acceptable tribological behavior in the piston ring-cylinder bore system.

Cast iron liners are the most preferred and most commonly used cylinder liners in production engines. Their material properties coupled with very effective honing methods create a tribo-system that has excellent wear resistance, and acceptable friction coefficients for the current set of environmental standards, both of which can be attributed to the graphite lamellas that exist within the alloy which act as a solid lubricant. These advantages to cast iron liners allow for good durability performance and long engine life. However, there are a few draw backs to cast iron liners such as a mismatch in the thermal expansion coefficients between the liner and the bulk material of the engine block which could cause deformation in the bore [5], leading to increased fuel and oil consumption. Additionally, the frictional coefficient of cast iron throughout all the dynamic lubrication regions is relatively higher than some available material alloys and coatings.

Some possible solutions to overcome the use of cast iron liners for greater friction and wear reduction are as follows [23]:

1. A strengthened aluminum alloy or composite cylinder liner inserted into a hypoeutectic engine block instead of the traditional cast iron liner.
2. The use of hypereutectic aluminum silicon alloy as the bulk material in monolithic engine blocks which would also act as the sliding surface in the cylinder bore.
3. Thermally sprayed coatings applied onto cylinder bores of hypoeutectic engine blocks.
4. Electroplated coatings applied onto cylinder bores of hypoeutectic engine blocks.

Some of the alternatives to cast iron liners in hypoeutectic aluminum silicon alloy engine blocks are already being used in production engines as shown in Table 1. Most of the preferred options are thermal spray coatings used by various manufacturers, mostly for high-end and high-performance vehicles with the exception of the Lichtbogendrahtspritzen (LDS) thermally sprayed bore coating used by BMW in their 2.0L Turbo I4 engine, production of which reaches into the millions of units.

Table 1: Production Bore Coatings by Manufacturers [24]

Manufacturer	Coating	Engine
Mercedes-Benz	LDS (Lichtbogendrahtspritzen)	6.3L V8
BMW	LDS (Lichtbogendrahtspritzen)	2.0L I4
Nissan	NPSC (Nissan Plasma Spray)	3.8L V6
Volkswagen	APS (Atmospheric Plasma)	5.0L V10
Bugatti	APS (Atmospheric Plasma)	8.0L W16
Ford	PTWA (Plasma Transferred Wire Arc)	5.4L V8

2.1. PLASMA TRANSFERRED WIRE ARC

Thermal spray coatings have proven to be the much more effective solution thus far to replacing cylinder liners and maintaining a hypoeutectic aluminum silicon alloy engine block that is light-weight and easier to machine than the competing solution of a monolithic hypereutectic aluminum silicon alloy engine blocks as both the bulk material and cylinder bore sliding surface. There exist several different types of thermal spray coating deposition systems that are used to create thin surface coatings. The main four systems are:

- Rota Plasma
- Twin Wire Arc
- High Velocity Oxygen Fuel (HVOF)
- Plasma Transferred Wire Arc (PTWA)

A thermal spray coating of particular interest is Plasma Transferred Wire Arc (PTWA) which is currently being utilized in a Ford 5.4L V8 high performance engine with plans to expand into different engine platforms produced by the Ford Motor Company. A schematic of PTWA operation is shown in Figure 5.

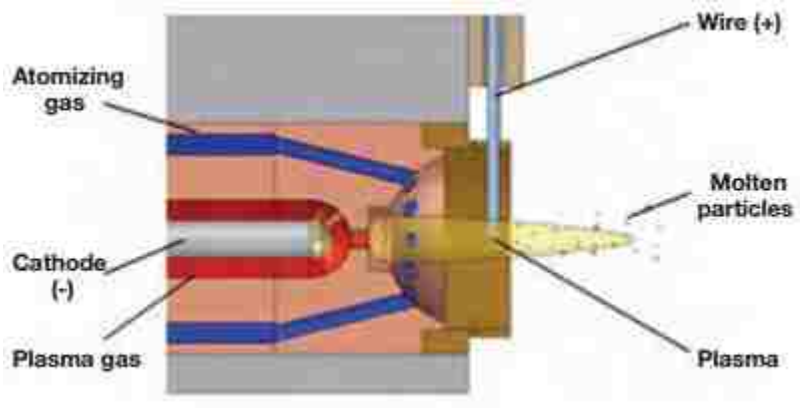

Figure 5: PTWA Spray Head Schematic [5]

PTWA application within internal combustion engines requires a coating thickness of about 200 - 300 microns, which is accomplished by accelerating ionized gas to supersonic speeds in the form of plasma through a nozzle. This is accomplished by an applied voltage of sufficient magnitude promoting the heating of supplied gas until plasma inducing temperatures are reached. The supersonic plasma hits an anodic feed wire that is usually

comprised of a type of steel. This collision of plasma gas and feed wire, combined with a high pressure gas for the purposes of atomization, breaks apart the feed wire and accelerates it towards the substrate which is to be coated, in a high velocity and high temperature stream of fine particles. It is important to note that the atomizing gas mentioned in the process be comprised of non-combustible compressed air. Additionally, the plasma gas is usually a mix of argon and hydrogen.

With this method for deposition of PTWA coating being well established, other issues such as adhesion arise. Adhesion of coating to substrate poses a challenge since the coating does not diffuse into the surface, therefore it provides no opportunity for inter-material bonding and consequently relies more on a mechanical bonding or interlocking method. For this reason, the PTWA coating package requires machining of bores prior to coating. Various methods of machining bores, otherwise referred to as pre-treatment, are available and are discussed below.

- Grit Blasting
- High Pressure Water Jet Blasting
- Flux Procedure: a material compound (NiAl) is applied to a flux which in turn is applied onto the substrate. The PTWA coating is then applied onto the material compound
- Mechanical Roughening: The best and now most commonly used method is by use of undercuts on surfaces in a “dove-tail” shape which was determined to provide the optimal material interlocking potential, subsequently providing greater adhesion characteristics between the coating and substrate surfaces. It is important to note that this procedure was developed as a lubricant-free process, removing the need for an extra rinse phase in the overall processing of the coating. A cross-sectional view of “dove-trail” mechanical roughening is provided in Figure 6.

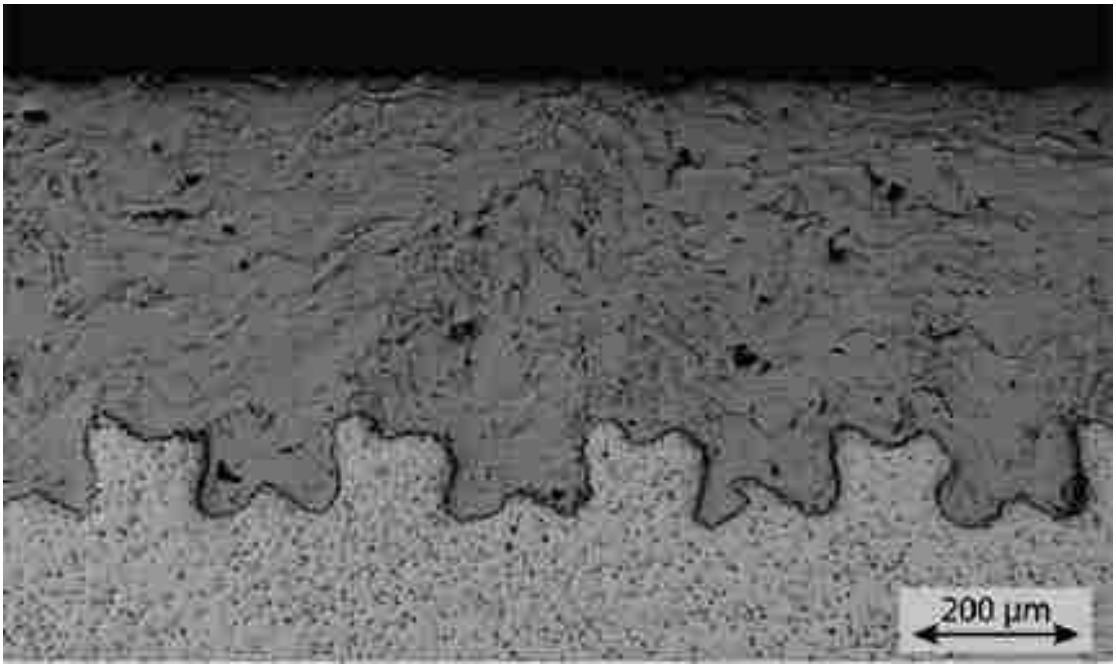

Figure 6: PTWA - Pre-treatment - Mechanical Roughening by "Dove-tail" Machining – Cross-sectional view [5]

2.1.1. TRIBOLOGY OF PTWA COATINGS

PTWA coatings tend to show very low coefficients of friction on cylinder bore surfaces along with low wear rates throughout all the regions of the Stribeck curve. These tribological advantages can be attributed to many process parameters. However, two main features for this advantage is the composition of the wire feed stock and the honing process that takes place after thermal spraying.

2.1.1.1. CARBON STEEL FEEDSTOCK

Feedstock wire usually comprised of 0.82% carbon steel provides good tribological qualities for a few reasons. Firstly, the iron component of the steel feed wire reacts with the oxygen within the air of the atomizing compressed gas to create Wuestite (FeO) [5]. Wuestite is a very hard material and serves as a solid lubricant in a sliding interface. Secondly, various levels of porosity may be achieved for increased oil retention volume, otherwise known as crevice volume, for further increase in tribological performance from the additional lubricant.

2.1.1.2. NANO-STRUCTURED FEEDSTOCK

To achieve nano-structure feed wires, a large amount of alloying is required, in some cases 25% of the composition would be made up of alloying elements. These highly alloyed feed wires are referred to as SUNA wires. Various SUNA grade wires are available and are varied by the type of alloying that they have. SUNA wires are known to have alloying elements such as:

- Chromium (Cr)
- Silicon (Si)
- Tungsten (W)
- Boron (B)

The high alloying composition induces high hardness characteristics which are good for decreasing the wear rate. Another way in which different grades of SUNA wires vary is through the morphology of the wire itself. Depending on the grain size and distribution of powered material used to make the wire, the porosity, and consequently, the oil retention of the coated surface would change. An oil retention comparison between various SUNA wires if provided in Figure 7.

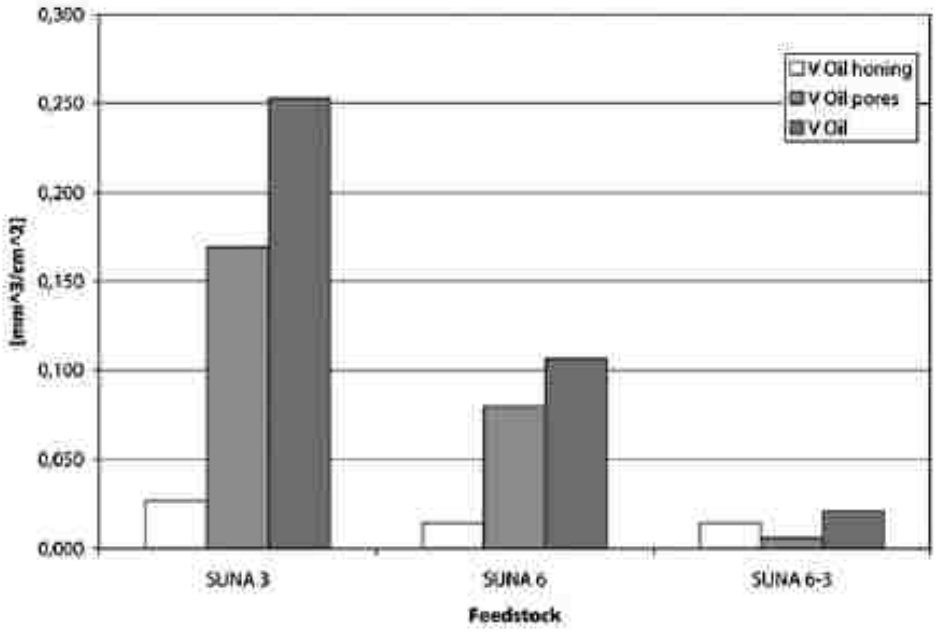

Figure 7: PTWA - Wire Feedstock – SUNA Wires - Oil Retention Comparison [5]

2.1.2. PTWA COATED BORES

As discussed, PTWA coatings have proven to possess the capabilities for increased tribological performance. Furthermore, as mentioned previously, the piston ring-to-cylinder wall interface was determined to account for about 20% of mechanical losses in a vehicle powertrain system [4]. Therefore, the application of PTWA coatings on monolithic engine block cylinder bores can reduce those losses and eliminate the use of liners along with their drawbacks.

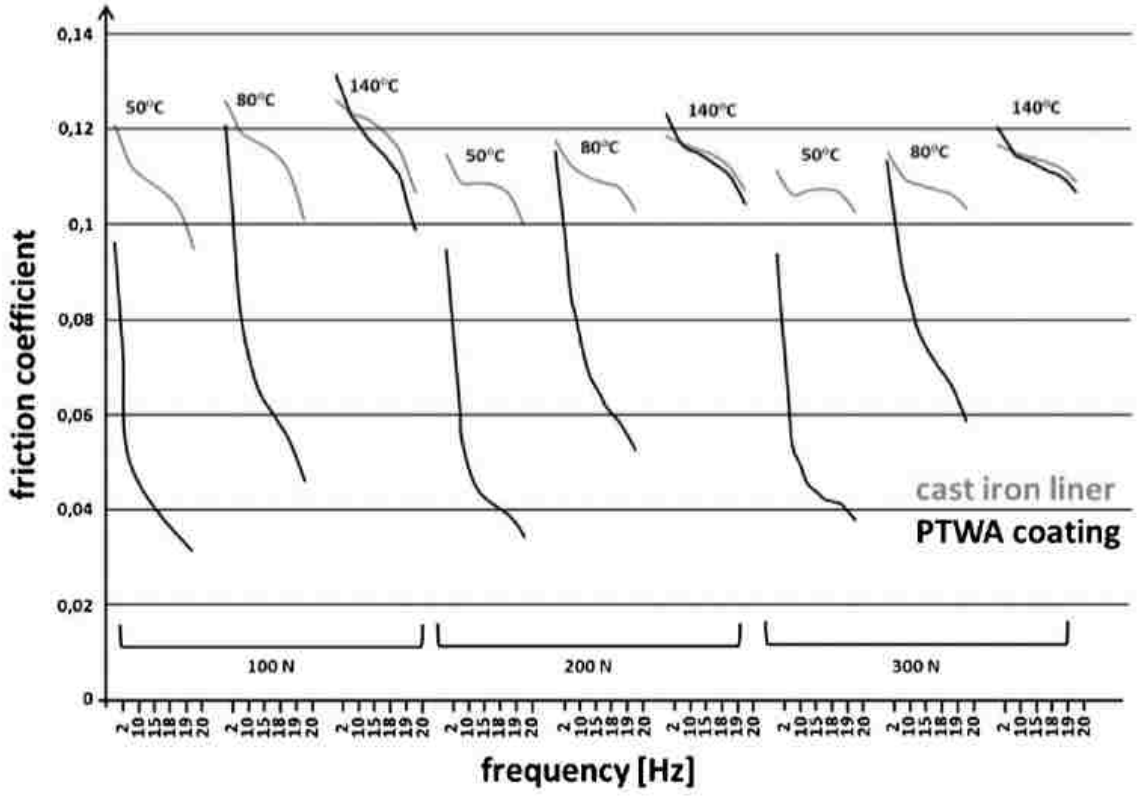

Figure 8: PTWA - Tribology Test - Cameron Plint TE77 - COF vs. Frequency vs. Lubricant Temperature [8]

Figure 8 displays a tribological comparison in terms of coefficient of friction between PTWA coated bores and cast iron liners, under varying conditions of sliding frequency and lubricant temperature. The comparison clearly shows the significant decrease in coefficient of friction when using PTWA coated bores.

Nevertheless, there are a few aspects of coated monolithic engine blocks that become very important and increase the need for caution. One of those being the casting process of the engine block, this factor becomes a lot more important when coating a cast surface. Casting defects have to be controlled very well as that will have an effect on coating quality, a feature that is less imperative when dealing with cast iron liners since the liner would cover a porous defect.

Another aspect of bore coatings that should be noted is the changing morphology throughout the cylinder. There are three morphological features noted to be present in a PTWA coated cylinder bore, each of which is displayed in Figure 9 [8]:

a) Highly Oxidized
b) Low Oxidized
c) Columnar

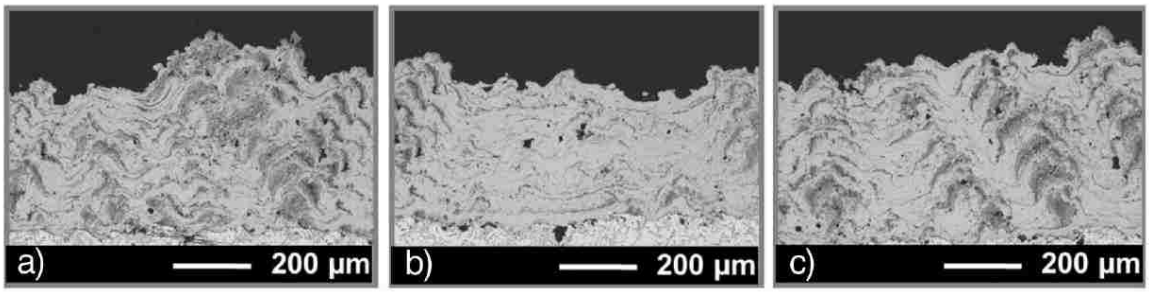

Figure 9: PTWA - Morphology Variation in Cylinder Bore [8]

As the spray head is operated within the bore, atmospheric properties change due to the constrictive geometry. This can be particularly noted by the higher oxide content in the middle of the cylinder (20%) as opposed to either ends (17%) and determined to be due to the restricted ventilation in that region. The ventilation limitations cause less heat to be dissipated which in turn promote an increase in oxidation. Additionally, it was observed that the constrictive geometry would affect the growth rate, ultimately having an effect on coating thickness, with thickness being slightly larger in the middle of the bore, as shown in Figure 10 and Figure 11 [8].

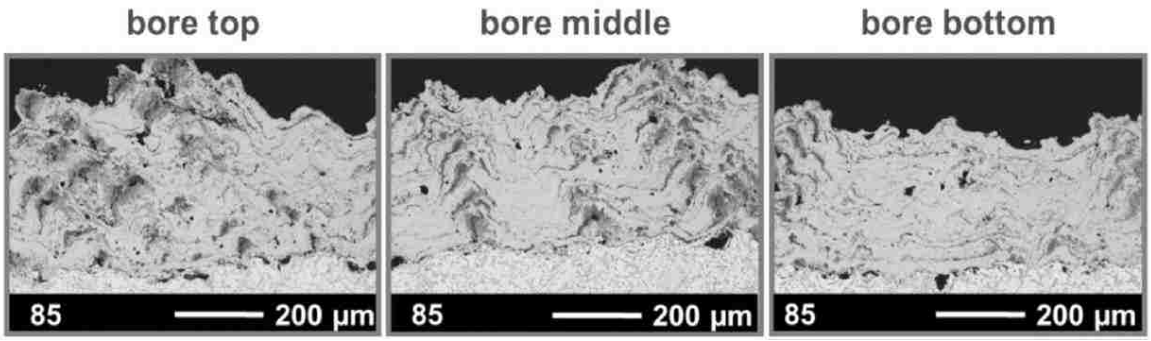

Figure 10: PTWA - Morphology & Thickness Variation in Cylinder Bore [8]

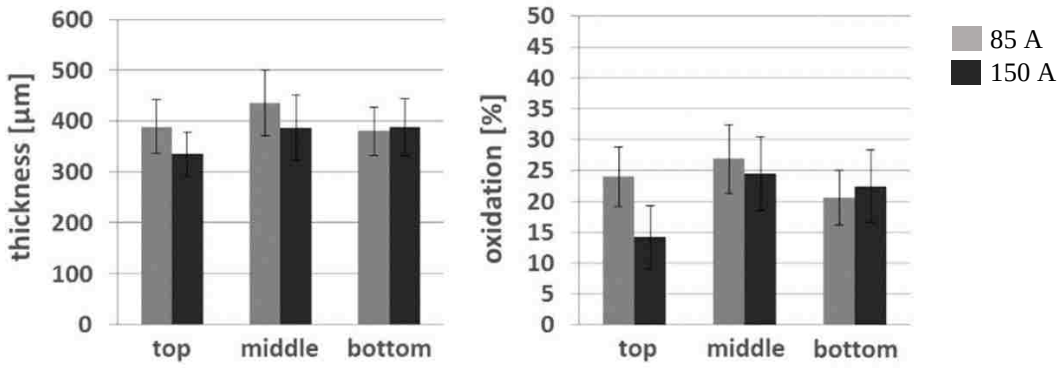

Figure 11: PTWA - Thickness Variation in Cylinder Bores with Varying Current [8]

All of the information provided and testing completed by numerous researchers and industry partners suggests that PTWA coatings possess a very high potential for increased engine performance, efficiency, and durability.

2.2. PEO COATINGS

Although PTWA coatings provide an attractive solution to reducing mechanical losses due to friction, researchers continue to develop new technologies, including new coating packages, in the hopes of reducing parasitic losses even further.

The coating package of Plasma Electrolytic Oxidation (PEO), otherwise referred to as Micro Arc Oxidation (MAO), is a type of electrochemical coating that has the potential to meet researcher requirements in the search for a new and improved generation of coatings for powertrain applications. With the ability for PEO coatings to adhere to surfaces such as aluminum or magnesium, their corrosion resistance, and increased oil retention through a large amount of naturally occurring porosity from the coating, this coating package

presents a promising solution. Additionally, through the use of alkaline solutions as an electrolyte in the deposition process, the deposition process for this coating package is environmentally friend and economical.

As with PTWA, PEO coatings only require a monolithic aluminum engine block, eliminating the requirement for cylinder liners, allowing for a reduction in manufacturing processes and decrease in weight, as well as many other tribological benefits.

2.2.1. PEO COATING PROCESS

PEO coatings are deposited using material from the electrolyte rather than a feed wire as with the case in PTWA. For this reason, there exist a set of characteristics by which PEO coating deposition processes abide by, and those are listed below [3].

- Application of different electrical potentials, an anode and cathode, between a work piece material and a counter electrode for the electrolysis of an aqueous environment (Electrolyte).
- Production of an electrical discharge at, or near, a work piece material

The way in which the electrical parameters such as voltage and current are applied to the system affects the mechanical, chemical, and physical properties of the final PEO coating.

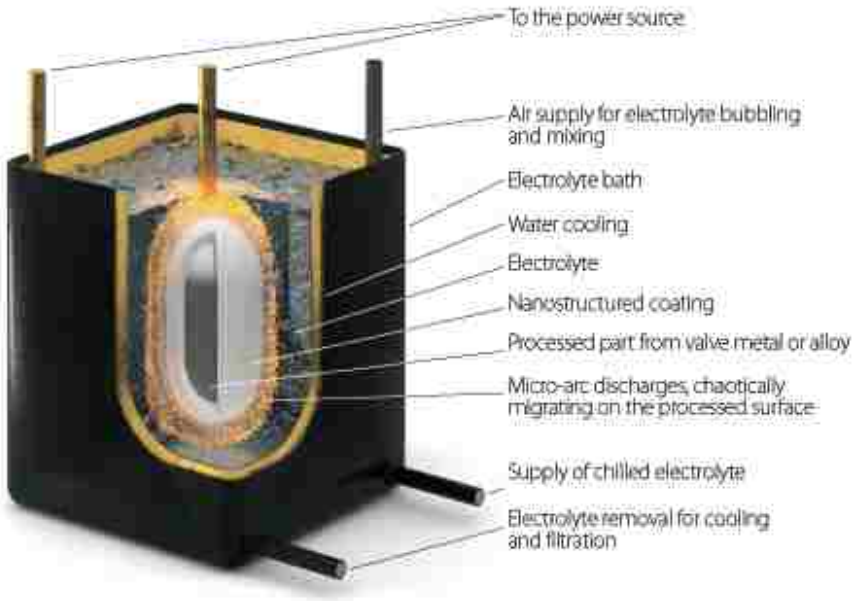

Figure 12: PEO Deposition System – Schematic [14]

Figure 12 is a basic representation and summary of the elements in a PEO coating system. It is important to note that the to-be-coated object is submerged into the electrolyte and all surfaces exposed to the electrolyte will be coated.

2.2.1.1. OXIDE FILM FORMATION

At the initializing point of the process, the passive film on the substrate that protects the base material from further oxidation begins to disband allowing for a more porous oxide film to grow; this is referred to as re-passivation. The voltage continues to rise until it reaches a critical value, after which the porous oxide film is broken. Once the film is broken, rapid sparking occurs across the surface of the oxide film, assisting in the growth of the oxide film. A buildup of negative charge in the expanding oxide film causes a discharge decay shortening effect. This effect shapes the low power and short arc discharges that subsequently occur, known as micro-discharges, or otherwise referred to as micro-arcs. These micro-discharges may also fuse the elements of the electrolyte to the porous oxide film that had gradually developed throughout the duration of the process and which has grown in both directions from the substrate surface. The plasma discharges and intense heat force the oxide growth on the substrate. The increase of voltage past that point would create much more powerful arcs and have detrimental effects such as thermal cracking of the film; therefore the careful control of electrical parameters is essential in this process. A sequence of events displaying the PEO coating process is shown via a current versus voltage plot in Figure 13.

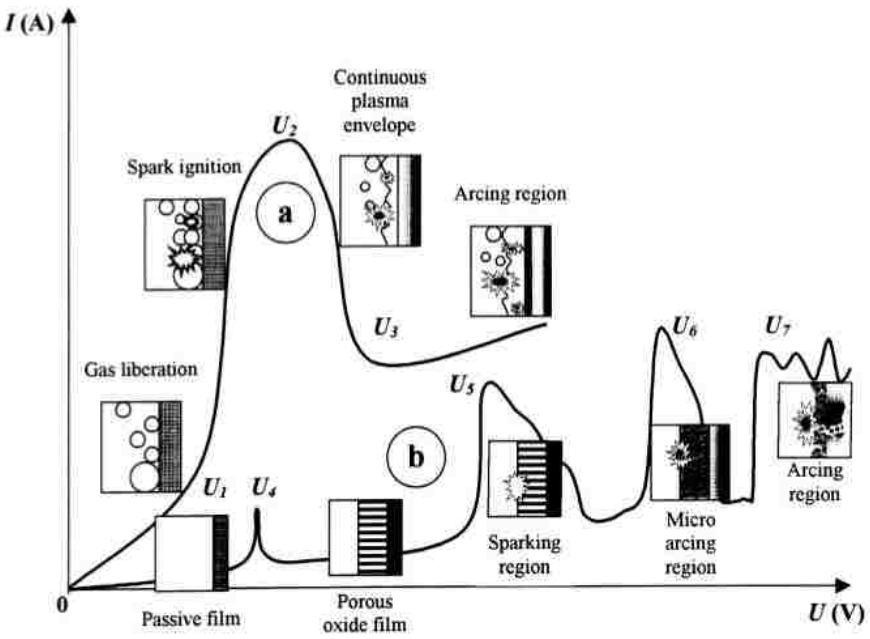

Figure 13: Current vs. Voltage Plot of (a) Surface Dissolution and (b) Oxide Film Formation [3]

2.2.2. TRIBOLOGY OF PEO COATINGS

Within PEO coatings exist three distinctive layers, each with a different response to friction and wear, due to the varying structures. In total, three domains of wear are associated with these coatings, each coinciding to one layer in the coating [3].

1. Porous Outer Region: High wear rate, attributed to the low hardness and high porosity.
2. Dense Inner Region: Minimum wear rate, attributed to the high hardness and low porosity.
3. Thin Interfacial Region: Highest wear rate, displayed by a sharp increase in wear, due to the soft characteristics of the substrate material.

Based on this information, it is sometimes undertaken to remove the porous outer region to reach the minimum wear rate of the dense inner region, for enhanced tribological results. However, under oil-lubricated conditions in the hydrodynamic lubrication region with the porous outer layer as the sliding interface, an extremely low value of friction was achieved. From tests conducted by Yerokin, Nie, Leyland, Matthews, and Dowey [3], coefficients of

friction as low as 0.015 were obtained for bench tests of PEO on steel in hydrodynamic lubrication regions.

2.2.2.1. POROSITY

Porosity of PEO coating is the governing factor for tribological performance due to the oil retention values that can be reached. For this reason, a strong emphasis is placed on process parameter effects on coating structure. Some of the elementary processes parameter modifications that can be made in the deposition process include, but are not limited to:

- Current Frequency
- Current Mode
- Electrolyte Composition

2.2.2.1.1. CURRENT FREQUENCY

During the production of PEO coatings, features known as “platelets” form on the outer region of the oxide surface. These “platelets” cause an increase in porosity as the odd shapes that form give way to surface voids, otherwise known as porosities. The “platelets” form due to the rapid solidification by quenching of molten alumina that occurs via the high arcing temperatures achieved during the creation of PEO coatings.

Through the variation of the current frequency during the production process, it was noticed that porosity and thickness could change. Test coatings under different current frequencies were completed, and via scanning electron microscope (SEM) analysis conducted by Tillous, Toll-Duchanoy, and Bauer-Grosse [2], the effect on the coating could be investigated through its cross-section.

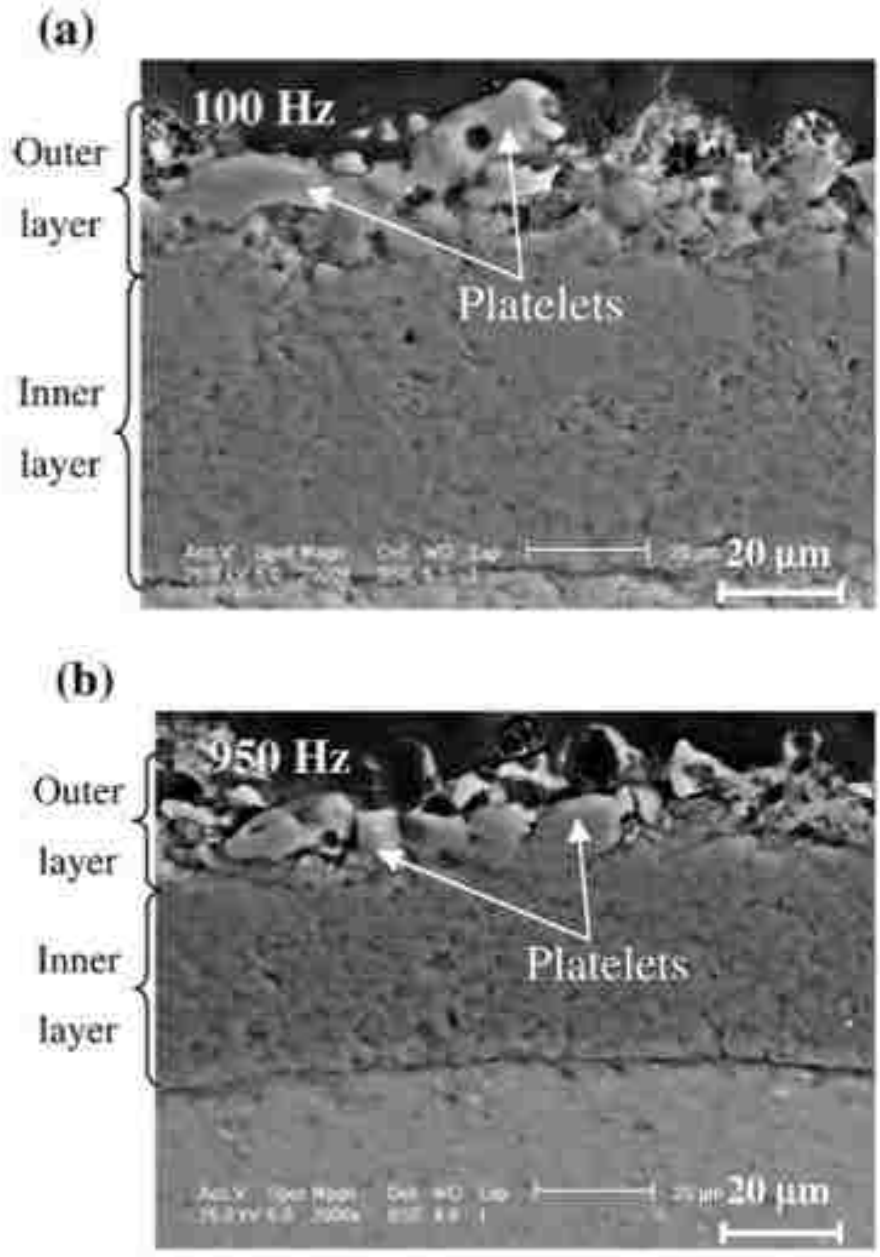

Figure 14: PEO - Current Frequency Variation Comparison – Cross-sectional View [2]

From Figure 14, a couple of changing characteristics are clearly noted. The effect of the "platelets" in provoking porosity noticeably diminishes with an increase in current frequency. This effect is due to the "platelets" becoming smaller during large current frequencies. Furthermore, an increase in current frequency decreases the coating thickness, as visible by the significantly reduced depths of the outer and inner layers of the coating.

2.2.2.1.2. CURRENT MODE

Although several current modes exist, PEO coating deposition processes focus on two main ones; unipolar and bipolar current. Unipolar current has very high discharge temperatures, which subsequently create “pancake” type features on the coating surface, as termed by Hussein, Nie, and Northwood [1].

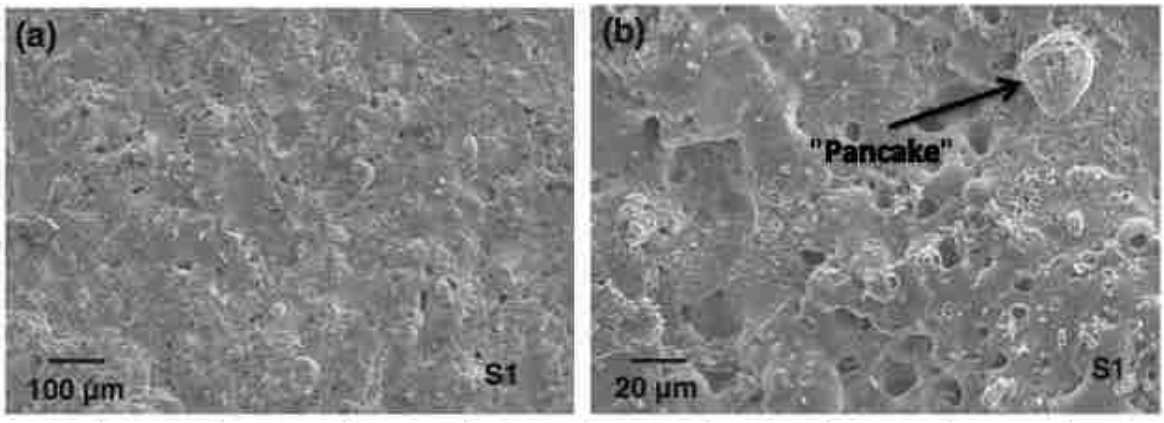

Figure 15: PEO - Unipolar Current Mode Microstructure – Top Surface View [1]

From the SEM image in Figure 15, many flat “pancake” features can be seen. Unipolar current mode discharge temperatures range from 4000K – 7000K, and these high temperatures cause volcano-like eruptions of molten alumina out of discharge channels on the coating surface, the molten aluminum then solidifies to create these “pancakes”. Furthermore, the high temperatures reached relate to stronger discharges, referred to as “B-type” discharges, while still maintaining a bulk surface temperature of approximately 100°C. B-type discharges of unipolar current modes penetrate deep into the coating surface leaving a region of high porosity. Therefore, “pancake” features and high porosity is associated with unipolar current modes.

Bipolar current modes create a largely different coating microstructure from unipolar current modes. Due to its current waveform, bipolar current modes do not reach temperatures as high as its unipolar counterpart. Bipolar temperatures range within 4000K-5500K, therefore reducing the effect of their “B-type” discharges.

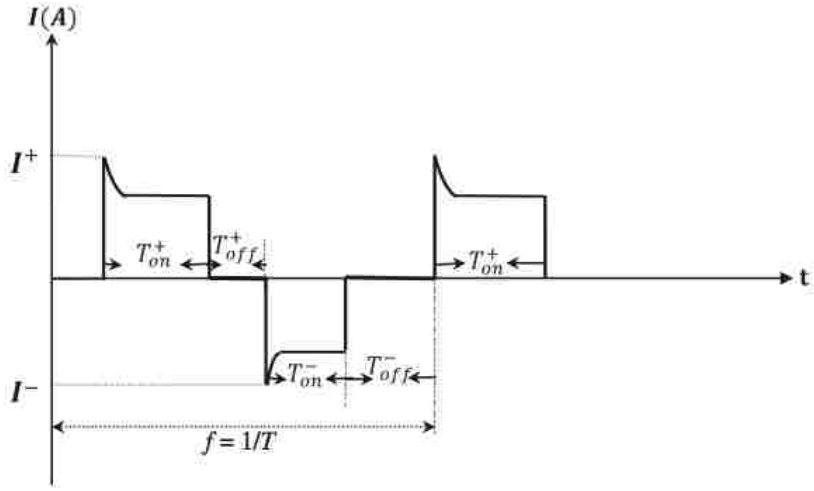

Figure 16: PEO - Bipolar Current Waveform – Schematic [2]

Figure 16 displays the current waveform of bipolar current mode. The negative current and off current time of the current mode, as seen from the waveform, provide the coating with a "balance of discharge" effect. This effect gives enough time for the local molten oxide to cool prior to the next pulse of current, which then sinters the recently cooled area. This type of procedure produces a hard, thick, and minimum porosity coating, as can be seen from Figure 17.

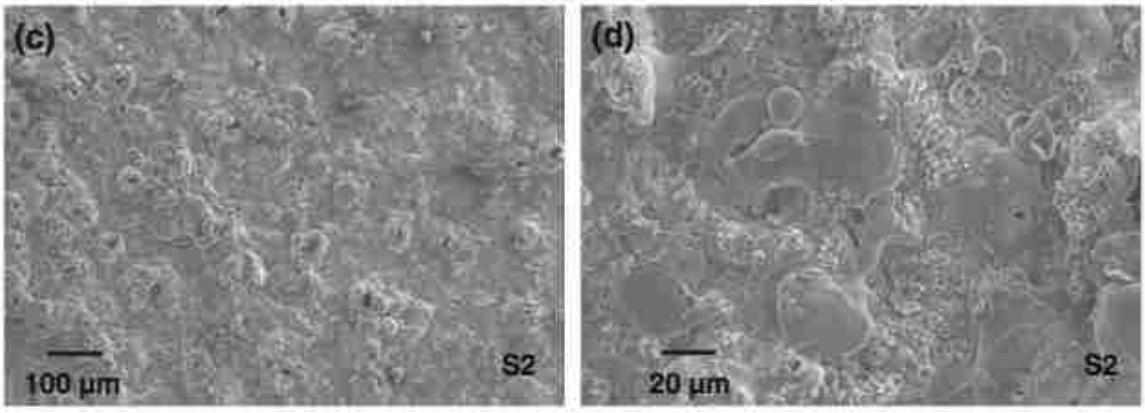

Figure 17: PEO - Bipolar Current Mode Microstructure – Top Surface View [1]

2.2.2.1.3. ELECTROLYTE COMPOSITION

As with most metals, alloying with other elements changes certain characteristics of the microstructure, generally creating a stronger material. This can also be achieved with PEO

coatings by changing the composition of the electrolyte. During production of the coating, the diffusion process fuses elements of the electrolyte into the coated surface. By adding elements into the electrolyte, it is possible to subsequently change the composition and microstructure of the coating itself, which therefore introduces another method of varying properties of the PEO coating surface.

A common elemental addition to the electrolyte is silicon. The silicon accelerates the growth of the coating due integration into the coating microstructure and subsequent formation of complex aluminum-silicon-oxide phases. The added silicon promotes a thicker porous outer layer, which is known to reach upwards of 90% of the total combined coating thickness. The thick outer layer contains very high levels of bulk porosities. However, due to the large porosities and depth of the outer layer, the dense inner and thin interfacial layers do not contribute as much to the overall performance of the coating and which therefore diminishes its mechanical properties. Moreover, the high levels of porosity on the outer layer inhibit the uniform distribution of chemical powders which could have been introduced to further change the coating composition, therefore creating non-isotropic coating properties [3].

2.2.3. PEO COATED BORES

Experience of PEO coating application with respect to cylinder bores of internal combustion engines is very limited in terms of results and analysis. The coating deposition processes on engine blocks are in their preliminary stages which causes there to be a lack of information with respect to PEO coated cylinder bores. However, it is known that for successful application of this coating into a fired engine for the purposes of increased engine performance, there are a series of challenges to be overcome. Firstly, all the process parameters need to be optimized for maximum tribological performance. Additionally, optimal coating thicknesses need to be determined, as this would relate to which stage of internal layering - Outer, inner, or interface - the sliding interface would be subjected to. Next steps for PEO coatings include tribological and fired engine tests, all of which will require a renewed optimization of parameters at each step including a thorough post-surface treatment process to obtain an optimal surface profile.

2.3. HONING

A major component dealing with engine cylinder bores, regardless of the surface treatment process or the cylinder bore material is the post-processing action of honing. Honing is well described by Goeldel et al. [25], which states "honing of a cylinder bore is a process of abrasion that removes materials to create a good quality surface finish". This statement could be further expanded to say that the goal is to obtain a surface finish that reduces friction and wear of the piston ring-to-cylinder bore interface.

Honing technology is an integral part of engine manufacturing and can be broken down into two categories of procedure or techniques and material selection. There are many different aspects of honing processes that can be combined to achieve optimal surface finish and consequently have the potential to improve not only the tribological performance of the piston ring-to-cylinder bore system, but also improve many engine characteristics such as:

- Reduction in oil consumption
- Reduction in performance degradation over time
- Reduced particle emissions
- Reduced hydrocarbon emissions
- Increased engine efficiency
- Increased engine life
- Increased fuel efficiency

An important topic directly related to honing is surface topography, which provides background information and fundamental principles of honing goals and processes. A surface profile can be a very complicated feature to explain because there are many parameters involved, for this reason, profilometry techniques consist of mathematical equations that produce a standardized series of values for surface features such as peaks, valleys, and overall roughness.

No matter how smooth a surface looks or feels it is never perfectly smooth. Even the smoothest surfaces have a surface profile at a micro level that could resemble cross-sections as pictured in Figure 18.

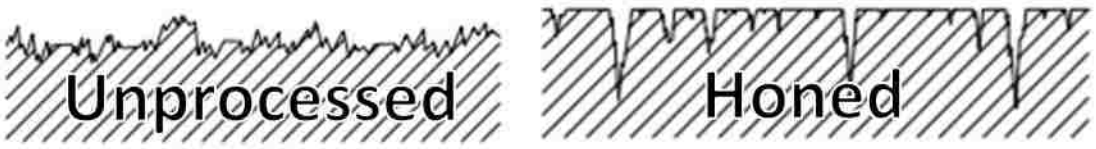

Figure 18: Surface Profile - Cross-Section – Schematic

To explain the features of these surface profiles in a clear and standardized way, they are measured using a profilometer that displays the data in graphical format for further evaluation and analysis, as shown in Figure 19. The data is usually displayed in terms of height and distance.

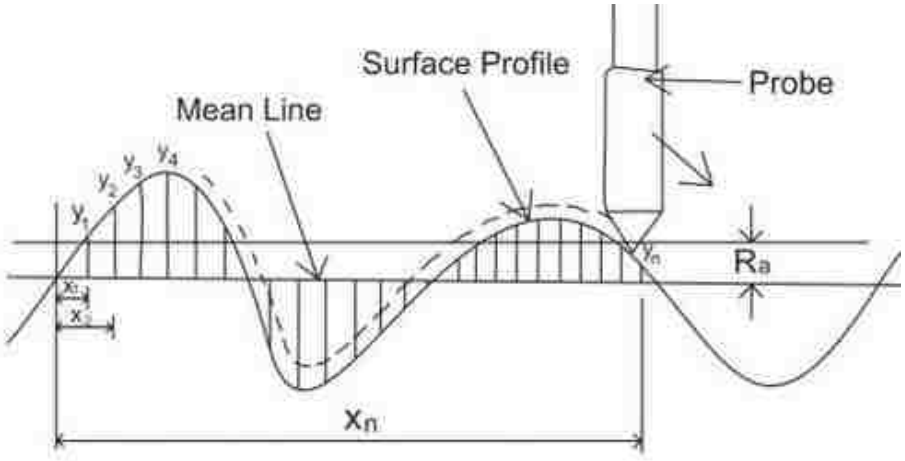

Figure 19: Profilometric Measurement - Schematic [36]

The data from the profilometer is then analyzed by mathematical methods to determine an array of different standardized features. Some basic surface features and their mathematical equations are presented in Table 2 [31].

Table 2: Surface Parameter Equations [31]

Surface Parameter	Symbol	Equation
Average Roughness	Ra	$Ra = \frac{1}{L}\int_0^L \lvert y(x)\rvert dx$

Root Mean Square Roughness	Rq	$R_q = \sqrt{\frac{1}{A}\int_0^{Ly}\int_0^{Lx}(Z(x,y))^2 dxdy}$
Skew of Surface Profile from Mean Height	Rsk	$R_{sk} = \frac{1}{Rq^3 A}\int_0^{Ly}\int_0^{Lx}(Z(x,y))^3 dxdy$
Kurtosis	Rku	$R_{ku} = \frac{1}{Rq^4 A}\int_0^{Ly}\int_0^{Lx}(Z(x,y))^4 dxdy$

The surface profile can be analyzed even further by the Abbot-Firestone curve in Figure 20 to give important information such as size and percentage of surface peaks and valleys and provide a material ratio curve such as the one in Figure 21.

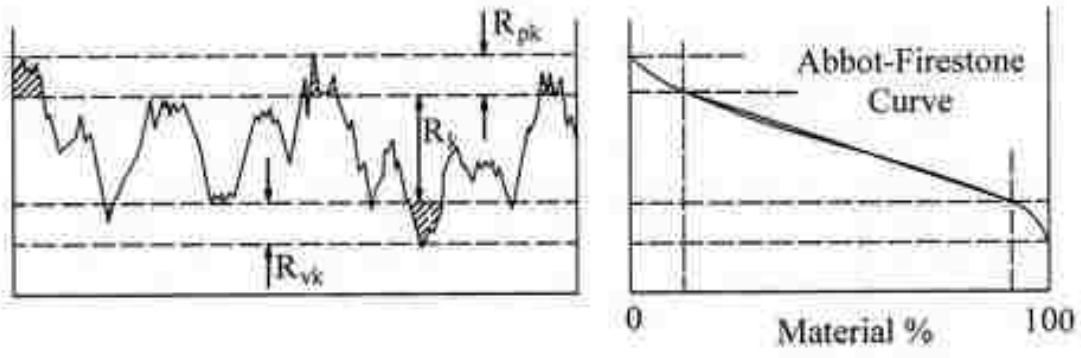

Figure 20: Surface Profile to Material Ratio Schematic [31]

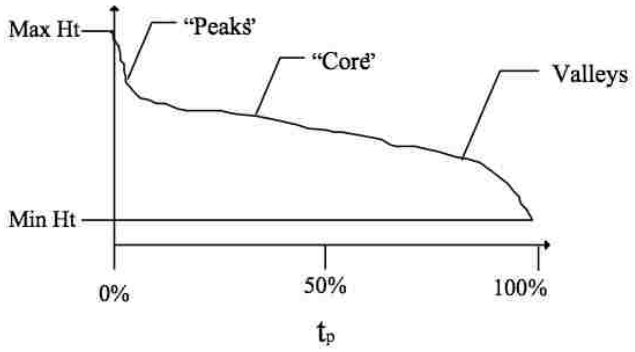

Figure 21: Material Ratio Curve [9]

All the surface parameters discussed assist in evaluating the honed profile and give targets of what kind of profile to achieve in order to maximize performance and durability. There are a few surface profile parameters with regards to cylinder bores of internal combustion engines that are important to mention. As discussed previously, surfaces profiles can have peaks and valleys that vary in size, quantity, and distribution. The goal of honing is to find a compromise between some of those parameters to obtain the best possible tribological solution [26].

- Roughness (Ra): Although it may seem intuitive to strive to achieve the smallest Ra value possible, meaning the smoothest surface, this is not the ideal case for an engine cylinder bore which requires oil retention capabilities.
- Surface Peaks (Rpk): It is important to get rid of the peaks as they can break off and create wear particles that further promote abrasive wear throughout the engine by circulating in the oil.
- Surface Valleys (Rvk): Large valleys are required for oil retention. Increased oil retention creates lubricated tribological conditions, which provide better friction and wear performance due to the formation of larger tribo-layers, subsequently separating the asperity contacts of the opposing sliding surfaces.

The abrasion and material removal that occurs during honing provides an opportunity to affect and control a few other parameters related to cylinder bores of an engine, such as:

- Bore Dimension: it is possible to control the bore dimensions very precisely and maintain a very small tolerance on bore sizes, eliminating the possible need for graded engine components to fit every combination of sizes that would be a result of large dimensional tolerances.
- Cylindricity/Roundness: maintaining roundness of the bore is also very critical for engine performance as it could eliminate all the advantages obtained from an ideal surface profile if the dimensions throughout the bore are not uniform and in-line with each other.
- Surface Features: some honing processes purposefully engrave “crosshatch” markings on the bore walls to increase control and influence of oil retention values. More advanced methods exist for the creation of surface features such as laser

texturing. Laser texturing creates uniform pits on the bore surface for even further reduction of oil consumption, emissions, friction, and wear [27].

2.3.1. HONING PROCESS

Honing is accomplished by a mechanism that has two degrees of freedom [25]:

1. Axial Translation
2. Rotation

An abrasive brush is inserted into the bore and moves longitudinally within the bore at a particular frequency for a set period of time, which is determined by the final surface profile specifications. Additionally, the abrasive brush rotates about the center axis of the bore to help achieve the required surface specifications. This combination of movements can also create the distinct crosshatch markings that are associated with honing as seen in Figure 23, which are also closely monitored to meet specifications. A schematic of this process is provided in Figure 22.

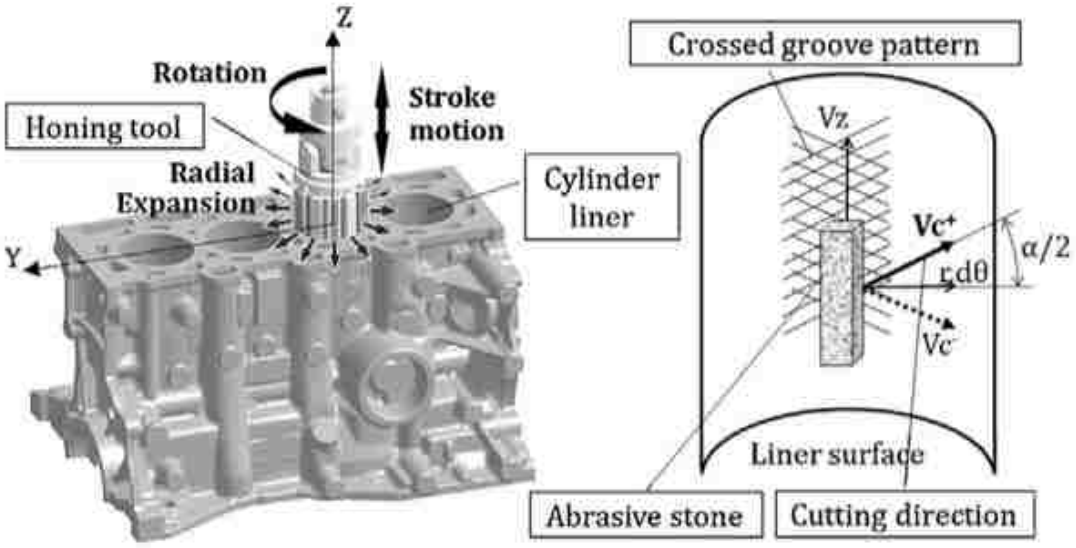

Figure 22: Honing Operation - Schematic [25]

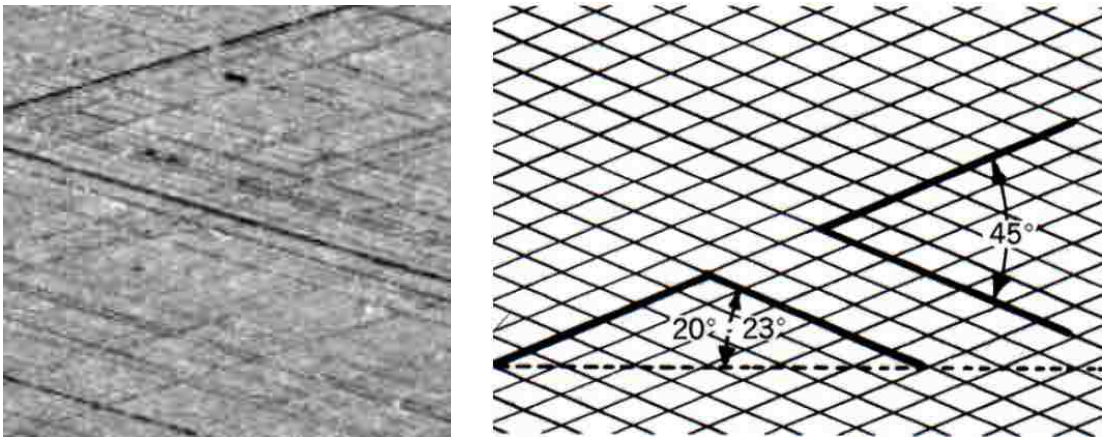

Figure 23: Honing Angle Measurements – Schematic [28]

Honing is usually not accomplished in a single step, but rather a series of steps, each consisting of varying honing brush materials or grit levels. This is done to superimpose one surface profile over another and further help in achieving the desired profile. These multi-step honing processes could vary from two-step to several-step [25], however, for mass-production purposes, it is always desired to reduce the number of steps required for this process.

2.3.1.1. HELICAL SLIDE & PLATEAU HONING

Due to the dynamics of the honing process, variations in surface appearance occur at the top and bottom of the cylinder bore when compared to the center. These variations are due to the longitudinal acceleration and deceleration when approaching the two ends of the cylinder bore. In these changing-velocity regions, rotational speeds remain constant. This combination of dynamic parameters creates parabolic surface features as opposed to the very liner crosshatching in the middle of the bore. The parabolic markings indicate what is known to be "Helical Slide Honing". The center region, with linear crosshatch marks is referred to as "Plateau Honing". The combination of helical slide honing on both ends of the bore and plateau honing in the center produces a "Mixed Liner" condition [25].

Plateau and helical honing can be easily distinguished by the degree of angle separation between the markings [29].

- Plateau: 40^0 - 60^0

- Helical: 120^0 - 140^0

Furthermore, helical slide honing provides several advantages over plateau honing, but due to the increased cost in production to conduct this method throughout the cylinder bore, it is not widely used. Nevertheless, the benefits of helical slide honing are important to be mentioned and are as follows [30]:

- Wear is reduced by up to 40% when increasing the helical honing angle to 140^0, compared with current honing production processes.
- Oil consumption was decreased by up to 50%.
- Oil consumption rate remained almost constant through running-in periods of the engine

2.3.1.2. ABRASIVE HONING STONES

Honing can be separated into two main categories, one being process and the other being material. The material aspect of honing is extremely important and it could encompass the bore material as well as the material used as the abrasive stones on the honing brush.

Silicon carbide or aluminum oxide abrasive honing stones have been commonly used and continue to be popular due to their cheap cost. However, as bore surfaces are becoming more intricate due to the many performance improvements that come along with those, honing materials are becoming more intricate as well. Although meeting surface specifications is important, the tool life of honing stones is critical in production. The conventionally used abrasive materials such as silicon carbide or aluminum oxide are known to wear equivalent to the surface they are honing. This wear of honing stones greatly affects the ability to keep uniform surface properties and although they have a low individual cost, they must be replaced often. Therefore, for production, a compromise between honing performance and tool life must be achieved. Some factors that must be considered when deciding on honing material are [27]:

- Hardness of the abrasive stones
- Hardness of the bore material
- Honing speed and frequency

- Honing load

Due to these factors, diamond abrasive honing stones have become popular for this application. Since diamond is the hardest material attainable, it experiences significantly less wear than any other honing stone. Subsequently, the reduced wear helps maintain uniform honing properties and significantly extends the tool life. These benefits come at an estimated cost of $600 - $700 for a brush set of stones [27], they are up to 47 times more expensive than conventional honing stones. However, over time, due to increased tool life, diamond honing stones have been known to pay themselves off.

Although diamonds seem to be a great solution, there are several drawbacks associated with them. Due to the mechanical properties of diamond material, specifically the large hardness values, diamond honing stones cut or hone different than conventional stones. Increased pressure on the bore by the honing brush is required to meet specifications when using diamond stones. Furthermore, diamond stones "plow" through the bore material rather than "cut" it. This "plowing" action affects the overall honing process in two substantial ways. Firstly, the "plowing" effect of diamond stones increases heat generation causing the need for precise control over pressure on the bore and lubrication parameters. Secondly, large rates of material removal are achieved which affects the ability to reach the required roughness. For this reason, at least two sets of diamond honing stones at different grits are required to obtain the desired surface profile. It is important to note that the grits used in diamond honing stones have to be much finer than conventional honing stones to achieve the same surface specifications. In some cases, a conventional honing brush is quickly used to further remove the surface peaks created from the plowing effect of diamond stones [27].

From this brief overview of the various types of honing processes, it is evident how important surface treatment techniques are and how complicated they may become. With that knowledge, it is possible to appreciate the many combinations of honing materials and processes that can be utilized to achieve the best compromise for efficient production and engine performance. Overall, honing is an important engine production process that continues to be developed. With the introduction of new coating materials for piston rings

and cylinder bores, honing will have to be optimized for each system including the PEO coating package which is the main focus of this study.

2.4. PISTON RINGS

A critical component of the piston assembly and the main opposing sliding surface to the bore itself is the piston ring pack. The piston rings affect important engine parameters such as performance, fuel economy, and emission control. Although they may have come from relatively simple origins such as plain steel rings, piston rings have evolved into immensely complicated engine components that greatly affect the engine itself. The main purpose of the piston rings is to provide a dynamic seal of the combustion chamber, separating it from the crankcase volume. A secondary and also vastly important purpose of the piston ring pack is to distribute and control the retention and flow of oil film between the cylinder bore and piston ring sliding surfaces. Along with the sealing and oil controlling, the piston ring pack must accomplish those responsibilities while maintaining low frictional coefficients in all regions of the piston stroke, significant wear resistance, as well as a resistance to thermal and mechanical fatigue [32].

Most current ring packs used in gasoline internal combustion engines consist of three stages:

1. Upper/Top/First Compression Ring: Used primarily in sealing the combustion chamber from the crankcase volume in order to maintain maximum compression in the combustion volume which would then translate into greater efficiency and increased power.
2. Lower/Bottom/Second Compression Ring: Distributes the oil along the cylinder bore walls and helps maintain a thin oil film thickness that assists in keeping a lubricated sliding interface and separating the opposing asperity contacts in order to produce more favorable tribological results with regards to lower friction and wear.
3. Oil Ring Pack: Consists of three separate entities that include two scraper rings and one spacer rings. The scraper rings remove excess oil off of the cylinder walls and direct it into the channels of the spacer ring which guides the oil back into the

crankcase for recirculation. The control and removal of excess oil off of the cylinder walls is important because it would otherwise be ignited in the combustion chamber creating hydrocarbon molecules which would degrade the emission output of the engine.

Additionally, piston rings are created with gaps which allow the rings to thermally expand without applying additional contact pressure on the cylinder walls. Moreover, all of the piston rings that make up the pack must be staggered so that their end gaps create a labyrinth for the flow of combustion gases, making it more difficult for them to pass into the crankcase, subsequently increasing engine efficiency and performance [32].

In order to accomplish all of the strict requirements of piston rings, their cross-sectional shape and overall material composition is critical for obtaining the proper mechanical and thermal properties that would help in achieving the goals of each individual ring. In order to meet these requirements, piston rings are usually made up of an array of different materials and surface treatments. Such a collection of different material properties is necessary to provide the following mechanical and thermal parameters expected by piston rings [32]:

- Elasticity: helps to provide a better dynamic seal that expands and contracts when necessary to accommodate for non-uniformity in the roundness of the bore which could be caused by bore deformation due to non-uniform thermal expansion throughout the stroke of the bore.
- Corrosion resistance: be able to resist corroding due to various types of fuels, including ethanol based fuels and chemical additives in the oil.
- Pairing to cylinder bore: piston ring sliding surfaces must have a favorable tribological reaction to cylinder wall materials. The pairing between piston rings and cylinder bore must create a tribological environment that has excellent abrasive resistance.
- Thermal conductivity: a major point of heat dissipation from the combustion chamber to the cooling system of the cylinder block is by conductive heat transfer via the piston rings. Therefore, they must also have favorable thermal conductivity properties to promote heat dissipation.

As important as all the mechanical and thermal parameters of may be, sufficient lubrication and lubrication regimes are also critical in piston ring performance. Ideally, the fully-flooded lubrication regime is desired in all areas of the stroke, as it is the regime that offers the least friction and wear. The fully-flooded lubrication regime occurs when the oil film completely separates the opposing surface asperities, leaving the contact pressure to be completely supported by the oil film. However, due to the harsh environment creating areas of high contact pressure, low velocities, and increased gas pressures that in-turn disturb the oil film, the most desired lubrication regime is not attainable through the entire engine cycle. Since fully-flooded lubrication occurs at high sliding velocity and low pressure values, this regime occurs mostly mid-stroke.

The other prevalent lubrication regime is the partially flooded regime. Occurring at both ends of the stroke, top dead and bottom dead centers, where velocity is at its lowest and contact pressure is significantly higher than in the rest of the stroke. The partially flooded lubrication regime causes the load to be carried by the surface asperities, causing increased friction and wear. The other remaining regime is starved lubrication where the sliding surface is exposed to the most severe friction and wear due to lack of oil film in the tribological system [32].

Monitoring and controlling the existence of these lubrication regimes throughout the stroke of the bore allows to decrease the risk of engine failure by piston seizure resulting from scuffing. Scuffing is detrimental to an engine and can be recognized by plastic deformation, abrasive ploughing, and material transfer [32]. Scuffing is the local micro-welding of surface asperities which occur when flash temperatures reach material melting temperatures. These types of micro-welding situations are most likely to occur in regions of poor lubrication, high contact pressure, and low sliding velocity.

Therefore, piston rings have a significant effect on an engine and can have detrimental effects if all their properties are not taken into account before being implemented into such an extreme environment. For this reason, the material composition, surface treatment, and deposition methods of piston rings are highly important.

2.4.1. PHYSICAL VAPOR DEPOSITION (PVD)

The most common form of material deposition onto piston rings is by physical vapor deposition (PVD). PVD processes work on the principles of vacuum science, which allows for the deposited coating to be composed of high purity material. Additionally, PVD processes are versatile in the sense that they can be combined with many other processes to create combination PVD processes, such as plasma-assisted chemical vapor deposition, and plasma nitriding-PVD surface coatings [13]. Furthermore, PVD is not limited to DLC coatings and its subgroups, but extends to include a whole range of various elements and their assorted alloys, including, but not limited to: aluminum, chromium, copper, zinc, indium, nickel, and titanium [12]. However, it is important to note that coating thickness by this method is limited to ranges from nanometers to several microns.

Although, as previously mentioned, various subsets of PVD processes exist when combining deposition methods, a general outline stands firm. A three point summary of this process is well described by Sigma-Aldrich [12], as follows:

1. Vaporization of material from a solid source (Target).
2. Transportation of the vaporized material to the substrate surface.
3. Condensation of the vaporized material onto the substrate surface.

The ways in which PVD processes vary has to do with how the target material is vaporized and transferred. A couple of different methods for vaporization and transportation are:

- Evaporation
- Sputtering

2.4.1.1. EVAPORATION

Evaporation PVD technique is characterized by transforming the target material into a gaseous state. This gaseous state is achieved by heating the high vacuum chamber until the target material reaches its vapor pressure, a characteristic which all materials possess and that signifies a temperature and pressure after which the material vaporizes.

PVD by evaporation has several defining characteristics that differ from the other PVD technique of sputtering. Evaporation PVD has a tendency to produce large grain sizes and

poor coating-to-substrate adhesion properties. These characteristics could be attributed to the low energy transfer of atoms from target to substrate material. However, due to the high vacuum environment required for this process, much less gas is found to be trapped within the deposited material. Additionally, evaporation PVD requires a direct line of sight from target to substrate for deposition due to the mechanism by which atoms are transferred [6].

PVD by evaporation can be further subcategorized into two modes of target heating:

- Filament
- Electron Beam

Evaporation by filament heating is achieved by passing an electrical current through a crucible, otherwise known as an evaporator, or filament. The target material is stored within this crucible and subjected to conductive heating. Multi-material coating deposition can also be achieved through using a variation of this method; using multiple crucibles. Each crucible would contain a separate material, producing a coating of more complicated composition. Figure 24 is a schematic displaying evaporation PVD by a filament process.

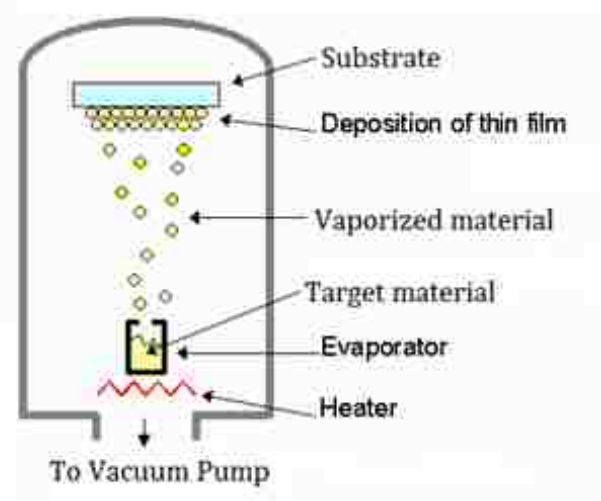

Figure 24: Evaporation PVD - Filament - Schematic [15]

2.4.1.1.1. ELECTRON BEAM

Evaporation by electron beam heating varies from filament type evaporation in many ways. The crucible which contains the target material to be evaporated is water-cooled so that to maintain a low bulk temperature of the target material, and subsequently keeping it in a

solid phase. The evaporation comes from heating the target material in a very small and locally concentrated area up to the materials critical vapor pressure. This evaporation technique is accomplished by a high energy electron beam. The electron bombardment is produced by a high voltage potential as well as a magnetic field which affects where the electrons are concentrated. This technique offers a lot of flexibility in terms of the deposition parameters, allowing for strict control over the evaporation rate and the evaporation and subsequent deposition of materials with high melting temperatures [15]. Furthermore, the local concentration of heating reduces possibilities of contamination from the crucible as is possible with filament evaporation. Figure 25 is a schematic displaying deposition by electron beam evaporation system.

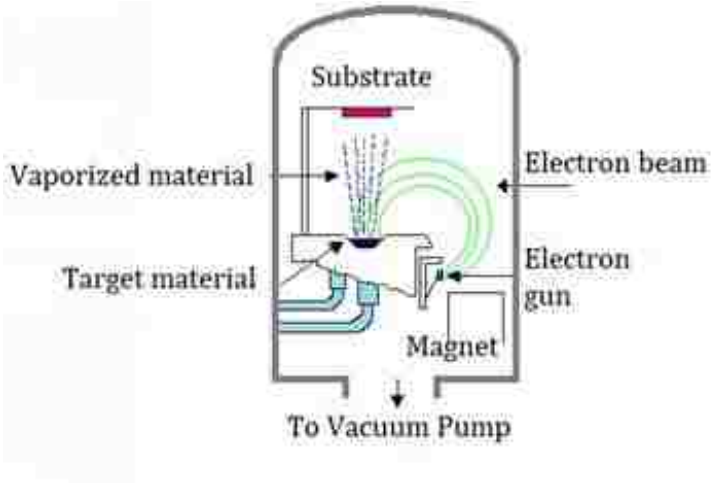

Figure 25: Evaporation PVD - Electron Beam - Schematic [15]

2.4.1.1.2. SPUTTERING

A different method of surface coating deposition is through sputtering. Sputtering can be defined as the bombardment of high energy atoms and subsequent transfer and deposition of target material to substrate by the passing of electrical discharge through a medium of working gas. The working gas is usually Argon, however, it may vary depending on the atomic weight of the target material. To achieve greater transfer efficiency from target to substrate, it is favorable to use an inert gas which closely matches the atomic weight of the target material. In the deposition of light atomic weight materials, neon has been known to

be used as the working gas. Conversely, Xenon or krypton have been used as a working gas for heavier target materials [15].

The sputtering system consists of opposing metal electrodes, the target material acting as the cathode, and substrate as the anode. The electrical discharge carries target material atoms through a state of plasma which is sustained by the collision of neutral argon atoms with electrons that subsequently form even more electrons and ions of argon [17]. A schematic of this sputtering technique is illustrated in Figure 26.

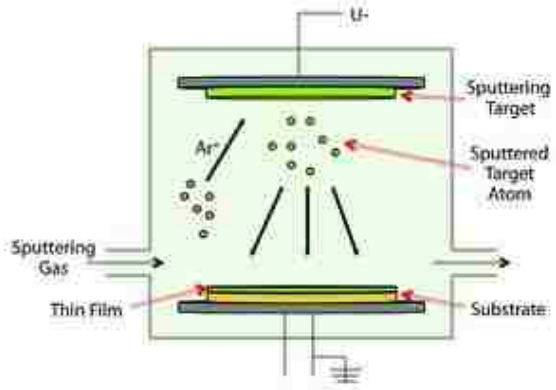

Figure 26: Sputtering PVD - General Technique – Schematic [12]

This deposition technique has several defining characteristics that vary from evaporation PVD. In part due to the high energy environment combined with the low vacuum required, the deposited material adheres well to the substrate surface, more so than evaporation PVD. Moreover, smaller grains are achieved in the coatings which signify a stronger and harder material due to basic material property principles that state microstructures with smaller grains have a greater number of grain boundaries preventing dislocation motion [6].

2.4.2. DIAMOND-LIKE CARBON COATINGS

Diamond-like Carbon (DLC) Coatings, otherwise known as near-frictionless carbon (NFC), have an amorphous structure and in the presence of inert gases, have been known to display near-frictionless performance with frictional coefficient values reaching as low as 0.001. DLC coatings lose their excellent tribological performance characteristics at high temperatures, as noted for NFC coatings to be above 250^0C [9]. Therefore, successful implementation of this coating within the combustion chamber where temperature and

pressure reach extreme values is difficult to achieve. However, the study of DLC coatings on piston rings still continues in order to overcome the technical challenges and utilize the excellent tribological qualities.

2.4.2.1. TRIBOLOGY OF DLC COATINGS

It would seem as though DLC coatings are an ideal solution to tribological systems. However, DLC coatings exhibit a few drawbacks that limit their implementation in some mechanical sliding interface systems. As mentioned previously in this report, the loss of enhanced tribological performance at extreme temperatures poses serious limitations. Furthermore, they are known to have poor adhesion properties to certain materials. For this reason multilayer composite DLC coatings are necessary to implement into these types of systems in order to find a compromise between all the parameters that would make this a functional coating.

To start, it is important to classify the types of coatings available for increased tribological performance. The generalization of these coatings is as follows:

- Wear Resistant: coating which is usually comprised of ceramic due to its resistance to high temperatures and good adhesion to alloys produced by the strong interatomic bonds within the oxides, carbides, or nitrides within the microstructure. However, this type of wear resistant coating generally suffers from higher than desired values for coefficient of friction.
- Low Coefficient of Friction: coating consisting of solid lubricants such as graphite lamellas. These lamellas provide low coefficient of friction due to their hexagonal crystal structures which have easy slip planes. However, these slip planes are detrimental with regards to wear, increasing the wear rate significantly due to the low hardness values.

As is described, each option has serious drawbacks, and this is where DLC coatings provide an excellent compromise. Consisting of diamond-like material, the coating naturally has high hardness and reduced coefficient of friction performance. However, to combat poor adhesion and temperature limitations, supporting layers have to be introduced.

Theoretically, numerous layers would be preferred to combat each one of the limitations. The theoretical layers required are as follows [16]:

1. DLC: Friction and wear resistant layer
2. Load Support
3. Stress Equalizing
4. Crack Braking
5. Diffusion Barrier
6. Adhesive

Although these layers provide a theoretical solution, for various reasons, including interlayer bonding, they are not possible to successfully produce. For this reason, only some supporting layers are integrated in this coating system. These layer combinations have their own benefits and drawbacks, and examples of a couple of these combinations are discussed below.

- Supporting Layers of Titanium Nitride and Titanium Carbo-nitride for Titanium DLC coatings.
- Patented coating layer structures by Federal-Mogul, commercially known as Carbo-glide applied to piston rings contains two supporting layers:
    - Bottom: Chromium adhesion
    - Intermediate: Tungsten carbide

2.4.2.2. DLC PISTON RINGS

From all the information discussed and gathered about DLC coatings, their application on piston ring-to-cylinder wall systems is the final step in affirming their positive tribological benefits. In tests conducted by various groups, the performance of DLC coatings compared with conventional piston ring materials is displayed below. It is important to note all tests were done by Cameron Plint Tribometer TE77 and conducted on cast iron cylinder liners. Furthermore, material noted as PVD is chromium nitride and Carboglide is a patented DLC coating package developed by Federal-Mogul.

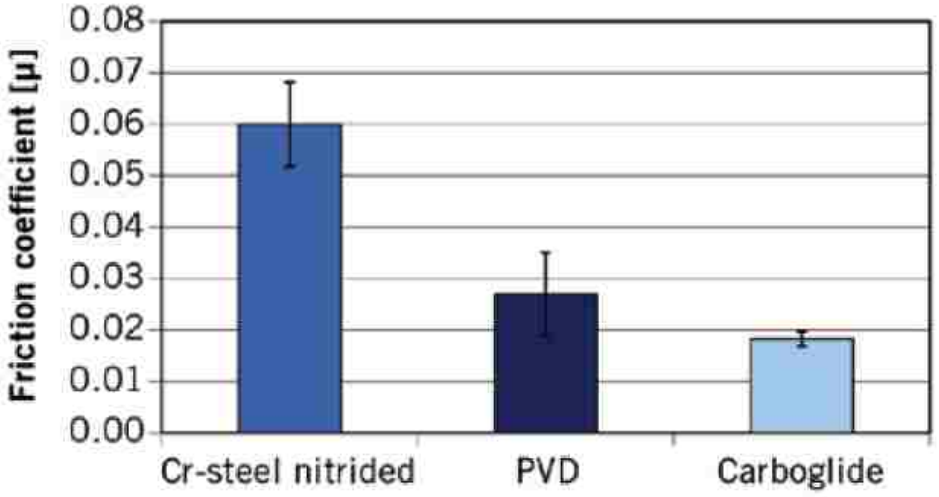

Figure 27: DLC Piston Ring Comparison - Coefficient of Friction [11]

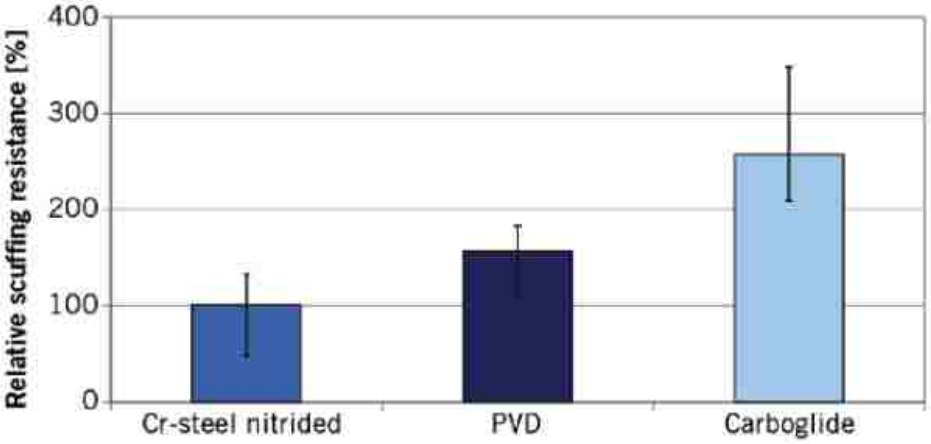

Figure 28: DLC Piston Ring Comparison - Relative Scuffing Resistance [11]

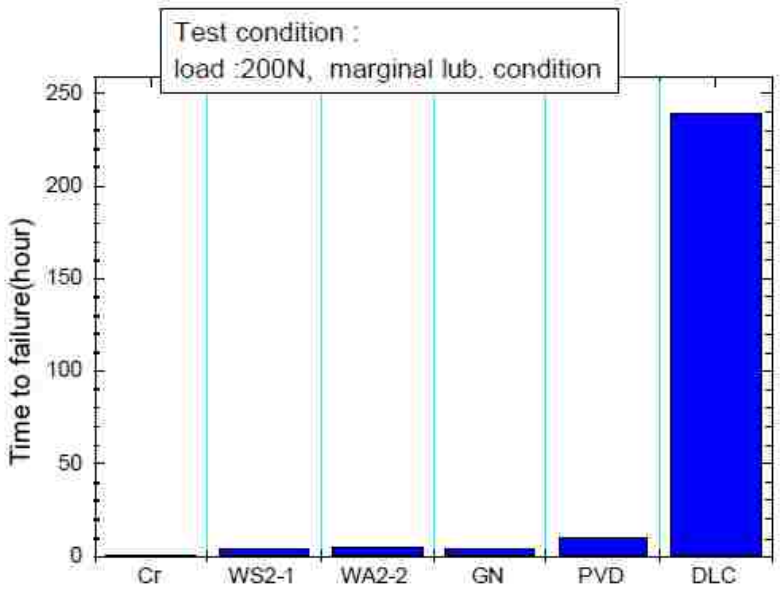

Figure 29: DLC Piston Ring Comparison - Durability (Scuffing) [7]

As is noted by Figure 27, Figure 28, Figure 29, independently studied by separate companies, both affirmed the excellent frictional, wear, and durability potential of DLC coatings when compared to other commercially available piston rings. Therefore, from the information gathered, it is clear that DLC coated piston rings have very favorable characteristics for use in piston ring-to-cylinder wall systems.

2.5. LITERATURE STATEMENT

The materials and application of PTWA, DLC, and honing techniques have been studied significantly, providing information about their properties and possible uses. However, it was noted that there was only limited information available about PEO coatings tribology and it was constrained to mostly bench tests. This literature review revealed that research into tribology of PEO coating in harsh environments such as combustion chambers was insufficient and provided an opportunity to enhance vehicle fuel economy and emissions. This study aimed to utilize the information available about DLC piston rings and honing techniques in order to investigate an area of limited research – PEO coated bores in internal combustion engines.

CHAPTER 3

3. INVESTIGATION METHODOLOGY

A series of measurements and processing procedures was developed in order to maintain a uniform testing methodology that could provide a basis for direct comparison between test results. The measurements, tests, and analysis conducted were done so to provide the best possible overview and data that could assist in development of further test iterations with the aim of improving wear resistance.

This study was limited to the number of independent variables, otherwise referred to as controlling parameters, available to modify in each iteration of testing. Even so, the limited number of changing parameters provided significantly varying results and sufficient data for analysis and evaluation.

3.1. CONTROLLING PARAMETERS

Many parameters must be optimized in order to reach ideal wear and friction in the combustion chamber tribo-system when utilizing PEO coated cylinder walls in internal combustion engines. Apart from the coating morphology itself, a significant number of non-coating parameters influence the wear rate and durability of the PEO coated bores. The piston assembly and physical aspects of the bore itself must be thoroughly monitored to determine optimal performance parameters. Within this study, the following four different controlling parameters were set to act as the independent test variables, each with their own subset of variables as shown in Figure 30:

- Coating Type
- Surface Profile
- Bore Size
- Piston Rings

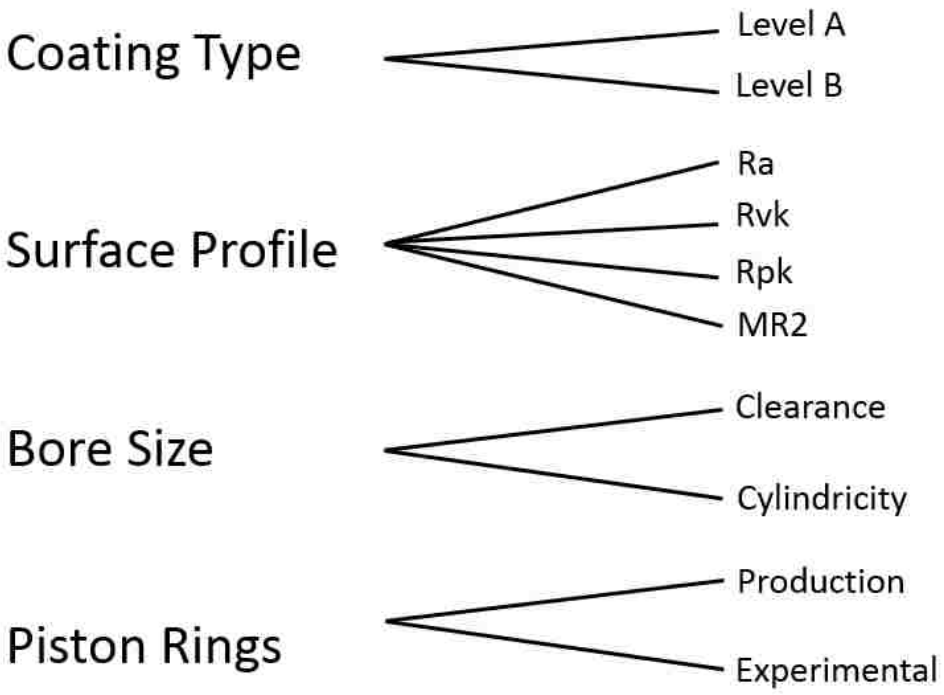

Figure 30: Controlling Parameters and Subset Variables

3.1.1. SLIDING SURFACE PROFILE

The sliding surface of cylinder bores, regardless of their material or coating, is a critical parameter which heavily affects all aspects and goals that the study is striving to achieve. The surface profile and its different features may affect emissions, oil consumption, frictional coefficient, and wear rate. In addition to achieving desired surface profile, whichever surface processing technique is used must compromise between and meet the requirements of coating thickness, bore dimension, as well as surface profile. As is known from Yerokhin et al. [3], the lowest wear rate occurs in the dense inner region of PEO coatings. Therefore it is preferred for the PEO coated cylinder bores to be within that region as well, which usually exists at around 10 μm of thickness. Maintaining the required bore dimensions is also critical and taken into account when altering cylinder bore surface profiles. Finally, surface profile must meet specifications along with all other parameters, and although the smoothest surface profile may seem ideal for sliding wear, it is not the desired profile for this type of application.

Average roughness (Ra) specifies the average variation in surface heights over a set measurement length. Although Ra is desired to be relatively low – ranging from 0.15 – 0.50 µm in automotive cylinder bores, its significance is outweighed by the importance of the surface peak and surface valley values, as well as their respective material ratios. Ideally, it is desired to have the lowest possible surface peak (Rpk) values to reduce the chance for abrasive wear and oil contamination – 0.15 µm in most cylinder bores, as well as low surface peak material ratios (MR1), a combination of which would mean that the surface profile has very few and small protruding peaks that would negatively influence tribological performance. Additionally, large and narrow surface valleys are desired to promote a lubricated sliding surface. Surface valley (Rvk) values of 1.0 µm combined with large surface valley material ratios (MR2) would signify deep and frequent valleys in the surface that would subsequently enhance tribological performance through oil retention.

However, ideal tribological conditions may sometimes contradict other project deliverables – as in the case of cylinder bores. Enhancing oil retention through surface profile modification is a useful tool in improving friction and wear but can negatively affect the emission output of an engine. Too much oil retention within the cylinder walls of a combustion chamber may lead to oil getting trapped and burned during combustion. This event may lead to poor engine emissions characteristics due to increased hydrocarbon output. Therefore, determining ideal oil retention is a compromise between acceptable surface profile parameters and emissions control. A mathematical tool in evaluating oil retention, which could assist in estimating the range and specifying a tolerance on surface profile features is the oil retention equation, otherwise known as crevice volume, and is displayed in units of oil retention volume normalized with respect to a unit area ($\mu m^3/\mu m^2$).

$$Crevice\ Volume\ (CV) = \frac{(100\% - MR2) * Rvk}{200}$$

There are a few different methods that this project utilizes in modifying the surface profile of cylinder bores.

1. Firstly, utilizing a sandpaper polishing technique, although very rudimentary, provides the ability to reach very low average roughness values and subsequently relies heavily on the natural porosity of the PEO coating to maintain acceptable oil

retention values. However, this method provides poor bore dimensional control and straightness. Ultimately, this type of polishing was a preliminary method in surface profile modification with a major benefit of its use being low cost and tool availability.

2. The second technique utilized for surface profile modification was via the use of Flex-Honing brushes. These brushes are off-the-shelf tools available for purchase and intended for re-honing the surface of cylinder bores during complete engine overhauls. The wide array of different size honing brushes for various sized bores, combined with a range of different grit options provided a versatile option for striving to achieve a desired surface profile while maintaining a low cost factor. These Flex-Honing brushes provide the ability to maintain relatively good dimensional control and uniformity throughout each bore.
3. The third option available for modification of the surface profile is by professional honing services. Gehring Technologies GmBH is an industrial supplier of honing solutions and conducted honing services for an engine block used within this study. Professional honing services are the preferred solution for achieving optimal surface profile. However, the cost of conducting such honing trials is very expensive and therefore other options such as Flex-Honing are utilized for other engines in this study. Advanced equipment and techniques allow for extremely accurate surface finishes. The honing done by Gehring Technologies GmBH achieved extremely low surface peak values, in some cases reaching values as low as 0.11 µm while maintaining deep surface valleys for the purpose of oil retention, reaching upwards of 11.86 µm in depth. These surface profile values can be attributed to the tools and processing used which are not available outside of professional honing services. Diamond honing stones of various grits, lubrication, and processing controls allowed the PEO coated cylinder bores to reach ideal surface profiles while maintaining strict bore dimensions.

3.1.2. BORE SIZE

While achieving ideal surface profile, the required bore size must simultaneously be met as it is an important factor in piston-to-bore clearance distance. Ideal bore size is highly

dependent on sliding surface material, oil retention, as well as all the characteristics associated with a particular piston ring pack. Additionally, although it may be instinctive to associate bore size to be as close to piston gauge diameter as possible, this is however not the case. In certain situations, having large clearances between the piston and bore could reduce the amount of friction and wear by promoting greater hydrodynamic lubrication area which would be a positive outcome and therefore relying heavily on the effectiveness of the piston ring pack to maintain combustion chamber sealing and oil scraping capacity. Conversely, having clearances between the piston and bore that are too big could induce severe wear via piston slap on both major and minor thrust sides of the bore. Therefore an array of bore sizes and subsequently, piston to bore clearances must be thoroughly monitored and a bore size compromise must be made to accommodate both aspects of piston-to-bore sliding wear in order to determine ideal bore size for this particular application. However, production dimensions and tolerances could be used as a guideline in determining testing ranges. The production bore diameter for the 2.0L GTDI engine used in this study was 87.510 +/- 0.010 mm and piston-to-bore clearance allowance of 25 – 45 µm.

In this study, the test of bore tolerance or piston-to-bore clearance extended across the whole range of allowable dimensions ranging from combined clearances of as low as 12 µm to 49 µm, or 6 µm to 24.5 µm on each side, respectively.

3.1.3. PISTON RINGS

The piston ring pack is an immensely important factor in any piston assembly as it acts as the main sliding surface opposing the cylinder bore, and must therefore display good tribological properties. Countless different piston ring pack variations exist, ranging from different substrates, surface treatment techniques, shapes, and coatings. The engine testing conducted in order to evaluate and improve upon the wear resistance of PEO bore coatings heavily analyzed the effectiveness of different piston rings in order to define a set that would provide minimal wear and friction, optimal oil dispersion over the stroke of the bore, and combustion chamber sealing capacity. Various combinations of piston ring packs were used, modifying either some or all of the upper compression, lower compression, and oil

ring sets in each cylinder in order to assist in determining the ideal piston ring pack solution. Piston rings used varied from current production models to experimental samples.

Some of the piston rings utilized throughout engine testing were production rings that are available in current models of the production 2.0L GTDI I4 engine used in this study. These rings are optimized for performance against a cast iron cylinder liner which the production engine implements. Table 3 provides a summary of the production ring characteristics.

Table 3: Production Piston Ring - Characteristics

Piston Ring	Substrate	Overall Surface Treatment	Outer Diameter Surface Treatment
Upper Compression	Tempered Chromium Silicon Alloy Steel (SAE 9254)	Zinc Phosphate	Chromium Nitride PVD (IN14A)
Lower Compression	Carbon Steel (SAE 1060)	Zinc Phosphate	Zinc Phosphate
Oil Control	Stainless Steel (SAE 440B)	Nitriding	Nitriding
Oil Spacer	Stainless Steel (SAE 304)	Nitriding	Nitriding

The experimental rings and their respective characteristics that were utilized instead of the production rings within this study are summarized in Table 4.

Table 4: Experimental Piston Ring - Characteristics

Piston Ring	Substrate	Overall Surface Treatment
Upper Compression	Steel	Diamond-like Carbon

Lower Compression	Steel	Chrome Plated
Oil Rings	Steel	Diamond-like Carbon

An additional piston ring factor, which may vary depending on piston ring substrate and material composition is the piston ring gap, a schematic of which is displayed in Figure 31.

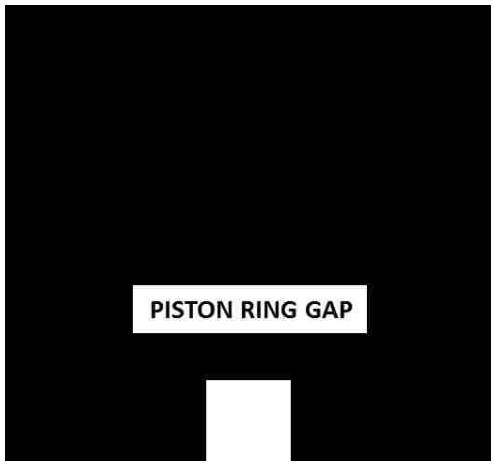

Figure 31: Piston Ring Gap Feature - Schematic

When the piston ring is compressed within a cylinder, this gap is considered to be a closed gap. The closed gap specifications are important to monitor so that to allow for sufficient area for thermal expansion during engine operation when the environment is subjected to increased temperatures. However, as with most engine components, a compromise has to be made. The closed gap distance cannot be made too large as it increases the likelihood of blow-by of combustion gases flowing past the rings and into the crankcase, which could ultimately reduce engine efficiency and performance – factors which need to be maximized in this study. On the other end of the spectrum, the piston ring gap cannot be made too small as it would then run the risk of insufficient room for thermal expansion. This type of scenario would lead to a piston ring which could no longer freely expand and then subsequently apply a greater normal force onto the cylinder walls, which would increase friction and wear, two factors that this study is aiming to minimize. For this reason, closed

ring gap specifications are closely monitored. The specifications used for experimental piston rings in this study as displayed in Table 5.

Table 5: Nippon Piston Ring Co. - Piston Ring Closed Gap Specifications for Cylinder Bore Size 75 - 89 mm

Piston Ring	Closed Gap Specifications [mm]	
	Minimum	Maximum
Upper Compression Ring	0.25	0.5
Lower Compression Ring	0.25	0.5
3 Piece Oil Ring Pack	0.25	1.00

3.1.4. COATING TYPE

It is important to note that electrolyte composition along with electrical process parameters that affect coating deposition and final PEO characteristics are not within the scope of this study. Modifying electrolyte and process parameters has the potential to change the morphology and physical characteristics of the coating which in turn could change the tribological effects. However, such an investigation is broad in its scope and greatly complex. For this reason, only two different PEO coating grades were utilized in this research, varying only through the alloying elements in their respective electrolyte compositions. An SEM image for each type of coating, showing their different morphologies is provided in Figure 32 and Figure 33.

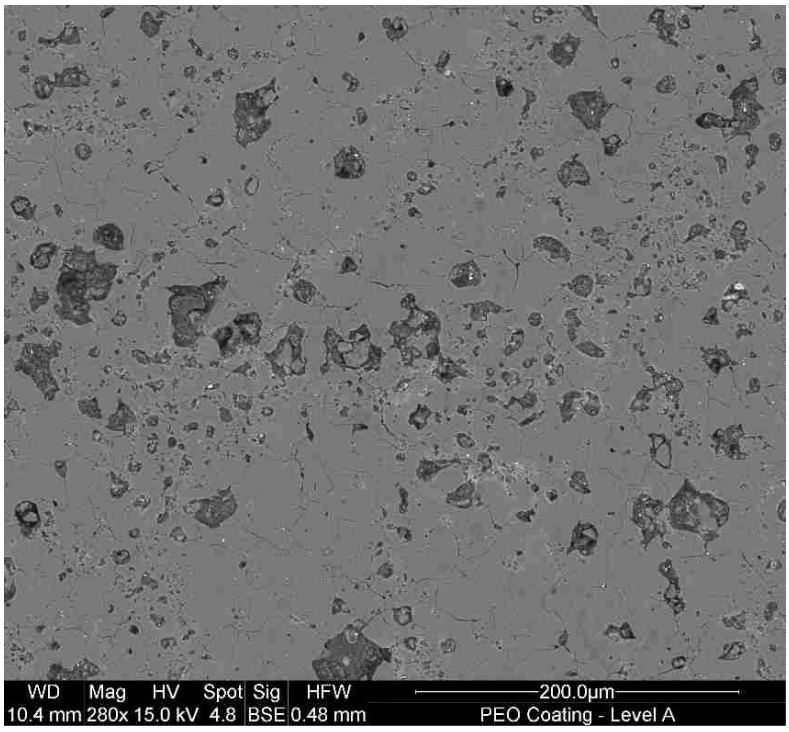

Figure 32: PEO Coating - Type A – Morphology – Top Surface View

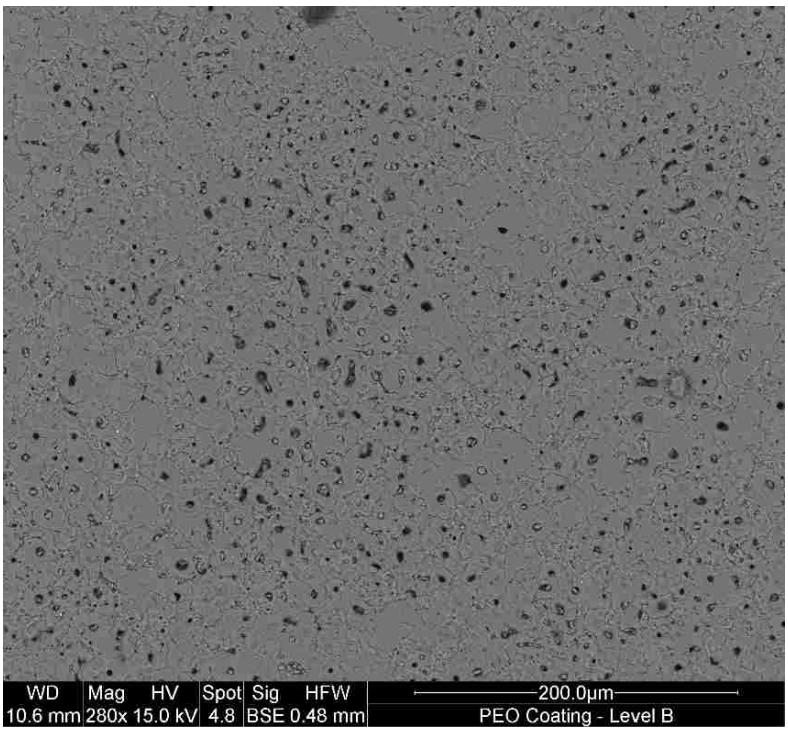

Figure 33: PEO Coating - Type B – Morphology – Top Surface View

CHAPTER 4

4. EXPERIMENTAL PROCEDURE

Beginning with a linerless A356 aluminum cylinder block from a 2.0L GTDI I4 engine, the bores were unprocessed and still fully exposing the aluminum substrate. The aluminum substrate possessed the mechanical properties shown in Table 6.

Table 6: A356 Mechanical Properties [37]

Mechanical Property	Value	Unit
Tensile Strength	230	MPa
Yield Strength	185	MPa
Elongation	3	%
Modulus of Elasticity	71	MPa
Brinell Hardness	75	BHN

The initial step was to precisely determine the bore size prior to any surface modification or processing being completed on the cylinder bores. The bore sizes were measured using a Coordinate Measuring Machine (CMM) or bore gauge, depending on the time and resource availability.

4.1. PRE-TREATMENT

The application of any coating, PEO in particular, requires the application surface to be as close to the desired final profile as possible as the coating would follow the contours and physical features on the surface to which it is being applied. This is especially true for thin coatings such as PEO as there would not be a lot of material for corrective surface processing if it was to be required after coating deposition. For this reason, it is necessary to conduct a pre-treatment on the aluminum substrate surface exposed in the bores and achieve a relatively smooth surface profile, removing and checking for casting defects along the way. For PEO application within cylinder bores, a substrate surface profile average roughness of 0.3 µm is targeted. In addition to the targeted substrate surface profile, the required bore dimensions and straightness needed to be simultaneously

achieved. Utilizing the initial bore dimensions gathered from the unprocessed cylinder block, a determination for bore dimensions had to be made for each stage of the process, including material removal during pre-treatment, material additional during coating deposition, material removal during final surface treatment, and ideal final bore size.

Pre-treatment material removal was conducted by utilizing Flex Honing brushes and aimed at achieving a desired surface profile along with a bore size that would allow attaining the ideal final bore size. To accomplish this, the ideal final bore size must be known. This type of hypothesis could be made from an informed decision based on data and analysis from an iterative methodology approach. A schematic portraying bore processing and its effect on bore diameter is displayed in Figure 34.

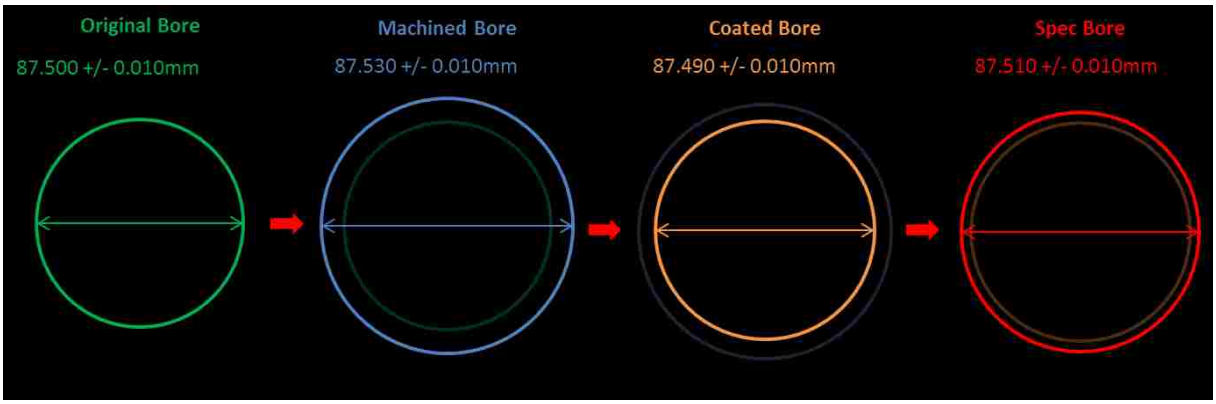

Figure 34: Cylinder Bore Processing Procedure Prior to Engine Trial

4.2. PEO COATING DEPOSITION

Deposition of PEO coating would follow once the pre-treatment surface profile and bore dimensions had been met. The deposition method for PEO coatings in cylinder bores is applied differently to conventional PEO coating deposition methods that may be used for smaller parts, such as for tribological testing or corrosion prevention. Cylinder bore geometry prevents the cylinder block from being submerged in a tank of electrolyte to coat the bores as it would require a substantially inefficient amount of electrolyte and risk coating other undesired areas of the cylinder block as sealing the undesired areas from the solution would be extremely difficult. This could also greatly affect current density and consequently, coating properties. For this reason, a method of localizing the deposition of

PEO coating to the cylinder bores exists and is utilized in this study – a spray head, as show in Figure 35.

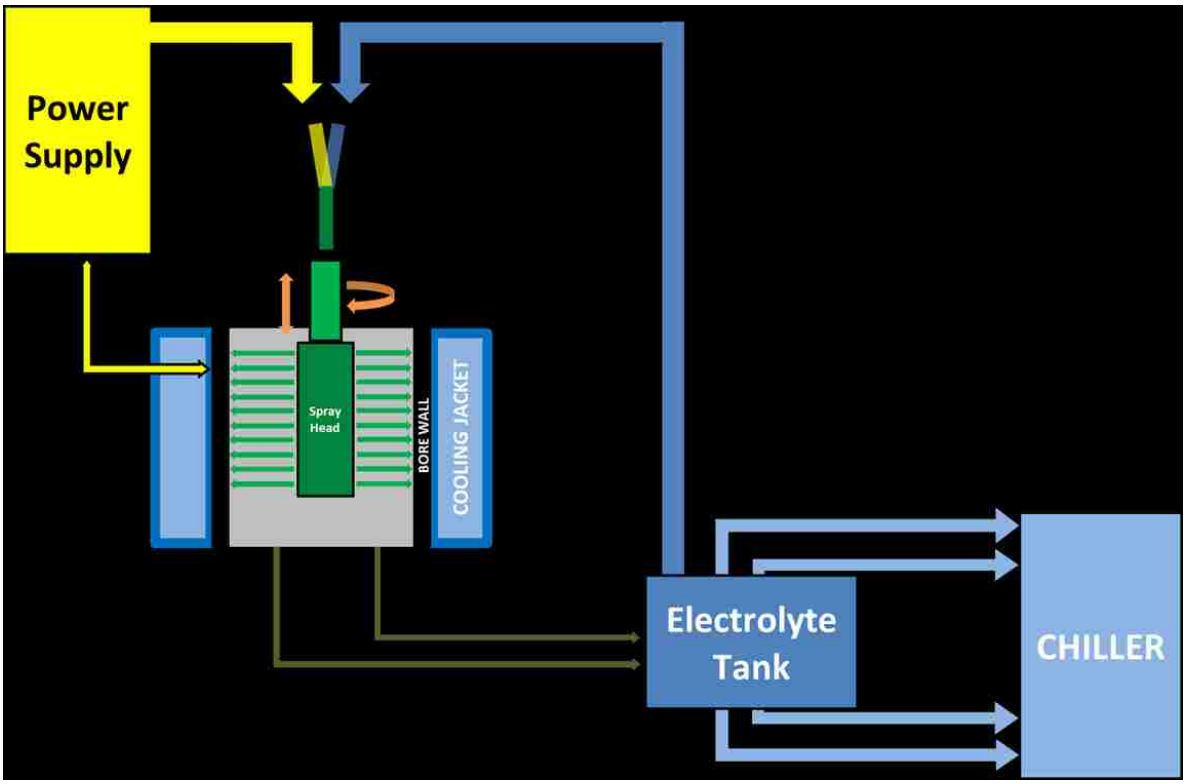

Figure 35: PEO Cylinder Bore Coating System - Schematic

With two degrees of freedom, the spray head mechanism can move along and rotate about the z-axis, allowing the spray head to be inserted in the bore and rotate at a constant rate of about 4 rpm in order to maintain a uniform coating thickness throughout the bore. To maintain the proper current density of 0.0016 A/mm^2, the electrolyte is discharged onto two narrow regions opposite each other, rather than the whole circumference of the bore. This type of deposition process is limited by the available power output from the 7 kW pulse power supply and current density required to achieve the desired PEO properties. PEO coating deposition via spray head would continue in each individual bore until the desired coating thickness was reached. Target coating thickness varied between 20 – 25 µm, depending on how much material removal was desired to achieve a target surface profile for the particular test iteration. Coating thickness was measured using a thickness gauge.

4.3. FINAL SURFACE PROFILE MODIFICATION

Depending on the final surface profile treatment method utilized, various surface profiles were achieved. However, the procedure to achieve the target surface profile remained constant. Whether through the use of sandpaper polishing, Flex-honing brushes, or professional honing equipment, various grit tools were used. Beginning with a low grit tool to remove large surface peaks and create a foundation for surface valleys for the purpose of oil retention, this level of grit was used cautiously so as to not remove a significant amount of material and risk ending up in an undesired region of the PEO coating such as the interfacial region, or end up with a bore size that was bigger than the target diameter. Throughout the polishing or honing process, the bore diameter would rigorously be checked with a profilometer to monitor the surface profile change and a bore gauge to note the amount of material removal.

The process would continue through each level of grit tools with constant profilometric and bore gauge evaluations to monitor the progress and help in achieving target values for surface profile and bore size. The highest level of grit available for sandpaper and Flex-Honing brushes was 1200 grit and 800 grit, respectively. Ultimately, the limiting factor for this type of procedure is material removal. The priority for this processing method was to achieve the targeted bore dimensions and straightness. This study utilized the full range of bore dimensions that were within safe mechanical operating tolerances for the particular engine being employed throughout all testing iterations.

The cylinder block with coated PEO cylinder bores would be evaluated once more in detail through profilometry, CMM or bore gauge, and thickness gauge to get final values prior to engine assembly.

4.4. ENGINE ASSEMBLY

A few production 2014 2.0L GTDI I4 engines were used as spare parts engines for this study. All the parts would be disassembled off of the production engine and reassembled onto the prepared cylinder block with PEO coated bores, essentially performing a swap of the cylinder block out of the production engine. Although a majority of the engine

components were able to be reused for reassembly off of the production spare parts engine, several parts required for assembly had to be new, such as:

- Cylinder head gasket
- Cylinder head bolts
- Rear crankcase seal
- Oil galley plugs

For consecutive tests which utilized the same production spare parts engine components, a full inspection of parts would be conducted to ensure that there was no wear that would negatively affect or influence performance and results of the following test iteration. If all parts determined to have minimal or normal wear, several other components would need to be replaced in addition to the standard set for complete engine reassembly. These parts include:

- Pistons
- Piston rings
- Oil sump pickup

Once the spare parts engine was disassembled, a couple parameters had to be measured and recorded since their role in the engine could have an effect on the performance of the PEO coating package. The pistons from the disassembled engine would be measured for diameter via an outside micrometer in order to determine exact clearance between piston and bore in each cylinder. In addition to determining exact piston-to-bore clearance, the piston and bore diameter information would allow to rearrange the pistons in specific bores to meet certain testing specifications for clearance set out for that particular test iteration.

Along with piston diameter measurements, piston ring gaps would also be measured via feeler gauges to determine the amount of expansion which is available for each piston ring and verify that they are within the specification set out by the manufacturer. The same measurements would be conducted again after completion of the test.

4.5. DYNAMOMETER

The intended purpose for the PEO coated bore package is for implementation within an internal combustion engine. Although bench tests are important for the evaluation of the coating under very specific conditions intended to replicate certain events in the engine cycle, there is no substitute for the extreme environment of dynamometer testing. Dynamometer testing provides the ability to replicate a full range of engine operation while maintaining full control of the system and providing the capability to rigorously monitor countless parameters to assist in evaluation of the coating and its effects on engine performance.

Dynamometer testing allows the coating package to be subjected to the extreme conditions of the engine cycle including high velocity sliding, piston slap, extreme temperatures, and high pressures. Exposing the coating package to this type of testing provides valuable wear results, and has the potential to allow for the study of the coating package effects on engine performance, emissions, and fuel economy.

However, prior to being able to complete the most rigorous of dynamometer tests which current production engines may be exposed to, such an experimental engine with PEO coated cylinder bores must be evaluated very carefully and its rate and type of wear must be analyzed, especially when dealing with an extremely thin coating thickness. For this reason, a standardized break-in test was utilized in order to conduct preliminary evaluations on coating wear and engine performance – 18 hour non-boosted break-in as pictured in Figure 36.

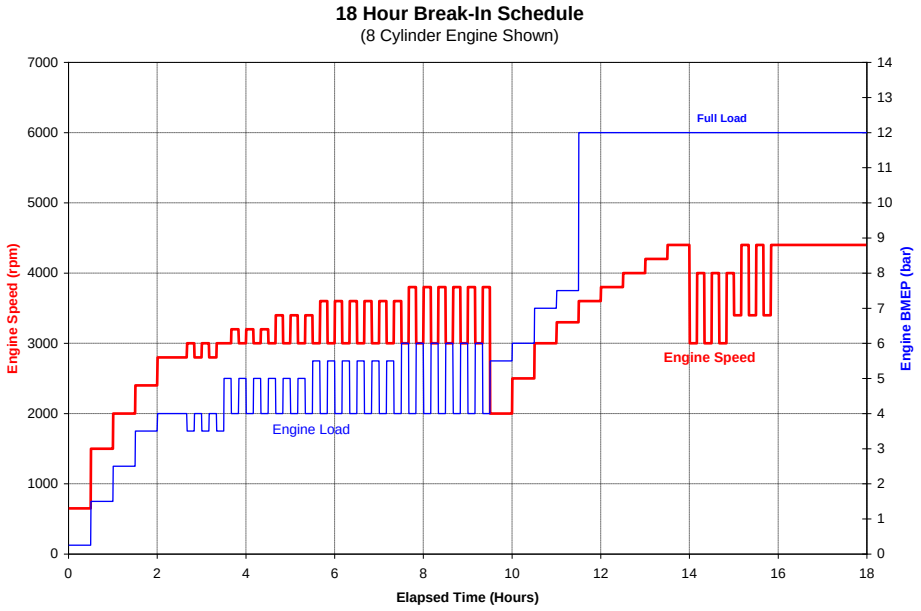

Figure 36: Dynamometer 18 Hour Break-In Curve

Break-in curves are designed to allow for a gradual run-in of all engine components subject to sliding wear. Break-in periods of an engine are subject to the highest wear rates due to all the tribological environments creating a natural wear pattern in their opposing sliding surfaces allowing for a more fluid integration of parts. A particular area of interest during a break-in period is the combustion chamber as the piston ring pack and cylinder bore are coupled to create a natural wear pattern and break-off any surface peaks off of their respective surface profiles. This type of running-in is usually followed by increased engine performance as the combustion chamber is able to withhold more pressure and provides greater stability throughout the engine as the engine components are uniquely seated to each other. It is important not to over-stress the engine during the period, before all the components are seated to each other, therefore the most extreme temperatures and pressures that the engine is designed to reach are usually avoided until the break-in curve is completed. For this reason, engines with forced induction components such as turbochargers, such as in the case of the 2.0L GTDI I4 engines used in this study, are carefully controlled in order to limit the amount of pressure and temperature in the combustion chamber during this dynamometer curve.

Although the main purpose of this preliminary dynamometer testing of PEO coated cylinder bores is to evaluate wear and coating durability, there are particular engine parameters that can provide real-time data and assist in analyzing the effect of the PEO coating package on engine performance along with real-time analysis of wear. It is important to note that the changes in values for the parameters in question, which assist in evaluating various aspects of PEO coated cylinder walls, require extremely precise measurement tools as some of the values may change in very small intervals.

- **Crankcase Pressure (mmH_2O)**: Sealing of the combustion chamber is a critical component of maintaining engine efficiency and power. Having the piston ring pack sealing the chamber, distributing and collecting the oil off of the cylinder walls helps achieve the most desirable tribological lubrication regimes throughout the stroke of the bore. The crankcase pressure can be a dynamic indication of the sealing conditions of the piston rings to the cylinder walls. If the crankcase pressure begins to increase beyond what is normally expected, this could be a sign that the cylinder wall or piston rings have been worn down creating gaps between the sliding surfaces, allowing for the exhaust gases to blow by past the rings and into the crankcase. The amount of crankcase pressure increase could allow for the determination of severity of the wear between the piston ring and cylinder wall sliding surfaces.
- **Fuel Flow/Power (lb/HP·Hr)**: Fuel consumption is an important factor and one of the main driving forces behind the application of PEO coatings in internal combustion engines. Therefore, monitoring fuel consumption is critical for the evaluation of this type of coating. The quantity and rate of fuel used can provide an indication of coating performance. Normalizing fuel flow with respect to power output displays the amount of mixture that was required to achieve those horsepower levels. Utilizing PEO coated cylinder walls has the potential to reduce friction and subsequently energy loss, leading to the theory that less fuel would be required to reach the same power values. Ideally, lower values are desired to display that engine operation has become more efficient when compared to production engines that had run similar dynamometer curves.

- **Coolant Out (˚F)**: Extracting heat out of the cylinder block is a critical factor for continued engine operation. The temperature of the coolant that has made a pass through the network of coolant channels throughout the engine is a helpful diagnostic tool for determining engine health but can also assist in evaluating the effect of PEO coated cylinder walls during engine operation. PEO coatings have very high thermal resistance and therefore create an effective thermal barrier. When applied onto cylinder bores, PEO coatings have the potential to provide better insulation inside the combustion chamber, maintaining more heat and subsequently energy within the bore walls. With more heat being transmitted into mechanical energy, the cooling system should theoretically have to withdraw less heat from the engine leading to the assumption that the coolant out temperature should be lower than a production engine that had run a similar dynamometer curve. Monitoring this temperature parameter can display the effectiveness of the PEO coating as a thermal barrier in the combustion chamber.

Throughout the dynamometer testing, it was important to closely monitor the performance of such a development engine. The real-time data such as crankcase pressure, coolant temperature, and fuel flow provided some degree of evaluation of the coating. However, a more in-depth analysis was required to track coating performance and durability throughout the dynamometer testing. For this reason, the test was paused at set intervals in order to conduct a borescope analysis, compression, leak-down, and blow-by tests. The combined results from these tests would give a relatively clear indication how the coating was standing up to the test conditions as well as determine whether the test may safely proceed or was required to be terminated due to the risk of damaging parts.

4.5.1. DYNAMOMETER CHECKS

An 18 hour dynamometer test would be paused at 4.5 hours, 9.5 hours, 13.5 hours, and 18 hours. While the test was paused, all dynamometer checks except borescope visual inspection would have to be conducted while the engine still retained most of the heat which was produced by friction and combustion. This was done to get the most accurate representation of engine health through the compression, leak-down, and blow-by tests, as

all engine components would still have been thermally expanded and closely represented actual engine operating conditions.

4.5.1.1. COMPRESSION TEST

A compression test is a standard test to determine how much air is being compressed within the combustion chamber. The values determined by this test would give an indication if piston rings were seated properly or if there was significant wear on the cylinder bore surfaces. High compression numbers are always good as they represent a good seal of the combustion chamber which would transfer to greater efficiency and performance of the engine due to less energy loss. However, the target compression values vary in each engine and are dependent on the compression ratio. Therefore is it necessary to know through engine specifications which values represent ideal compression. In the case of 2.0L GTDI I4 engines used in this study, compression values of over 200 psi were desired. The compression test was conducted in each cylinder individually. The ignition system of the engine would be disengaged and the spark plug would be removed. An air hose would be inserted into the cylinder through the spark plug hole, connecting it to a pressure gauge. The engine crankshaft would then be spun by the dynamometer at 360 rpm until a stable compression reading was able to be recorded off of the pressure gauge. This process was repeated for each cylinder individually.

4.5.1.2. LEAK-DOWN TEST

A leak-down test is a static engine test designed to determine the exact percentage of air being retained in the combustion chamber. For this test, each cylinder is done individually. The piston in the cylinder that is being tested is brought up to top dead center (TDC) position to ensure that both the intake and exhaust values are fully closed. An air hose is inserted into the threaded hole, replacing the spark plug. Compressed air at a known pressure is fed into the combustion chamber while a pressure gauge simultaneously takes pressure readings.

$$Leakdown\ \% = 1 - \frac{Cylinder\ Chamber\ Pressure}{Shop\ Air\ Pressure}$$

Leak-down from the combustion chamber can occur through many different components in an engine, especially for an engine that has seen heavy use or experienced part failures. Air pressure leakage could possibly occur through the following:

- Intake and exhaust value seats
- Piston rings
- Ruptured cylinder head gasket

If a significant pressure leak does exist, it can be narrowed down through sound. Listening to passing air through various engine orifices allows to determine the path from which the pressure is leaking. However, for the purposes of this study, all leakage was assumed to have occurred through the piston rings. This assumption was confidently made because all components that could have caused a pressure leak were new and only exposed to relatively mild engine operation conditions. The break-in dynamometer test was designed to only evaluate the PEO coating package and therefore all the engine components including the valves, valve seats, and gaskets were well within their usage life and specifications.

4.5.1.3. BLOW-BY TEST

A blow-by test can be considered as a dynamic version of a leak-down test. This type of test can be conducted at different engine speeds and loads to determine the amount of air passing through the piston rings in units of cubic feet per minute (CFM). Blow-by test results cannot be narrowed down to evaluate dynamic conditions of each cylinder individually, as the test measures passing air through the crankcase and therefore measures the accumulative combustion pressure passing through all the piston ring packs together. The test is conducted at various engine operating levels to determine the piston ring pack sealing performance under an array of conditions. This type of analysis provides a greater understanding of combustion chamber sealing performance due to piston rings or cylinder bore walls and therefore allows to make more informed decisions and analysis of piston ring or coating conditions. The blow-by tests conducted in this study were done at the following speeds and loads:

- 1500 RPM at 76 ft·lb
- 1500 RPM at 30 ft·lb

- 3000 RPM at 0 inHg of manifold intake pressure

The ignition for a blow-by test is enabled and the engine functions normally with the exception of all orifices which could release crankcase pressure being blocked or replaced with a gauge to measure passing crankcase air flow.

4.5.1.4. BORESCOPE

The final evaluation completed at each interval is a visual inspection of the combustion chamber done by a borescope. Each cylinder is evaluated and visually inspected by first turning over the engine until the piston is at bottom dead center (BDC) for the cylinder in question. This piston position allows inspections of the entire stroke of the bore including the compressed volume and swept volume regions. Furthermore, the versatility of the borescope allows for the visual inspection of the piston crown, valves, and valve seats. The most critical borescope inspection done in this study is examining the bore walls. Visual inspection of the bore walls allows monitoring of any wear or general surface condition. Additionally, it is possible to note whether the aluminum substrate of the cylinder block is exposed in the cylinder due to excessive wear.

The combined results from these dynamometer checks and visual inspections provided reasonable indication of the condition of the PEO coating package in the engine throughout dynamometer testing. Moreover, the evolution of these values throughout the test at the designated intervals can show a valuable trend of information. This trend can indicate a general wear rate of the coating.

Table 7: Equipment Specifications

Equipment	Name	Model	Resolution
CMM	Zeiss	UMESS	0.1 µm
Bore Gauge	Fowler	Xtender	0.0005 in
Thickness Gauge	PosiTector 6000	NRS1	0.5 µm
Profilometer	Mitutoyo	SJ-210	0.01 µm
Outside Micrometer	Starrett	75 – 100 mm	1 µm

Borescope	Medit	Rigel	0.5 Megapixel
Pressure Gauge	Snap-On	-	2 psi

4.6. TEARDOWN ANALYSIS

Although the periodic dynamometer tests provide a reasonable evaluation of coating durability, a full teardown after test failure or completion is necessary to investigate the wear mechanisms or reasons for failure. There are many components that affect the PEO coating package which cannot be evaluated during testing through the dynamometer checks. Some of these measurements include:

- **Bore dimensional changes**: repeating bore measurements by CMM or bore gauge to have a complete set of "before" and "after" values may indicate wear severity throughout the stroke of the bore or determine the amount of material removed through wear in all regions of the bore, both of which are important factors in determining wear rate of the PEO coating package.
- **Surface profiles at TDC, mid-stroke, and BDC**: since the piston travels at different speeds at various regions in the bore, there are many tribological variations through the stroke due to changing lubrication regimes. With some lubrication regimes known to be more demanding on the sliding surfaces, the evaluation of the surface profile in these different lubrication regimes can assist in improving durability by isolating worst case tribological conditions and their effect on the coating surface. Moreover, by comparing the surface profiles before and after dynamometer tests, it is possible to study the evolution of the surface profile and the effects the whole system has on the sliding surface including their changing surface features and oil retention capabilities. The oil retention variation can have a significant influence on the understanding of PEO coatings in these types of applications and assist in improving on further iterations of the coating or parts of the system as a whole to promote more desired lubrication regimes.
- **Surface profiles on major and minor thrust sides**: as with varying piston speeds having an influence on severity of wear, normal forces to the bore walls also have an influence. The normal forces are taken into account within a function of the

Stribeck curve (Figure 3) to determine in which lubrication regime a certain system falls. Normal forces change significantly against a cylinder bore on the major and minor thrust sides due to the combustion event. The combustion event causes the piston to rock and impart greater forces on one side of the cylinder wall, depending on the direction of rotation, via the piston rings and piston skirt. These thrust sides, with the major thrust side in particular, are considered to be the worst case tribological conditions in cylinder bores as they experience the most severe normal forces and wear.

- **Severe wear at TDC**: The worst region for friction and wear of the Stribeck curve is the boundary lubrication regime. This regime is created when opposing sliding surface asperities contact each other due to a minimized layer of lubrication. This deficiency of lubrication could be caused by an increase in normal forces or reduced sliding speed. Although an operating engine has very high piston sliding speeds, the sliding speeds still have a momentary velocity of 0 m/s at TDC and BDC, and very slow sliding speeds in the regions of deceleration and acceleration of the piston before TDC and BDC. Although the area of these boundary lubrication regimes within the bore is relatively small, they still present a limiting factor for the implementation of the PEO coating application package. Friction and wear increase greatly in this narrow region. The effect of boundary lubrication in the areas surrounding TDC and BDC, including the TDC and BDC points themselves, can be evaluated through profilometry. By measuring the profile surrounding and over the point where the upper compression ring reaches its highest point in the stroke, which is usually distinguishable by the change in wear pattern between the swept volume and compression volume, the amount of surface wear can be determined in the form of surface height variation and comparing it to a surface area which has experienced no sliding wear and that has only been exposed to the combustion event

– the compression volume. The profilometric setup for measuring surface profile at TDC is shown in Figure 37.

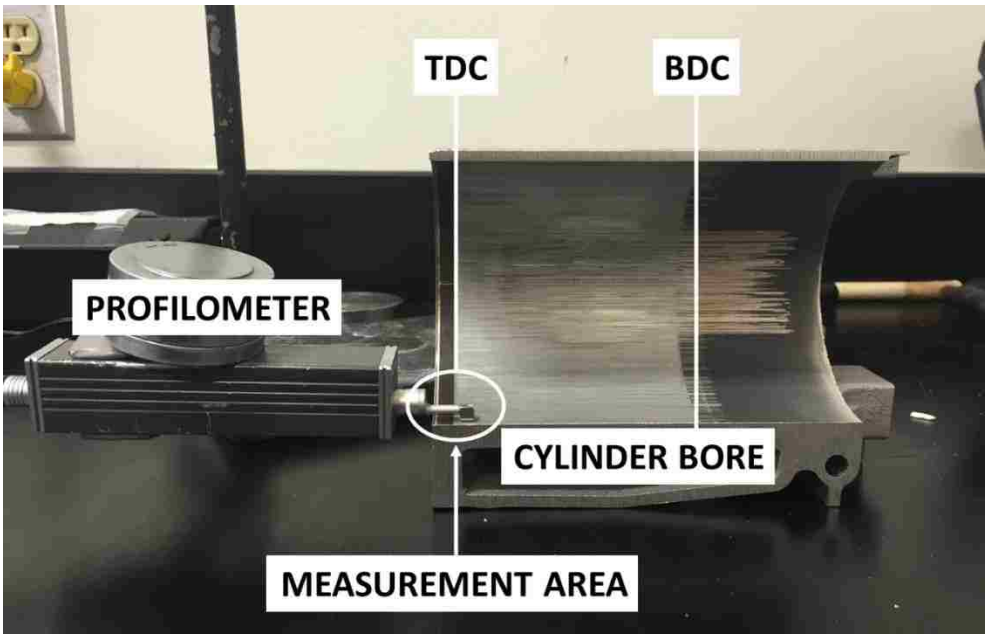

Figure 37: Measurement of Depression via Wear at TDC - Setup

- **Coating thickness**: Tribological properties change with varying surface conditions, including surface profile and coating morphology. PEO coatings have varying morphology throughout their entire thickness and in each of their outer, inner, and interfacial regions. The changing morphology has an effect on friction and wear performance, therefore it is important to note and understand which PEO region is exposed to the sliding surfaces. When PEO coatings are applied within a cylinder bore, the dense inner region is initially exposed as it had been shown to possess the most favorable wear properties, as shown through bench tests and literature review [3]. However, during engine operation the coating thickness changes as it is slowly worn and the piston rings are seated to the bore walls. The evaluation of coating thickness after test completion is important in order to determine the rate of wear for the PEO coating. Moreover, measurements of PEO coating in different areas of the bore such as at the top, middle, and bottom of the piston stroke can reveal different wear rates and therefore coating thicknesses. This array of coating thickness measurements can display different trends of wear

through the bore and assist in analyzing and determining limiting factors of the PEO coating package.

- **Piston sizes changes**: As with wear on the PEO coated cylinder bores, piston skirts also have a surface treatment for enhanced tribological performance and improved scuffing resistance that are subject to wear. The pistons used in this study had piston skirts coated with a graphite based coating to act as a solid lubricant. With the given trade name of Nanofriks-1, this graphite coating was applied on each skirt until a thickness between 7 µm and 17 µm was reached. Measuring the piston diameters allowed analyzing the piston deformation or piston skirt coating wear to determine the effect of the PEO coating package on one of the sliding surfaces opposite to the bore walls.
- **Piston skirt wear**: With the clearance between piston and bore being measured in microns, the space between the two components still allows for the piston to rotate about the wrist pin causing the piston skirt to impact the bore walls creating a phenomenon known as piston slap. The impact and sliding forces acting on this piston skirt during moments of piston slap could have detrimental effects on piston skirts in the form of severe wear through scuffing or polishing off of the piston skirt coating. A compromise between all the components in the piston assembly and bore wall coating properties must be met in order to mitigate piston skirt wear and preserve the anti-wear and friction reduction of the piston skirt coating.
- **Piston ring wear**: A sliding surface opposite the bore wall which is in constant contact at various pressures and sliding velocities throughout the entire stroke of the bore and covering the entire circumferences is the piston ring. This range of tribological characteristics makes piston ring wear a critical point for analysis and a major limiting factor in the progression of the PEO coating package. From the many material choice combinations available for piston ring packs including different substrates and surface treatments, a compromise must be met between durability, friction reduction, sealing capabilities, and wear resistance to the opposing PEO sliding surface. Piston ring wear can be analyzed through SEM microscopy and compared to baseline production piston rings or untested rings with the same characteristics. Points of interest in the analysis of piston rings would be

looking at surface features of tested piston rings and comparing them to their untested counterparts. Additionally, it is possible to look at the scratch marks engraved on the surface and to notice their depth, size, and regularity.

- **Material transfer between piston ring and the PEO cylinder bore coating**: The resistance to wear for the opposing sliding surface of piston rings is an important consideration when choosing piston ring properties through various substrate and surface treatment combinations. Therefore, evaluation of piston ring wear resistance to PEO is necessary. This evaluation can be done in the form of analysis of material transfer. Through the use of SEM and EDS, it is possible to visually determine the quantity of material transfer as well as material composition, respectively. The type of material which has been transferred onto the surface of the piston rings could consist of oxidized PEO coating or aluminum substrate. The quantity of each material transferred would assist in evaluating the level of wear experienced on the sliding interface during the test.
- **Visual evaluation of bore walls**: The simplest type of analysis that may be conducted after a test is a visual analysis. There are many different parameters to observe on the bore walls at a macro and micro level.

  At the macro level, discoloration can be seen and noted throughout the stroke of the bore which could signify different levels of coating thicknesses. The PEO coating layers have varying morphology which causes the layers to exhibit a different color. Wear patterns such as scuffing or galling can be seen on the bore walls, as well as any exposed aluminum substrate material.

  A micro level evaluation of the PEO coated bore walls would require sectioning of the cylinder block. If sectioning of the cylinder block was completed, it would be possible to look at the surface of the walls at a high enough magnification to determine which level of layer the coating is in, or if there is any coating remaining on a scuffed section of a bore. The determination of coating layer or overall existence of coating could be seen by detecting discharge channels or platelet morphology features that are common to PEO coatings. Additionally, a cross-sectional analysis would enable the exact thickness of the remaining coating to be

determined in that section, if any did still exist. Moreover, the horizontal surface profile would be able to be seen and evaluated, especially if significant scuffing and wear had occurred, a type of profilometric analysis that a profilometer could struggle with due to the large curvature in the section owing to the cylinder bore shape.

The description of various positions in the cylinder bores cited in teardown analysis data and pictures is displayed in Figure 38.

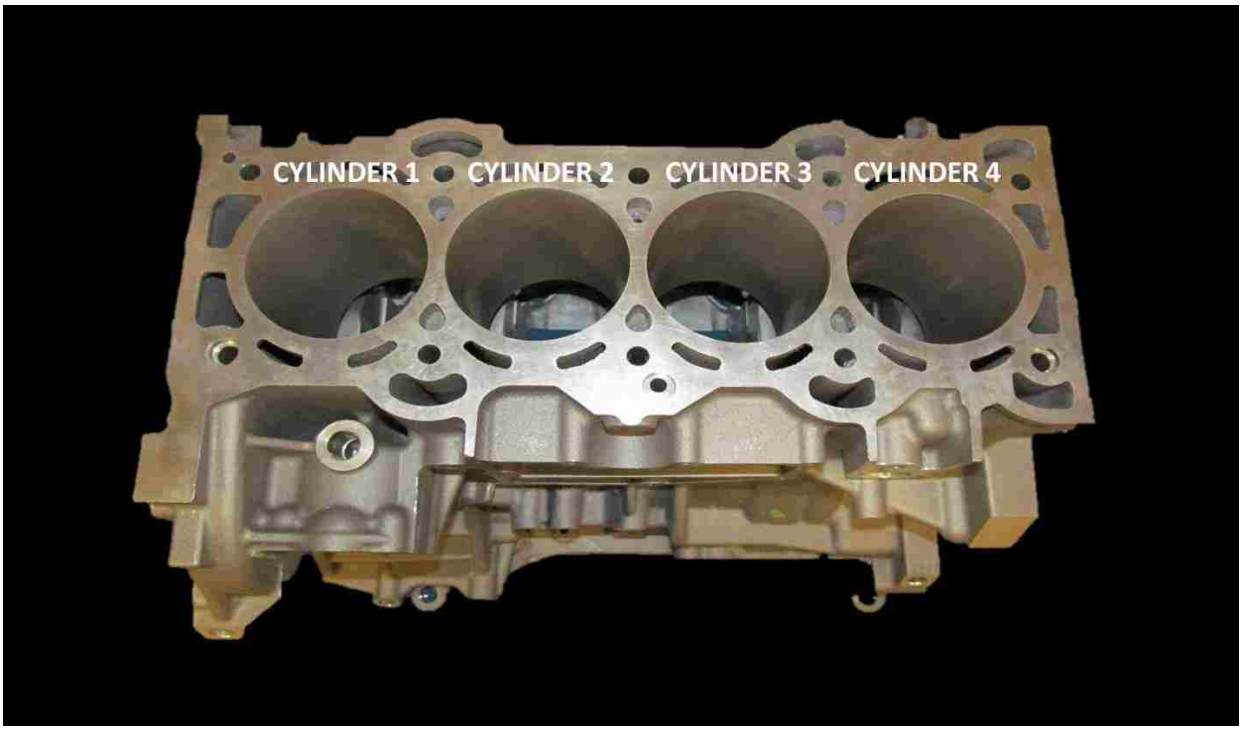

Figure 38: Cylinder Bore - Measurement Location Terminology

The combination of results from a detailed teardown analysis is able to provide the necessary information required to further improve the durability of the PEO coating or emphasize a weak point in the system that could be modified for the following test iteration of the study.

CHAPER 5

5. EXPERIMENTAL RESULTS

A series of engines with PEO coated cylinder bores were tested with varying parameters that directly influence the performance of the coating in terms of friction and wear. This section discusses the outcome of those tests, measurements taken, and analysis that was conducted on the respective engines. The data gathered from tests was used in order to make changes to parameters for the following test iteration. The trial and error process was conducted for four 2.0L GTDI I4 engine blocks produced by Nemak and made for the Ford Motor Company. The test goals were to continuously improve upon the wear resistance of PEO coatings through reduced wear during dynamometer testing.

5.1. TRIAL 1 – ENGINE 2599

The first cylinder block tested had parameters aimed at staying within known production engine specifications. Additionally, with being the first test iteration of this study, the influence of many parameters were unknown and therefore this test strived to highlight areas of concern and factors that would limit PEO coating durability. Additionally, the procedures used were preliminary. However, the procedural knowledge gained through this engine trial were of significant importance and helped in achieving more effective testing, measuring, and analyzing methods for future test iterations. All engine components were transferred from an unused production 2.0L GTDI engine.

5.1.1. PRE-TEST PARAMETER SELECTION

The following section describes the controlling parameters chosen for engine trial 1 with engine block 2599.

5.1.1.1. SURFACE PROFILE

The cylinder bores of labeled engine number 2599 were coated with PEO process parameters that produced coating type A. The large discharge channels were assumed to increase oil retention volume and create more desirable lubricated tribological conditions throughout the stroke of the bore by separating surface asperities of the opposing sliding

surfaces. This increase in oil retention volume was especially desired considering the surface processing techniques that were going to be used were not going to leave any cross-hatch markings as seen on production cylinder liners or other surface treated cylinder bores for additional oil retention volume and control. The surface processing technique used for the bores in this engine trial was the sandpaper polishing method. Figure 39 provides the surface profile values for the cylinder block bores used in engine trial 1.

Stroke Length: 4mm													
Cylinder No.	Position	Variable											
		Ra (µm)			Rpk (µm)			Rvk (µm)			Oil Retention Volume (µm^3/ µm^2)		
		Top	Middle	Bottom	Top	Middle	Bottom	Top	Middle	Bottom	Top	Middle	Bottom
1	Back	1.14	0.73	0.69	0.39	0.36	0.60	2.68	1.26	1.69	0.21	0.08	0.13
	Left	0.55	1.19	0.67	0.25	0.22	0.35	1.16	4.76	1.57	0.09	0.36	0.11
2	Back	0.86	0.70	0.59	0.54	0.46	0.40	2.60	1.72	1.56	0.26	0.14	0.14
	Left	0.81	1.04	0.65	0.30	0.45	0.28	2.53	2.62	2.34	0.19	0.29	0.20
3	Back	1.11	0.89	0.69	0.46	0.48	0.33	3.60	1.73	1.75	0.38	0.12	0.12
	Left	0.84	1.09	0.47	0.37	0.31	0.28	3.45	1.99	1.83	0.26	0.18	0.16
4	Back	0.89	0.77	0.81	0.76	0.34	0.61	2.94	1.43	2.01	0.24	0.10	0.23
	Left	0.77	0.96	0.56	0.39	0.16	0.40	1.50	2.39	2.20	0.10	0.25	0.18

Figure 39: Dynamometer 1 - Engine 2599 - Surface Profile Values – Before Dynamometer

5.1.1.2. BORE DIAMETER, COATING THICKNESS, & CLEARANCE

The surface processing technique aimed at achieving a surface profile with Ra, Rvk, and Rpk values of 0.5 µm, 1 µm, and 0.3 µm, respectively. However, in order to achieve targeted coating thickness and bore diameter simultaneously, the surface profile values had to be compromised. For that reason, some surface profile measurements exceeded or did not meet the targeted values. The target bore diameter for this engine trial was to be on the lowest end of the tolerance specifications set out for a 2.0L GTDI engine which allowed for anywhere between 87.500 – 87.520 mm. Table 8 summarizes the average diameter, coating type, and coating thickness of each bore in engine trial 1. Additionally, Figure 40 graphically displays bore straightness of engine trial 1.

Table 8: Dynamometer 1 - Engine 2599 - Diameter, Coating Type, and Coating Thickness

Cylinder	1	2	3	4
Avg. Diameter (mm) - CMM	87.505	87.504	87.503	87.502
Coating Type	Type A	Type A	Type A	Type A
Coating Thickness (µm)	5-10	5-10	5-10	5-10

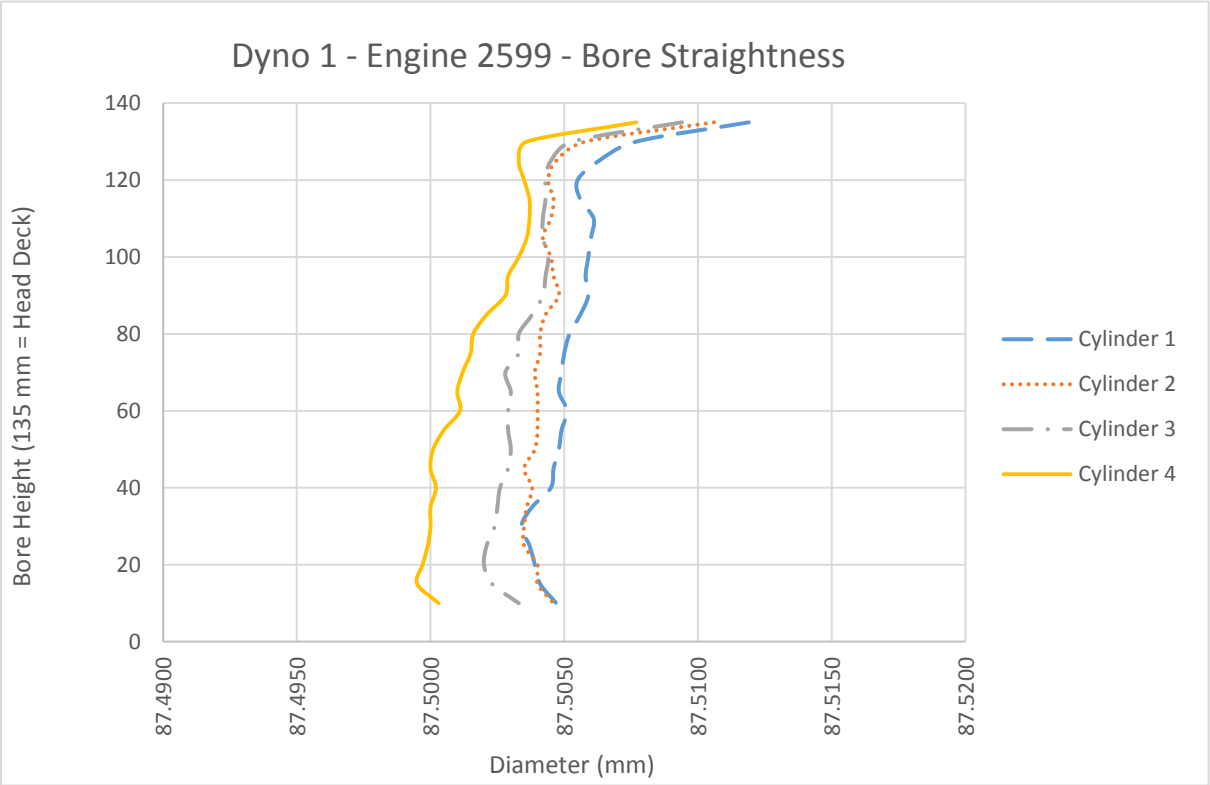

Figure 40: Dynamometer 1 - Engine 2599 - Bore Straightness - Before Dynamometer Test

The lowest end of the bore diameter tolerance was chosen for the intention of deterring two possible issues. Firstly, with a large bore clearance between piston and cylinder wall, there is an increased chance of piston slap which could have a detrimental effect on the piston skirt and PEO coating. By reducing the bore clearance, it was thought that the piston would have less ability to rock about its wrist pin and impact the bore walls on the major and minor thrust sides after the combustion event. Secondly, the sealing capacity of the

combustion chamber was a concern. With no honing cross-hatching marks and oil retention volume limited to the natural porosity in the PEO coating topography, maintaining piston ring pressure against the cylinder walls was assumed to be necessary to be able to sustain a dynamic seal and prevent a large amount of combustion gases blowing-by the piston ring pack into the crankcase, as that would have decreased engine performance by reducing efficiency and counteracted any possible parasitic loss reductions that the PEO coating package could have presented.

The piston diameters were not measured, but their diameter and tolerances were available from released drawings - 87.4800 +/- 0.0075 mm. A stack-up was performed to determine range of clearances available in each bore as shown in Table 9.

Table 9: Dynamometer 1 - Engine 2599 - Clearance Stack-Up

Total Clearance - Both sides (mm)	Cylinder	1	2	3	4
	Minimum	0.0159	0.0160	0.0145	0.0120
	Maximum	0.0394	0.0381	0.0369	0.0352

5.1.1.3. PISTON RINGS

Piston rings for this engine trial were the standard rings for a production 2.0L GTDI engine as displayed in Table 10.

Table 10: Dynamometer 1 - Engine 2599 - Piston Ring Selection

Piston Ring	Substrate	Overall Surface Treatment	Outer Diameter Surface Treatment
Upper Compression	Tempered Chromium Silicon Alloy Steel (SAE 9254)	Zinc Phosphate	Chromium Nitride PVD (IN14A)

Lower Compression	Carbon Steel (SAE 1060)	Zinc Phosphate	Zinc Phosphate
Oil Control	Stainless Steel (SAE 440B)	Nitriding	Nitriding
Oil Spacer	Stainless Steel (SAE 304)	Nitriding	Nitriding

5.1.2. DYNAMOMETER TEST

The following section describes the dynamometer test results for engine trial 1 of engine block 2599. The procedure for this dynamometer test varied from other tests conducted as this was the first PEO coated block of the engine trial series to be tested and the experimental procedure for this phase of the trial was still being developed and enhanced based off the experience and results obtained from such a preliminary test.

5.1.2.1. DYNAMOMETER CHECKS

5.1.2.1.1. 0 TEST HOURS

This low clearance engine setup produced very high leak-down and blow-by results throughout the test, much greater than the standard engine warning values of 15% and 0.5 CFM, respectively. Consequently, the compression test values for each cylinder were much lower than the target pressure of 200 psi as shown in Figure 43 Regardless of the poor dynamometer check values at the start of the test, the test was still conducted to evaluate coated bore wear.

From the beginning of the test, the engine experienced high crankcase pressures caused by the significant blow-by around the piston ring pack. Ideal crankcase gauge pressure is below 0 mmH_20, which would signify there would be no resistance to piston motion by pressure as well as no significant blow-by of combustion gases. Unfortunately, crankcase pressure for this test reached values as high as 43 mmH_2O therefore reducing engine efficiency, as shown in Figure 41.

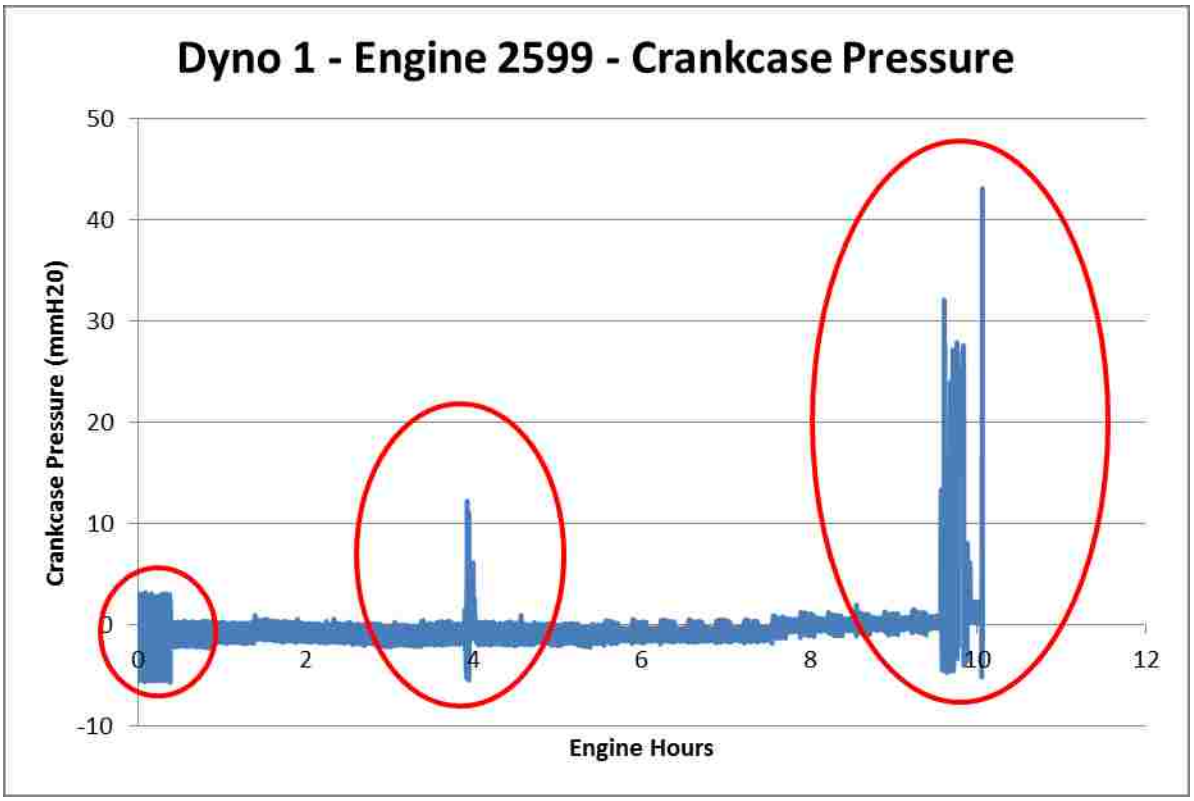

Figure 41: Dynamometer 1 - Engine 2599 - Crankcase Pressure vs. Engine Hours

5.1.2.1.2. 9.5 TEST HOURS

The dynamometer checks were repeated once more at 9.5 engine test hours. Unfortunately, the dynamometer check values did not improve over the first half of the break-in curve as is usually the case with an engine since the parts get seated to their respective sliding surfaces and create better dynamic seals and wear tracks.

Through a borescope visual inspection, severe wear was noticeable on the bore walls of each cylinder as seen in Figure 42. Although some PEO coating was still visible, distinguishable by its dark color and surface porosity, the majority of the surface had been worn down to expose the aluminum substrate of the cylinder block which was noted by its silver and extremely reflective surface. Furthermore, the wear had been uneven and left visible ridges in the direction of piston travel, emphasized on the major and minor thrust sides, leading to the assumption of piston skirt scuffing and abrasive wear through debris in the circulating oil. An oil change at this stage confirmed the significant oil contamination determined through discoloration in the oil by having a silver-metallic shade rather than

the opaque black shade expected of oil at that stage in engine life. Although an oil analysis was not conducted, it was assumed a majority of the oil contamination came from the worn high hardness PEO coating, further expediting the wear on the bore walls.

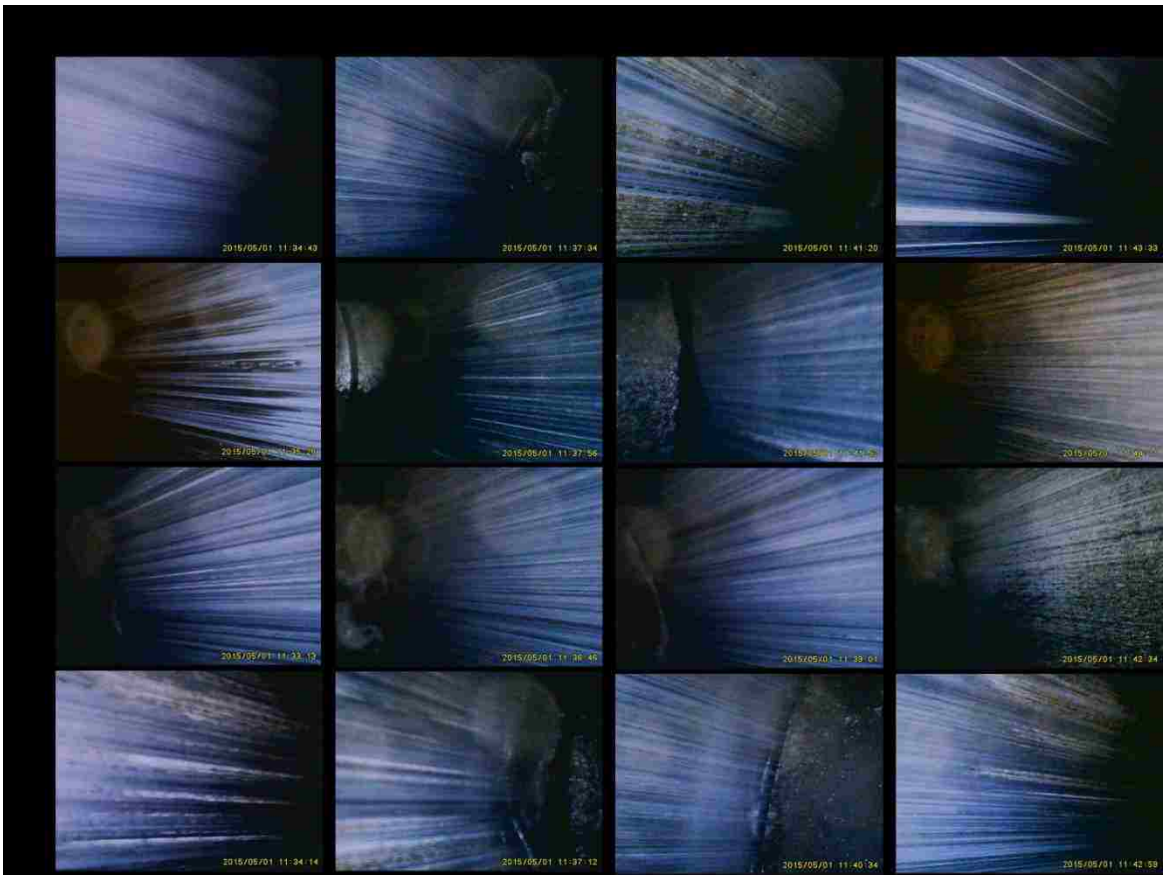

Figure 42: Dynamometer 1 - Engine 2599 - Borescope - 9.5 Test Hours

Following completion of dynamometer checks and oil change, the engine was put back to running the test. However, shortly after resuming the test, the engine experienced severe vibrations so the test was stopped. Thus, the engine did not complete the full 18 hour dynamometer curve and was stopped at 9.54 engine test hours, at which point it was disassembled to investigate the cause of failure.

Cylinder	Test Type	Test Hours		UNITS
		0	9.5	
1	Compression	191	190	PSI
	Leakdown	27	30	%
2	Compression	185	189	PSI
	Leakdown	40	29	%
3	Compression	180	189	PSI
	Leakdown	38	25	%
4	Compression	198	194	PSI
	Leakdown	17	30	%
Blow-by	1500 rpm @ 76 ft lb	2.16	2.54	CFM
	1500 rpm @ 30 ft lb	N/A	N/A	CFM
	3000 rpm @ 0 inHg ManVac	N/A	N/A	CFM

Figure 43: Dynamometer 1 - Engine 2599 - Dynamometer Check Results

5.1.3. TEARDOWN ANALYSIS

The following section discusses the investigation into the failure mode of PEO coating engine trial 1 of cylinder block 2599. An array of measurements were taken along with visual, microscopic, and elemental analysis to assist in determining a limiting factor in the one of the controlling parameters chosen for the engine setup. A macroscopic visual display of the bore wear is visible in Figure 44.

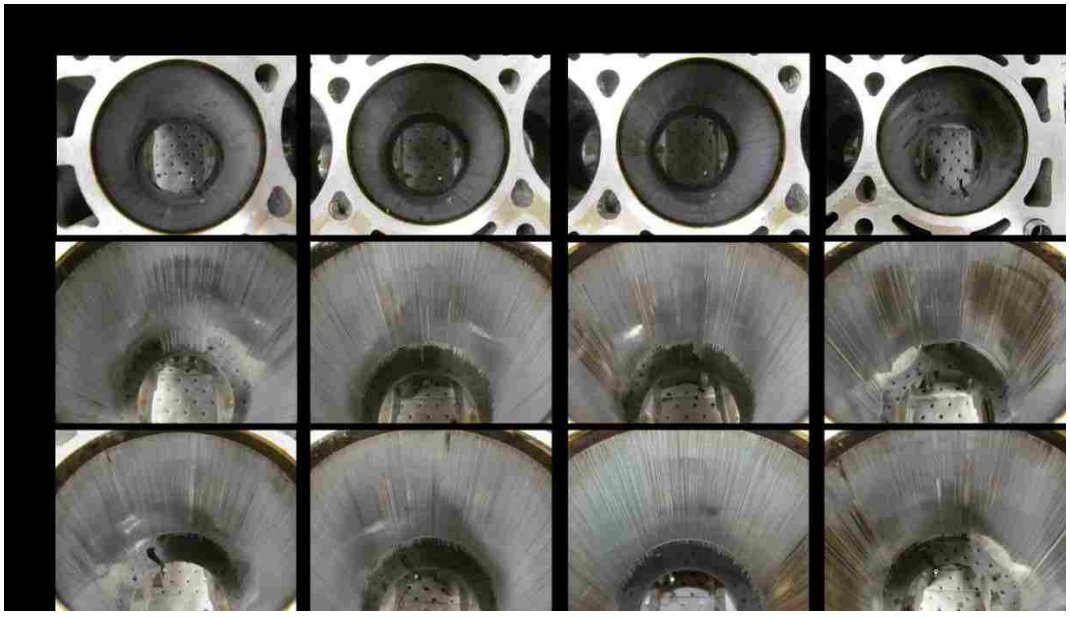

Figure 44: Dynamometer 1 - Engine 2599 - Teardown - Cylinders

5.1.3.1. SURFACE WEAR

The bore wall was investigated for coating material, surface profile, and surface depression by wear. The profile over TDC was studied to determine the amount of depression experienced through sinking-in while in a boundary lubrication region. The top point of upper compression ring travel caused a significant depression in the bore walls, noticeable in all of the cylinders, reaching values greater than 50 µm depression below the compression volume coated surface that was used as a datum. Profilometry curves for each measurement taken can be found in Appendix A and their maximum depression values are presented in Table 11.

Table 11: Dynamometer 1 - Engine 2599 - Maximum Values of Surface Depression via Wear at TDC

Dynamometer 1 (Engine 2599) – Maximum Depression by Wear at TDC [µm]				
Location	**Cylinder 1**	**Cylinder 2**	**Cylinder 3**	**Cylinder 4**
Front	25	30	35	25
Right	20	N/A	25	20
Back	30	N/A	50	35
Left	35	N/A	25	45

The severely worn surface was analyzed by SEM to investigate whether any PEO coating remained even if not macroscopically visible, as the interfacial region could have still existed without being immediately noticeable. Cross-sectional analysis in the direction of piston travel revealed no visible PEO coating layers remaining in the stroke volume of the cylinder as would have been noticeable by a change in color from the aluminum substrate to PEO coating such as is visible in a cross-sectional coating thickness analysis taken in the area of compression volume seen in Figure 45. This PEO coating was confirmed to be completely worn away via EDS point analysis of the surface, noted particularly by the lack of oxidized elements as represented in Figure 47, compared to an EDS point analysis of existing coating in the compression volume as shown in Figure 46.

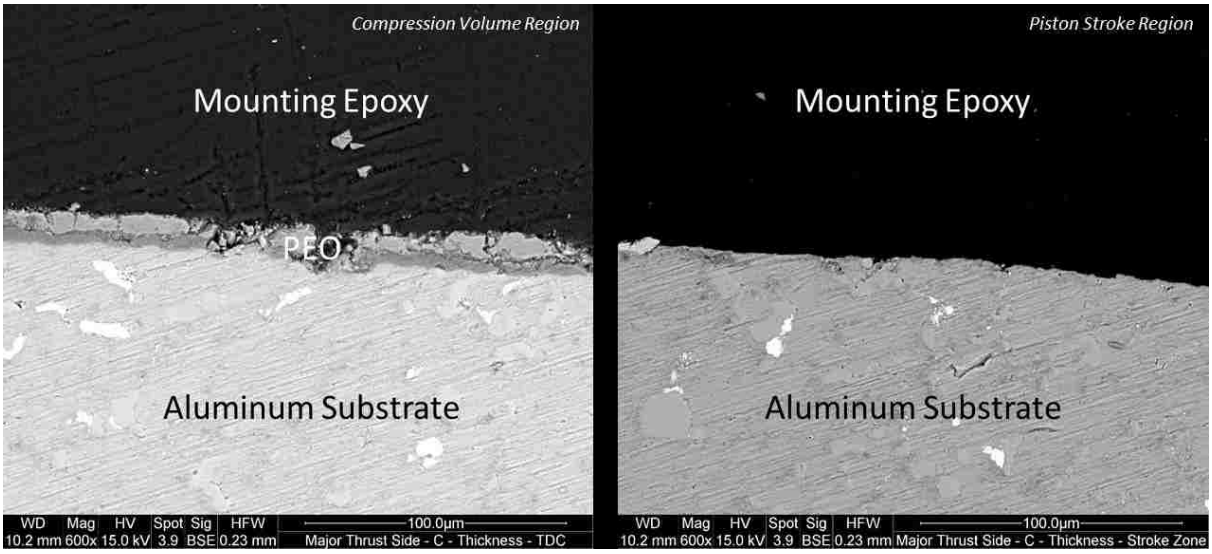

Figure 45: Longitudinal Cross-Section - Cylinder 2 - Compression Volume Region vs. Piston Stroke Region - Coating Thickness

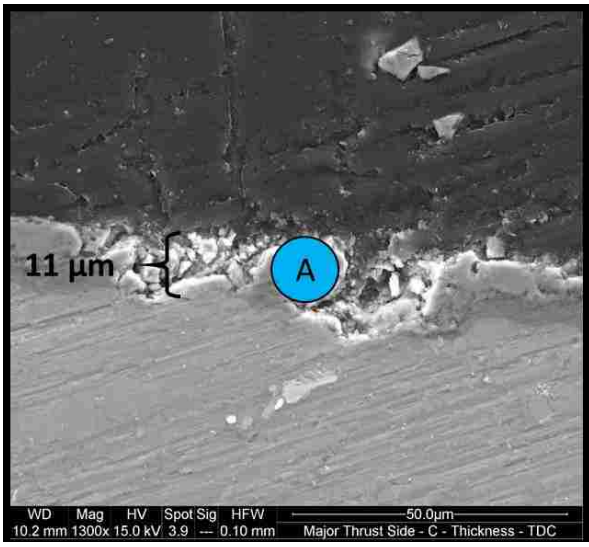

Element	Weight %	Atomic %	Error %
O K	46.49	59.47	6.82
AlK	51.44	39.02	3.29
SiK	2.06	1.50	11.12

Figure 46: Cylinder 2 - Compression Volume - Coating Thickness - EDS Point Analysis

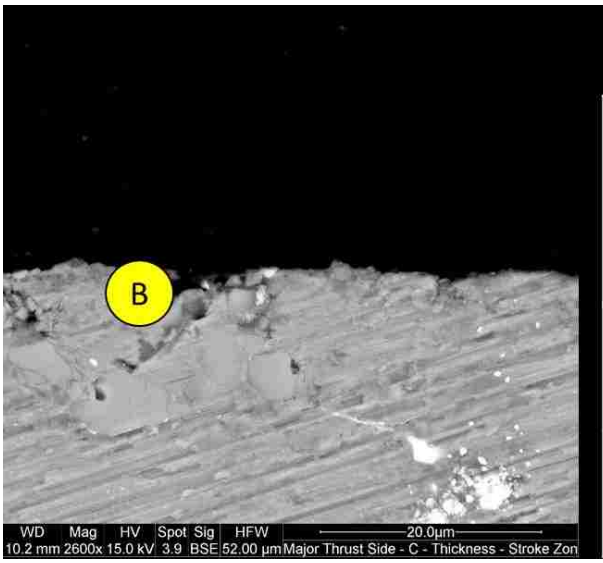

Element	Weight %	Atomic %	Error %
AlK	2.44	2.54	4.12
SiK	97.56	97.46	1.73

Figure 47: Cylinder 2 - Piston Stroke Volume - Coating Thickness - EDS Point Analysis

Surface profile measurement was completed by sectioning the cylinder block and mounting a cross-sectional sample to investigate the depth and width of ridges formed by the piston ring pack and piston skirt sliding surfaces during dynamometer testing. A SEM analysis of such a sample pictured in Figure 48 revealed a rough surface profile transverse to piston travel with variations in height from peak to valley as large as 13.6 µm.

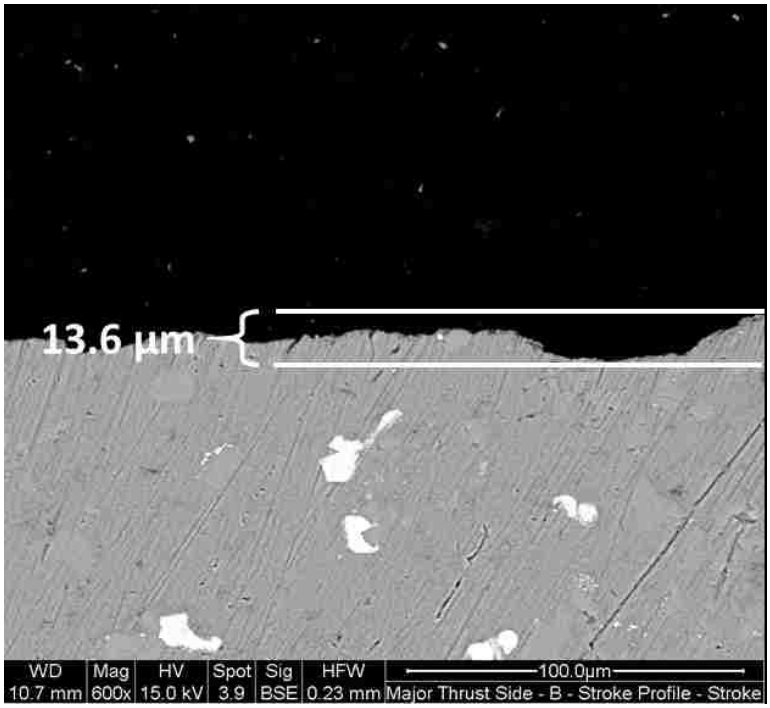

Figure 48: Cylinder 2 - Horizontal Cross-Section - Stroke Profile

Visual inspection of the piston skirts revealed severe scuffing on the major thrust sides of the pistons as shown in Figure 49. The scuffing completely wore off the graphite-based Nanofriks1 coating leaving large scoring marks in the direction of piston travel. The galling that had occurred on the major thrust side of the piston skirts could have accelerated wear of the bore walls by aggressively ploughing the sliding interface causing surface profile changes in the form of scratches and through contamination of the oil.

Although the major thrust side piston skirts experienced the most severe scuffing as shown in Figure 49, there was still detrimental wear that had occurred on the minor thrust sides as is visible in Figure 50. The polishing off of the piston skirt coating was beginning to occur as is visible on the bottom of the minor thrust side piston skirts. This type of wear does not normally occur in standard production engines, especially at such an early period in engine operation of only 9.54 test hours.

Figure 49: Dynamometer 1 - Engine 2599 – Teardown - Piston Skirts - Major Thrust Side

Figure 50: Dynamometer 1 - Engine 2599 – Teardown - Piston Skirts - Minor Thrust Side

5.1.3.2. PISTON RINGS

Significant material transfer from the bore walls to the piston rings was noticeable, especially on the upper compression rings and visible in Figure 51. Through EDS point analysis it was noted that the transferred material onto the upper compression rings

contained a large weight percentage of aluminum and oxide elements, leading to the conclusion that the transferred material was the aluminum substrate.

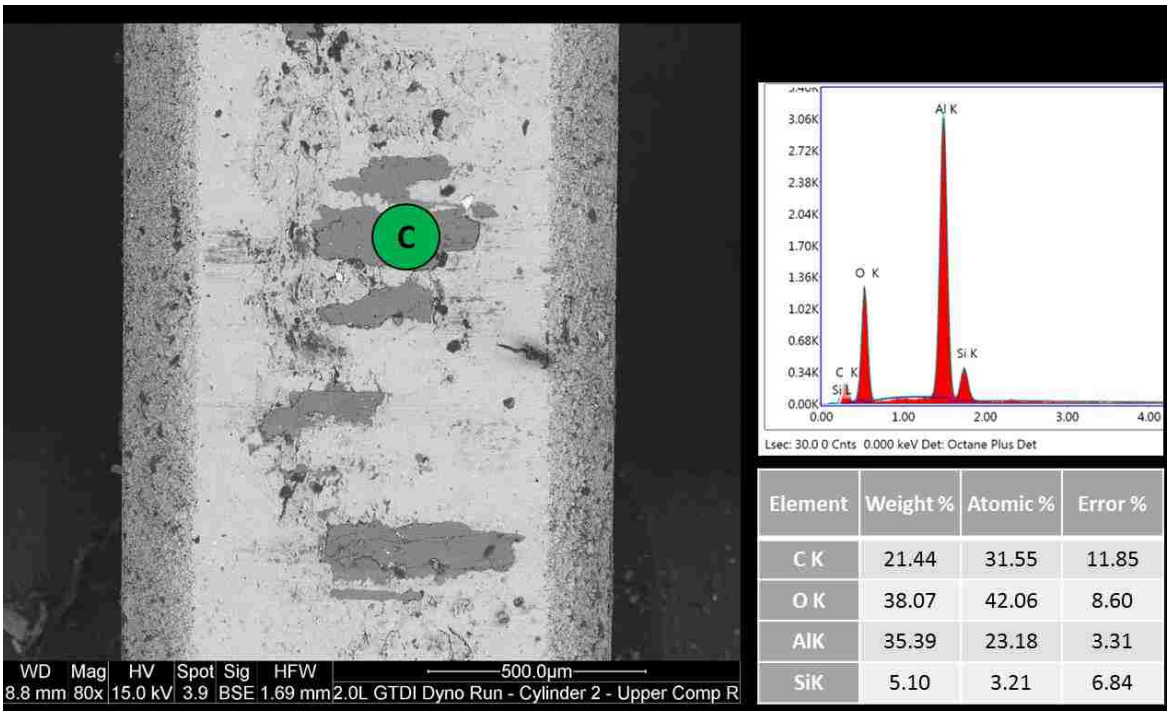

Element	Weight %	Atomic %	Error %
C K	21.44	31.55	11.85
O K	38.07	42.06	8.60
AlK	35.39	23.18	3.31
SiK	5.10	3.21	6.84

Figure 51: Cylinder 2 - Upper Compression Ring - SEM & EDS

Similar analysis was conducted on the lower compression rings which displayed comparable results seen in Figure 52. Although less quantity of material transfer was noticed on the outer diameter piston ring surface, the elemental composition of the transferred material contained significant weight percentages of aluminum and oxide meaning aluminum substrate was the transferred material.

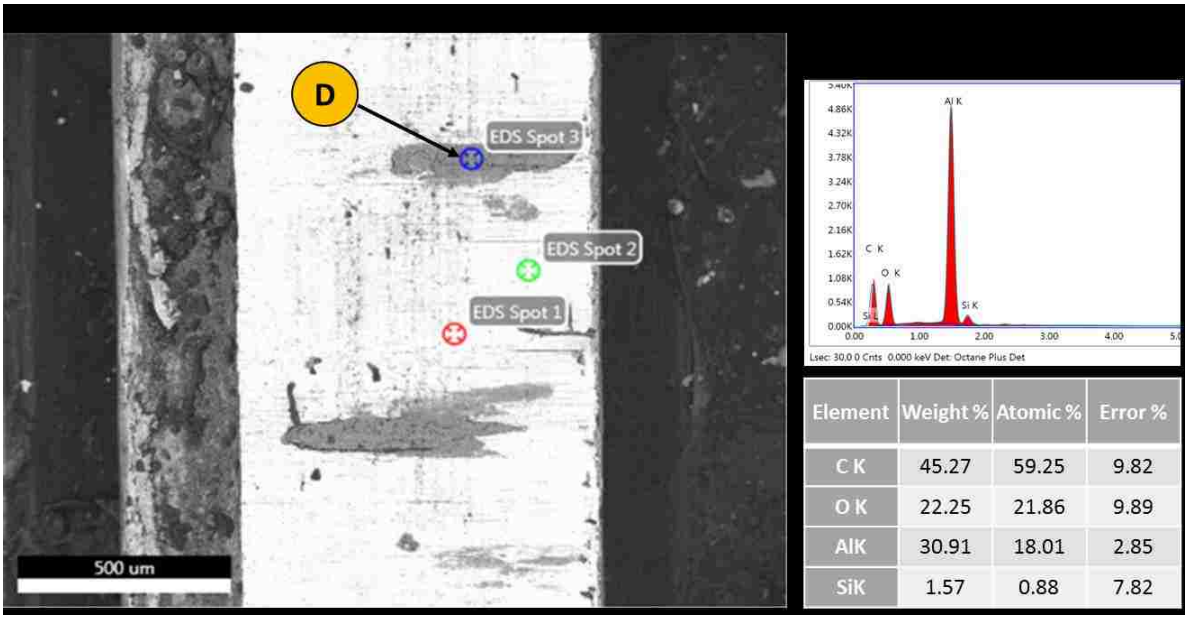

Element	Weight %	Atomic %	Error %
C K	45.27	59.25	9.82
O K	22.25	21.86	9.89
AlK	30.91	18.01	2.85
SiK	1.57	0.88	7.82

Figure 52: Cylinder 2 - Lower Compression Ring - SEM & EDS

5.2. TRIAL 2 – ENGINE 2633

Many of the controlling parameters in the second engine trial were modified to be outside of their specification range, significant resource investment was made into surface profile modifications, non-production parts were utilized, and the cylinders were not all coated the same. All engine components were transferred from an unused production 2.0L GTDI engine.

5.2.1. PRE-TEST PARAMETER SELECTION

The following section describes the reasoning and controlling parameter selection for the second engine used in the PEO coating study.

5.2.1.1. SURFACE PROFILE

The ideal surface profile with values below 0.3 µm, and 0.5 µm for Rpk and Ra, respectively, were targeted. Large Rvk values above 1 µm were also targeted to achieve sufficient oil retention without requiring cross-hatch honing marks. Extremely low surface peaks combined with large oil valleys all while maintaining straightness is very difficult to achieve and can only be done through professional surface profile modification methods. For this engine trial, professional honing surfaces from Gehring Technologies GmBH were

engaged to prepare the coated surface profile for fired-engine testing. This task was also experimental for Gehring Technologies GmBH and required significant time investment to determine the proper procedures and tools necessary to reach the target surface profile values. The honing methods utilized by Gehring are outside the scope of this study and will not be discussed. The subsequent surface profiles did not reach exact target values but came extremely close as seen in Figure 53, resulting in a high oil retention and preferred surface profile, one that otherwise would not have been able to be achieved through the manual polishing or Flex-Honing options available.

Stroke Length: 8mm													
Cylinder No.	Position	Variable											
		Ra (micron)			Rpk (micron)			Rvk (micron)			Oil Retention Volume (µm^3/µm^2)		
		Top	Middle	Bottom	Top	Middle	Bottom	Top	Middle	Bottom	Top	Middle	Bottom
1	Back	1.29	0.60	1.11	3.24	0.15	0.17	7.25	1.95	2.82	0.87	0.30	0.37
	Left	1.58	0.55	1.96	1.41	0.25	0.69	11.15	1.87	3.85	0.89	0.27	0.29
2	Back	1.68	1.62	0.57	0.70	0.52	0.16	4.61	3.69	1.99	0.67	0.54	0.30
	Left	2.17	1.45	1.54	4.54	0.54	0.19	5.98	2.32	4.53	0.72	0.12	0.77
3	Back	0.97	1.17	1.25	0.33	0.27	0.13	3.32	3.27	4.68	0.51	0.44	0.70
	Left	1.84	1.83	1.42	1.34	0.36	0.33	11.86	6.75	4.04	1.36	0.98	0.59
4	Back	0.63	0.55	0.61	0.45	0.18	0.11	2.24	1.70	1.89	0.27	0.22	0.24
	Left	0.62	0.64	0.85	0.19	0.08	0.21	2.07	1.95	2.22	0.25	0.25	0.30

Figure 53: Dynamometer 2 - Engine 2633 - Surface Profile Values – Before Dynamometer

5.2.1.2. BORE DIAMETER, COATING THICKNESS, & CLEARANCE

The bore diameter was able to be precisely controlled due to the professional honing services that were utilized and the equipment at their disposal. The target bore diameter was to be relatively large and to rely more on the piston ring pack for dynamic combustion sealing. With a production specification range of 87.500 – 87.520 mm, the target bore diameter for this test iteration was 87.530 mm. The aim was to combine the test results from high bore diameter and low bore diameter from the previous test iteration to be able to narrow down on the optimal bore size for non-crosshatched PEO coated bores. The priority for the professional honing services conducted was to achieve optimal surface profile. For this reason, once cylinder 4 reached the maximum benefits for surface profile from the surface processing, it was left at a smaller bore size than targeted. It is important to note this same cylinder block had been PEO coated before, had the coating stripped by

Flex Honing brushes and re-coated before being professionally honed in preparation for fired-engine testing. This reworking of the block could have attributed to the subsequent bore size variation in cylinder 4 when compared to the rest of the cylinders. A summary of average diameter, coating type, and coating thickness for each bore in engine trial 2 is provided in Table 12 along with a visual representation of bore straightness shown in Figure 54.

Table 12: Dynamometer 2 - Engine 2633 - Diameter, Coating Type, and Coating Thickness

Cylinder	1	2	3	4
Avg. Diameter (mm) - CMM	87.530	87.530	87.529	87.509
Coating Type	Type B	Type B	Type A	Type A
Coating Thickness (µm)	10-12	10-12	10-12	10-12

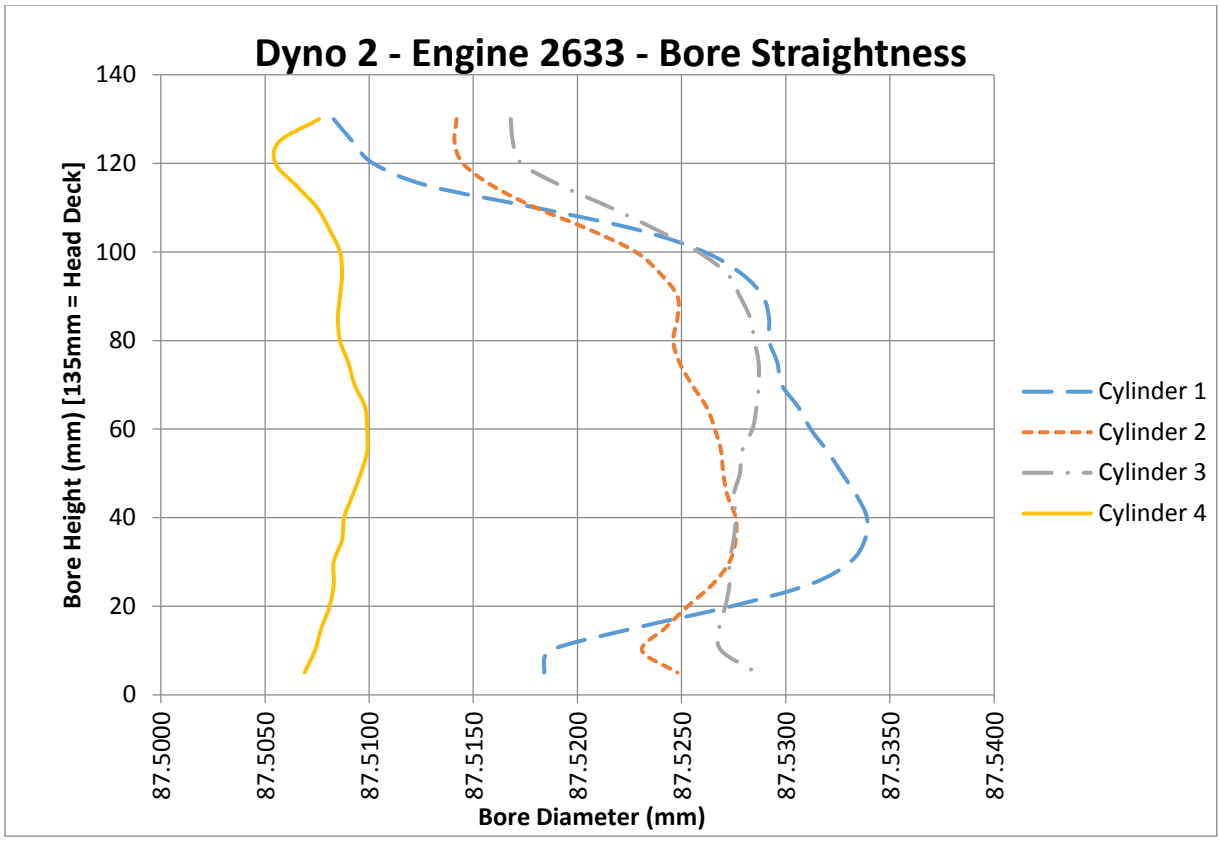

Figure 54: Dynamometer 2 - Engine 2633 - Bore Straightness - Before Dynamometer Test

This engine was also unique as it had two different PEO coatings types. Varying only through electrolyte composition in their deposition methods they were characterized by two different surface morphologies visible in Figure 32 and Figure 33. The coating variation in the same engine provided an opportunity to thoroughly evaluate the performance of the coating type controlling parameter.

The piston sizes were not measured prior to test but the tolerances from their drawing specifications allowed to determine a stack-up for largest and smallest bore clearances possible in each bore as shown in Table 13.

Table 13: Dynamometer 2 - Engine 2633 - Clearance Stack-Up

Total Clearance - Both sides (mm)	Cylinder	1	2	3	4
	Minimum	0.0208	0.0266	0.0293	0.0180
	Maximum	0.0614	0.0551	0.0562	0.0374

5.2.1.3. PISTON RINGS

The piston rings utilized in this test iteration were all non-production experimental rings provided by Nippon Piston Ring Co., Ltd as shown in Table 14.

Table 14: Dynamometer 2 - Engine 2633 - Piston Ring Selection

Piston Ring	Substrate	Overall Surface Treatment
Upper Compression	Steel	Diamond-like Carbon
Lower Compression	Steel	Chrome Plated
Oil Control	Steel	Diamond-like Carbon
Oil Spacer	Steel	Diamond-like Carbon

5.2.2. DYNAMOMETER TEST

The following section describes the dynamometer test and checks conducted on the second PEO coated engine trial of cylinder block 2633.

5.2.2.1. DYNAMOMETER CHECKS

5.2.2.1.1. 0 TEST HOURS

Before the test even started, the preliminary dynamometer checks at 0 test hours showed optimistic values. Although the bore sizes were larger than the tolerances specified for the bore on this type of engine, the piston rings and oil retention capacity was sufficient enough to provide very good static and dynamic combustion chamber sealing as was visible from the leak-down and blow-by dynamometer check results, respectively. Consequently, the compression values were good as well, reaching and even surpassing the desired values of 200 psi. It is important to note that even cylinder 4, which had a bore diameter 21 µm smaller than the other three cylinders experienced similarly positive dynamometer check values. These numbers proved that the combination of surface profile, clearance, and piston

rings chosen had a beneficial result on engine performance while their effect on coating wear resistance still had to be evaluated.

5.2.2.1.2. 4.5 TEST HOURS

At 4.5 test hours, the dynamometer test was paused to conduct additional dynamometer checks, results for which are provided in Figure 57 and visually inspect the bores using the borescope. The dynamometer check values in all the bores worsened slightly but were well within safe engine operation conditions.

The visual borescope analysis conducted at the 4.5 test mark showed initial signs of wear on cylinders 3 and 4 with faint marks in the direction of piston travel, particularly noticeable on the major and minor thrust sides. Cylinders 1 and 2 did not exhibit the same marks and from a close visual inspection did not display any wear that was visible by the resolution available via the borescope as seen in Figure 55. This was a clear indication that the coating type had a large effect on PEO coating wear resistance since the wear was visible only on cylinders which had PEO coating type A deposited on them.

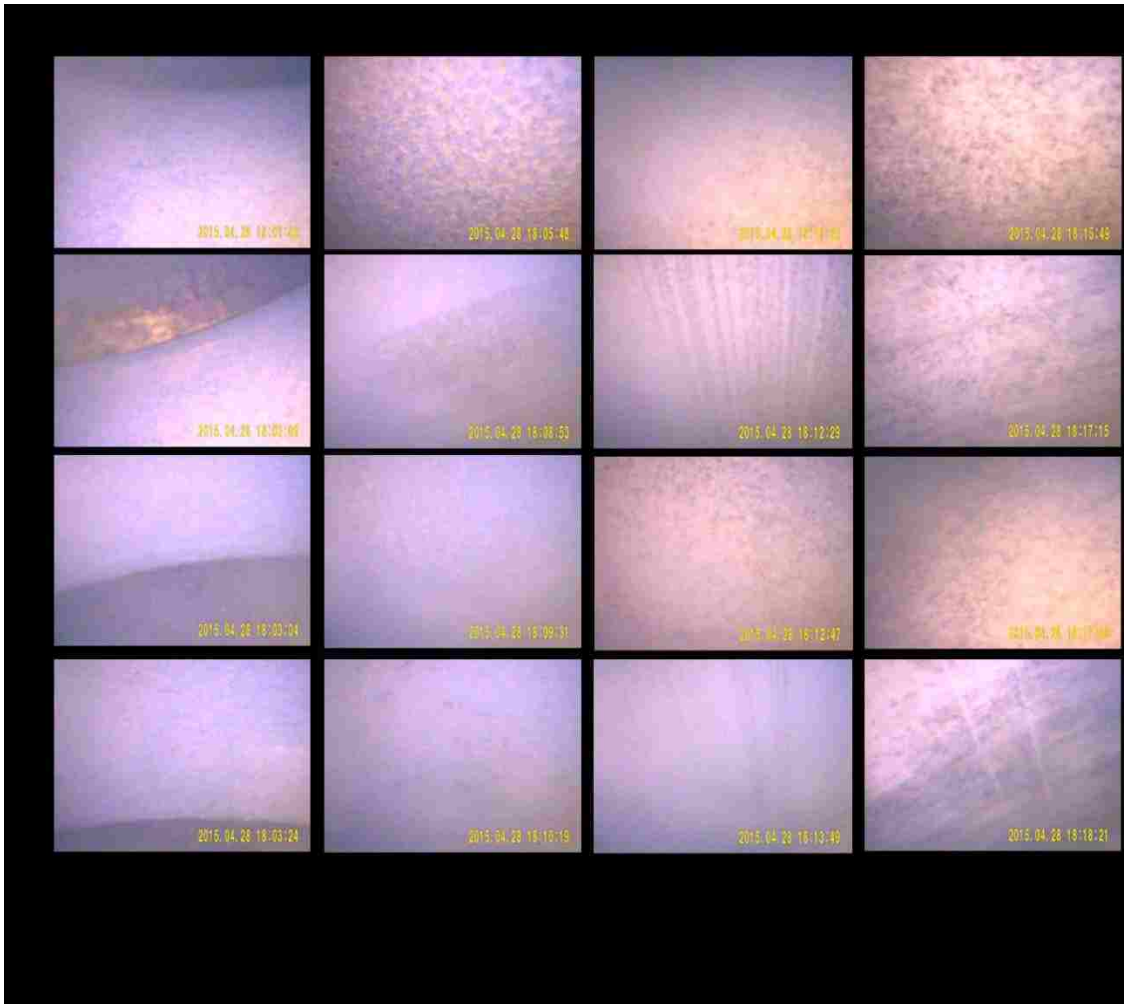

Figure 55: Dynamometer 2 - Engine 2633 - Borescope - 4.5 Test Hours

Throughout the test, the engine operated within normal conditions expected of a 2.0L GTDI. The real-time engine performance data was well within the operating ranges expected for temperature and pressure for all the main monitoring parameters. Additionally, the crankcase pressure stayed below 0 mmH_20, signifying a relatively good dynamic seal of the combustion chamber that could be attributed to the piston ring pack and oil retention in the bore walls.

5.2.2.1.3. 9.5 TEST HOURS

At 9.5 test hours, the test was paused to conduct another set of dynamometer checks. For cylinders 1 and 2, the leak-down and compression numbers stayed the same as the 4.5 hour mark, signifying that no damaging wear had occurred in the elapsed time since the previous

set of dynamometer checks. However, cylinders 3 and 4 did show negative signs of performance as the leak-down and compression numbers deteriorated further, especially for cylinder 3. Leak down of 30% was measured in cylinder 3, far greater than the standard warning value of 20%.

A borescope analysis conducted at the 9.5 test hour mark verified the detrimental wear in cylinders 3 and 4 as displayed in Figure 56. Severe wear in the form of longitudinal scratch marks were noticeable on all sides of cylinders 3 and 4, and with bare aluminum substrate exposed in some areas of cylinder 3. Conversely, cylinders 1 and 2 did not display any wear that was visible through the resolution of the borescope, creating a clear distinction between coating type A for cylinders 3 and 4, and type B for cylinders 1 and 2.

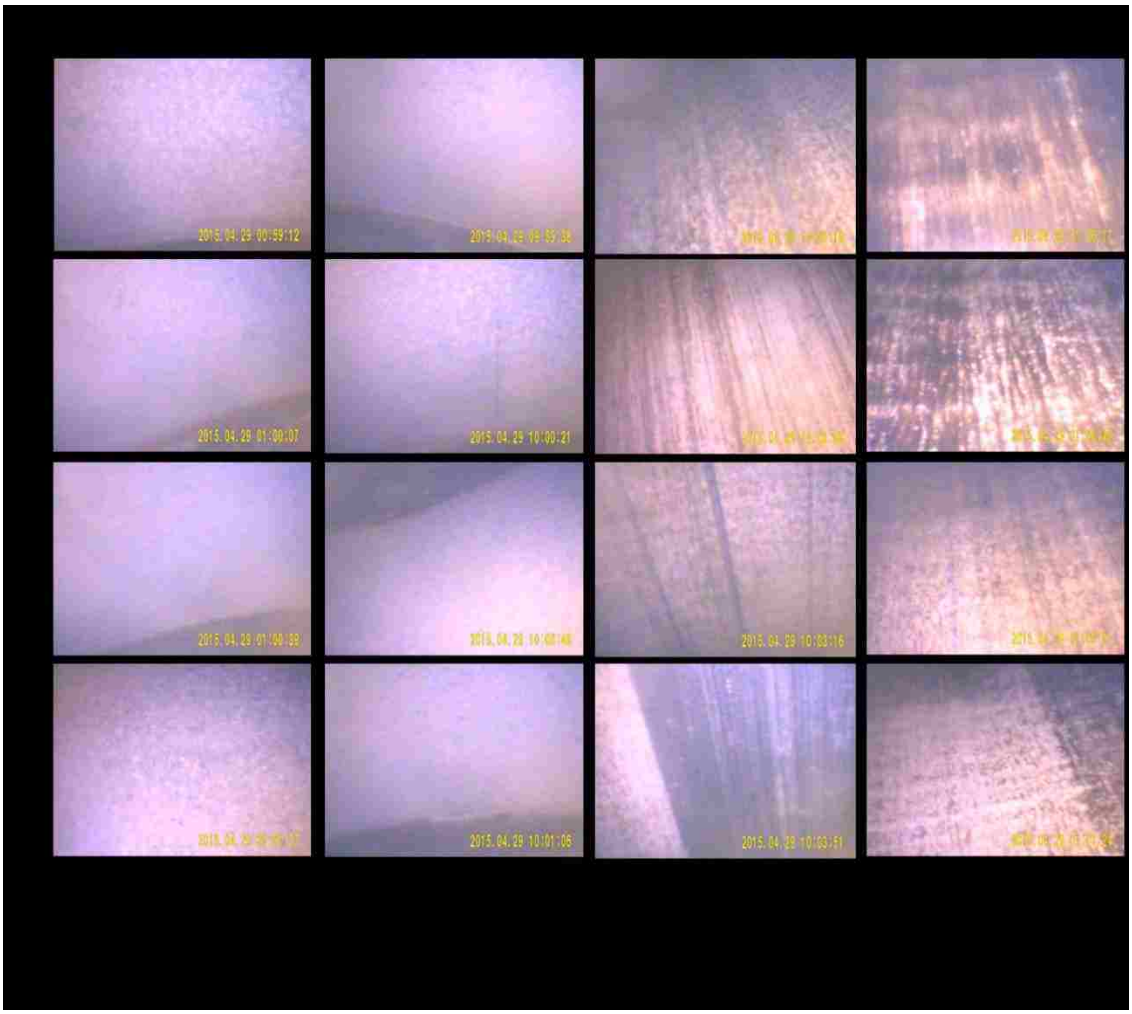

Figure 56: Dynamometer 2 - Engine 2633 - Borescope - 9.5 Test Hours

As the borescope displayed exposed bare aluminum substrate and the leak-down value for cylinder 3 was very poor, the engine was deemed to be beyond safe operating conditions. Therefore, the test was terminated and the engine extracted for teardown analysis.

Cylinder	Test Type	Test Hours			UNITS
		0	4.35	9.5	
1	Compression	205	200	200	PSI
	Leakdown	4	5	5	%
2	Compression	208	200	200	PSI
	Leakdown	4	6	6	%
3	Compression	210	200	190	PSI
	Leakdown	4	6	30	%
4	Compression	210	205	200	PSI
	Leakdown	4	6	14	%
Blow-by	1500 @ 76 ft lb	0.53	0.62	1.35	CFM
	1500 @ 30 ft lb	N/A	0.15	0.6	CFM
	3000 @ WOT & 0 inHg	N/A	0.83	1.57	CFM

Figure 57: Dynamometer 2 - Engine 2633 - Dynamometer Check Results

5.2.3. TEARDOWN ANALYSIS

The following section discusses the teardown analysis of the dynamometer tested engine 2633 which completed 9.5 test hours and was stopped due to the wear on cylinders 3 and 4. Furthermore, the teardown analysis investigated the low wear properties of cylinders 1 and 2 in order to determine the fundamental differences between the two sets of cylinders.

5.2.3.1. CYLINDERS 1 AND 2

The teardown analysis of cylinders 1 and 2 will be discussed in this section followed by cylinders 3 and 4 in the following section due to the considerably different test results from the same engine trial. A macroscopic display of cylinders 1 and 2 is shown in Figure 58.

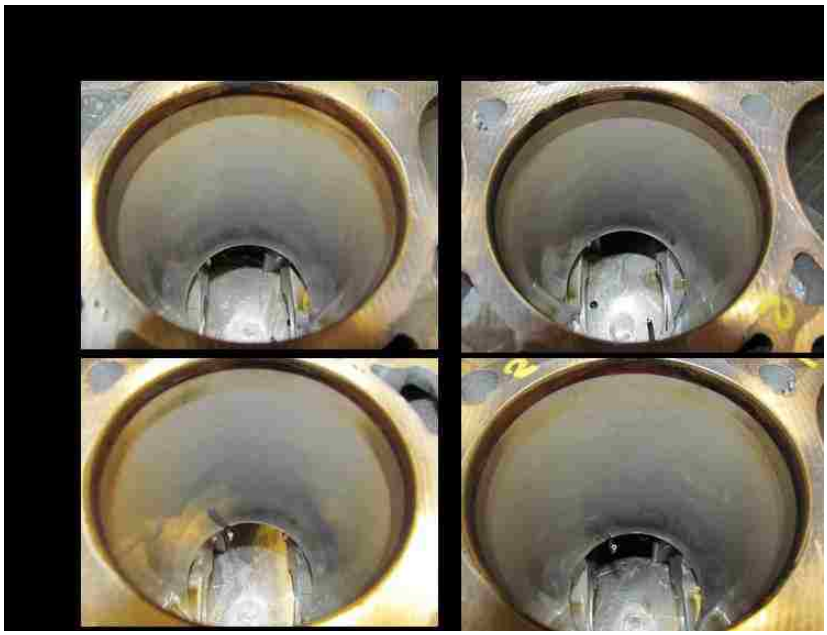

Figure 58: Dynamometer 2 - Engine 2633 - Teardown - Cylinders 1 & 2

5.2.3.1.1. SURFACE WEAR

Visually, it seemed that cylinders 1 and 2 did not experience any detrimental wear. Profilometry was used to determine the quantity and severity of microscopic wear and depression by wear that had occurred in these cylinders. The variation in color towards the top of the stroke was only due to the bore wall being exposed to different sliding surfaces or none at all, as seen in Figure 59.

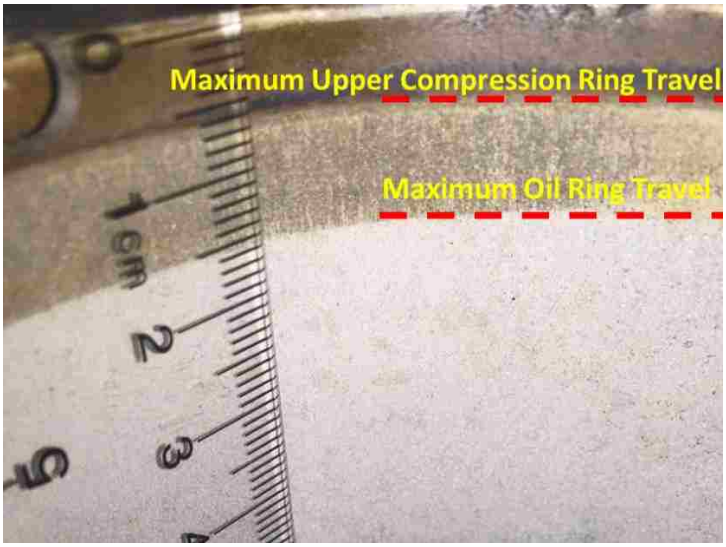

Figure 59: Dynamometer 2 - Engine 2633 - Cylinder 1 - Back – Piston Ring Travel Schematic

The profile over TDC displayed that depression had occurred in cylinders 1 and 2, the amount of which was consistently uniform at approximately 10 µm. Additionally, the profilometry confirmed that the coating stayed intact while the substrate was depressed since the micro-porosity surface profile of the PEO coating remained similar to the areas which did not experience any depression. Profilometry curves over TDC are visible in Appendix A and maximum values of surface depression at TDC as displayed in Table 15.

Table 15: Dynamometer 2 - Engine 2633 - Maximum Values of Surface Depression via Wear at TDC – Cylinder 1 & 2

Dynamometer 2 (Engine 2633) – Maximum Depression by Wear at TDC [µm]		
Location	**Cylinder 1**	**Cylinder 2**
Front	3	35
Right	7	35
Back	25	30
Left	35	20

The surface depression at TDC would have been superimposed on the general depression that the piston caused on the cylinder walls. A CMM dimensional analysis of the bores after the dynamometer as displayed in Figure 60 and Figure 61 revealed that cylinder 1 had experienced an average of 0.65 µm depression, meaning that there was almost no dimensional difference in the bore after 9.5 test hours of fired-engine conditions, apart from the top 20 mm of the stroke which experienced upwards of 12.2 µm dimensional change. The dimensional changes in cylinder 2 were more prominent than cylinder 1 with an average dimensional change of 5.62 µm and a maximum of 14.6 µm.

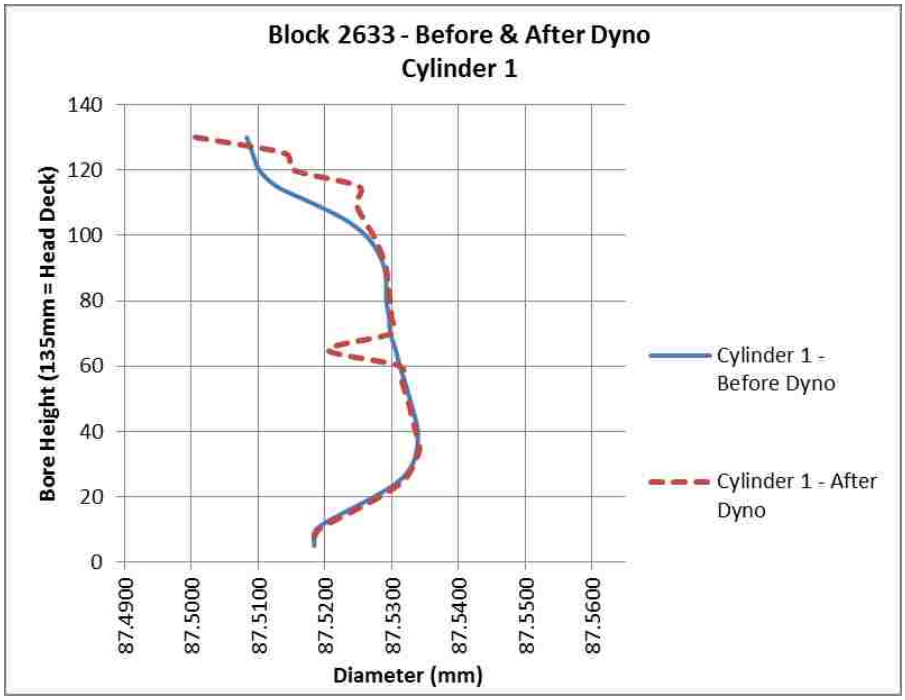

Figure 60: Dynamometer 2 - Engine 2633 - Bore Dimensional Comparison - Before & After Dynamometer – Cylinder 1

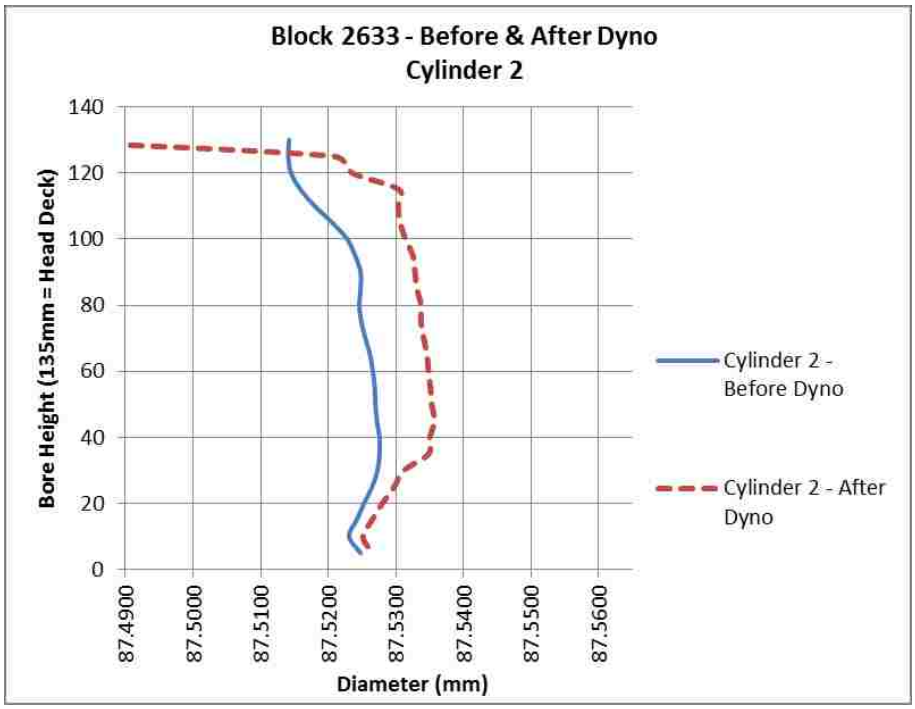

Figure 61: Dynamometer 2 - Engine 2633 - Bore Dimensional Comparison - Before & After Dynamometer - Cylinder 2

The surface profile throughout cylinders 1 and 2 became smoother than before the dynamometer test as the sliding surfaces broke off surface peaks and found their natural wear patterns, as shown via a comparison of surface profile values in Figure 62.

Before Dyno	Average	1.18	0.99	4.82	1.51	1.11	3.85	1.41	0.46	5.65	0.65	0.20	2.01
	Standard Deviation	0.50	1.10	3.36	0.48	1.55	1.38	0.33	0.40	3.01	0.09	0.12	0.19

Figure 62: Dynamometer 2 - Engine 2633 - Surface Profile - Statistical Comparison - Before & After Dynamometer

5.2.3.1.2. PISTON SKIRTS

The piston skirts for cylinder 1 and 2 did not experience any significant wear and stayed completely intact with the exception of slight discoloration towards the center of the skirt on both the major and minor thrust sides as shown in Figure 63.

Figure 63: Dynamometer 2 - Engine 2633 - Teardown - Piston Skirts - Cylinders 1 & 2

5.2.3.1.3. PISTON RINGS

There was no noteworthy material transfer that had occurred between the bore walls and upper or lower compression piston rings of cylinder 1 and 2, this was determined through both SEM and EDS analysis pictured in Figure 64 and Figure 65. There was only small debris consisting of iron particles trapped under the groove of the lower piston ring for cylinder 1 as shown by EDS analysis in Figure 66.

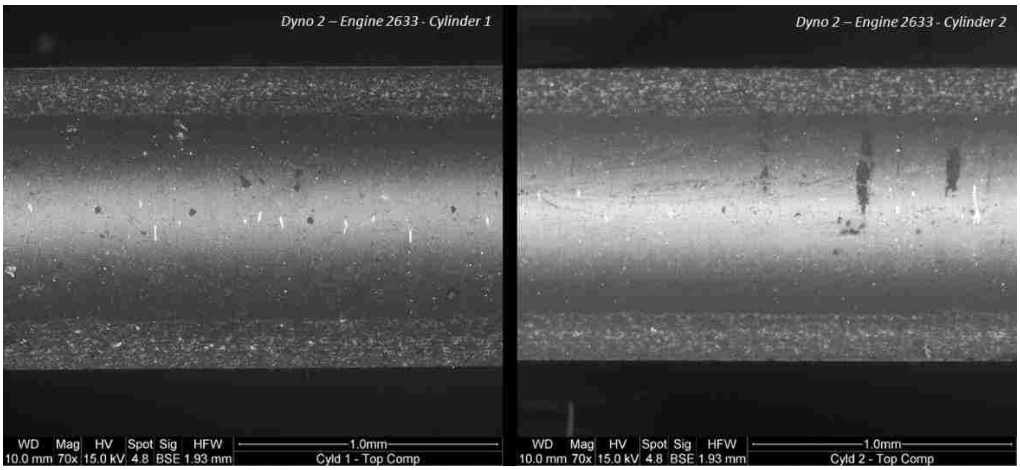

Figure 64: Dynamometer 2 - Engine 2633 - Teardown - Upper Compression Rings - Cylinders 1 & 2

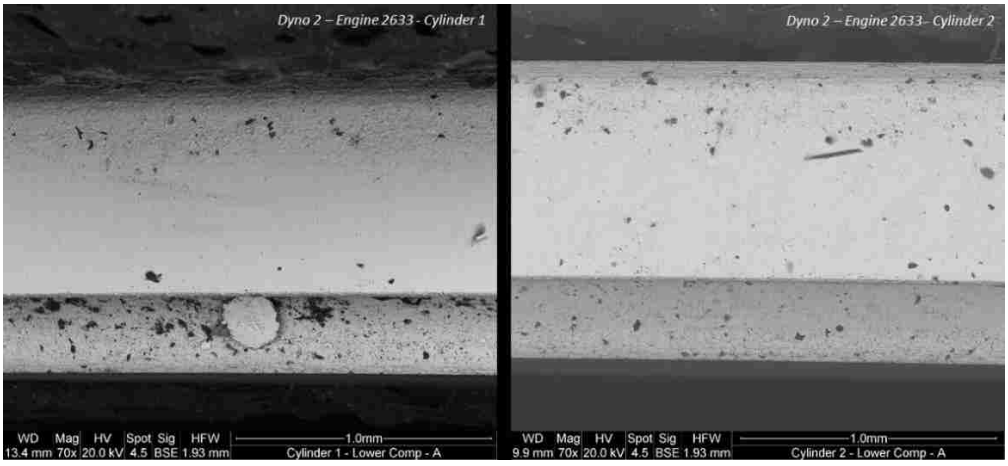

Figure 65: Dynamometer 2 - Engine 2633 - Teardown - Lower Compression Rings - Cylinder 1 & 2

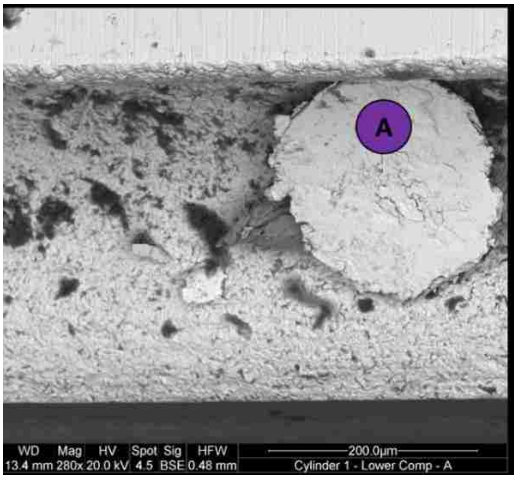

Element	Weight %	Atomic %	Error %
C K	19.33	52.66	9.68
CrK	2.11	1.33	4.76
FeK	78.56	46.02	1.70

Figure 66: Dynamometer 2 - Engine 2633 - Teardown - Lower Compression Ring Groove – Cylinder 1 - EDS Analysis

5.2.3.2. CYLINDERS 3 AND 4

This section covers the tear down analysis of cylinders 3 and 4 of engine 2633 in the second PEO coated engine trial which were coated with PEO type A deposition process parameters. A macroscopic view of bores 3 and 4 after teardown is visible in Figure 67.

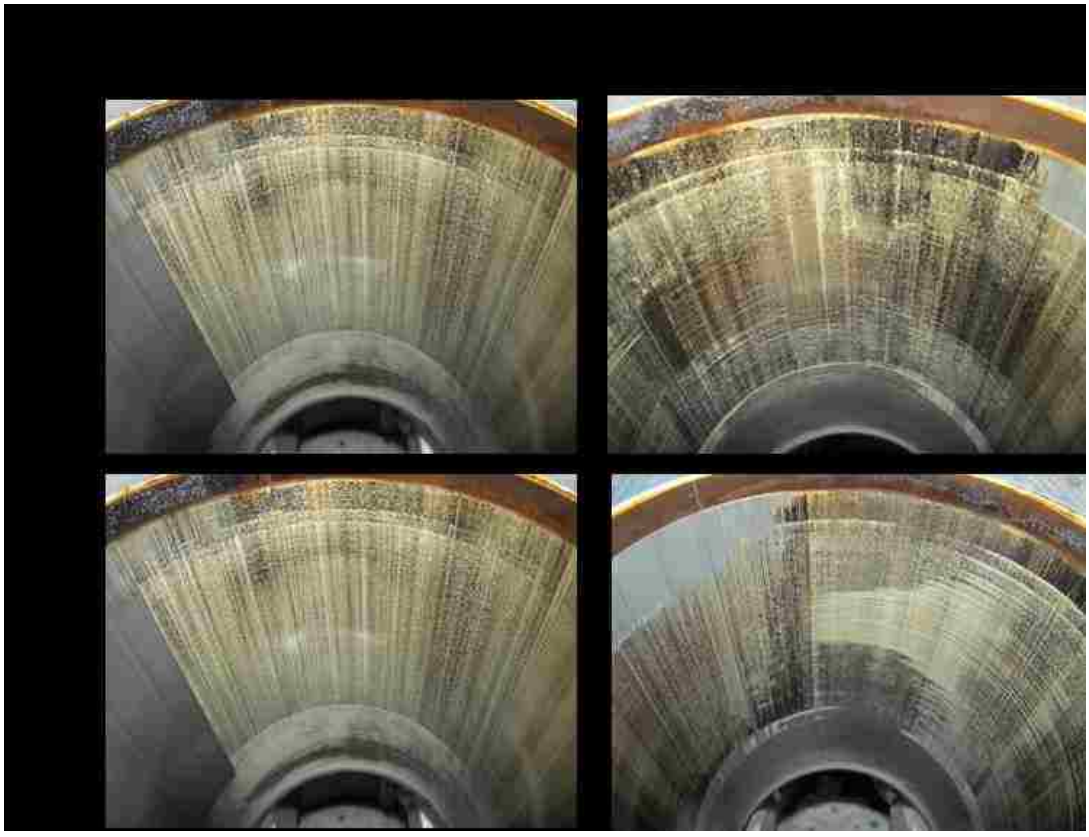

Figure 67: Dynamometer 2 - Engine 2633 - Teardown - Cylinders 3 & 4

5.2.3.2.1. SURFACE WEAR

Cylinders 3 and 4 experienced detrimental wear and completely wore off the PEO coating in some areas. The areas of exposed aluminum were emphasized at TDC and BDC where the sliding surface experienced boundary lubrication. The profilometry confirmed the severity of wear by displaying deep depressions in the bores over TDC as shown in Table 16, as well as distinct lack of micro-porosities in the profile that would have signified remaining PEO coating, visible in the surface profile data over TDC provided in Appendix A.

Table 16: Dynamometer 2 - Engine 2633 - Maximum Values of Surface Depression via Wear at TDC – Cylinder 3 & 4

Dynamometer 2 (Engine 2633) – Maximum Depression by Wear at TDC [µm]		
Location	**Cylinder 3**	**Cylinder 4**
Front	40	120
Right	35	35
Back	30	27
Left	100	30

An important factor to note is the 20 µm difference in diameter between cylinders 3 and 4, with cylinder 4 being the smaller bore at an average diameter of 87.509 mm. This difference in dimensions could be visible in the areas of wear as shown in Figure 68. Cylinder 4 experienced removal of PEO coating at TDC and BDC. Conversely, cylinder 3 had coating removed uniformly throughout the bore, and on cylinder sides which had some coating remaining, the coating was not removed at TDC and BDC. This could lead to the assumption that a smaller bore is more demanding on TDC and BDC regions.

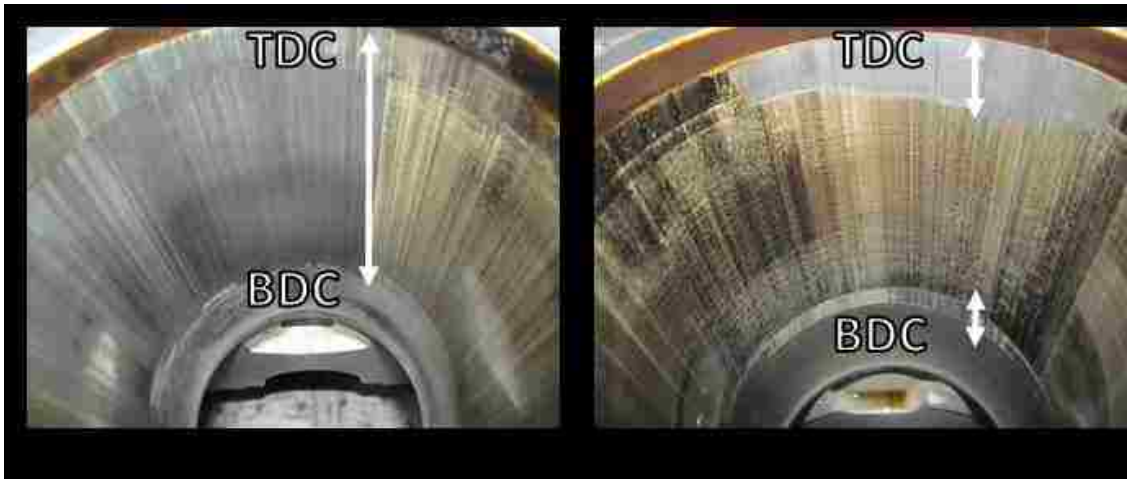

Figure 68: Dynamometer 2 - Engine 2633 - Wear Pattern - Large (Cyld. 3) vs. Small (Cyld. 4) Bore Size

The wear on the bores and removal of PEO coatings on cylinders 3 and 4 was in addition to the substantial deformation experienced throughout the bores as pictured in Figure 69 and Figure 70, and summarized in Table 17. Deformation was measured to be up to 37.40

µm on cylinder 3 and up to 16.20 µm of deformation on cylinder 4 from the original measurements. This amount of surface depression penetrated into the substrate causing aluminum particles to mix into the circulating oil and increase abrasive wear.

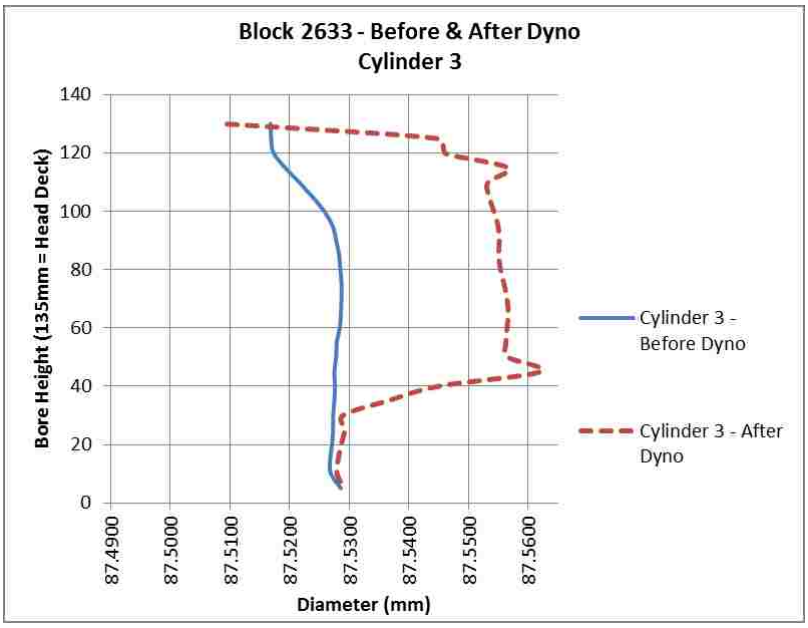

Figure 69: Dynamometer 2 - Engine 2633 - Bore Dimensional Comparison - Before & After Dynamometer - Cylinder 3

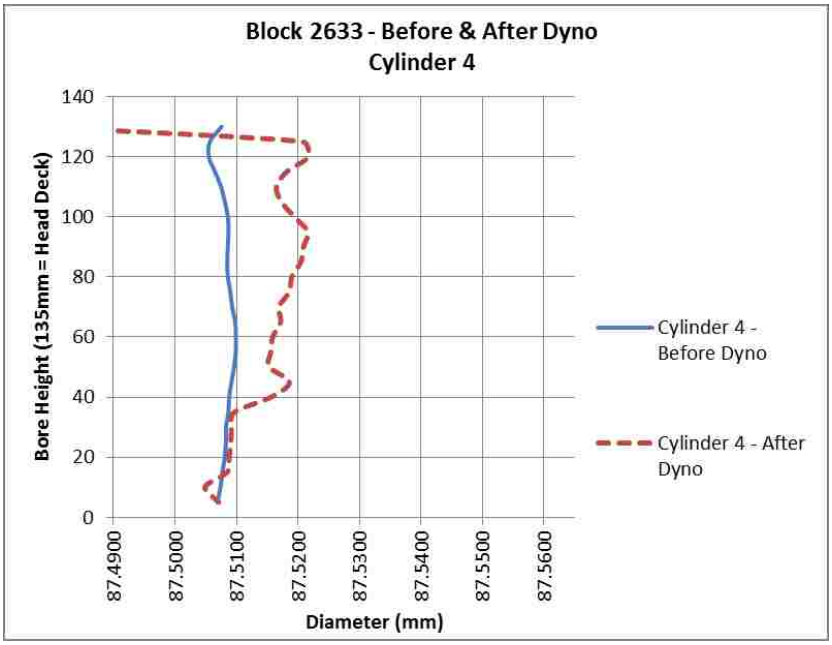

Figure 70: Dynamometer 2 - Engine 2633 - Bore Dimensional Comparison - Before & After Dynamometer - Cylinder 4

Table 17: Dynamometer 2 - Engine 2633 - Bore Dimension Statistical Summary - Before & After Dynamometer - All Cylinders

Difference - Bore Dimensions - Before & After Dynamometer				
(µm)	Cylinder			
	1	2	3	4
MAX	12.20	14.60	37.40	16.20
MIN	-10.20	-40.30	-7.20	-30.30
AVG	0.65	5.62	20.14	5.75
STANDEV	3.95	9.68	13.16	8.74

In the regions of the bore in which there was PEO coating remaining, those areas did possess a surface profile that was smoother judging by off Ra values compared to profilometry data that was gathered before dynamometer testing as visible in Figure 62.

5.2.3.2.2. PISTON SKIRTS

The piston skirts for cylinders 3 and 4 did not experience any unfavorable wear on either the major or minor thrust sides, despite the severe wear on the cylinder bores as pictured in Figure 71.

Figure 71: Dynamometer 2 - Engine 2633 - Teardown - Piston Skirts - Cylinders 3 & 4

5.2.3.2.3. PISTON RINGS

Some notable material transfer did exist on the piston rings used in cylinders 3 and 4 as shown in Figure 72, Figure 73, Figure 74, and Figure 75. On the piston rings used in

cylinder 3 in particular, there was a significant amount of material impregnated onto the sliding surface of the upper and lower compression rings. The foreign material on the upper compression ring of cylinder 3 consisted of carbon, aluminum, and oxygen elements. The carbon elements could have been oil that had been oxidized due to the high combustion chamber temperatures reached during engine operation [32]. Aluminum and oxygen elements could have been material transfer from the aluminum oxide based PEO coating that had been applied on the cylinder bores. The aluminum oxide PEO coating could have transferred onto the piston rings after the PEO coating began to wear off the bore walls.

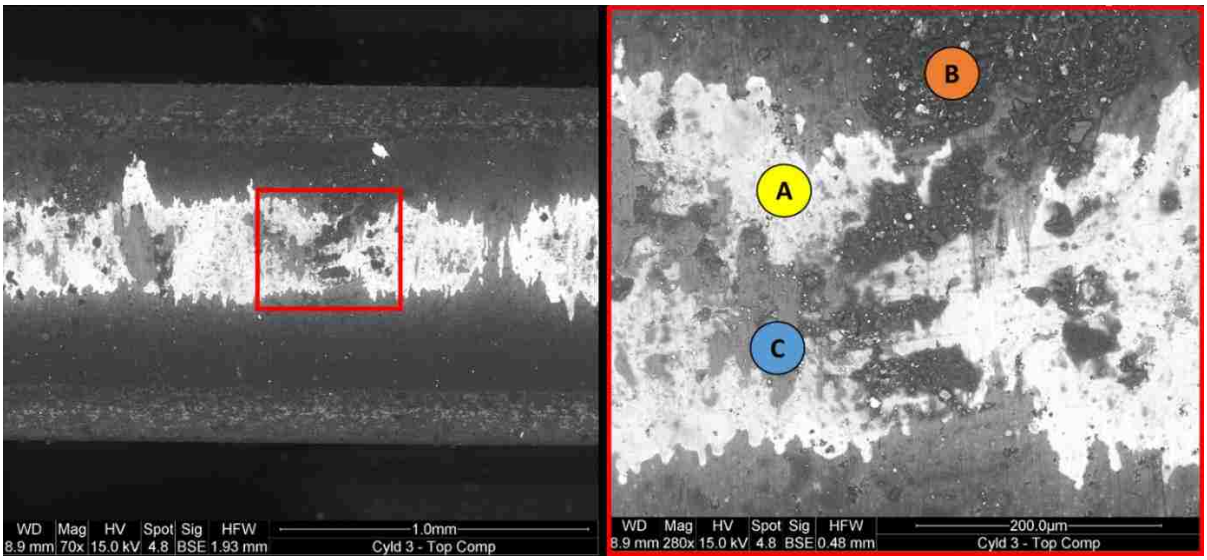

Figure 72: Dynamometer 2 - Engine 2633 - Teardown - Upper Compression Ring - Cylinder 3 – SEM - x70 Mag. vs. x280 Mag.

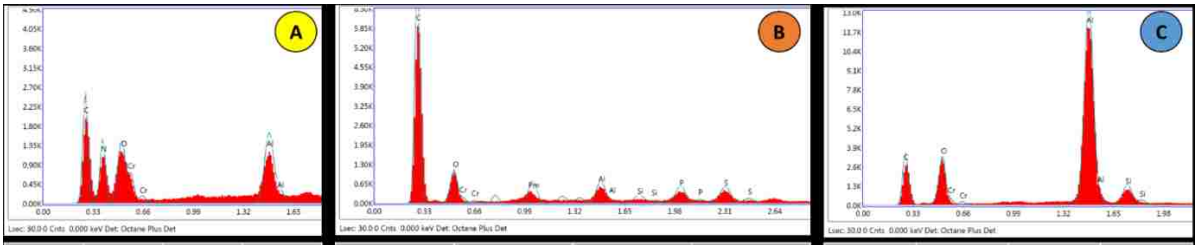

Element	Weight %	Atomic %	Error %
C K	37.11	45.82	7.53
N K	24.95	26.41	11.03
O K	18.36	17.02	10.85
Al K	19.57	10.75	9.86

Element	Weight %	Atomic %	Error %
C K	67.16	81.39	8.11
O K	7.26	6.60	11.28
Al K	3.71	2.00	12.20
P K	7.65	3.60	11.96
S K	14.09	6.40	11.06

Element	Weight %	Atomic %	Error %
C K	14.19	25.97	10.49
O K	7.70	10.57	7.57
Al K	72.08	58.73	5.37
Si K	6.04	4.72	8.97

Figure 73: Dynamometer 2 - Engine 2633 - Teardown - Upper Compression Ring - Cylinder 3 - EDS Point Analysis

The lower compression ring used in cylinder 3 did not have any aluminum oxide material transfer, however, there was a measureable amount of carbon on the sliding surface that was examined through EDS analysis.

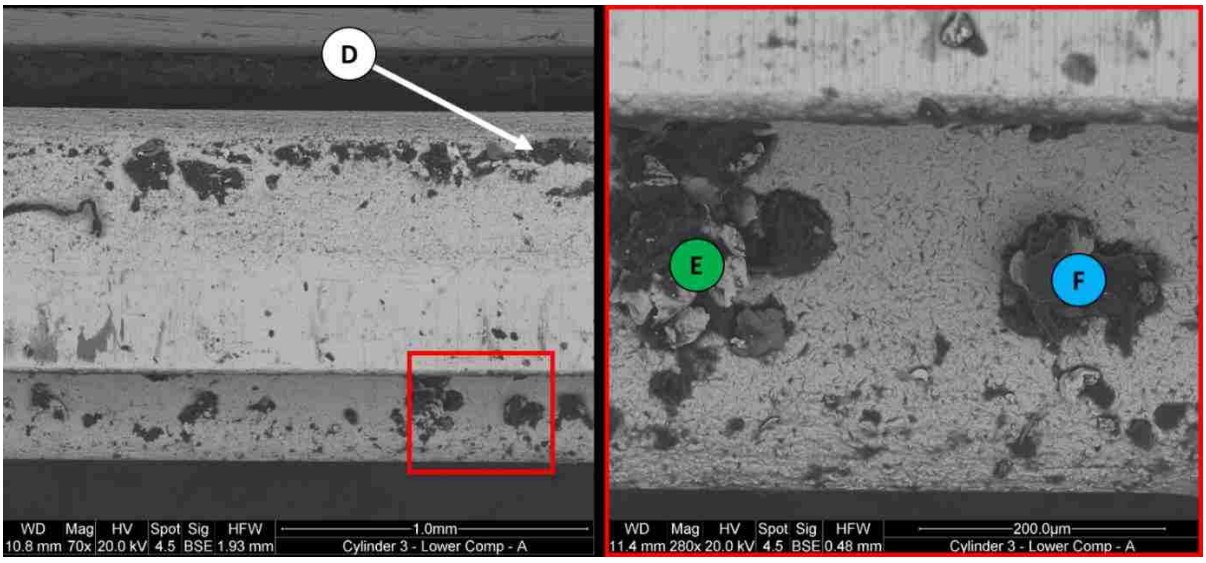

Figure 74: Dynamometer 2 - Engine 2633 - Teardown - Lower Compression Ring - Cylinder 3 – SEM - x70 Mag. vs. x280 Mag.

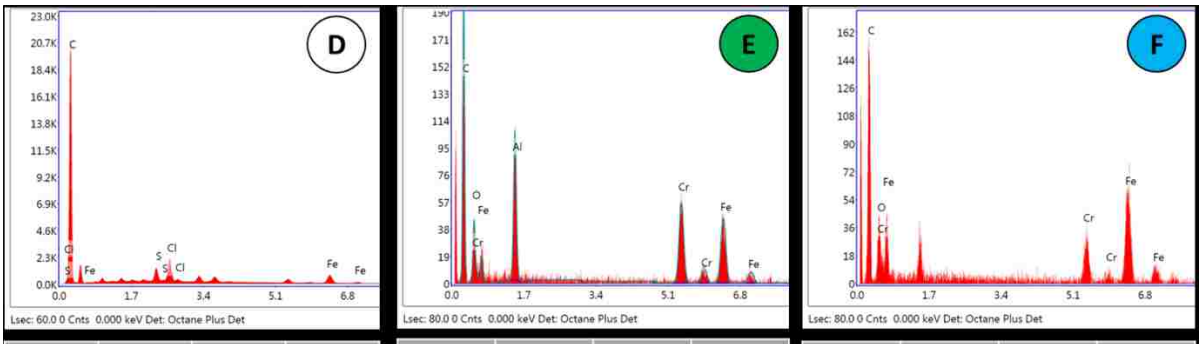

Element	Weight %	Atomic %	Error %
C K	94.75	98.45	4.99
S K	0.91	0.35	2.50
Cl K	1.80	0.64	1.97
Fe K	2.54	0.57	3.15

Element	Weight %	Atomic %	Error %
C K	60.68	76.13	9.10
O K	16.98	15.99	17.32
Al K	5.91	3.30	8.83
Cr K	7.37	2.14	5.48
Fe K	9.06	2.44	5.91

Element	Weight %	Atomic %	Error %
C K	61.44	76.80	8.18
O K	19.04	17.86	17.82
Cr K	4.46	1.29	9.12
Fe K	15.07	4.05	5.10

Figure 75: Dynamometer 2 - Engine 2633 - Teardown - Lower Compression Ring - Cylinder 3 - EDS Point Analysis

The upper and lower compression rings used in cylinder 4 experienced almost no material transfer and had only a minimal amount of debris on their sliding surfaces, as pictured in

Figure 76 and Figure 77. The lower compression ring of cylinder 4 had a small quantity of foreign material on its surface that was determined to consist of mostly carbon and aluminum oxide.

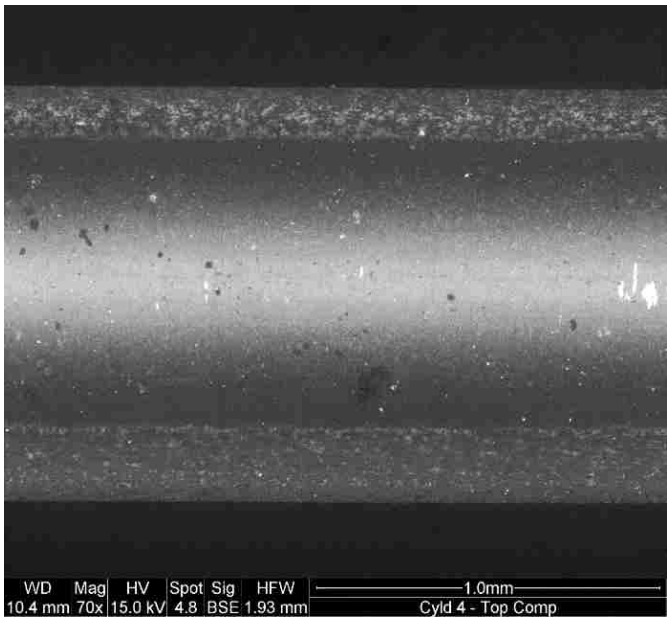

Figure 76: Dynamometer 2 - Engine 2633 - Teardown - Upper Compression Ring – Cylinder 4 - SEM

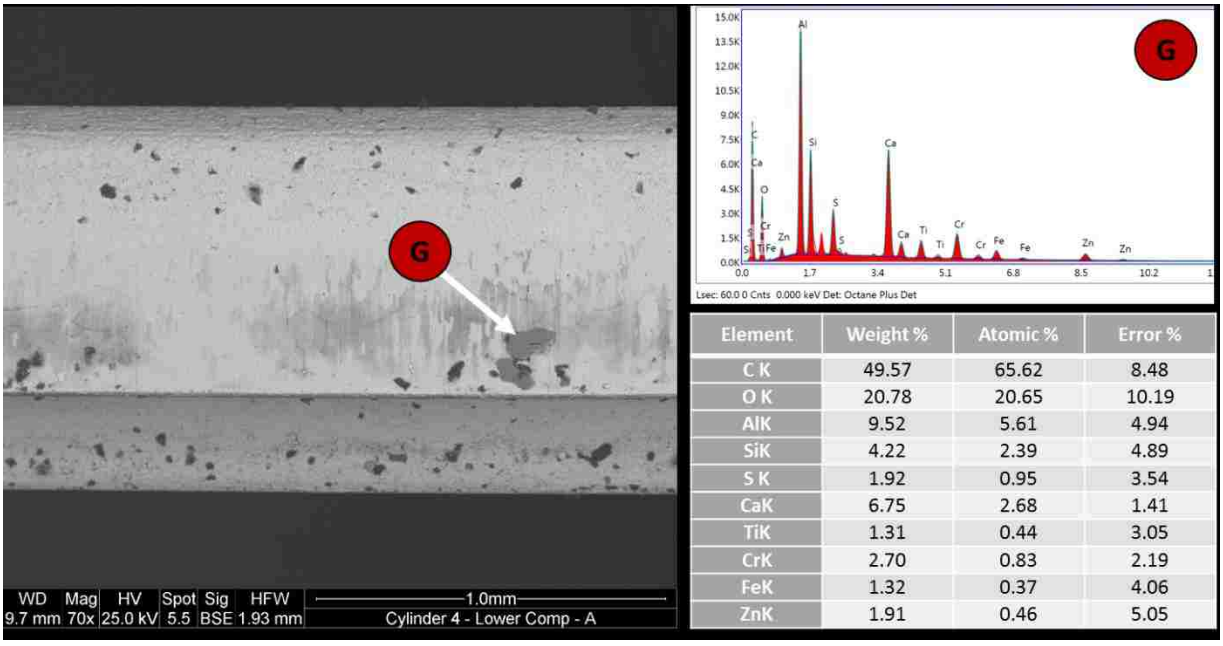

Element	Weight %	Atomic %	Error %
C K	49.57	65.62	8.48
O K	20.78	20.65	10.19
AlK	9.52	5.61	4.94
SiK	4.22	2.39	4.89
S K	1.92	0.95	3.54
CaK	6.75	2.68	1.41
TiK	1.31	0.44	3.05
CrK	2.70	0.83	2.19
FeK	1.32	0.37	4.06
ZnK	1.91	0.46	5.05

Figure 77: Dynamometer 2 - Engine 2633 - Teardown - Lower Compression Ring - Cylinder 4 - EDS Point Analysis

5.3. TRIAL 3 – ENGINE 2595

The third engine in the series of PEO bore coating trials had uniform parameters throughout all 4 cylinders and utilized information gathered from previous PEO engine trials in order to optimize the controlling variables. All engine components were transferred from an unused production 2.0L GTDI engine.

5.3.1. PRE-TEST PARAMETER SELECTION

The following section discusses the selection of the controlling parameters for the third engine trial in this study.

5.3.1.1. SURFACE PROFILE

Due to the resources available at the time of this engine trial, professional honing services were not engaged to prepare the surface profile of the PEO coated cylinder bores. Flex-Honing brushes were instead used to modify the surface profile and prepare the surface for fired-engine testing. Various grits of Flex-Honing brushes were used in an attempt to attain a high oil retention, low surface peak, and smooth surface all while monitoring coating thickness in order to not strip the coating completely during this process.

The surface profile values attained and provided in Figure 78 through the Flex-Honing brush method achieved values lower than the target value of maximum 0.50 µm surface peaks, which was favorable. However, the surface valley numbers were relatively low at an average of 1.18 µm, which kept oil retention values lower than desired at 0.08 $\mu m^{3/}\mu m^2$ when combined with the roughness values averaging 0.55 µm. The combination of these values were the best possible solution attainable while maintaining a desired coating thickness of around 8 – 10 µm and dimensional control towards the upper end of production bore diameter tolerance of 87.520 mm.

Stroke Length: 8mm													
Cylinder No.	Position	Variable											
		Ra (µm)			Rpk (µm)			Rvk (µm)			Oil Retention Volume (µm^3/µm^2)		
		Top	Middle	Bottom	Top	Middle	Bottom	Top	Middle	Bottom	Top	Middle	Bottom
1	Back	0.57	0.54	0.59	0.51	0.46	0.40	1.10	1.09	1.02	0.09	0.07	0.07
2		0.57	0.48	0.58	0.49	0.52	0.50	1.26	1.13	1.27	0.08	0.08	0.09
3		0.54	0.42	0.50	0.47	0.30	0.60	1.16	1.02	0.95	0.09	0.07	0.07
4		0.55	0.74	0.54	0.36	0.43	0.47	1.45	1.46	1.28	0.09	0.12	0.08

Figure 78: Dynamometer 3 - Engine 2595 - Surface Profile Values – Before Dynamometer

5.3.1.2. BORE DIAMETER, COATING THICKNESS, & CLEARANCE

The target bore diameters for this test iteration were to be on the upper end of the tolerance based on specifications set out for 2.0L GTDI engines at 87.520 mm. The clearance between piston and bore coated with PEO coating B would also be on the larger end of the specification tolerance, which was also desired as a controlling parameter for this engine trial. The bore diameters were measured by bore gauge via use of a cylinder bore with a known diameter rather than CMM due to resource availability, therefore bore straightness or cylindricity measurements were not recorded for this engine trial. Average diameter, coating type, and coating thickness for each bore of engine trial 3 are provided in Table 18.

Table 18: Dynamometer 3 - Engine 2595 - Diameter, Coating Type, and Coating Thickness

Cylinder	1	2	3	4
Avg. Diameter (mm) – Bore Gauge	87.515	87.520	87.515	87.510
Coating Type	Type B	Type B	Type B	Type B
Coating Thickness (µm)	8-10	8-10	8-10	8-10

The pistons used in this engine trial were measured by outside micrometer in order to more precisely determine and control the clearance available between pistons and bore walls. The clearance values calculated for each bore are provided in Table 19.

Table 19: Dynamometer 3 - Engine 2595 - Clearance

Total Clearance - Both sides (mm)	Cylinder	1	2	3	4
	Piston Size	87.490	87.494	87.492	87.497
	Clearance	0.0250	0.0260	0.0230	0.0130

5.3.1.3. PISTON RINGS

The piston rings used in this test iteration were all experimental non-production rings as shown in Table 20.

Table 20: Dynamometer 3 - Engine 2595 - Piston Ring Selection

Piston Ring	Substrate	Overall Surface Treatment
Upper Compression	Steel	Diamond-like Carbon
Lower Compression	Steel	Chrome Plated
Oil Control	Steel	Diamond-like Carbon
Oil Spacer	Steel	Diamond-like Carbon

5.3.2. DYNAMOMETER TEST

The following section describes the results from dynamometer testing of the third engine in the PEO coated cylinder bore study.

5.3.2.1. DYNAMOMETER CHECKS

5.3.2.1.1. 0 TEST HOURS

The dynamometer checks for leak-down, compression, and blow-by were all conducted at the 0 test hour mark to determine the health of the engine and evaluate the sealing of all piston assembly and combustion chamber components chosen as part of the controlling parameters for this engine trial prior to test start. The dynamometer check values did not reach target numbers for compression at the 0 test hour mark. However, the leak-down and blow-by numbers were well within engine tolerances.

5.3.2.1.2. 4.5 TEST HOURS

The test operated within expected temperatures and pressures for the first stage of the test prior to being paused for scheduled dynamometer checks at 4.5 test hours. Additionally, crankcase pressures were in a vacuum state below 0 mmH_20, which served as an indicator for acceptable dynamic combustion chamber sealing conditions. The various dynamometer checks conducted at 4.5 test hours showed an increase in both static and dynamic combustion chamber sealing capacity. Notably improved leak-down, compression, and blow-by numbers in each cylinder, respectively, indicating that opposing sliding wear components had created natural wear patterns in their respective tribological systems and became better seated to each other.

A borescope analysis at this 4.5 test hour stage of dynamometer checks did not reveal any noticeable wear marks on any of the bore surfaces throughout all 4 cylinders as pictured in Figure 79. The PEO coating and its defining surface pattern was still clearly visible.

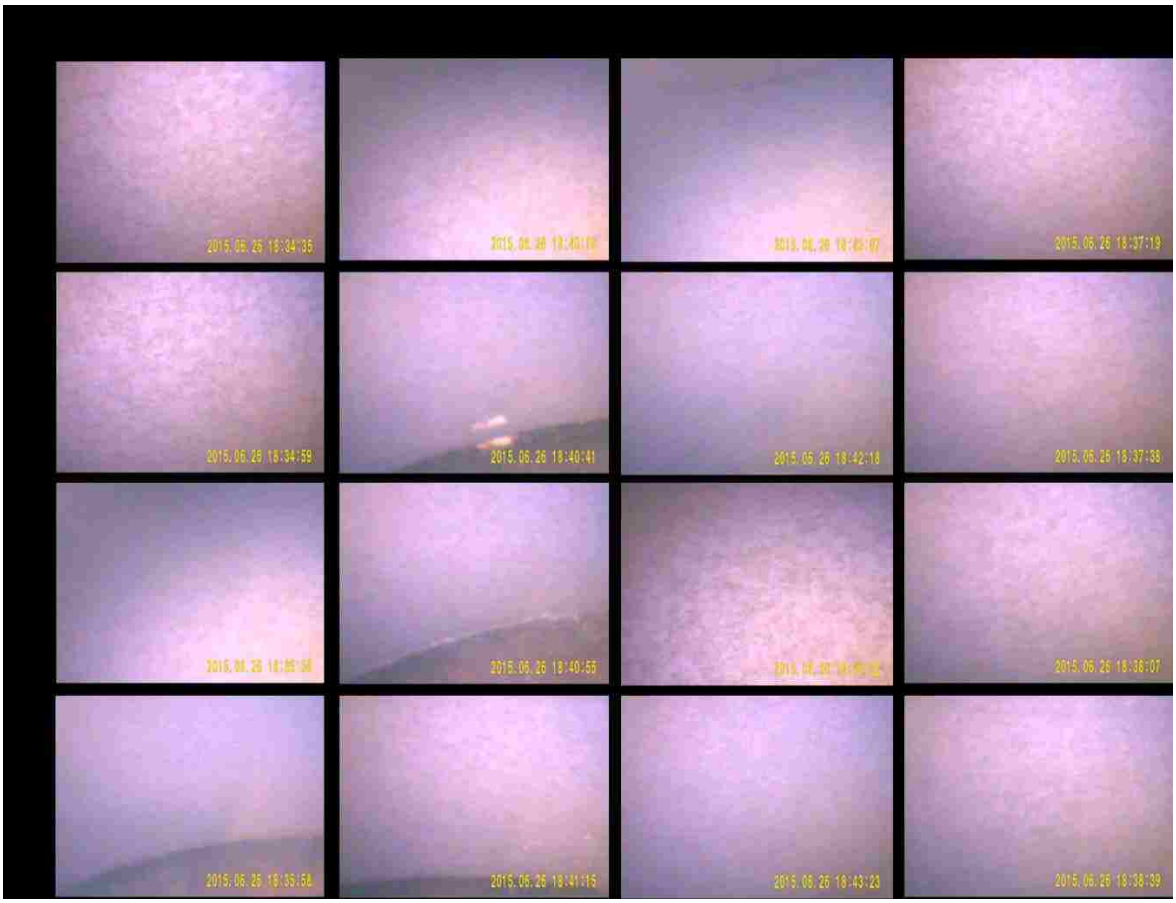

Figure 79: Dynamometer 3 - Engine 2595 - Borescope - 4.5 Test Hours

5.3.2.1.3. 9.5 TEST HOURS

The test was resumed until the dynamometer checks were repeated at the 9.5 test hour mark. The dynamometer check values remained relatively stable with only minor variations for leak-down and compression when compared to the numbers attained at the 4.5 test hour mark. Additionally, the dynamic combustion chamber sealing had improved as determined through slightly reduced blow-by values.

Visual analysis of the cylinders via borescope revealed a few notable surface features that indicated the onset of wear as pictured in Figure 80. The side of the bore wall facing towards the front of the engine in cylinders 1 and 4 displayed faint longitudinal scratch marks. Moreover, cylinder 2 showed a distinct pattern of linear markings perpendicular to piston travel, originating on the left side of the bore. It is interesting to note that the markings had a very constant pattern with seemingly uniform spacing between the

markings. Although the markings did disrupt the surface pattern and color of the PEO coating, the markings did not reflect the light from the borescope, which lead to the assumption that although this may be an onset of wear, the aluminum substrate of the cylinder block was still not exposed and this could be a different layer of the PEO coating displaying a color variation due to uneven wear.

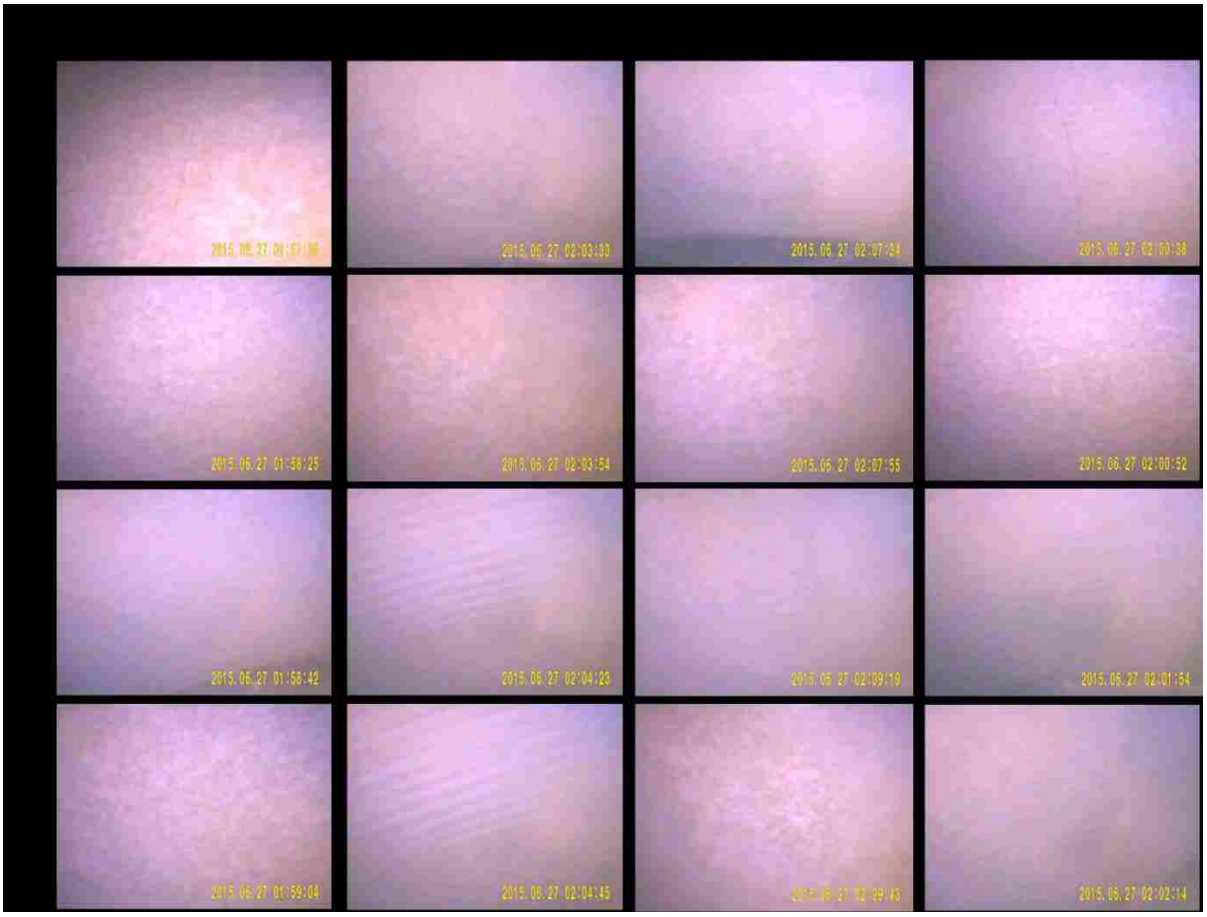

Figure 80: Dynamometer 3 - Engine 2595 - Borescope - 9.5 Test Hours

With no aluminum substrate exposed and dynamometer check values well within operating conditions, the engine test was continued.

5.3.2.1.4. 13.5 TEST HOURS

Dynamometer checks completed at the 13.5 test hour mark displayed greater uniformity throughout all the bores as well as increased compression pressure. Blow-by data remained

relatively uniform from the previous set of dynamometer checks completed at 9.5 test hours and were well within safe operating conditions.

A borescope inspection revealed wear in all 4 bores as pictured in Figure 81. The wear in each bore varied in severity but consisted of the same wear pattern of linear markings perpendicular to piston travel. In all bores, the aluminum substrate of the cylinder block was visible as the PEO coating was worn away. Although the wear pattern was visible on all sides of the bores, the more severe wear was concentrated on the front and back sides of the cylinder.

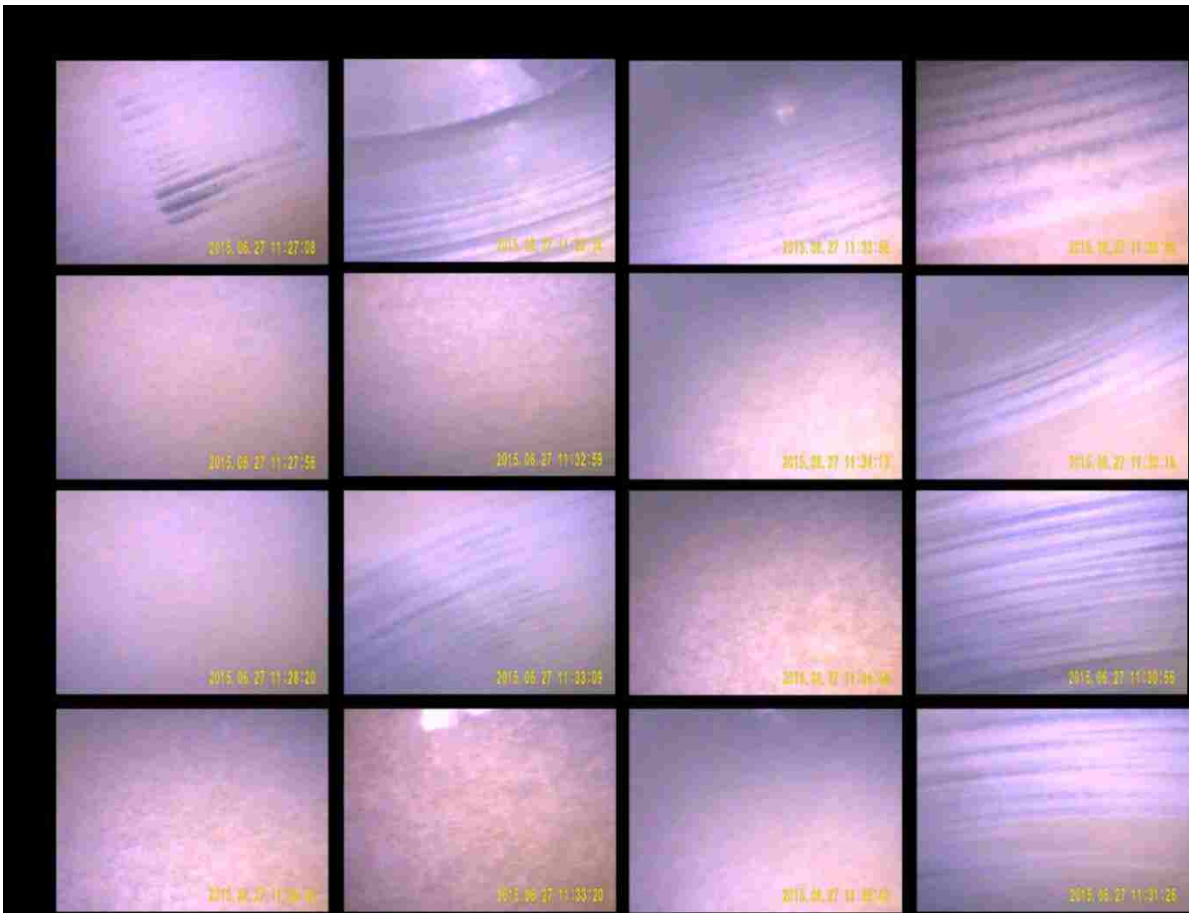

Figure 81: Dynamometer 3 - Engine 2595 - Borescope - 13.5 Test Hours

There was no visible scuffing on the bores and the dynamometer check values were within safe operating conditions, therefore the test was continued.

5.3.2.1.5. 18 TEST HOURS

The test completed the full 18 hour dynamometer curve for which it was scheduled. The engine operating temperatures and pressures stayed within expected operating levels throughout the test, even after bore wear was discovered to be increasing in severity. The dynamometer checks were conducted after test completion and revealed almost no change in values from the previous set of checks at 13.5 test hours for compression and blow-by results. The leak-down results did increase but were still far under the leak-down warning levels of 20%. A summary of all dynamometer check values is provided in Figure 83.

Visual analysis via borescope of the bores after 18 test hours revealed an increase in wear severity as shown in Figure 82. The horizontal linear marking pattern covered a greater percentage area of the bore on all sides, as well as increased the amount of exposed aluminum substrate.

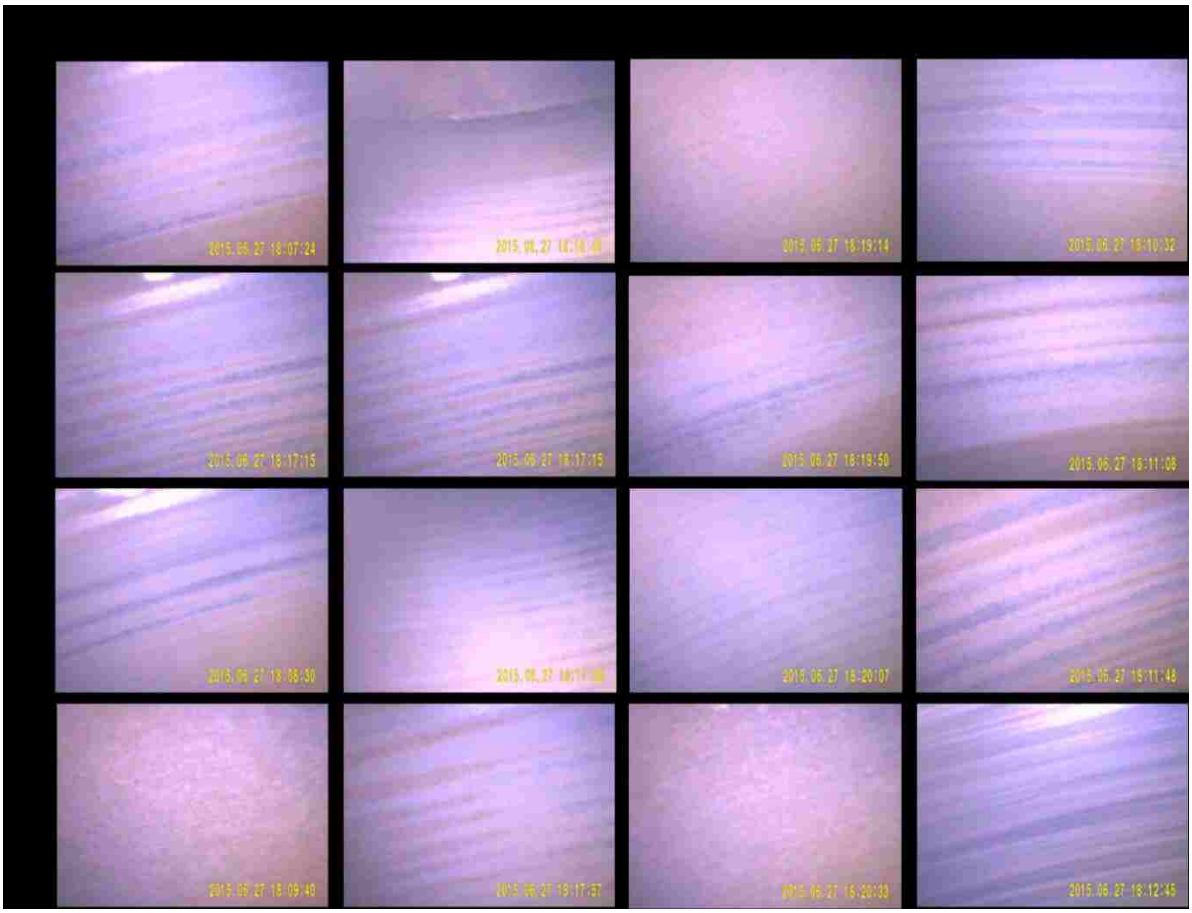

Figure 82: Dynamometer 3 - Engine 2595 - Borescope - 18 Test Hours

Cylinder	Test Type	Test Hours					UNITS
		0	4.5	9.5	13.5	18	
1	Compression	190	190	190	205	205	PSI
	Leakdown	5	4	7	4	8	%
2	Compression	180	190	190	205	205	PSI
	Leakdown	6	6	5	6	8	%
3	Compression	190	195	190	205	205	PSI
	Leakdown	7	6	5	6	9	%
4	Compression	185	200	190	205	205	PSI
	Leakdown	8	5	6	6	7	%
Blow-by (CFM)	1500 rpm @ 76 ft lb	0.54	0.64	0.63	0.65	0.66	CFM
	1500 rpm @ 30 ft lb	0.34	0.23	0.17	0.22	0.2	CFM
	3000 rpm @ 0 inHg ManVac	N/A	0.83	0.78	0.77	0.78	CFM

Figure 83: Dynamometer 3 - Engine 2595 - Dynamometer Check Results

5.3.3. TEARDOWN ANALYSIS

The following section discusses the teardown analysis results of the third PEO coated and dynamometer tested engine – engine 2595. This engine trial completed the full 18 hour dynamometer test. However, it did experience a unique wear pattern which will further be examined and discussed. It is important to note the CMM was unavailable to conduct after-dynamometer cylinder bore measurements for diameter and straightness of this engine trial. A macroscopic display of the wear in each bore is provided in Figure 84.

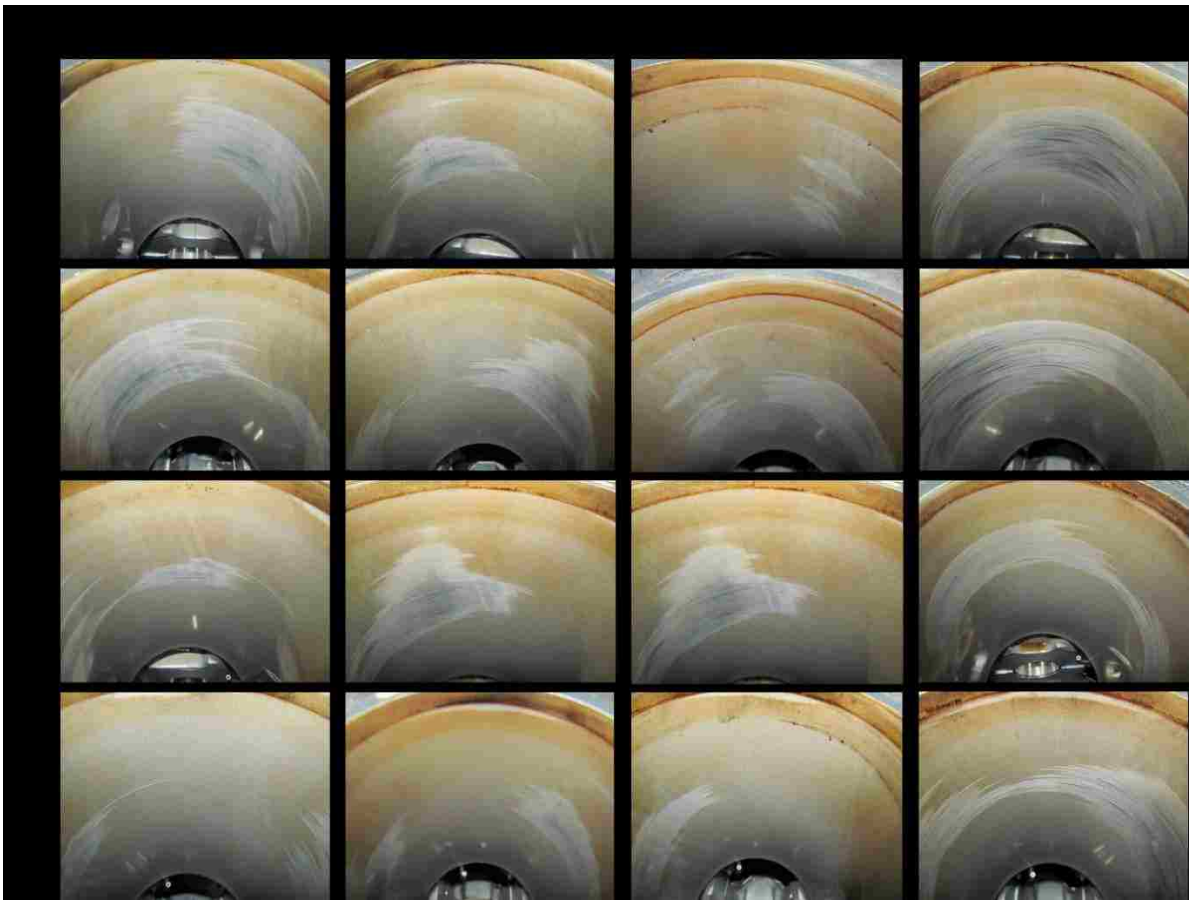

Figure 84: Dynamometer 3 - Engine 2595 - Teardown - Cylinders

5.3.3.1. SURFACE WEAR

Depression at TDC in most areas throughout all four bores was found to be relatively small at around 10 µm of depression or even as low as 0 µm in some locations. However, at one location in each bore, the surface depressions reached extremely large values leading up a maximum of 150 µm. Profilometry curves for the profile over TDC are provided in Appendix A and a summary of their maximum values are displayed in Table 21.

Table 21: Dynamometer 3 - Engine 2595 - Maximum Values of Surface Depression via Wear at TDC

Dynamometer 3 (Engine 2595) – Maximum Depression by Wear at TDC [µm]				
Location	**Cylinder 1**	**Cylinder 2**	**Cylinder 3**	**Cylinder 4**
Front	0	65	150	50
Right	100	0	10	10

Back	0	0	0	0
Left	10	15	10	12

Measuring the surface profiles of areas unaffected by the detrimental wear revealed a surface profile similar in values to measurements that were taken before the dynamometer test, as shown in Figure 85.

Before Dyno	Average	0.57	0.46	1.07	0.54	0.50	1.22	0.49	0.46	1.04	0.61	0.42	1.40
	Standard Deviation	0.02	0.04	0.04	0.04	0.01	0.06	0.05	0.12	0.09	0.09	0.05	0.08

Figure 85: Dynamometer 3 - Engine 2595 - Surface Profile - Statistical Comparison - Before & After Dynamometer

The unique wear pattern was measured and revealed distinct fluctuations in surface height ranging up to 9 µm (Cylinder 4, Front) from peak to valley in some areas. This pattern visible in Figure 86, Figure 87, Figure 88, and Figure 89.

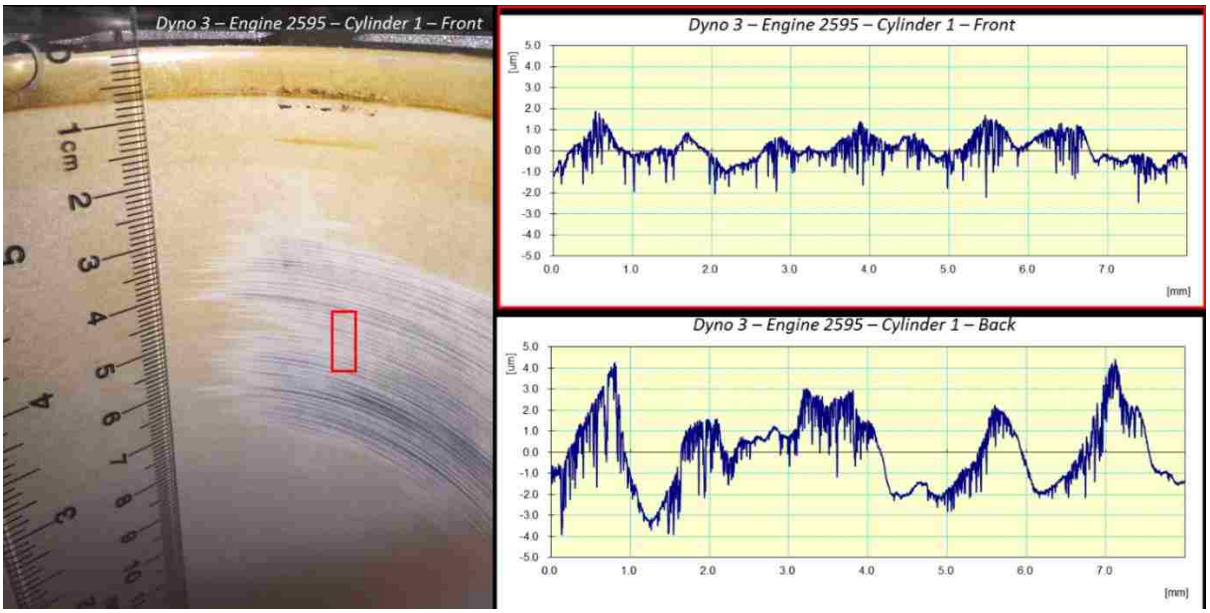

Figure 86: Dynamometer 3 - Engine 2595 - Profilometry - Ring Flutter - Cylinder 1

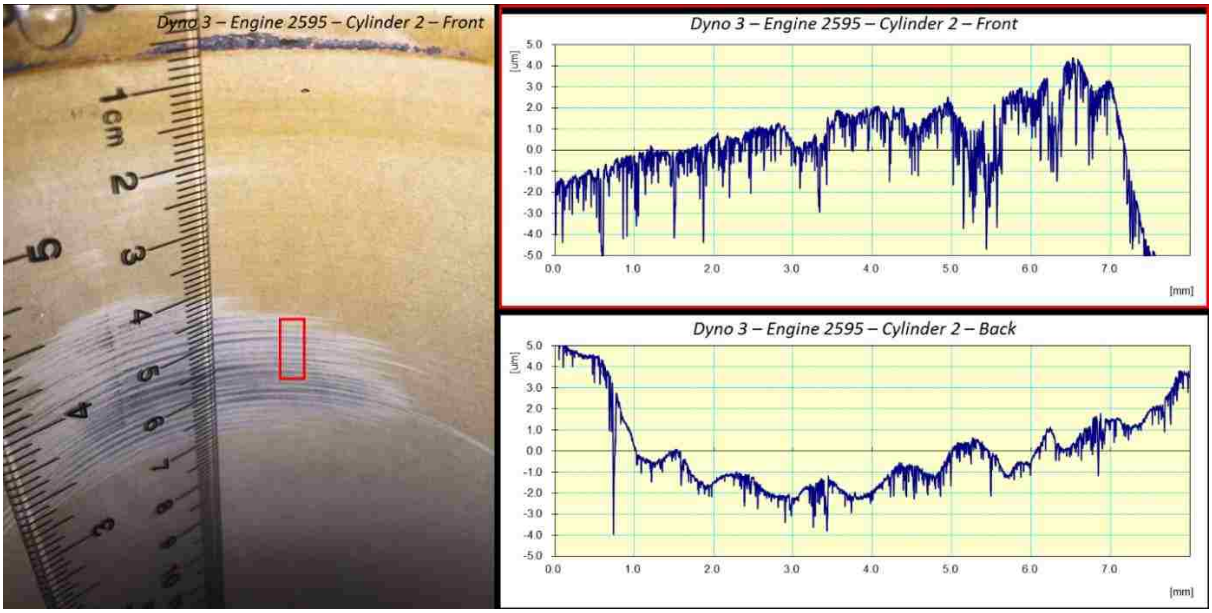

Figure 87: Dynamometer 3 - Engine 2595 - Profilometry - Ring Flutter - Cylinder 2

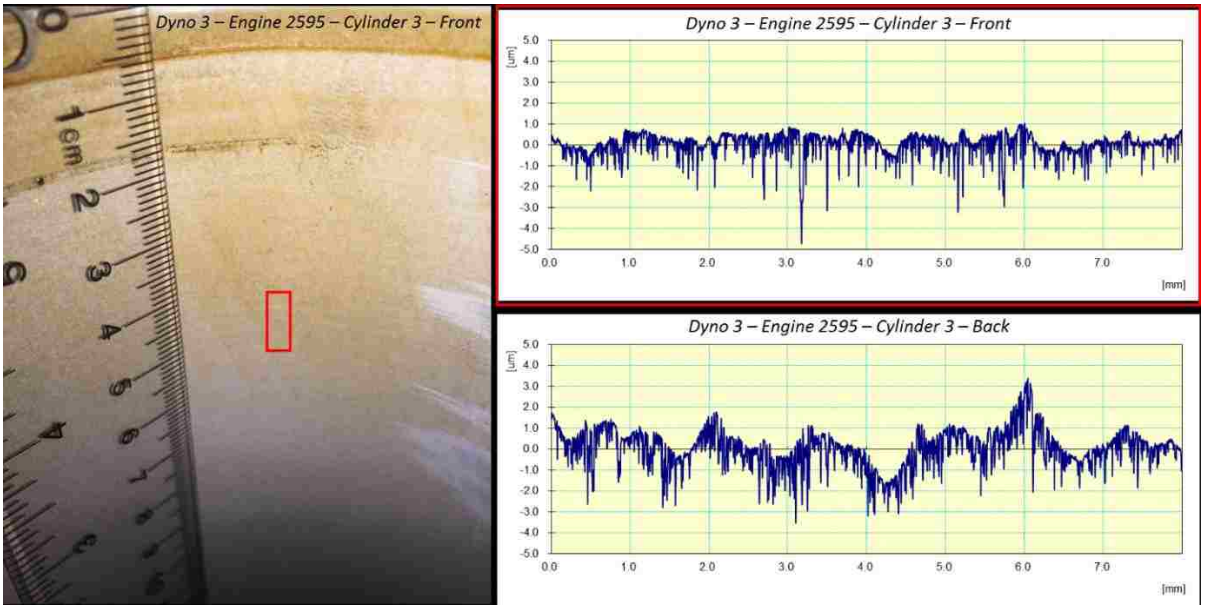

Figure 88: Dynamometer 3 - Engine 2595 - Profilometry - Ring Flutter - Cylinder 3

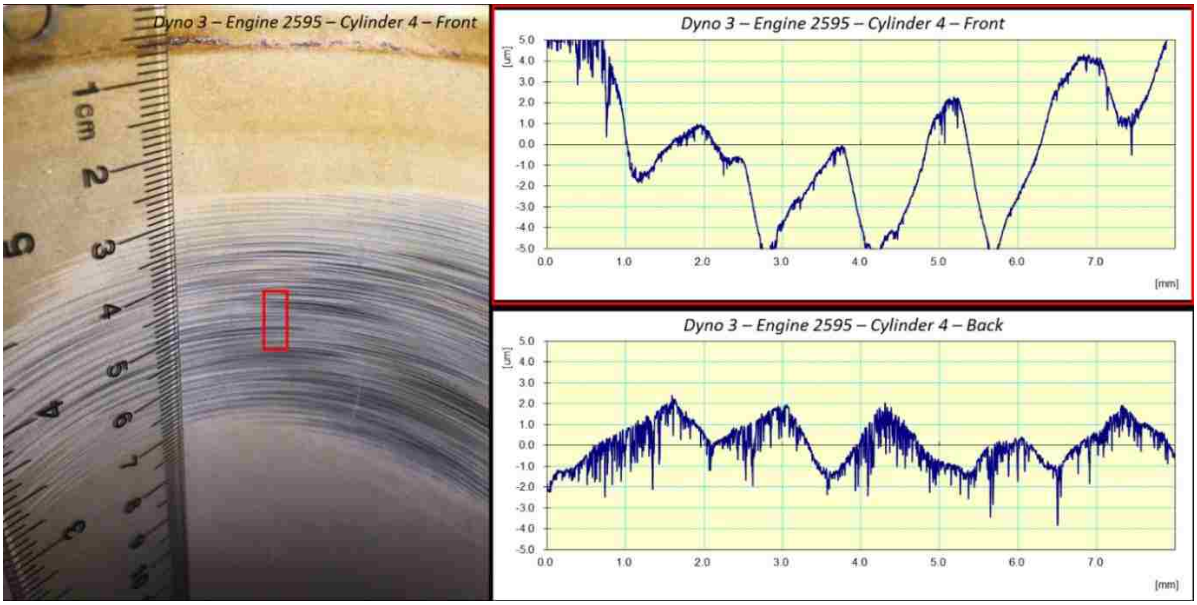

Figure 89: Dynamometer 3 - Engine 2595 - Profilometry - Ring Flutter - Cylinder 4

5.3.3.2. PISTON SKIRTS

The piston skirts experienced acute wear, mostly on the major thrust side. On the major thrust side, there was noticeable discoloration at the bottom of the Nanofriks1 coated piston skirts as pictured in Figure 90. In addition to the discoloration, piston 1 and 2 major thrust sides, which experienced the largest piston to bore clearances, had faint linear marks in the direction of piston travel extending over the entire piston skirt. Moreover, piston 4, which experienced the smallest bore clearance, had the piston skirt coating polished off at the bottom edge on the major thrust side.

Figure 90: Dynamometer 3 - Engine 2595 - Teardown - Piston Skirts - Major Thrust Side

The minor thrust side of all pistons experienced little to no wear as seen in Figure 91. Pistons 2 and 4 had faint linear markings on their minor thrust sides.

Figure 91: Dynamometer 3 - Engine 2595 - Teardown - Piston Skirts - Minor Thrust Side

5.3.3.3. PISTON RINGS

The upper compression rings did not experience any material transfer from the PEO coated bores. However, there was noticeable carbon debris scattered over the entire outside diameter surface of the piston rings as determined through EDS analysis, pictured in Figure 92.

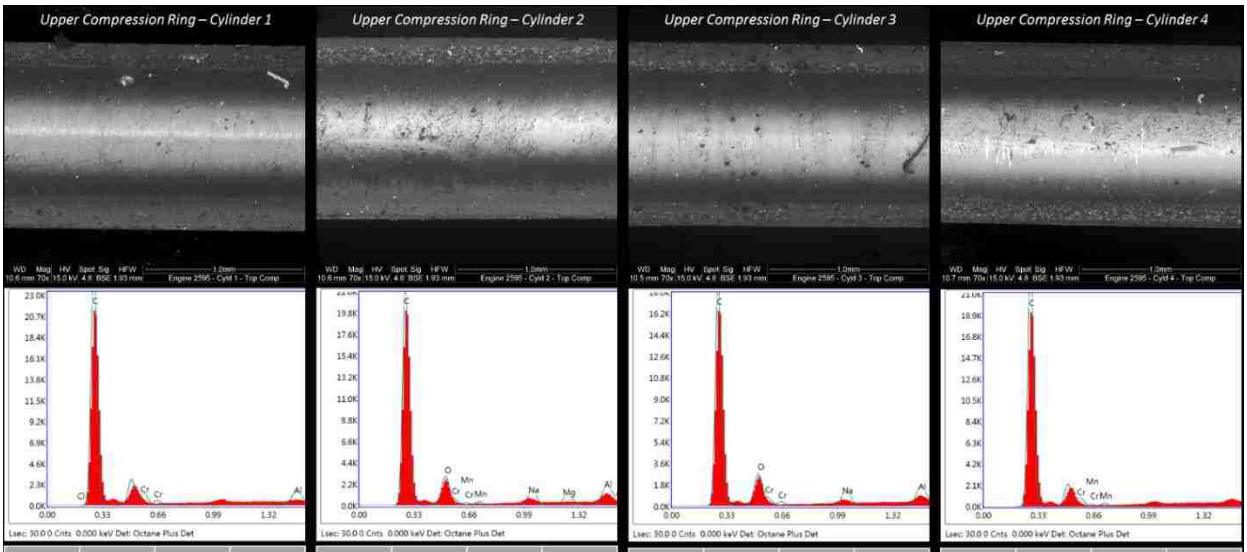

Element	Weight %	Atomic %	Error %
C K	85.72	94.87	6.68
CrL	1.93	0.49	12.21
ClK	12.35	4.63	13.38

Element	Weight %	Atomic %	Error %
C K	76.60	90.81	4.82
O K	8.09	7.20	10.80
AlK	1.39	0.73	23.98
MoL	3.81	0.57	56.19
AtM	10.11	0.69	28.14

Element	Weight %	Atomic %	Error %
C K	73.97	89.83	4.65
O K	9.69	8.84	10.72
MoL	1.96	0.30	64.16
AtM	14.31	0.99	24.09

Element	Weight %	Atomic %	Error %
C K	98.76	99.71	3.98
CrL	1.24	0.29	22.20

Figure 92: Dynamometer 3 - Engine 2595 - Upper Compression Rings - SEM & EDS - Debris

All of the lower compression rings used in this engine did not experience any material transfer on their sliding surfaces. However, there were varying amounts of debris collected under the bottom groove as visible in Figure 93. Most of the debris collected under the piston ring groove was made up of elemental carbon, aluminum, and oxygen. These elements lead to the assumption that oxidized oil and worn material from the PEO coated cylinder bores was collected in this area. The lower compression ring used in cylinder 3 had the greatest quantity of debris collected.

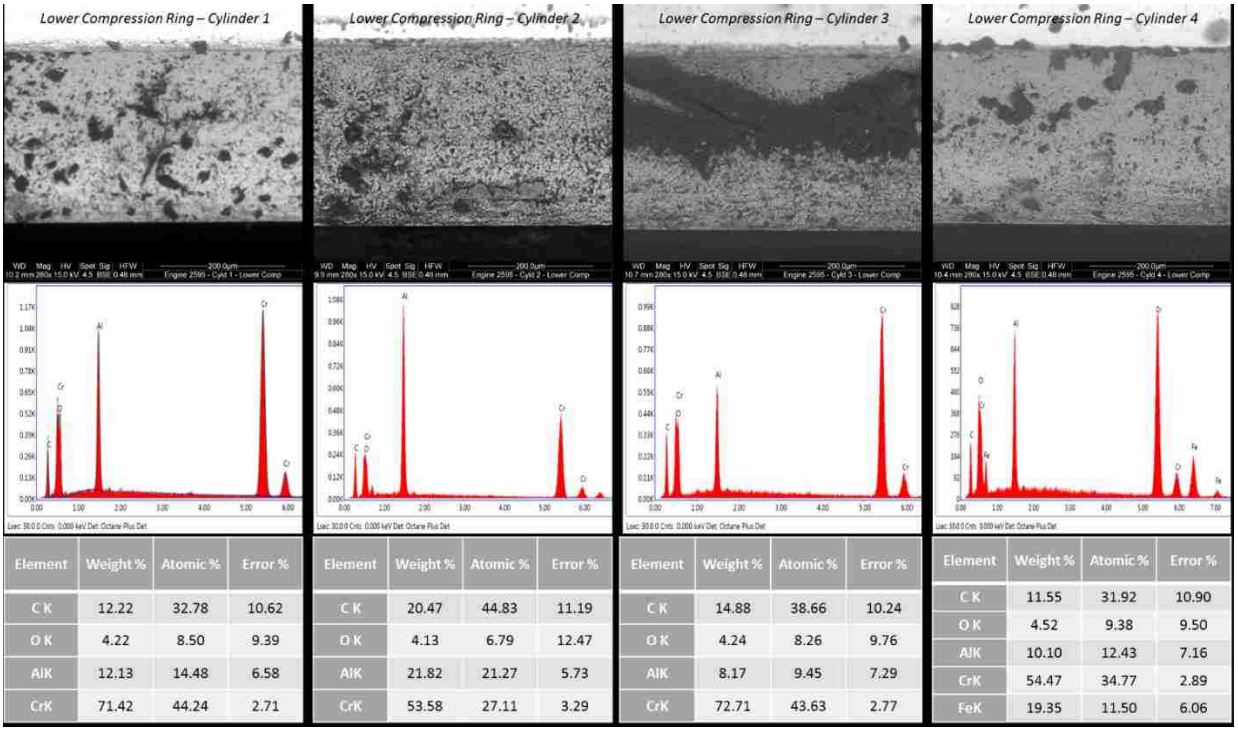

Element	Weight %	Atomic %	Error %
C K	12.22	32.78	10.62
O K	4.22	8.50	9.39
AlK	12.13	14.48	6.58
CrK	71.42	44.24	2.71

Element	Weight %	Atomic %	Error %
C K	20.47	44.83	11.19
O K	4.13	6.79	12.47
AlK	21.82	21.27	5.73
CrK	53.58	27.11	3.29

Element	Weight %	Atomic %	Error %
C K	14.88	38.66	10.24
O K	4.24	8.26	9.76
AlK	8.17	9.45	7.29
CrK	72.71	43.63	2.77

Element	Weight %	Atomic %	Error %
C K	11.55	31.92	10.90
O K	4.52	9.38	9.50
AlK	10.10	12.43	7.16
CrK	54.47	34.77	2.89
FeK	19.35	11.50	6.06

Figure 93: Dynamometer 3 - Engine 2595 - Lower Compressing Ring - Groove - SEM & EDS - Debris

An important observation is the height of wear on the lower compression ring sliding surfaces. The original surface profile of the lower compression rings is worn to create a seemingly smooth surface visible from a SEM visual inspection. A visual representation for the difference between the original and worn surface profiles is evident in Figure 94 and Figure 95.

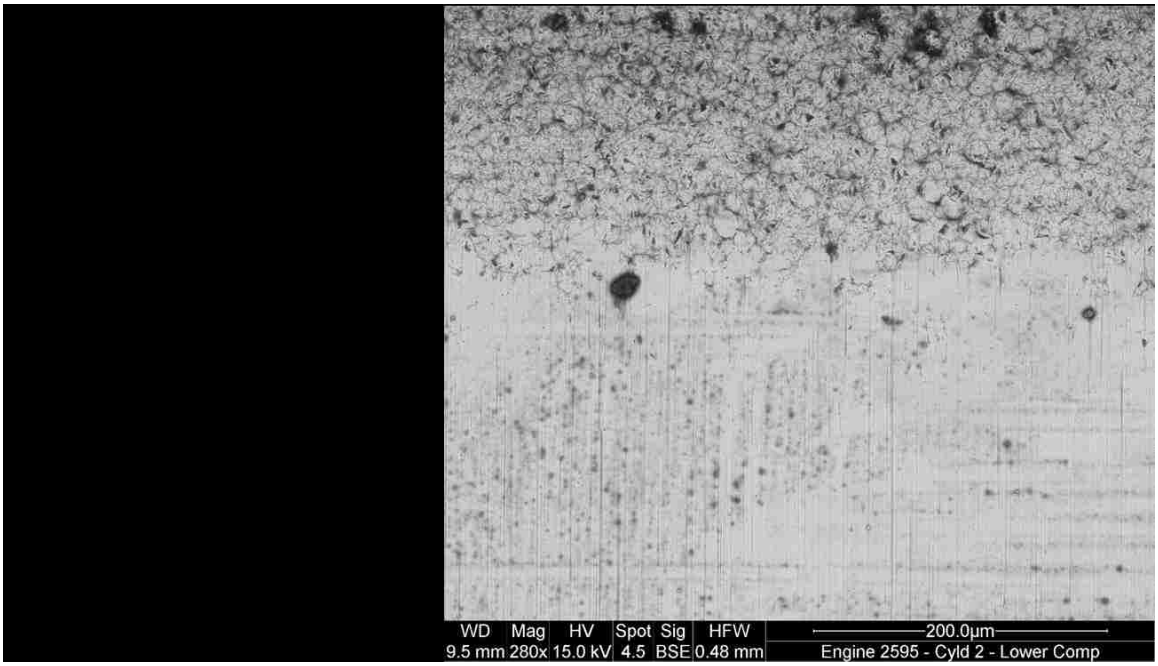

Figure 94: Dynamometer 3 - Engine 2595 - Teardown - Piston Rings - Lower Compression Rings - Wear - Cylinder 2

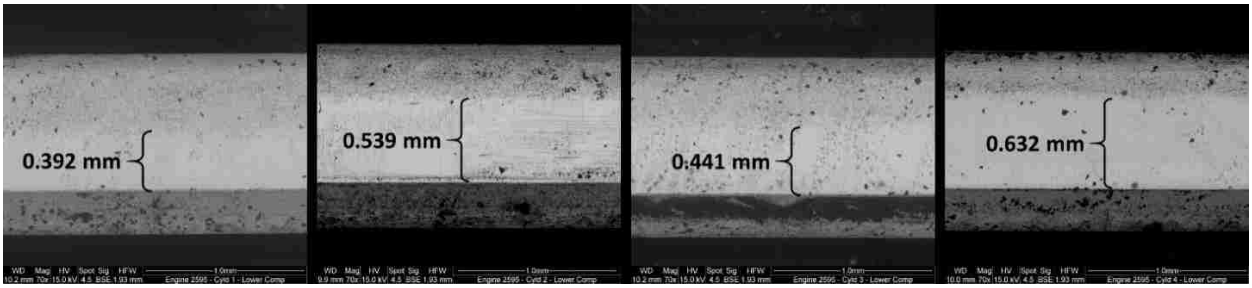

Figure 95: Dynamometer 3 - Engine 2595 - Teardown - Lower Compression Rings - Wear Height

5.4. TRIAL 4 – ENGINE 2595R

The fourth and final engine trial in this series utilized a cylinder block previously used in this PEO coating engine trial series. The cylinder block was used in the third engine trial and had the coating stripped after test completion. The block had then been recoated and underwent a new engine trial test which will be discussed in this section. This engine trial served the purpose for testing new independent test parameters as well as displaying proof of concept that a cylinder block with PEO coated cylinder bores may be overhauled after being damaged and continue serving as a functional engine component. It is important to note that this engine experienced a failure due to destroyed crankshaft journal bearings at

8.48 test hours which was attributed to an engine assembly issue as all the engine components were reused from the third engine trial. The fragmentation of the journal bearings at failure affected the teardown analysis results as the fragments caused damage to internal components and contaminated the recirculating oil.

5.4.1. PRE-TEST PARAMETER SELECTION

The following section discusses the independent variables applied in this engine trial. The decisions for selection of these parameters were made by applying knowledge gained from results and analysis of the previous engine trials in this study.

5.4.1.1. SURFACE PROFILE

Flex Honing brushes were used to modify the surface profile and achieve surface features that would be acceptable for a fired-engine test, a summary of those surface profile values is provided in Figure 96. The surface profile that was able to be achieved while maintaining sufficient coating thickness and target diameter had Rpk values that were higher than 0.5 µm, which were undesirable. However, a positive factor of the surface profile was the Rvk values that were achieved, which provided a lot of potential for oil retention capacity with no Rvk value lower than 1.91 µm and an average of 2.63 µm throughout all the cylinders.

Stroke Length: 8mm													
Cylinder No.	Position	Variable											
		Ra (micron)			Rpk (micron)			Rvk (micron)			Oil Retention Volume (µm^3/µm^2)		
		Top	Middle	Bottom	Top	Middle	Bottom	Top	Middle	Bottom	Top	Middle	Bottom
1	Back	0.93	0.74	0.88	0.94	0.45	0.47	2.74	2.39	2.59	0.23	0.19	0.22
2		0.79	0.71	0.82	0.55	0.25	0.50	1.91	2.18	2.85	0.11	0.16	0.20
3		1.09	0.71	0.75	1.05	0.48	0.45	3.26	1.99	1.94	0.26	0.14	0.17
4		0.94	0.85	0.97	0.84	0.79	0.91	2.49	3.63	3.53	0.22	0.25	0.23

Figure 96: Dynamometer 4 - Engine 2595R - Surface Profile Values – Before Dynamometer

5.4.1.2. BORE DIAMETER, COATING THICKNESS, & CLEARANCE

The type B PEO coated bore diameters targeted for this engine were to be larger than specification and combined with pistons in the mid-range of their specified diameter tolerance. This grouping created relatively large clearances in each cylinder, ranging from 45 µm to 49 µm in total, or 22.5 µm to 24.5 µm from piston gauge point to bore wall on each side, shown in Table 23. Average diameter, coating type, and coating thickness for each bore in engine trail 4 is summarized in Table 22 along with a graphical representation of bore straightness provided in Figure 97.

Table 22: Dynamometer 4 - Engine 2595R - Diameter, Coating Type, and Coating Thickness

Cylinder	1	2	3	4
Avg. Diameter (mm) – CMM	87.532	87.531	87.533	87.534
Coating Type	Type B	Type B	Type B	Type B
Coating Thickness (µm)	7 - 9	7 - 8.5	7 - 9	8 – 10.5

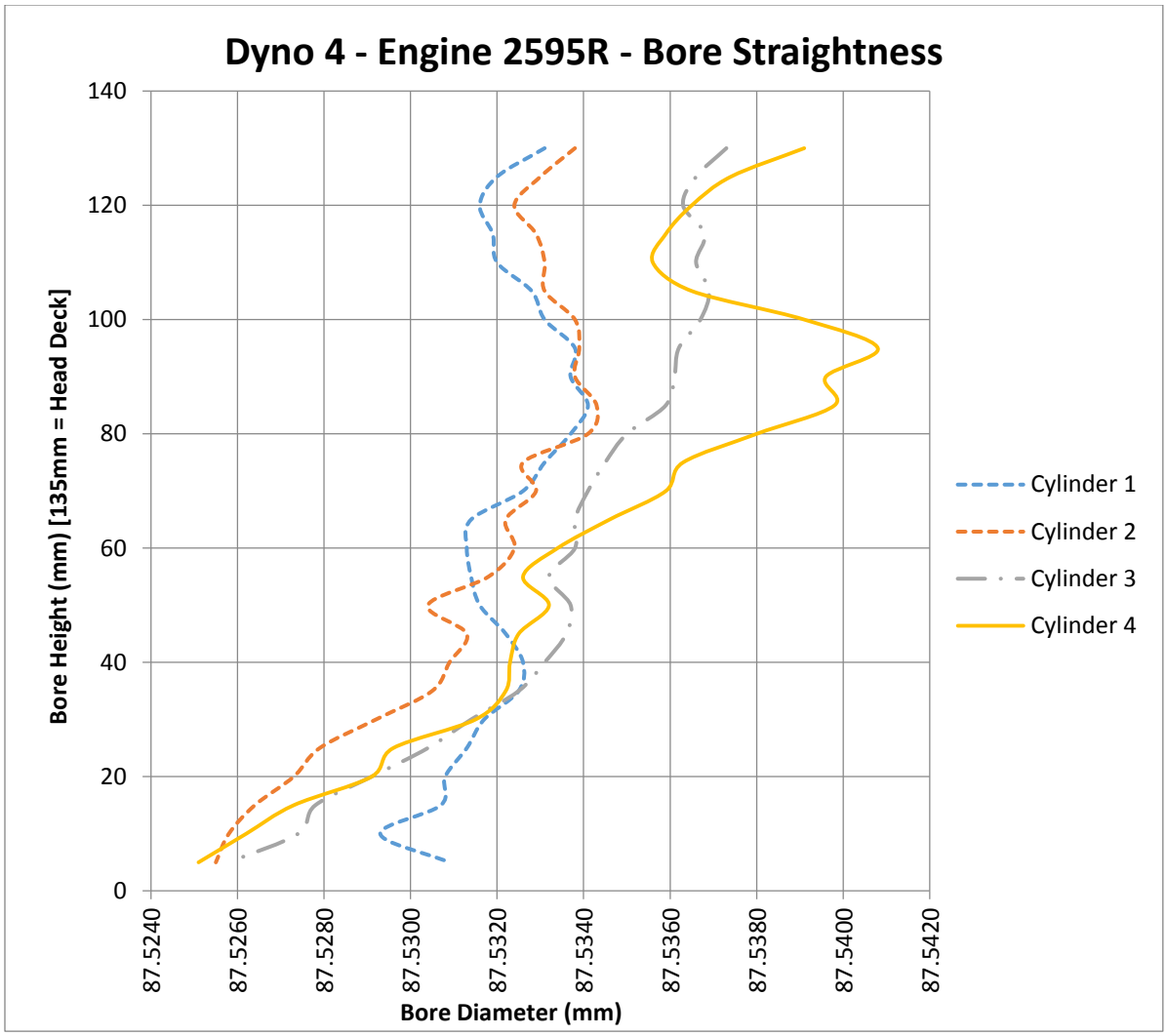

Figure 97: Dynamometer 4 - Engine 2595R - Bore Straightness – Before Dynamometer Test

Table 23: Dynamometer 4 - Engine 2595R - Clearance

Total Clearance - Both sides (mm)	Cylinder	1	2	3	4
	Piston Size	87.485	87.486	87.489	87.485
	Clearance	0.0470	0.0450	0.0440	0.0490

5.4.1.3. PISTON RINGS

Two different sets of piston ring packs were used in this engine trial. Cylinder 1 to 3 had the same piston ring packs while cylinder 4 had a mix of both experimental and production

piston ring parts to further study the effect of piston ring materials on PEO coated bore with large piston to bore clearances. A summary of the piston rings used in each bore is provided in Table 24.

Table 24: Dynamometer 4 - Engine 2595R - Piston Ring Selection

Cylinder	1	2	3	4
Upper Compression	Diamond-like Carbon	Diamond-like Carbon	Diamond-like Carbon	Chromium Nitride PVD (IN14A)
Lower Compression	Chrome Plated	Chrome Plated	Chrome Plated	Chrome Plated
Oil Control	Diamond-like Carbon	Diamond-like Carbon	Diamond-like Carbon	Nitriding
Oil Spacer	Diamond-like Carbon	Diamond-like Carbon	Diamond-like Carbon	Nitriding

5.4.2. DYNAMOMETER TEST

The following section describes the results from dynamometer testing of the fourth engine in the PEO coated cylinder bore study.

5.4.2.1. DYNAMOMETER CHECKS

5.4.2.1.1. 0 TEST HOURS

Dynamometer checks conducted at the 0 test hour mark revealed high compression and low leak-down numbers, signifying a good seal within the combustion chamber even with the high clearances between piston and bore.

5.4.2.1.2. 4.5 TEST HOURS

The engine operated normally with no issues, all monitoring parameters were within safe operating conditions in the first stage of this test. At 4.5 test hours, the test was paused for scheduled engine checks, the values for which are provided in Figure 99. Although there

was a slight degradation in combustion chamber sealing that was determined via a reduction in compression pressure and an increase in leak-down results, the numbers were still above target values. Dynamic sealing was also determined to be within normal operating conditions based on the array of blow-by results obtained.

A borescope inspection did not display any visible wear in any of the cylinders. PEO coating was still visible to be fully intact on the bore walls as seen in Figure 98.

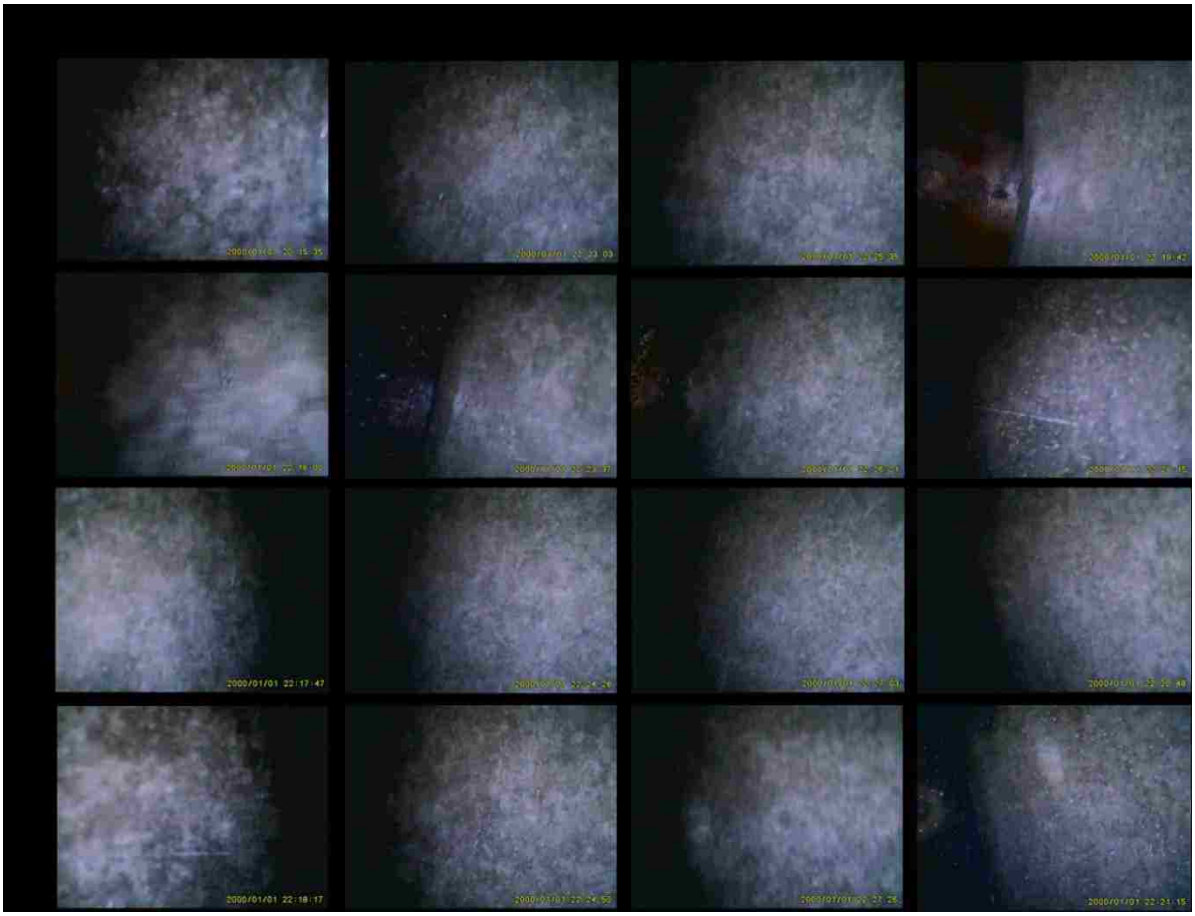

Figure 98: Dynamometer 4 - Engine 2595R - Borescope - 4.5 Test Hours

5.4.2.1.3. 8.48 TEST HOURS

The engine experienced an automatic shutdown at 8.48 test hours triggered by high oil sump temperature. The high oil sump temperature was accompanied by loud engine knocking. The engine was not run after this point and therefore only a static leak-down test and borescope inspection was able to be completed before engine teardown and analysis.

The leak-down test that was able to be performed showed values that indicated good static combustion chamber sealing before the engine being torn down to investigate cause of failure and bore wear.

Cylinder	Test Type	Test Hours			UNITS
		0	4.5	8.48	
1	Compression	218	212	N/A	PSI
	Leakdown	6	6	8	%
2	Compression	215	215	N/A	PSI
	Leakdown	7	6	6	%
3	Compression	212	212	N/A	PSI
	Leakdown	7	9	8	%
4	Compression	215	212	N/A	PSI
	Leakdown	8	8	10	%
Blow-by (CFM)	1500 rpm @ 76 ft lb	N/A	0.63	N/A	CFM
	1500 rpm @ 30 ft lb	N/A	0.23	N/A	CFM
	3000 rpm @ 0 inHg ManVac	N/A	0.91	N/A	CFM

Figure 99: Dynamometer 4 - Engine 2595R - Dynamometer Check Results

5.4.3. TEARDOWN ANALYSIS

The following section discusses the results of the test through measurements and visual inspection to determine the wear resistance of the PEO coating and combination of independent experiment parameters used. Due to failure and disintegration of the journal bearings, subsequent measurements taken of the coated bore surfaces may have been affected due to fragmentation and oil contamination. A macroscopic display of bore wear is provided in Figure 100.

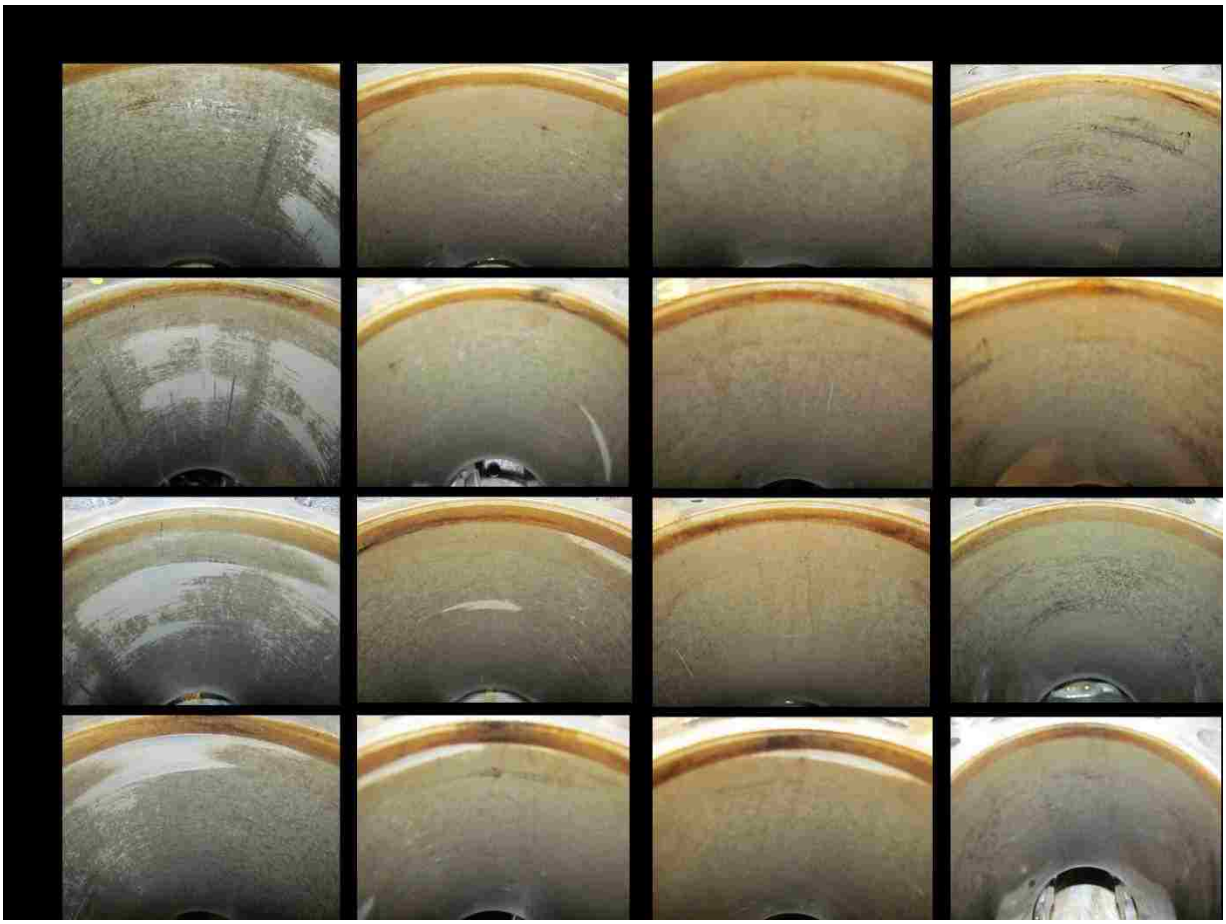

Figure 100: Dynamometer 4 - Engine 2595R - Teardown - Cylinders

The reason for failure was assumed to be engine parts or engine assembly and not due to the coated bores as there was not enough significant wear on the bore walls to cause such a failure. Journal bearings associated with cylinders 1 and 4 were destroyed. The destroyed journal bearing associated with cylinder 4 is pictured in Figure 101. Cylinders 1 and 4 had also shown the most significant wear by visual inspection. It is assumed that the journal bearings fragmented into their respective cylinders consequently affecting the PEO coated bore surfaces.

Figure 101: Dynamometer 4 - Engine 2595R - Journal Bearing - Cylinder 4

5.4.3.1. SURFACE WEAR

Each cylinder was subjected to various levels of wear during this dynamometer test. Cylinder 1 experienced the worst wear with delaminating PEO coating. In addition to PEO coating wear, scratch marks were visible on the major thrust side following direction of piston travel as seen in Figure 103. Cylinders 2 was subjected to minimal wear, mostly occurring by delamination at TDC of each bore on their minor thrust sides as pictured in Figure 102. Cylinder 3 had also experienced relatively minimal wear with delamination occurring at TDC on its minor thrust side, in addition to the onset of scratch marks located on the major thrust side in the direction of piston travel. Cylinder 4 began seeing linear markings and discoloration parallel to piston travel on the major and minor thrust sides which indicated piston slap occurring.

Figure 102: Dynamometer 4 - Engine 2595R - Teardown - Cylinders – Wear Marks – Minor Thrust Side

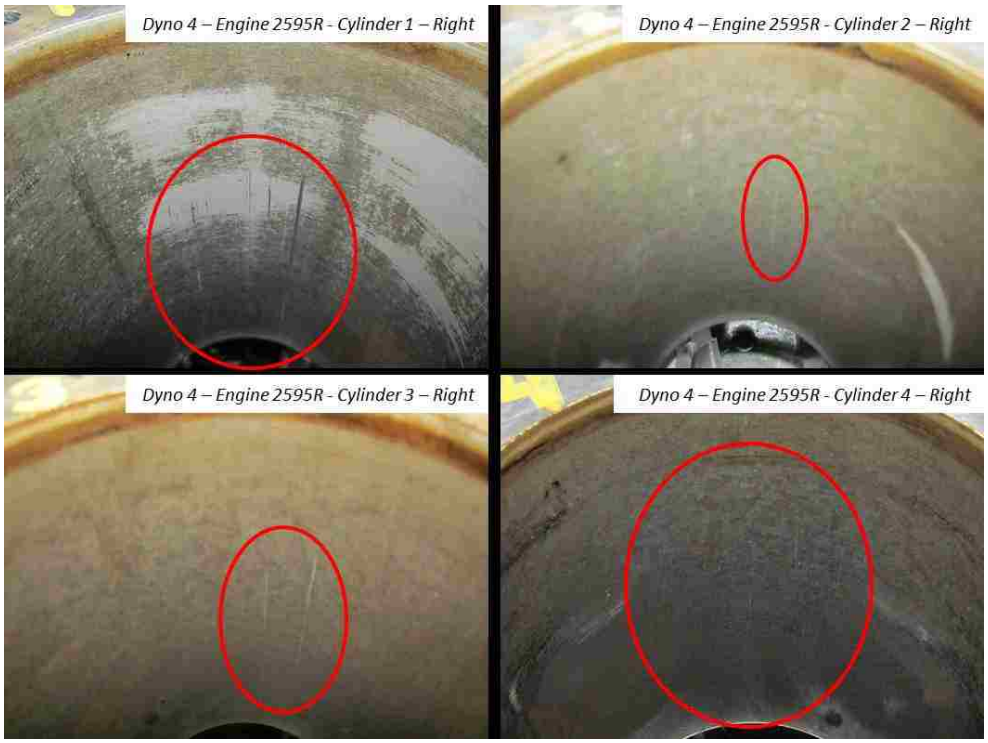

Figure 103: Dynamometer 4 - Engine 2595R - Teardown - Cylinders – Wear Marks – Major Thrust Side

Depression at TDC was minimal from most of the measurements taken and in some cases no visible depression at all as summarized in Table 25. Cylinder 3 experienced the most prominent depression by wear at TDC reaching values greater than 40 µm. Some minor ploughing was visible to have occurred on the left side of both cylinder 1 and 2, creating peaks reaching a maximum height of 13 µm as is visible in Appendix A - 49.

Table 25: Dynamometer 4 - Engine 2595R - Maximum Values of Surface Depression via Wear at TDC

Dynamometer 4 (Engine 2595R) – Maximum Depression by Wear at TDC [µm]				
Location	**Cylinder 1**	**Cylinder 2**	**Cylinder 3**	**Cylinder 4**
Front	0	15	20	10
Right	5	14	40	0
Back	0	0	0	0
Left	4	20	25	0

The surface profile measurement taken indicated that the bore surface became rougher after undergoing dynamometer testing. Ra and Rpk values increased, while Rvk values remained relatively similar as shown in Table 26.

Table 26: Dynamometer 4 - Engine 2595R - Surface Profile - Statistical Comparison - Before & After Dynamometer

Surface Profile Comparison		Cylinder											
		1			2			3			4		
		Ra	Rpk	Rvk	Ra	Rpk	Rvk	Ra	Rpk	Rvk	Ra	Rpk	Rvk
Before Dyno	Average	0.85	0.62	2.57	0.77	0.43	2.31	0.85	0.66	2.40	0.92	0.85	3.22
	Standard Deviation	0.08	0.23	0.14	0.05	0.13	0.40	0.17	0.28	0.61	0.05	0.05	0.52
After Dyno	Average	1.18	1.03	3.54	0.78	0.69	2.32	0.95	0.72	2.69	1.06	0.70	3.07
	Standard Deviation	0.42	1.02	1.34	0.07	0.23	0.57	0.21	0.12	1.33	0.25	0.30	0.90

Bore shape of each cylinder remained relatively close to the measurements that were taken before dynamometer testing as shown in Figure 104, Figure 105, Figure 106, and Figure 107. Cylinder 1 experienced the worst bore deformation with a maximum dimensional change of 7.30 µm and an average of 1.98 µm. These values closely relate to the quantity of visible wear as Cylinder 1 also experienced significantly more delamination and scratch marks than the other bores. Cylinders 2 through 4 did not experience large dimensional changes and retained the profile of the original bore throughout the test. The minor dimensional changes that Cylinders 2, 3 and 4 did experience are noted in Table 27.

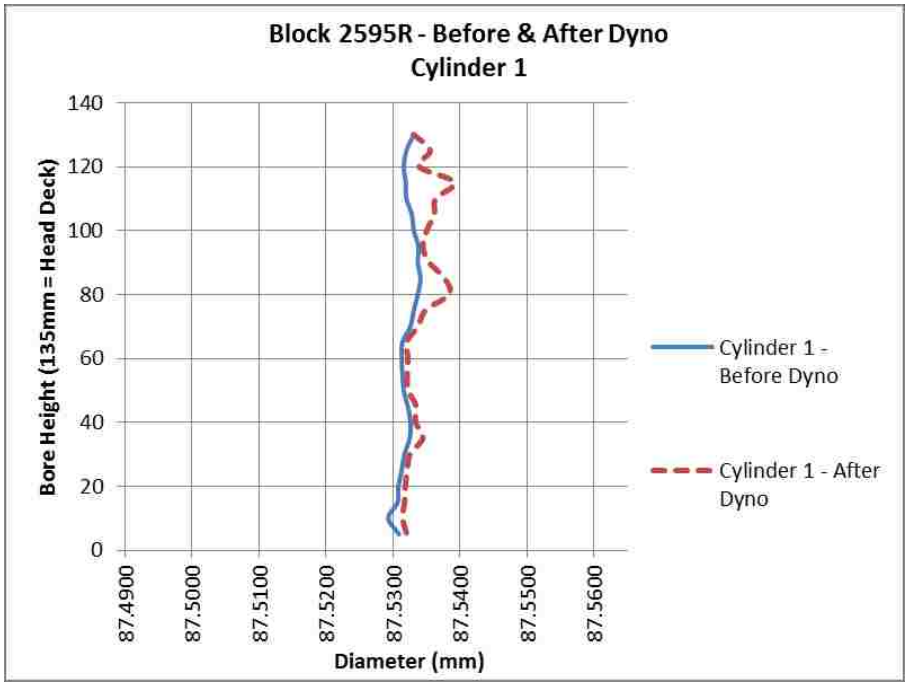

Figure 104: Dynamometer 4 - Engine 2595R - Bore Dimensional Comparison - Before & After Dynamometer - Cylinder 1

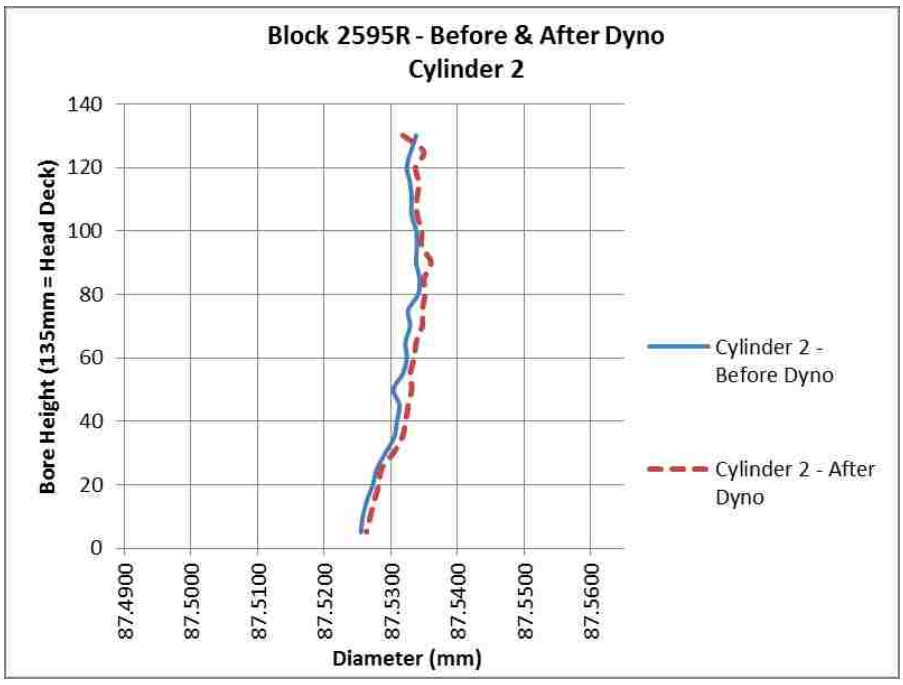

Figure 105: Dynamometer 4 - Engine 2595R - Bore Dimensional Comparison - Before & After Dynamometer - Cylinder 2

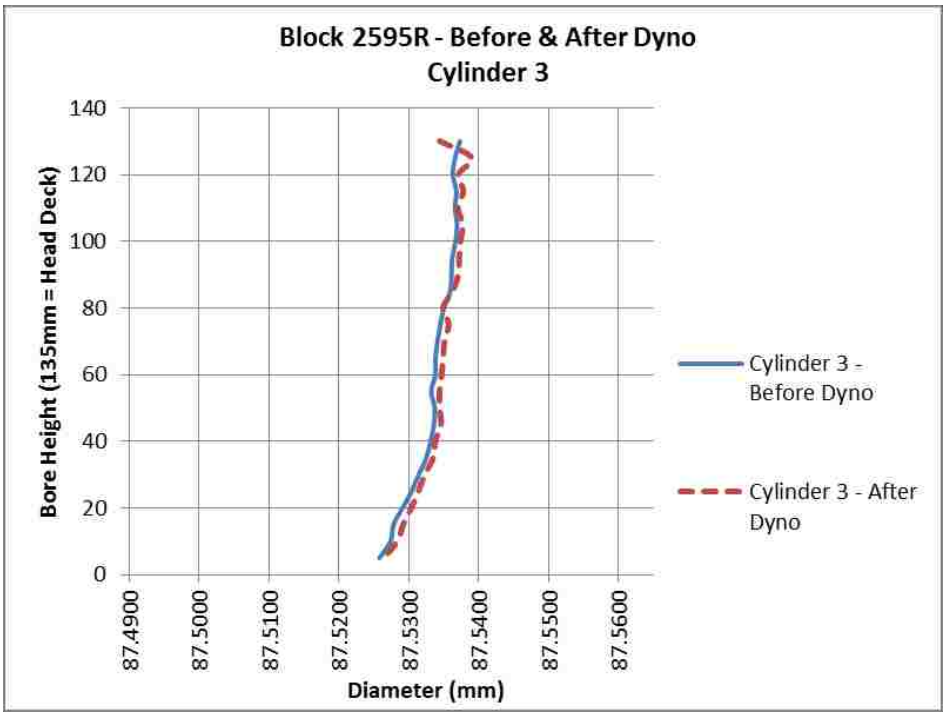

Figure 106: Dynamometer 4 - Engine 2595R - Bore Dimensional Comparison - Before & After Dynamometer - Cylinder 3

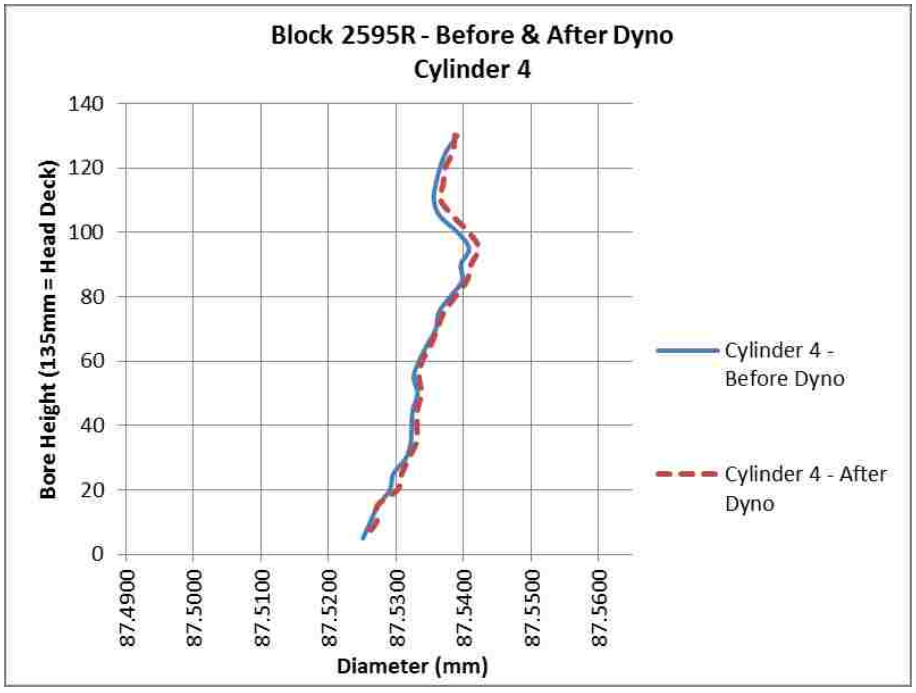

Figure 107: Dynamometer 4 - Engine 2595R - Bore Dimensional Comparison - Before & After Dynamometer - Cylinder 4

Table 27: Dynamometer 4 - Engine 2595R - Bore Dimension Statistical Comparison - All Cylinders

Difference - Bore Dimensions - Before & After Dynamometer				
(µm)	**Cylinder**			
	1	**2**	**3**	**4**
MAX	7.30	2.70	2.40	1.90
MIN	0.00	0.00	-0.10	0.00
AVG	1.98	1.21	0.90	0.85
STANDEV	1.61	0.56	0.46	0.46

5.4.3.2. PISTON SKIRTS

The piston skirts in this engine trial experienced varying levels of wear, closely correlating to the quantity and severity visible on their respective bore counter surfaces. Cylinder 1 major thrust side skirt coating was polished off while the minor thrust side was mostly intact with the exception of linear markings along the entire skirt face as pictured in Figure 108.

Figure 108: Dynamometer 4 - Engine 2595R - Teardown - Piston Skirts - Piston 1

Pistons 2 and 3 experienced similar wear. Both the major and minor thrust side coatings were unaffected by any wear with the exception of faint scratch marks along the skirt faces as shown in Figure 109 and Figure 110.

Figure 109: Dynamometer 4 - Engine 2595R - Teardown - Piston Skirts - Piston 2

Figure 110: Dynamometer 4 - Engine 2595R - Teardown - Piston Skirts - Piston 3

Piston 4 experienced severe wear on both the major and minor thrust side piston skirts, visible in Figure 111. Substantial longitudinal linear wear marks covered the surface of the skirt in addition to the visible fading of the skirt coating concentrated towards the center of the skirts, distinguishable by the color variation.

Figure 111: Dynamometer 4 - Engine 2595R - Teardown - Piston Skirts - Piston 4

5.4.3.3. PISTON RINGS

Correlating closely to visible wear on the bores, the respective piston rings experienced relatable material transfer and deposited foreign debris on their sliding surfaces. The upper compression ring from cylinder 1 had a noteworthy amount of carbon deposited on its surface as seen in Figure 112. In contrast, the upper compression rings from Cylinders 2, 3, and 4 did not have any material transfer or deposited carbon on their sliding surfaces, as pictured in Figure 113. It is important to note that the upper compression ring for cylinder 4 was Chromium Nitride PVD coated while the other rings were DLC coated rings. The variation in piston ring material did not display notable differences on piston ring surface through material transfer or debris deposits.

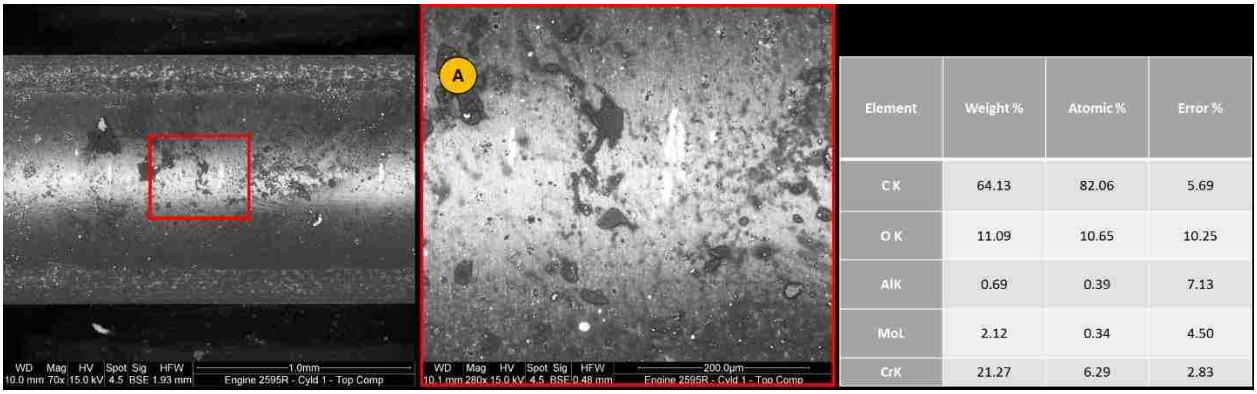

Element	Weight %	Atomic %	Error %
C K	64.13	82.06	5.69
O K	11.09	10.65	10.25
Al K	0.69	0.39	7.13
Mo L	2.12	0.34	4.50
Cr K	21.27	6.29	2.83

Figure 112: Dynamometer 4 - Engine 2595R - Upper Compression Ring - Cylinder 1 - SEM & EDS

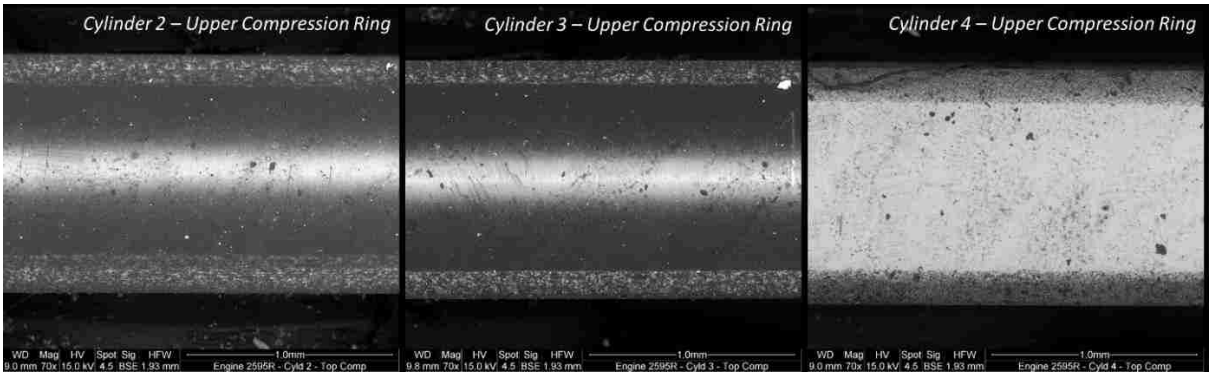

Figure 113: Dynamometer 4 - Engine 2595R - Upper Compression Rings - Cylinder 2-4

All lower compression rings used in this engine trial had debris with high weight percentage of elemental carbon trapped under the groove of the ring. Lower compression rings from Cylinders 1, 2, and 3 had similar quantities of carbon debris trapped under the

ring groove. Cylinder 4 had a significantly higher amount of carbon debris trapped under its ring groove with some of it also deposited on its sliding surface. The wear height was similar throughout all four lower compression rings, distinguishable by the variation in surface pattern. SEM and EDS analysis of the trapped carbon under the lower compression ring piston ring grooves is shown in Figure 114 and Figure 115.

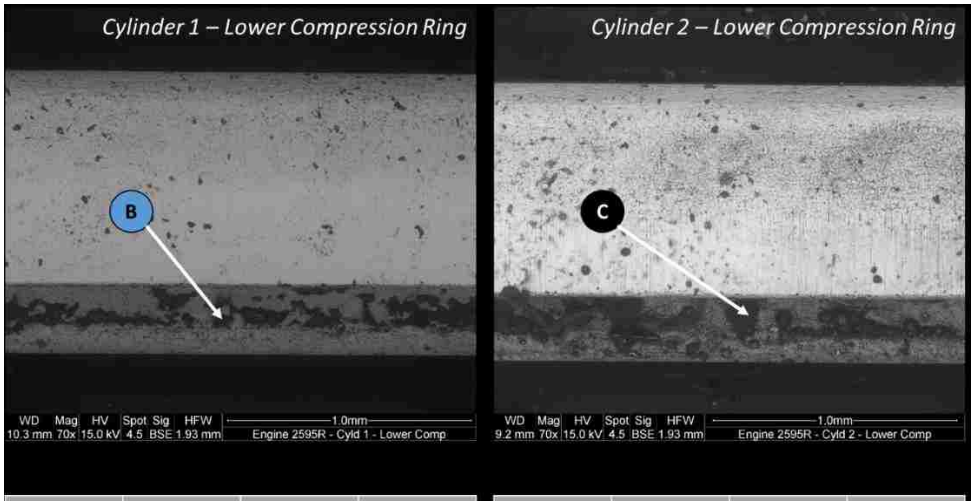

Element	Weight %	Atomic %	Error %
C K	12.45	33.42	10.75
O K	4.10	8.26	10.25
Al K	11.46	13.69	6.75
Cr K	71.98	44.62	2.76

Element	Weight %	Atomic %	Error %
C K	21.05	49.26	10.11
O K	3.80	6.67	12.13
Al K	6.87	7.16	7.96
Cr K	68.28	36.91	3.15

Figure 114: Dynamometer 4 - Engine 2595R - Lower Compression Rings - Cylinder 1 & 2 - SEM & EDS

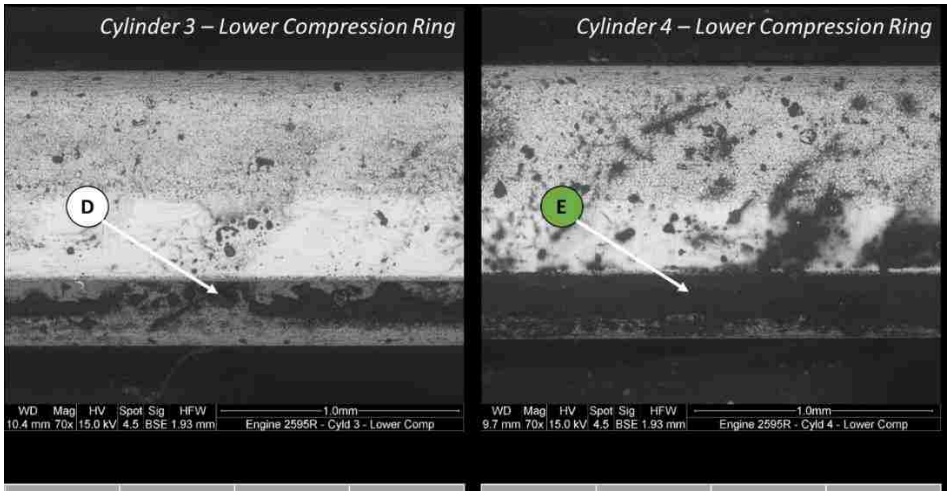

Element	Weight %	Atomic %	Error %
C K	21.50	49.08	9.69
O K	3.34	5.72	11.26
Al K	11.42	11.60	6.29
Cr K	63.74	33.60	2.75

Element	Weight %	Atomic %	Error %
C K	30.95	58.43	9.76
O K	4.47	6.33	12.10
Al K	17.50	14.71	5.37
Cr K	47.08	20.53	3.05

Figure 115: Dynamometer 4 - Engine 2595R - Lower Compression Rings - Cylinder 3 & 4 - SEM & EDS

CHAPTER 6

6. DISCUSSION

The following section summarizes and discusses the results obtained throughout the study in order to distinguish factors that improved on coating wear resistance. Each of the controlling parameters will be mentioned and compared relative to all the dynamometer tests conducted. It is important to note there were many varying parameters in each test that may have influenced the results and therefore those results are trend-based more so than providing numerical value outcomes for each independent variable.

6.1. SUMMARY

This section provides an overview and summary of the controlling parameters in each test iteration along with their dynamometer test results. Values associated with surface profile provided in the following summary are an overall average of all positions and levels in all 4 cylinder bores of each engine test iteration. Figure 116 provides a comprehensive summary of the controlling parameters and test results.

CONTROLLING PARAMETERS						
Parameter	**Unit**		**Dyno 1**	**Dyno 2**	**Dyno 3**	**Dyno 4**
			Engine 2599	**Engine 2633**	**Engine 2595**	**Engine 2595R**
Bore Diameter	**mm**		Cylinder 1: 87.505 Cylinder 2: 87.504 Cylinder 3: 87.503 Cylinder 4: 87.502	Cylinder 1: 87.530 Cylinder 2: 87.530 Cylinder 3: 87.529 Cylinder 4: 87.509	Cylinder 1: 87.515 Cylinder 2: 87.520 Cylinder 3: 87.515 Cylinder 4: 87.510	Cylinder 1: 87.532 Cylinder 2: 87.531 Cylinder 3: 87.533 Cylinder 4: 87.534
Coating Type			Level A	Cylinder 1-2: Level B Cylinder 3-4: Level A	Level B	Level B
Coating Thickness	**µm**		5-10	10-12	8-10	7-10
Ra	**µm**	**Avg**	0.81	1.19	0.55	0.85
		Std.Dev	0.19	0.51	0.07	0.11
Rpk	**µm**	**Avg**	0.40	0.69	0.46	0.64
		Std.Dev	0.13	1.04	0.08	0.24
Rvk	**µm**	**Avg**	2.22	4.08	1.18	2.63
		Std.Dev	0.82	2.73	0.16	0.57
Oil Retention	**µm3/ µm2**	**Avg**	0.19	0.51	0.08	0.20
		Std.Dev	0.08	0.30	0.01	0.05
Clearance	**µm**		Cylinder 1: 16 - 40 Cylinder 2: 16 - 38 Cylinder 3: 15 - 37 Cylinder 4: 12 - 35	Cylinder 1: 21 - 61 Cylinder 2: 27 - 55 Cylinder 3: 29 - 56 Cylinder 4: 18 - 37	Cylinder 1: 25 Cylinder 2: 26 Cylinder 3: 23 Cylinder 4: 13	Cylinder 1: 47 Cylinder 2: 45 Cylinder 3: 44 Cylinder 4: 49
Piston Rings		**Upper Compression**	Chromium Nitride	DLC	DLC	Cylinder 1-3: DLC Cylinder 4 : CrN
		Lower	Zinc Phosphate	Chrome Plated	Chrome Plated	Chrome Plated
		Oil Ring Pack	Nitrided	DLC	DLC	Cylinder 1-3: DLC Cylinder 4 : Nitrided
POST-TEST RESULTS						
Test Time	**Hours**		9.67	9.50	18.00	8.48
TDC Deformation	**µm**		Cylinder 1: 25 - 50 Cylinder 2: 30 Cylinder 3: 25 - 50 Cylinder 4: 25 - 45	Cylinder 1: 3 - 35 Cylinder 2: 20 - 35 Cylinder 3: 30 - 100 Cylinder 4: 27 - 120	Cylinder 1: 0 - 100 Cylinder 2: 0 - 65 Cylinder 3: 0 - 150 Cylinder 4: 0 - 50	Cylinder 1: 0 - 5 Cylinder 2: 0 - 20 Cylinder 3: 0 - 40 Cylinder 4: 0 - 10
Piston Skirt Wear			Cylinders 1-4: Severe Scuffing/Galling	Cylinder 1-4: No wear	Cylinder 1: Minor Discoloration/Linear Marks Cylinder 2: Minor Discoloration/Linear Marks Cylinder 3: No Wear Cylinder 4: Minor Polish	Cylinder 1: Severe Polish/Linear Marks Cylinder 2: Faint Linear Marks Cylinder 3: Faint Linear Marks Cylinder 4: Severe Wear Marks
Bore Wear			Cylinders 1-4: Severe Scuffing	Cylinder 1: No wear Cylinder 2: No wear Cylinder 3: Delamination Cylinder 4: Delamination	Cylinder 1: Ring Flutter Cylinder 2: Ring Flutter Cylinder 3: Ring Flutter Cylinder 4: Significant quantity of ring flutter	Cylinder 1: Delamination/Linear Wear Marks Cylinder 2: Minor Delamination Cylinder 3: No Wear Cylinder 4: Minor Delamination
Piston Rings Material Transfer		**Upper Compression**	Cylinder 1-4: Aluminum and carbon transfer	Cylinder 1: No Transfer Cylinder 2: No Transfer Cylinder 3: Aluminum and carbon transfer Cylinder 4: No Transfer	Cylinder 1: No Transfer Cylinder 2: No Transfer Cylinder 3: No Transfer Cylinder 4: No Transfer	Cylinder 1: Minor quantity carbon transfer Cylinder 2: No Transfer Cylinder 3: No Transfer Cylinder 4: No Transfer
		Lower Compression	Cylinder 1-4: Aluminum and carbon transfer	Cylinder 1: No Transfer Cylinder 2: No Transfer Cylinder 3: Minor quantity aluminum and significant carbon transfer Cylinder 4: Minor aluminum and carbon	Cylinder 1: No Transfer Cylinder 2: Minor quantity trapped carbon Cylinder 3: Significant quantity trapped carbon Cylinder 4: No Transfer	Cylinder 1: Minor quantity trapped carbon Cylinder 2: Minor quantity trapped carbon Cylinder 3: Minor quantity trapped carbon Cylinder 4: Significant quantity trapped carbon
Limiting Factor			Clearance	Coating Level A	Ring Flutter	Journal Bearing Failure

Figure 116: Summary - Controlling Parameters & Results

6.2. COATING TYPE

A controlling parameter that had a significant influence on test results was coating type. There were only two different coating types available to implement within this study. However, these two coating types varied significantly in surface morphology by porosity size and porosity distribution. Coating A had relatively large porosities which were assumed to help with increased oil retention and promote lubricated sliding surfaces. However, the porosities were non-uniformly distributed over the surface. Coating B had much smaller porosities in comparison to coating A. However, the porosities in Coating B were uniformly spread out over the coating surface and at greater regularity.

6.2.1. ENGINE TRIAL 2

Following the poor performance of dynamometer test 1, many controlling parameters were modified for dynamometer test 2. For dynamometer test 2, it was undertaken to evaluate the direct effect of the coating types. All the controlling parameters were either the same or relatively similar for Cylinders 1, 2, and 3, with the exception of coating type. It is important to note that cylinder 4 had a piston-to-bore clearance much smaller than the rest of the cylinders, therefore it will be excluded from this discussion of direct comparison with regards to coating type.

Coating type among the three cylinders under direct comparison was coating level A for Cylinders 1 and 2, and Coating level B for Cylinder 3. A comparison of the three cylinders in discussion in provided in Table 28.

Table 28: Dynamometer 2 - Engine 2633 - Coating & Dynamometer Checks

Dynamometer 2				
Engine 2633				
Parameter		**Cylinder**		
		1	**2**	**3**
Coating Type		B	B	A
Leakdown (%)	**0 Hours**	4	4	4

	4.35 Hours	5	6	6
	9.5 Hours	5	6	30
Compression (PSI)	**0 Hours**	205	208	210
	4.35 Hours	200	200	200
	9.5 Hours	200	200	190
Visual Analysis of Bore		No Wear	No Wear	Delamination
Visual Analysis of Skirt		No Wear	No Wear	No Wear

Coating type B performed significantly better than coating type A. Severe coating wear occurred on cylinder 3 to such an extent that leak down results increased up to 30% from initial values of 4% and cylinder compression values dropped from 210 psi to 190 psi. Simultaneously, dynamometer check results for Cylinder 1 and 2 coated with PEO type B retained their good dynamometer check values in the same time frame.

Borescope inspection at the 4.35 test hour mark revealed the onset of wear through longitudinal wear marks on coating type A in Cylinder 3 as opposed to cylinders 1 and 2 with coating type B which did not display any signs of wear. Additionally, teardown analysis revealed substantial coating delamination in cylinder 3. Cylinders 1 and 2 did not experience detrimental wear and displayed uniform coating color and surface pattern throughout their respective bores.

Coating type B was determined to be a superior coating with respect to resisting cylinder bore wear in a fired-engine test through this direct comparison. The evenly distributed but smaller porosities had a more beneficial impact on cylinder bore tribological performance than the more sparsely distributed and larger size surface porosities.

6.3. CLEARANCE

A combination of bore diameter and respective piston size determined the clearance between piston skirts and bore wall in each cylinder. Although there was no control over piston gauge diameter sizes, bore diameter was an independent variable as it was able to be controlled. The test iterations conducted in this study covered a wide range of clearances that even surpassed both ends of production tolerance (25 – 45 μm) to investigate relatively extreme clearance cases.

Piston-to-bore clearance must be a compromised factor that takes into consideration the consequences of having too large or too small clearance distances. This comprise must be met in order to determine an effective solution between wear and engine efficiency. Smaller piston-to-bore clearances increase contact pressure of the piston rings which subsequently affect oil film formation, asperity contact, and frictional coefficients. The other end of the spectrum for piston-to-bore clearance is having a clearance distance that is too large which may reduce combustion chamber sealing, subsequently reducing engine efficiency, and increase opportunity for piston slap which may lead to wear issues as well as noise, vibration, and harshness concerns due to piston movement about its wrist pin [34].

The evaluation method for effect of piston-to-bore clearance included cross-sectional SEM assessment of cylinder bores, profilometry of wear regions, and visual analysis of cylinder bore and piston skirt wear. Clearance issues were evaluated through comparison of individual cylinders in the same trial engine, with engine trials 1 and 3 providing the greatest opportunity for analysis of clearance effect due to their particular setup of controlling parameters.

A valuable analysis in determining wear rate after post-test analysis was by normalizing surface depression via wear at TDC with respect to test hours on the dynamometer, as shown in Table 29.

Table 29: Wear Rate - Comparison - Depression by Wear at TDC

Wear Rate (µm/hr)	Dynamometer 1	Dynamometer 2		Dynamometer 3	Dynamometer 4
		Cyld. 1 & 2	Cyld. 3 & 4		
	3.08	2.50	5.49	1.50	1.13

6.3.1. ENGINE TRIAL 1

Clearance distance was a large issue and limiting factor in the first engine trial which was superimposed over the issue of poor coating wear resistance. However, clearance was a distinguishable problem that could be evaluated separately from coating type because of the noticeable scuffing and wear that occurred on all sliding surfaces including bore walls, piston skirts, and piston rings. For scuffing to occur, significant asperity contact and pressure must be present in the tribosystem, usually due to insufficient lubrication [33]. The clearance between piston and bore for the first engine trial was available as a stack-up with possible minimum values as low as total 12 µm (6 µm between piston and bore on each side). Furthermore, from a cross-sectional evaluation of cylinder 2 in engine trial 1, surface depressions greater than 13 µm were visible in the swept volume region of the bore indicating significant contact pressure between the sliding surfaces.

6.3.2. ENGINE TRIALS 2 & 3

Engine trial 3 provided additional data to support the claim of lower clearance distances increasing wear. All cylinders in engine trial 3 had the same wear type, denoted as “Ring Flutter” in this study, as well as cylinder 4 in engine trial 2. A visible comparison between the similar wear patterns over two different engine trials is seen in Figure 117. The common controlling parameter between these sets of cylinders was the bore size and clearance distance being 87.509 mm – 87.520 mm.

Additionally, all cylinders in engine trial 3 possessed the same controlling parameters with the exception of clearance distance. Cylinder 4 had a combined clearance total of 13 µm, much smaller than the next smallest clearance total in the same engine trial which occurred in cylinder 3 and had a total combined clearance of 23 µm. A post-test visual inspection of

the bores revealed a significantly larger area of the cylinder bore covered by the ring flutter phenomenon, and with more aluminum substrate exposed. In addition to the greater ring flutter region, the depth of each wear mark was more severe in cylinder 4 than the rest of the cylinders with peak to valley heights being consistently large and reaching values up to 9 µm in height. Moreover, the piston in cylinder 4 experienced a different wear with the piston skirt coating being polished off on the bottom end of the major thrust side. This comparison between engines of similar clearance distance as well as individual cylinders with different clearance distances suggests that the ring flutter phenomenon occurs due to small clearance distances. The severity of ring flutter wear is enhanced as the clearance distances become smaller until eventual scuffing due to extremely small clearances creating high contact pressure on the bores, as seen in engine trial 1.

Figure 117: Discussion - Ring Flutter Wear – Comparison Between Engine Trials 2 & 3

6.3.3. ENGINE TRIAL 4

Clearances for engine trial 4 were very large and past the upper end of production tolerances, a combination of bore sizes greater than 87.531 mm and piston sizes no more than 87.489 mm created total combined clearances ranging between 44 µm – 49 µm. The outcomes of having clearances so large in PEO coated cylinder bores was visible on the major and minor thrust sides with discoloration and scratching occurring in a pattern and shape that signified piston slap. Although the engine failed early due to journal bearing failure, it is clear that the wear being created by piston slap would have been a detrimental factor in the engine test due to the high clearance between piston and bore.

6.4. SURFACE PROFILE

Surface profile was a controlling parameter which consisted of the most variables and subsequently produced widely varying surface profiles in each engine trial within this study. The method of evaluation for effect of surface profile was through dynamometer checks and visual inspection of wear on piston and cylinder bore. Engine trials 2, 3, and 4 provided the greatest opportunity for analysis of surface profile effect.

6.4.1. ENGINE TRIAL 2

Professionally honed bores of the second engine trial with very high oil retention values formed by extremely high surface valley data and large surface valley material ratios produced excellent leak-down and compression results signifying sufficient dynamic and static combustion chamber sealing. The surface profile is known to have had a significant effect on the combustion chamber sealing as cylinder 4 was a much smaller size than cylinders 1, 2, and 3, but it still possessed the same sealing capabilities until failure, therefore ruling out dependence on clearance distance between piston and bore in this particular scenario. Additionally, the visual surface profiles of the professionally honed engine were extremely flat although numerically the surface peak values were misleadingly large with an average from 0.65 µm in cylinder 4 and upwards to 1.51 µm in cylinder 2. Although the test was limited by coating type failure in cylinders 3 and 4, cylinders 1 and 2 with the superior coating type B were left fully intact with even wear throughout, no delamination, and no visible scratch or wear marks on either the cylinder bores or piston skirts.

6.4.2. ENGINE TRIAL 3

Engine trials 3 and 4, had drastically different surface profiles when compared to engine trial 2 as distinguishable by a data comparison and visual comparison of surface profile data. These differences can be attributed to the surface processing techniques used. Engine trials 3 and 4 were processed by utilizing Flex-Honing brushes rather than enlisting professional honing services. A consequence of utilizing Flex-Honing brushes is the wavy surface profile visible in the surface profile curves - a common trait between the two Flex-

Honed engines (Engine Trial 3, Engine Trial 4) even with their different surface profile values.

6.4.3. ENGINE TRIAL 4

Engine trial 4 had surface profile values in the moderate ranges, no surface value parameters were on the extreme ends of the spectrum when compared to all engines tested in this study. The following are the cylinder average surface profile ranges for engine trial 4:

- Ra: 0.77 – 0.92 µm
- Rpk: 0.43 – 0.85 µm
- Rvk: 2.31 – 3.22 µm
- CV: 0.16 – 0.24 $\mu m^3/\mu m^2$

The post-test analysis results of engine trial 4 showed minor signs of delamination wear in all bores to varying degrees. However, with the destroyed journal bearing debris adding wear marks, it is difficult to conclusively separate the superimposed wear marks of journal bearing debris abrasive wear and evaluate surface profile effect. Nevertheless, the cylinders in which their respective journal bearings did not experience destructive failure such as cylinder 2 and 3, experienced minimal to no wear.

6.5. PISTON RINGS

The various combination of piston rings used did not display any conclusive results within this study. Material transfer onto piston ring sliding surfaces was only seen in cylinders which experienced severe delamination or scuffing and had the aluminum substrate of the cylinder block exposed in the combustion chamber. In the instances where there was significant wear and aluminum substrate exposed in the cylinders, elemental analysis determined the existence of aluminum, oxide, and carbon elements on both upper and lower compression ring outside surfaces. In environments where there was no significant bore wear such as in the cases of engine trials 3 and 4, there was no aluminum or oxide material transfer on any of the piston rings. However, for engine trials 3 and 4, there were varying

quantities of carbon elements impregnated or trapped on piston ring surfaces. The carbon elements were a collection of oxidized oil or unburnt fuel [32].

CHAPTER 7

7. RECOMMENDATIONS

From the various fired-engine tests conducted in this study and the array of controlling parameters utilized, it is possible to make recommendations for each controlling parameter based on the post-test analysis and discussions conducted. As the results of the PEO coated engine trials were trend-based, recommendations for controlling parameters can only be given with large tolerances and guide following tests of PEO coated cylinder bores in a progressive direction in order to achieve goals of reduced wear.

7.1. COATING TYPE

A conclusive result based off a direct comparison of both types of coatings from this study determined coating type B with small surface porosities evenly distributed across the sliding surface was the optimal type of coating for use within cylinder bores of fired-engine tests. It is the recommendation of the study to continue using coating type B in future fired-engine trials.

7.2. CLEARANCE

The suggested total combined clearance between piston and bore for future engine trials of 2.0L GTDI I4 engines with PEO coated bore would be 30 +/- 5 µm. The range recommended was determined through the comparison of engine trials with various clearance distances and their subsequent effect on wear with particular emphasis on piston ring contact pressure and piston skirt effect on major and minor thrust sides of cylinder bores. Clearances below the suggested range noticed a ring flutter effect and even scuffing occurring when clearances were extremely low based on bore sizes bordering the lower end of production tolerances. Increasing the clearances beyond the suggested range lead to greater piston slap effect on the cylinder bores evident from scratch marks, discoloration, and wear.

7.3. SURFACE PROFILE

Professional honing is highly suggested for future surface processing techniques of PEO coated cylinder bores as it the method which provides the most control over surface profile features, cylindricity, and bore size. The surface profile features which provided the most beneficial results were composed of large surface valleys and material ratios which created large crevices for increased oil retention. An important added benefit seen from professional honing and the extremely flat profile was the ability to attain dynamic and static combustion chamber sealing properties. A suggested surface profile target for PEO coated bores would be a professionally honed surface with surface features meeting the criteria listed in Table 30.

Table 30: Recommendations - Surface Profile Parameters

Surface Profile Parameter	Criteria
Rpk	< 0.7 µm
Rvk	> 4.0 µm
MR2	74 +/- 5 %
CV	0.51 +/- 0.3 $\mu m^3/\mu m^2$

It is important to note a specification for Ra was not given as it is not representative of an ideal surface profile condition since Ra may rise with increased surface valleys which are beneficial for tribological conditions. Additionally, a low Ra value may not signify a good surface profile either as it may still produce a wavy profile as seen from Flex-Honed profilometry data.

7.4. PISTON RINGS

Through the study which was conducted, the use of various piston ring pack combinations did not display any conclusive effect on wear of PEO coated cylinder bores. However, it is still suggested to use DLC coated upper compression and oil rings as well as chrome plated lower compression rings as part of the piston ring pack for use in PEO coated cylinder bores as those types of piston rings are known to have low friction properties [11]. The low friction properties of DLC coated piston rings could superimpose their beneficial

tribological effect on the low friction PEO coating to create even more favorable sliding surface conditions.

7.5. RECOMMENDED FUTURE WORK

The work of reducing wear in PEO coated cylinder bores is very complex and extends beyond the controlling parameters considered in this study. For this reason there are several other factors that are suggested to be investigated in future iterations of PEO coated engine trials. Understanding the effects of the following parameters has the potential to assist in further decreasing PEO coating wear in cylinder bores.

7.5.1. DECK PLATE

Bore measurements conducted by CMM provided a resolution of up to 1 µm, this type of measurement precision was necessary because such small changes to bore size and cylindricity have a large effect on the overall performance of the coating. However, measurements of the cylinder block were conducted on a bare block with no other engine components torqued on. Once the cylinder head and main bearing tray for the crankshaft are torqued on, their addition has an effect on bore geometry. Understanding the way in which these components affect bore geometry could further explain wear patterns visible on the cylinder walls and provide data to portray a bore shape that is more representative of engine conditions. A deck plate, otherwise known as a torque pate, can be torqued on in the same sequence and to the same values as a cylinder head but without inhibiting the ability to measure the bores as a regular cylinder head would. For this reason it is suggested to conduct a deck plate study and gather data on how the addition of a cylinder head and main bearing tray changes bore shape. It is important to note that although the addition of such components would give a better understanding of in-engine bore shape, fired engine conditions and the thermal expansion of the various components would further affect that bore geometry, however, that type of information and at the precision levels this study is exposed to is unattainable and can only be simulated.

7.5.2. PISTON RINGS

Being the main opposing sliding surface to PEO coated bored, piston rings present a large opportunity for modifying wear outcomes. In addition to the limited piston ring material surface treatments investigated in this study, it is also important to understand the effect on piston ring gap and piston ring tension.

7.5.2.1. PISTON RING GAP

Piston ring gap is the distance between the two ends of the piston ring which allows for installation onto the piston as well as thermal expansion during fired-engine operation. For future studies regarding PEO coating wear, it is suggested to monitor the size of the piston ring gap and determine whether the piston ring gap size is sufficient for thermal expansion in combustion chamber environments with PEO coated cylinder bores. It is possible for the gap to be insufficiently large, preventing the piston ring from freely expanding and subsequently increasing the contact pressure on the cylinder bores and negatively affecting cylinder bore tribology.

7.5.2.2. PISTON RING TENSION

Piston ring contact pressure on cylinder bores is an important consideration in combustion chamber tribological systems. Finding a compromise between sufficient contact pressure to maintain combustion chamber sealing and reducing normal force on the bore walls for decreasing wear is a controlling parameter that is suggested to be added in future PEO coated engine trials.

7.5.3. HONING

Professional honing provides the greater control over surface feature and provides optimal surface profiles for cylinder bore tribological systems. However, further honing features such as cross-hatching marks as seen on cast iron cylinder liners and PTWA thermally sprayed bores should be investigated to evaluate the effect the increased crevice volume and oil control created by the supplementary surface features has on PEO coated cylinder bores.

CHAPTER 8

8. CONCLUSIONS

The investigation into the use of PEO coated cylinder bores in fired-engine conditions provided research results which in turn helped improve on coating wear resistance and extend the duration of testing. Additionally, the information gathered provided greater understanding of the effects of certain controlling parameters used in this study. The following is a summary addressing each of the objectives set out prior to the study being undertaken and a brief description of what was achieved.

1. A literature survey was conducted which investigated various features associated with the cylinder bore to piston ring sliding system. The topics which were reviewed as part of the literature survey include:
    a. The deposition process and parameters of low-friction PTWA coatings utilized by the Ford Motor Company. Additionally, the review of PTWA coatings covered topics such as deposition parameters, the tribological conditions associated with PTWA coatings, application of PTWA in cylinder bores, and bench test results from academic literature.
    b. The purpose and functionality of piston rings was reviewed which included their effect on tribological conditions as well as combustion chamber sealing.
    c. The experimental piston ring surface treatment of DLC was investigated to establish the deposition characteristics and tribological benefits.
    d. Honing technology and its effect on tribological conditions via surface profile and oil retention was conducted to be able to apply that knowledge in cylinder bore testing of PEO coated cylinders.
2. Four fired engine tests were conducted using engines with PEO coated cylinder bores.
    a. Each trialed engine had varying independent variables of bore size, surface profile, coating type, and piston rings. Three of the four engine tests failed prematurely, while one engine test completed the full dynamometer curve.

Regardless of dynamometer curve completion, the teardown analysis results from each engine test provided valuable information on failure mechanisms which lead to greater understanding of the controlling parameters and their respective effects on coating wear resistance. The following is a summary of the effects for each variable:

i. Coating Type: coating type B (small, distributed, uniform porosity) was able to conclusively resist wear far greater than coating type A (large, non-uniform porosity).
ii. Surface Profile: greater values of oil retention promoted oil-film formation and enhanced the hydrodynamic lubrication regime by separating the opposing sliding surfaces. Therefore, flat surface profiles with large and frequent surface valleys improved wear resistance and combustion chamber sealing.
iii. Bore Clearance: determined to be one of the most important influencing factors, a narrow range of operation was distinguishable for optimal results. Values of clearance below or above the optimal range would experience increased wear.
iv. Piston Rings: differences in wear patterns and performance between different piston ring types were indistinguishable and produced inconclusive results.

b. From the pre-test metrology information, real-time dynamometer test results, and post-test analysis, the study was able to outline optimal operating ranges for the independent variables for the purposes of improving wear resistance of PEO coated cylinder bores with the resources available. The following is a summary of the recommendations made for the independent variables covered by this study:

i. Coating Type: small, distributed, and uniform surface porosities – Coating Type B
ii. Surface Profile: professionally honed surface profile
    1. Rpk: < 0.7 µm
    2. Rvk: > 4.0 µm

3. MR2: 74 ± 5 %
4. CV: 0.51 ± 0.3 $\mu m^3/\mu m^2$

iii. Bore Clearance: total combined clearance of 30 ± 5 µm

iv. Piston Rings: experimental piston rings

1. Upper Compression Ring: DLC Coated
2. Lower Compression Ring: Chrome Plated
3. Oil Ring Set: DLC Coated

c. Additionally, the results obtained and their subsequent analysis also provided guidance as to what additional work and resources would be best suited to optimize the coating package even further.

REFERENCES

[1] Hussein, R.O., X. Nie, and D.O. Northwood. "Influence of Process Parameters on Electrolytic Plasma Discharging Behaviour and Aluminum Oxide Coating Microstructure." Surface & Coating Technology (2010): 1659-667. Print.

[2] Tillous, E.K., T. Toll-Duchanoy, and E. Bauer-Grosse. "Microstructure and 3D Microtomographic Characterization of Porosity of MAO Surface Layers Formed on Aluminum and 2214-T6 Alloy." Surface & Coating Technology (2009): 1850-855. Print.

[3] Yerokhin, A.L., X. Nie, A. Leyland, A. Matthews, and S.J. Dowey. "Plasma Electrolysis for Surface Engineering." Surface & Coating Technology (1999): 73-93. Print.

[4] Bedajangam, S., & Jadhav, N. (2013). Friction Losses Between Piston Ring-Liner Assembly of Internal Combustion Engine: A Review. International Journal of Scientific and Research Publications, 3(6), 2250-3153.

[5] Bobzin, K., Ernst, F., Richardt, K., Schlaeder, T., Verpoort, C., & Flores, G. (2008). Thermal Spraying of Cylinder Bores with the Plasma Transferred Wire Arc Process. Surface & Coating Technology, 202, 4438-4443.

[6] Christensen, D. T. (2000). Physics of Thin Films. Retrieved from UCCS Teach: http://www.uccs.edu/~tchriste/courses/PHYS549/549lectures/index.html

[7] Daewoo Heavy Industry Co. (1995). DLC Coated Piston Rings for Diesel Engine. KIST, 1-8.

[8] Darut, G., Liao, H., Coddet, C., Bordes, J. M., & Diaby, M. (2014). Steel Coating Application for Engine Block Bores by PTWA Spraying Process. Surface & Coating Technology, 1-8.

[9] Hershberger, J., Ozturk, O., Ajayi, O., Woodford, Erdemir, A., Erck, R., et al. (2004). Evaluation of DLC Coatings for SIDI Fuel Systems. Surface Coatings & Technology, 237-244.

[10] Hironaka, S. (1984, July 1). Boundary Lubrication and Lubricants. Technical News, 1-8.

[11] Kennedy, D. M., Hoppe, D. S., & Esser, J. (2012). Piston Ring Coating Reduces Gasoline Engine Friction. Development Friction, 40-43.

[12] PVD. (2015). Retrieved from Sigma-Aldrich: http://www.sigmaaldrich.com/materials- science/material-science-products.html?TablePage=108832720

[13] PVD Process. (2014). Retrieved from Oerlikon: http://www.oerlikon.com/metco/en/products- services/coating-services/dlc-coatings/processes/processes-pvd/

[14] Rusnano. (2010). Porous Nanostructured Inorganic Nonmetallic Coatings. Retrieved from Rusnano: http://en.rusnano.com/portfolio/companies/manel

[15] Thin Film Deposition. (2013). Retrieved from Hivatec: http://hivatec.ca/consulting-design/thin-film-deposition

[16] Voevodin, A., Schneider, J., Rebholz, C., & Matthews, A. (1996). Multilayer Composite Ceramic-metal DLC Coatings for Sliding Wear Applications. Tribology International, 29(7), 559-570.

[17] Nie, X.. "Physical Vapour Deposition" Thin Films and Coatings. University of Windsor. , Windsor. Winter 2015. Lecture.

[18] Office of the Press Secretary. (2012, August 28). Obama Administration Finalizes Historic 54.5 MPG Fuel Efficiency Standards. Retrieved from https://www.whitehouse.gov/the-press-office/2012/08/28/obama-administration-finalizes-historic-545-mpg-fuel-efficiency-standard

[19] Office of Transportation and Air Quality. "EPA and NHTSA Propose to Extend the National Program to Reduce Greenhouse Gases and Improve Fuel Economy for Cars and Truck." EPA. United States Environmental Protection Agency, 1 Nov. 2011. Web. <http://www.epa.gov/oms/climate/documents/420f11038.pdf>.

[20] Office of Transportation and Air Quality. "Average Annual Emissions and Fuel Consumption for Gasoline-Fueled Passenger Cars and Light Trucks." EPA. United States Environmental Protection Agency, 1 Oct. 2008. Web. <http://www.epa.gov/otaq/consumer/420f08024.pdf>.

[21] Fenske, George, Robert Erck, Layo Ajayi, Ali Erdemir, and Osman Eryilmaz. "Parasitic Energy Loss Mechanisms Impact on Vehicle System Efficiency." Heavy Vehicle Systems. Argonne National Laboratory, 1 Apr. 2006. Web. http://www1.eere.energy.gov/vehiclesandfuels/pdfs/hvso_2006/07_fenske.pdf>.

[22] D'Agostino, V., P. Maresca, and A. Senatore. "Theoretical Analysis for Friction Losses Minimization in Piston Rings." AITC-AIT (2006): 1-12. Print.

[23] Lenny Jr., John. "Replacing the Cast Iron Liners for Aluminum Engine Cylinder Blocks: A Comparative Assessment of Potential Candidates." Thesis – Rensselaer Polytechnic Institute (2011). Print.

[24] Verpoort, Clemens. "Development of Nano-Crystalline Thermal Spray Coatings for Cylinder Bores of Aluminum Combustion Engines." Ford Motor Company. University of Windsor, Windsor. Oct. 2014. Presentation

[25] Goeldel, B., J. Voisin, D. Dumur, M. El Mansori, and M. Frabolot. "Flexible Right Sized Honing Technology for Fast Engine Finishing." *CIRP Annals - Manufacturing Technology* (2013): 327-30. Print.

[26] Pawlus, P., T. Cieslak, and T. Mathia. "The Study of Cylinder Liner Plateau Honing Process." *Journal of Materials Processing Technology* (2009): 327-30. Print.

[27] Carley, Larry. "The Smooth Science of Cylinder Honing." *Engine Builder*. Babcox, 1 Jan. 2002. Web. <http://www.enginebuildermag.com/2002/11/the-smooth-science-of-cylinder-honing/>.

[28] BRM. "Common Practices in Cylinder Boring, Honing, and Wall Finishing." 1-12. Print.

[29] Sabeur Mezghani, Ibrahim Demirci, Mohamed El Mansori, Mohammed Yousfi "Mutual influence of cross hatch angle and superficial roughness of honed surfaces on friction in ring-pack tribo-system". Tribology international. Vol. 66, p.54-59 – 2013

[30] Wos, Pawel, and Jacek Michalski. "Effect of Initial Cylinder Liner Honing Surface Roughness on Aircraft Piston Engine Performances." *Tribol Lett* (2011): 555-67. Print.

[31] "Surface Texture Parameters." International Joint Tribology Conference. , . Lecture.

[32] Andersson, Peter, Jaana Tamminen, and Carl-Erik Sandstrom. "Piston Ring Tribology: A Literature Survey." VVT Research Notes (2002): 1-108. Print.

[33] Blau, Peter J. *Scuffing: From Basic Understanding to Engine Materials Testing.* Proc. of DEER Conference, Detroit, MI. Oak Ridge National Laboratory. Wed. 2007.

[34] Kuppast, Vinay V., and S. N. Kurbet. "Dynamic Simulation of Piston Motion to Predict the Piston Slap Using Radioss." HTC (2010): 1. Web.

[35] Donahue, Raymond, and Philip. A. Fabiyi. “Manufacturing Feasibility of All-Aluminum Automotive Engines Via Application of High Silicon Aluminum Alloy.” Society of Automotive Engineers (2000): 1-11. Web.

[36] "Rock Surface Roughness Measurement Using Microcontroller." Rickey's World. 1 Feb. 2011. Web. <http://www.8051projects.net/t44365/project-help/poll-rock-surface-roughness-measurement-using-microcontroller.htm>.

[37] "A356 Aluminum Casting Alloy." Hadleigh Castings. Web. <http://www.hadleighcastings.com/uploads/A356.0 Alloy Detail.pdf>.

BIBLIOGRAPHY

[38] Yerokhin, A.L., L.O. Snizhko, N.L. Gurevina, A. Matthews, and A. Pilkington. "Spatial Characteristics of Discharge Phenomena in Plasma Electrolytic Oxidation of Aluminum Alloy." Surface & Coating Technology (2004): 779-83. Print.

[39] Al Bosta, Mohannad M.S., and Kung-Jeng Ma. "Suggested Mechanism for the MAO Ceramic Coating on Aluminum Substrates Using Bipolar Current Mode in the Alkaline Silicate Electrolytes." Surface & Coating Technology (2014): 121-35. Print.

[40] Liu, Run, Jie Wu, Wenbin Xue, Yao Qu, Chaolin Yang, and Bin Wang. "Discharge Behaviors during Plasma Electrolytic Oxidation on Aluminum Alloy." Materials Chemistry & Physics (2014): 284-92. Print.

[41] Peng, Zhijing, "Plasma Electrolytic Oxidation (PEO) Coatings on an A356 Alloy for Improved Corrosion and Wear Resistance" (2013). Electronic Theses and Dissertations. Paper 4764. Print.

[42] Ladwig, A. M., Koch, R. D., Wenski, E. G., & Hicks, R. F. (2009). Atmospheric plasma deposition of diamond-like carbon coatings. Diamond and Related Materials, 1-5.

[43] Nie, X.. "Introduction to Vacuum Science and Technology" Thin Films and Coatings. University of Windsor. , Windsor. Winter 2015. Lecture.

[44] Nie, X.. "Plasma, Discharges, and Ion-Surface Interactions" Thin Films and Coatings. University of Windsor. , Windsor. Winter 2015. Lecture.

[45] Nie, X.. "Structure/Property Relationship for Hard Coatings" Thin Films and Coatings. University of Windsor. , Windsor. Winter 2015. Lecture.

[46] "Basic Concepts & Elements of Surface Topography." Innovation & Integration. B.C. MacDonald & Co.. , . Lecture.

[47] Malburg, Dr. Mark C.. "Cylinder Bore Surface Texture Analysis." Digital Metrology Solutions. , . 1 Jan. 2002. Lecture.

[48] Deutz. "Less Wear and Oil Consumption Through Helical Slide Honing of Engines." *Development: Tribology* 70 (2012): 46-51. Print.

[49] Hennink, Susanna Contini. "Laser Texturing Slashes Cylinder Wear." *Photonics Spectra*. 1998. Web. <http://www.photonics.com/Article.aspx?AID=2304>.

[50] Gehring L.P. "Honing Technology for a Higher Return." *Advanced Honing Technology*. Gehring L.P. Web. <http://www.gehring.de/en/international-locations/usa/>.

[51] R&L Engines. "Piston Ring Tech." *R&L Engines*. Web. <http://www.rlengines.com/Web_Pages/pistonrings.html>.

APPENDICIES

APPENDIX A

Appendix A - 1: Dynamometer 1 - Engine 2599 - Cylinder 1 – Front

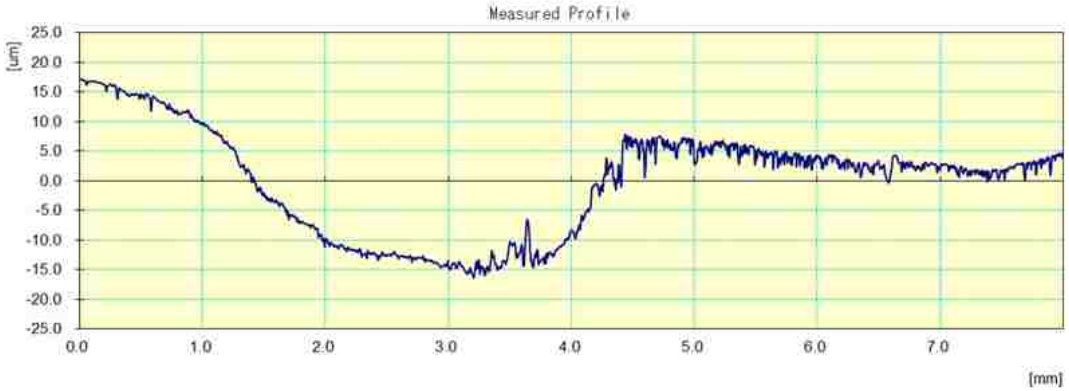

Appendix A - 2: Dynamometer 1 - Engine 2599 - Cylinder 1 – Right

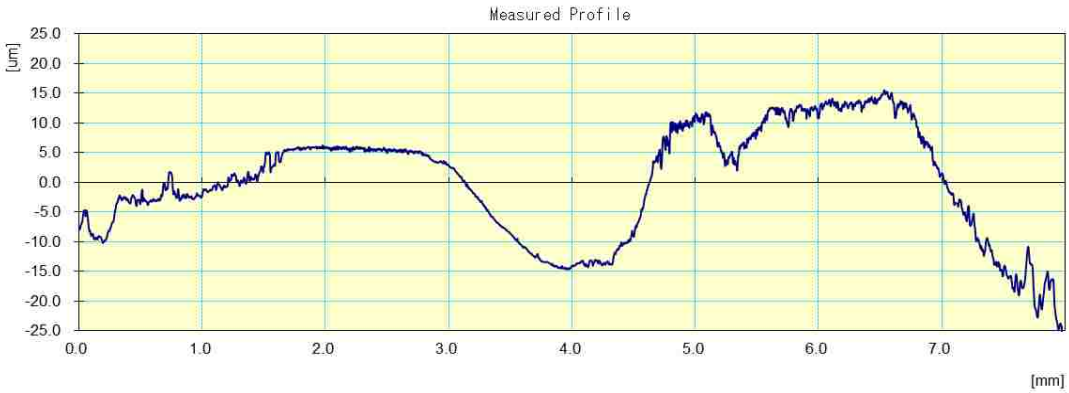

Appendix A - 3: Dynamometer 1 - Engine 2599 - Cylinder 1 – Back

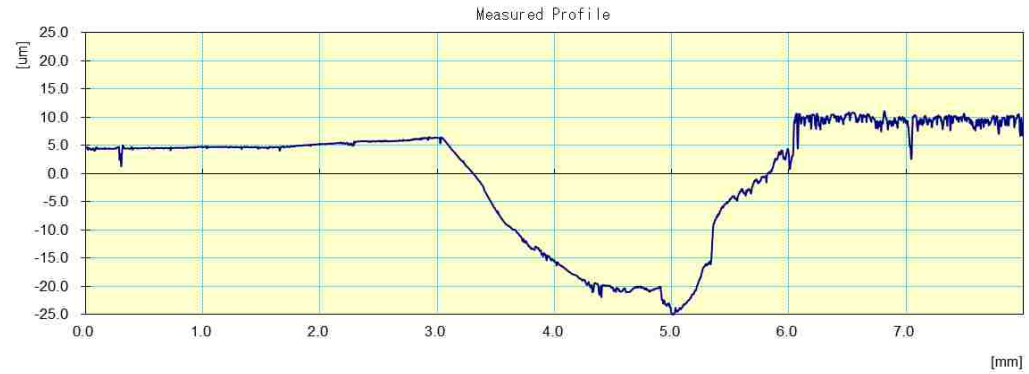

Appendix A - 4: Dynamometer 1 - Engine 2599 - Cylinder 1 – Left

Appendix A - 5: Dynamometer 1 - Engine 2599 - Cylinder 2 – Front

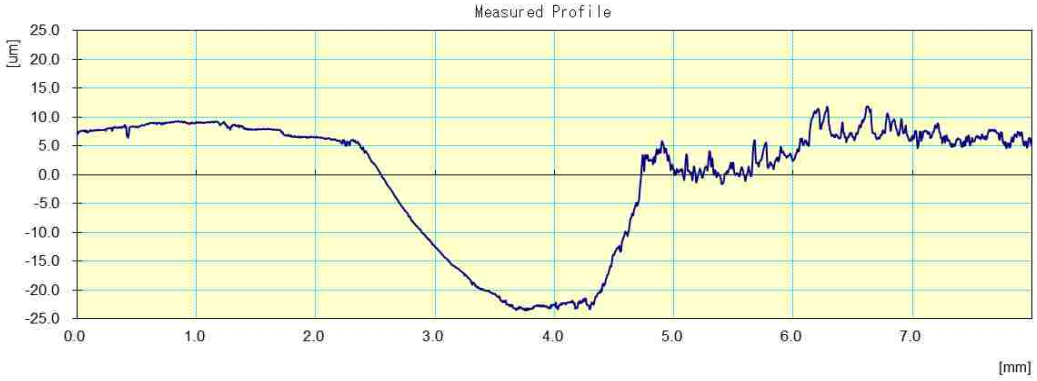

Appendix A - 6: Dynamometer 1 - Engine 2599 - Cylinder 3 – Front

Appendix A - 7: : Dynamometer 1 - Engine 2599 - Cylinder 3 – Right

Appendix A - 8: : Dynamometer 1 - Engine 2599 - Cylinder 3 – Back

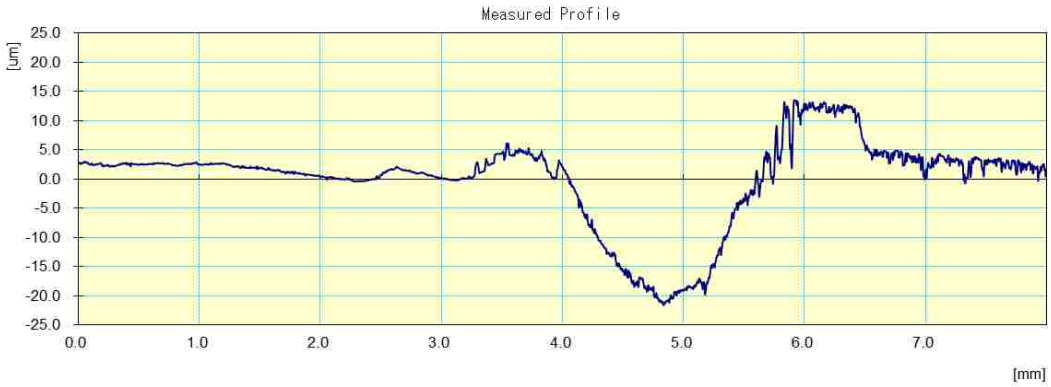

Appendix A - 9: : Dynamometer 1 - Engine 2599 - Cylinder 3 – Left

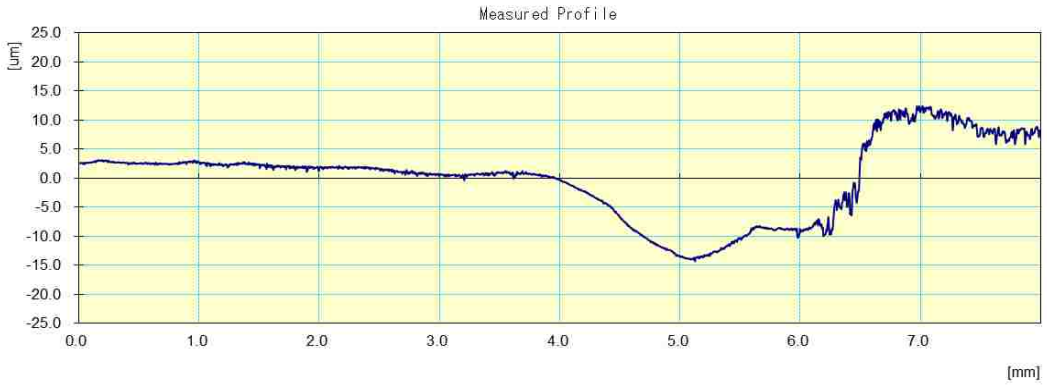

Appendix A - 10: Dynamometer 1 - Engine 2599 - Cylinder 4 – Front

Appendix A - 11: Dynamometer 1 - Engine 2599 - Cylinder 4 – Right

Appendix A - 12: Dynamometer 1 - Engine 2599 - Cylinder 4 – Back

Appendix A - 13: Dynamometer 1 - Engine 2599 - Cylinder 4 – Left

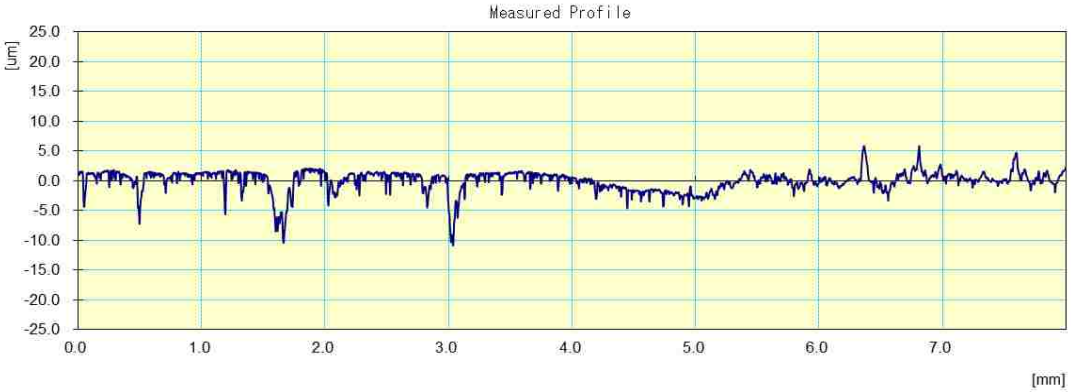

Appendix A - 14: Dynamometer 2 - Engine 2633 - Cylinder 1 – Front

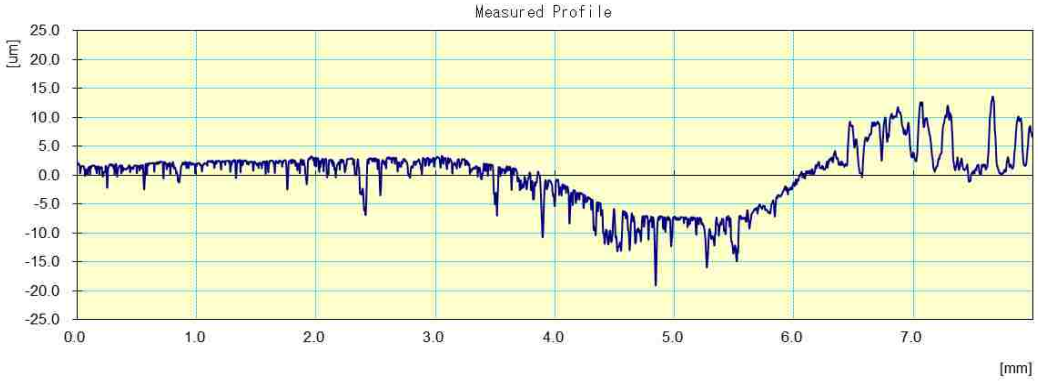

Appendix A - 15: Dynamometer 2 - Engine 2633 - Cylinder 1 – Right

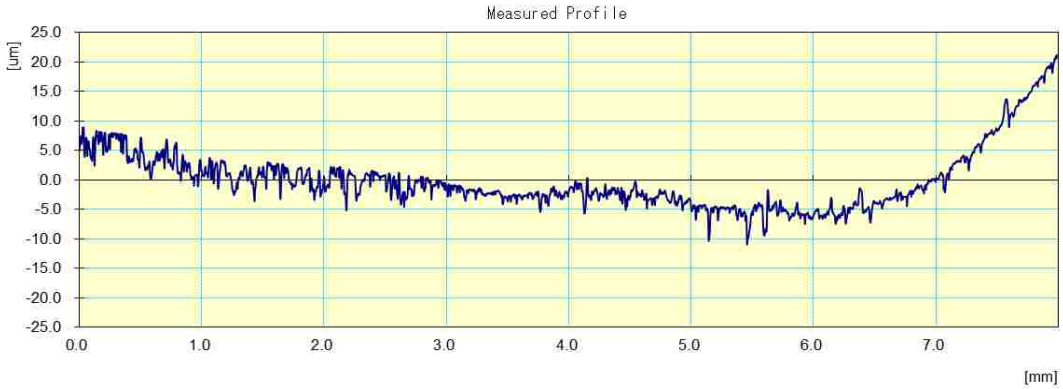

Appendix A - 16: Dynamometer 2 - Engine 2633 - Cylinder 1 – Back

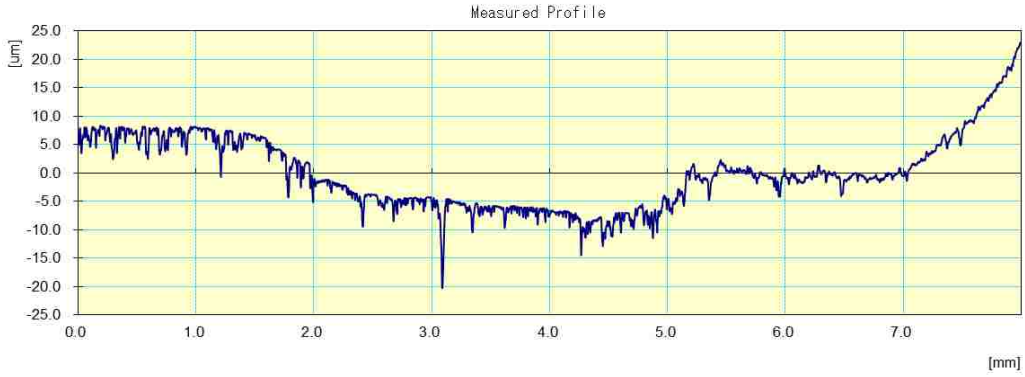

Appendix A - 17: Dynamometer 2 - Engine 2633 - Cylinder 1 – Left

Appendix A - 18' Dynamometer 2 - Engine 2633 - Cylinder 2 - Front

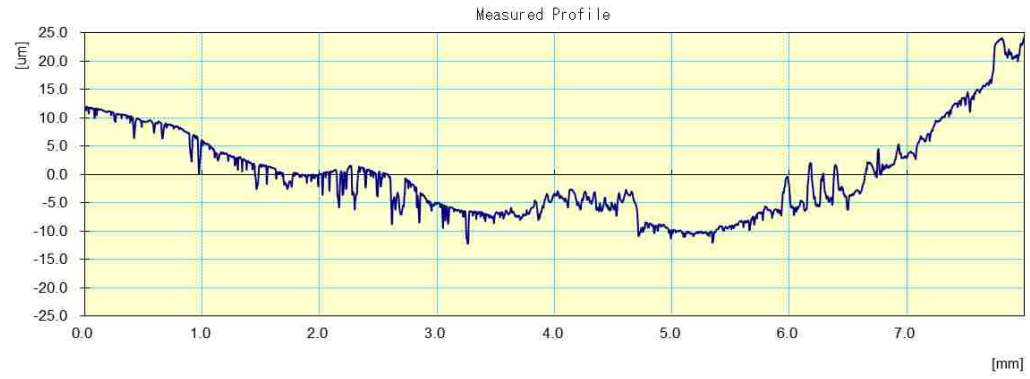

Appendix A - 19: Dynamometer 2 - Engine 2633 - Cylinder 2 - Right

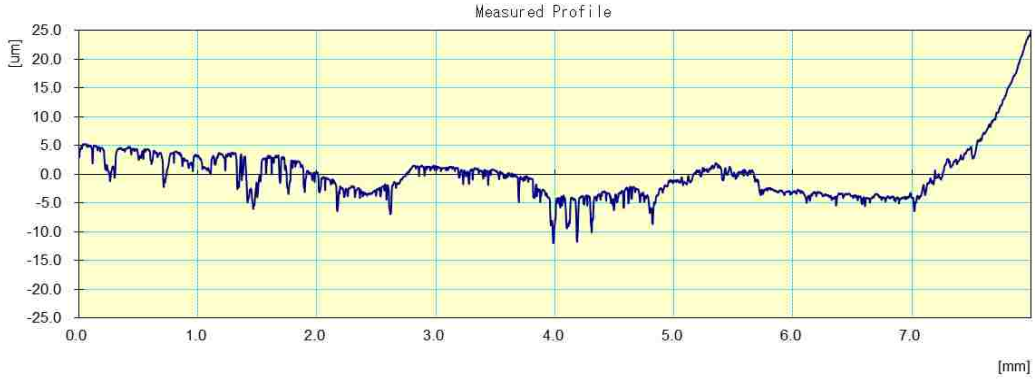

Appendix A - 20: Dynamometer 2 - Engine 2633 - Cylinder 2 - Back

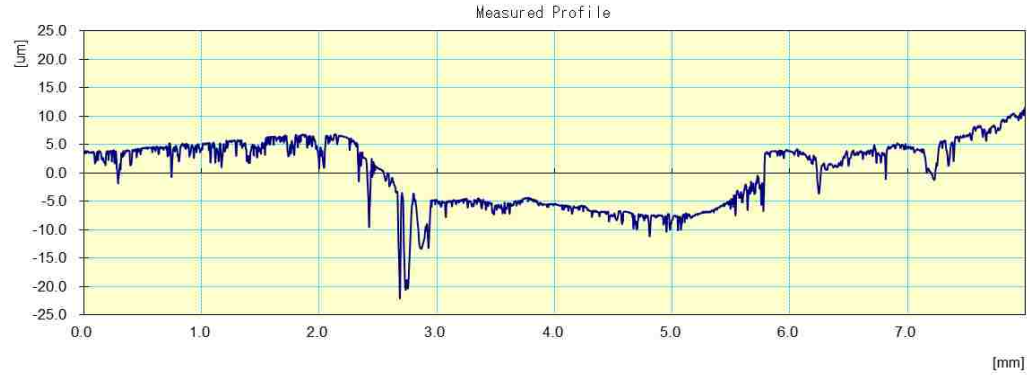

Appendix A - 21: Dynamometer 2 - Engine 2633 - Cylinder 2 – Left

Appendix A - 22: Dynamometer 2 - Engine 2633 - Cylinder 3 - Front

Appendix A - 23: Dynamometer 2 - Engine 2633 - Cylinder 3 - Right

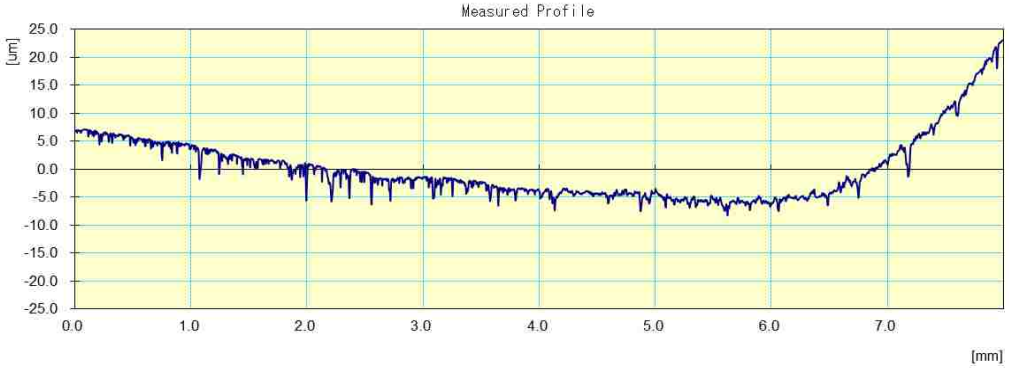

Appendix A - 24Dynamometer 2 - Engine 2633 - Cylinder 3 - Back

Appendix A - 25: Dynamometer 2 - Engine 2633 - Cylinder 3 – Left

Appendix A - 26: Dynamometer 2 - Engine 2633 - Cylinder 4 - Front

Appendix A - 27: Dynamometer 2 - Engine 2633 - Cylinder 4 - Right

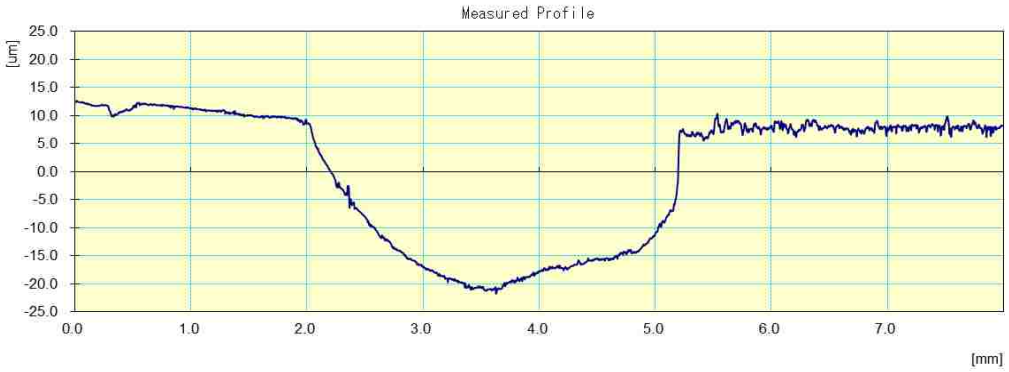

Appendix A - 28: Dynamometer 2 - Engine 2633 - Cylinder 4 - Back

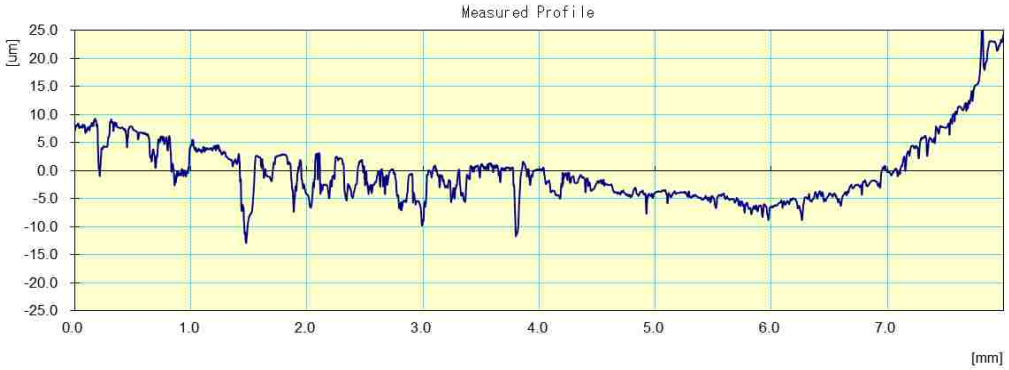

Appendix A - 29: Dynamometer 2 - Engine 2633 - Cylinder 4 – Left

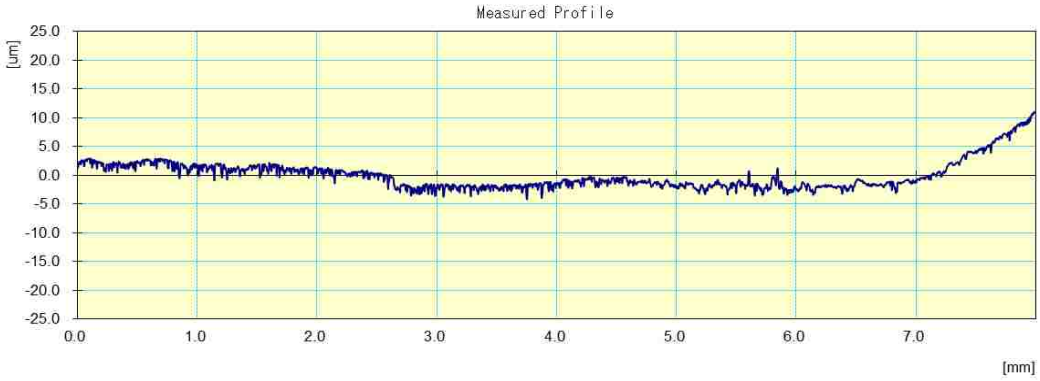

Appendix A - 30: Dynamometer 3 - Engine 2595 - Cylinder 1 – Front

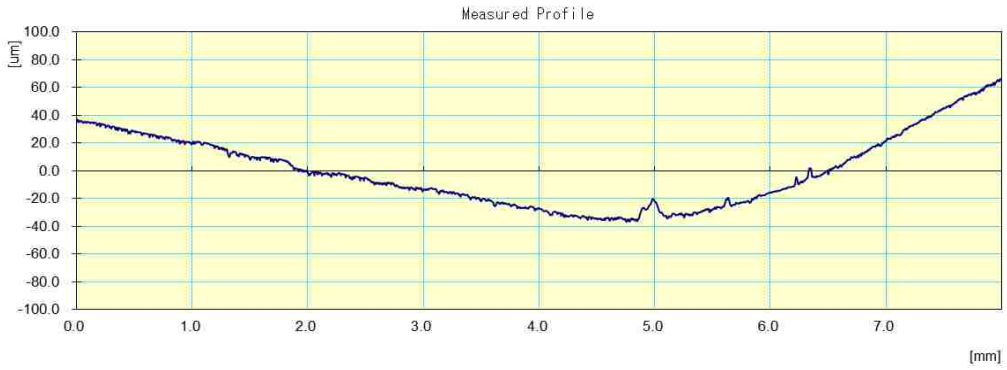

Appendix A - 31: Dynamometer 3 - Engine 2595 - Cylinder 1 – Right

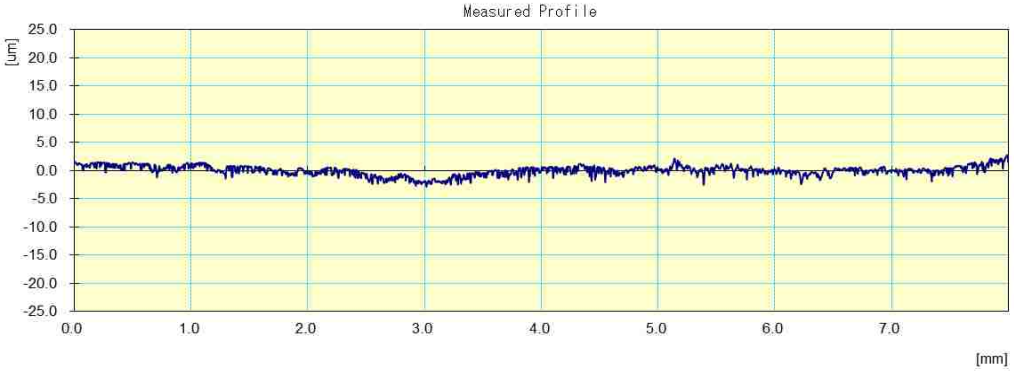

Appendix A - 32: Dynamometer 3 - Engine 2595 - Cylinder 1 – Back

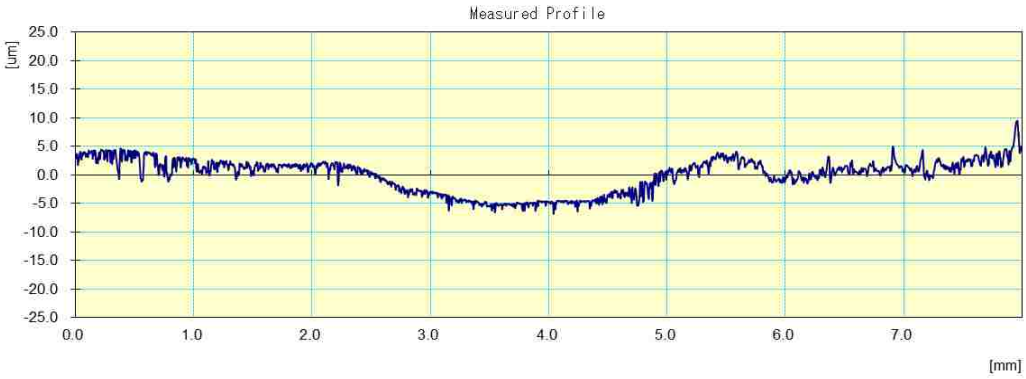

Appendix A - 33: Dynamometer 3 - Engine 2595 - Cylinder 1 – Left

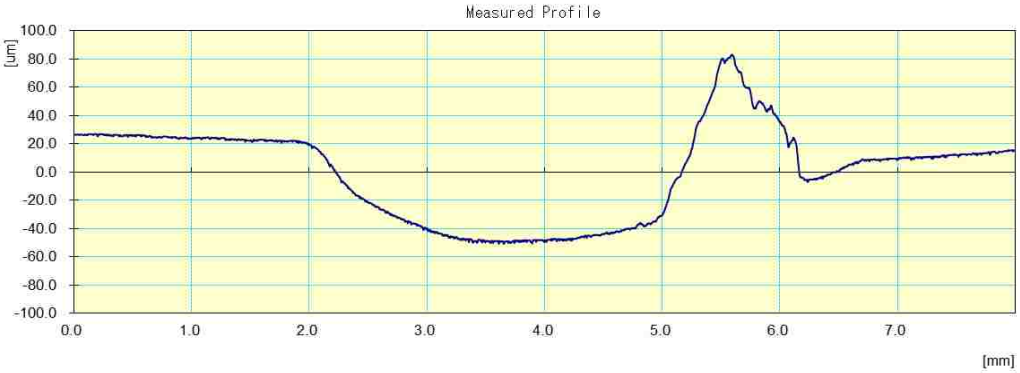

Appendix A - 34: Dynamometer 3 - Engine 2595 - Cylinder 2 – Front

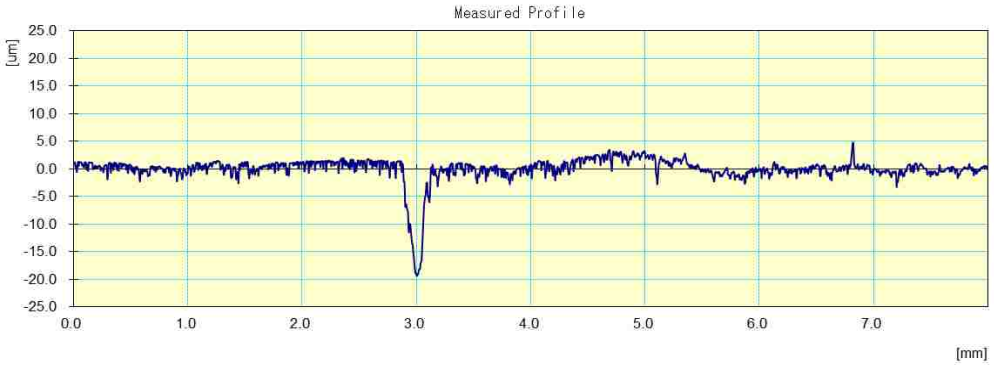

Appendix A - 35: Dynamometer 3 - Engine 2595 - Cylinder 2 – Right

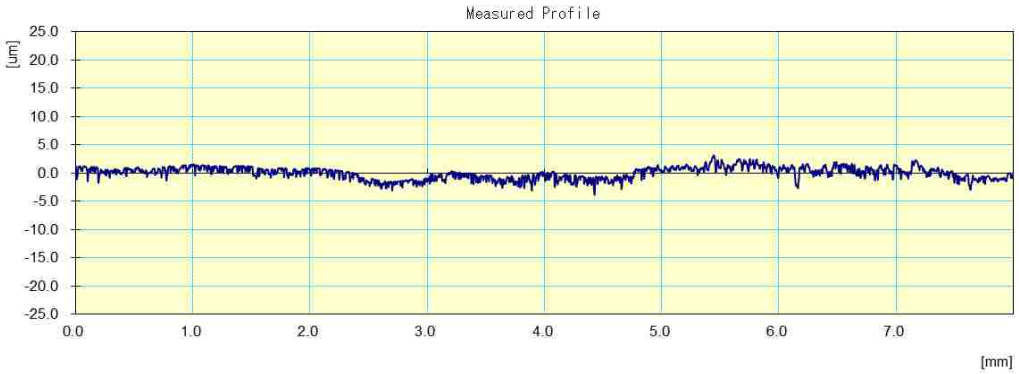

Appendix A - 36: Dynamometer 3 - Engine 2595 - Cylinder 2 – Back

Appendix A - 37: Dynamometer 3 - Engine 2595 - Cylinder 2 – Left

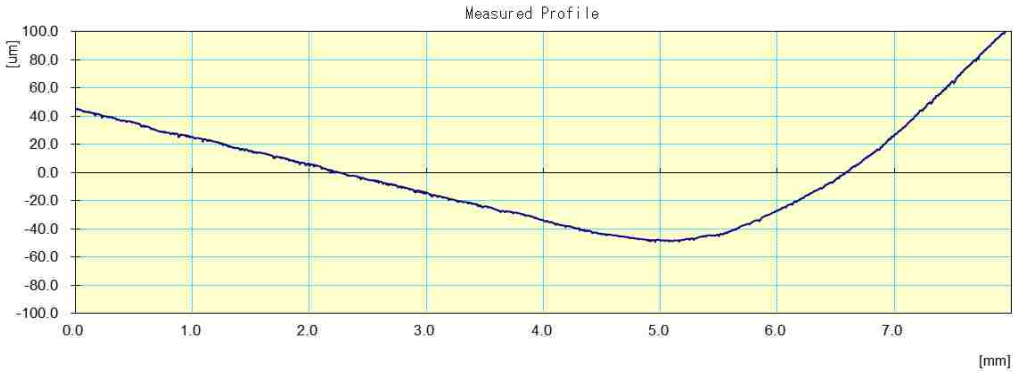

Appendix A - 38: Dynamometer 3 - Engine 2595 - Cylinder 3 – Front

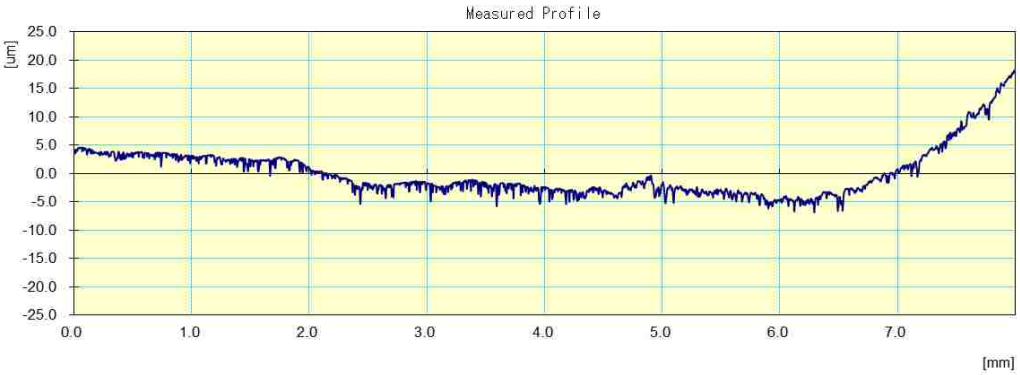

Appendix A - 39: Dynamometer 3 - Engine 2595 - Cylinder 3 – Right

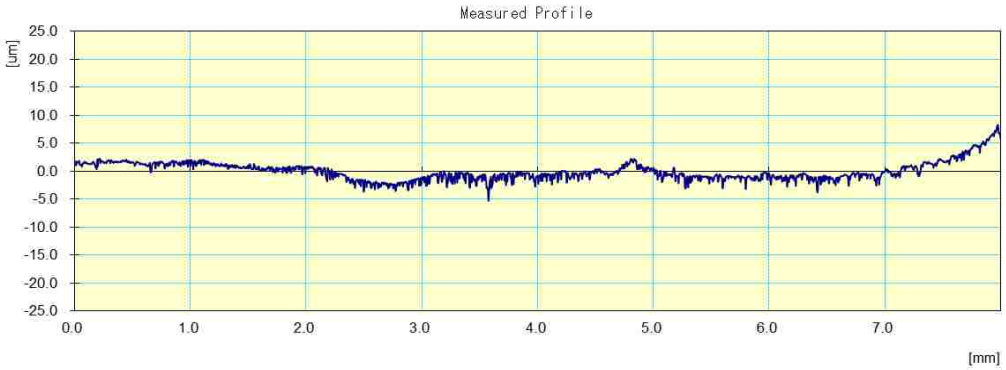

Appendix A - 40: Dynamometer 3 - Engine 2595 - Cylinder 3 – Back

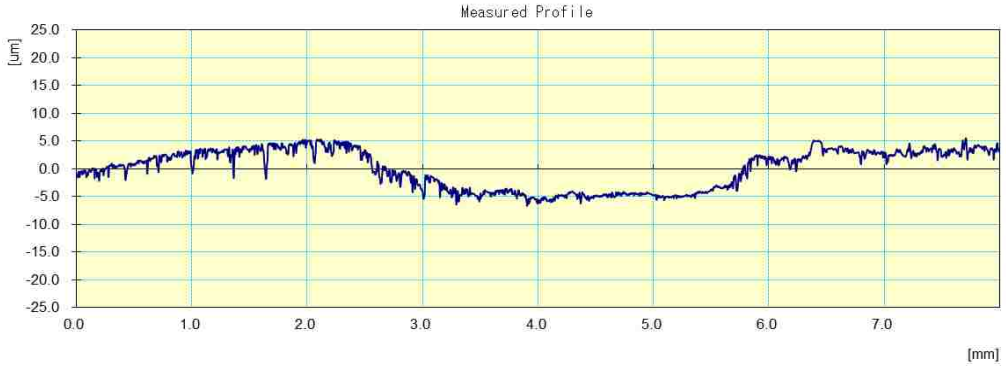

Appendix A - 41: Dynamometer 3 - Engine 2595 - Cylinder 3 – Left

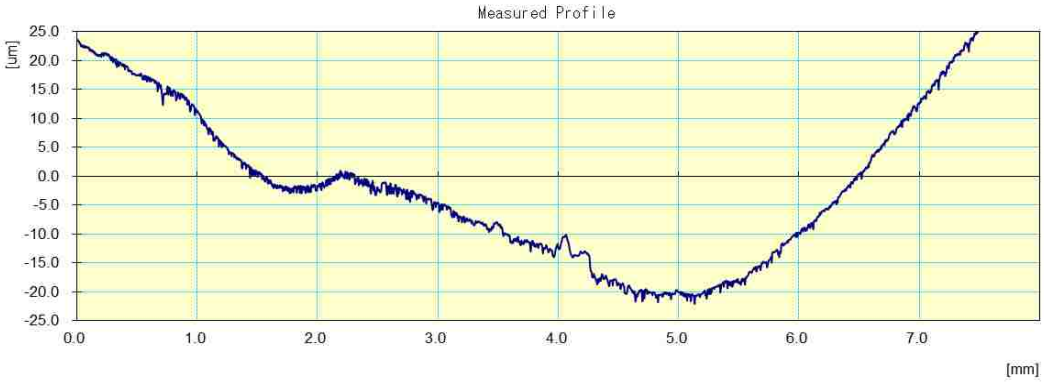

Appendix A - 42: Dynamometer 3 - Engine 2595 - Cylinder 4 – Front

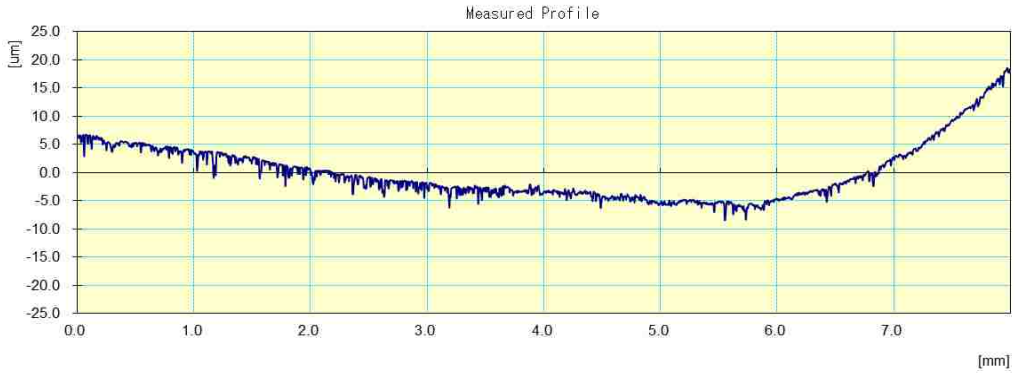

Appendix A - 43: Dynamometer 3 - Engine 2595 - Cylinder 4 – Right

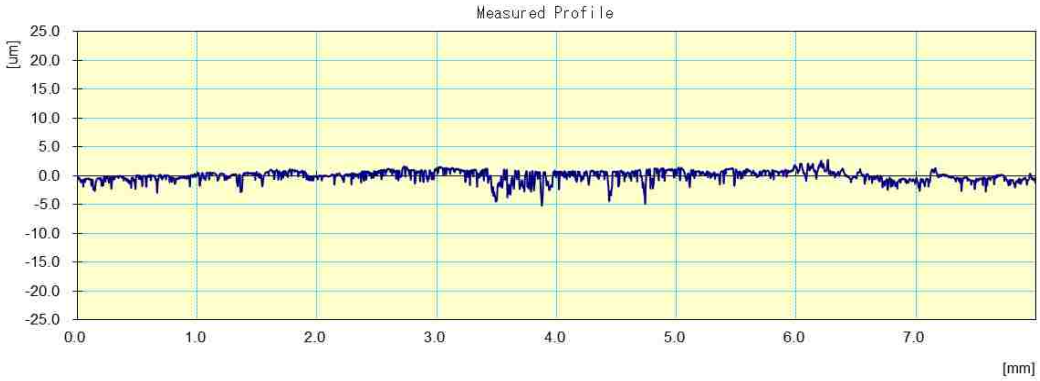

Appendix A - 44: Dynamometer 3 - Engine 2595 - Cylinder 4 – Back

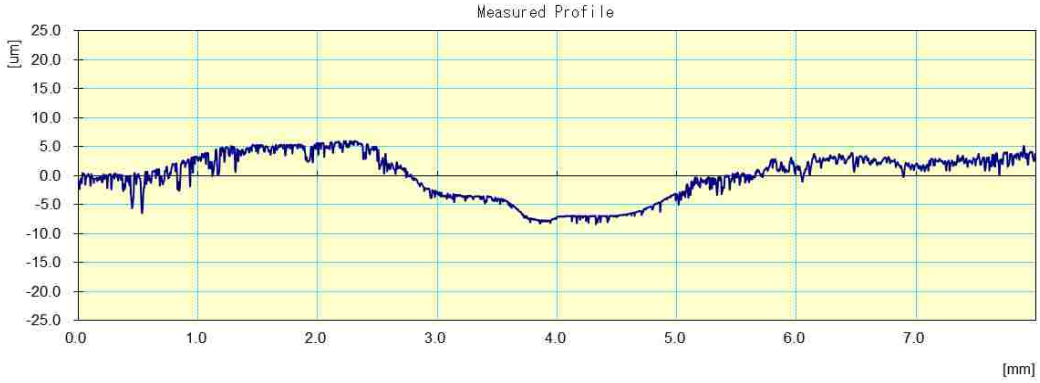

Appendix A - 45: Dynamometer 3 - Engine 2595 - Cylinder 4 – Left

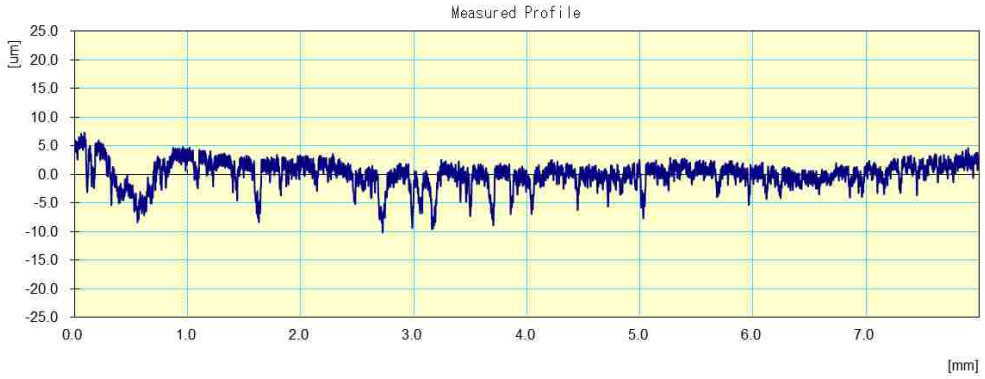

Appendix A - 46: Dynamometer 4 - Engine 2595R - Cylinder 1 – Front

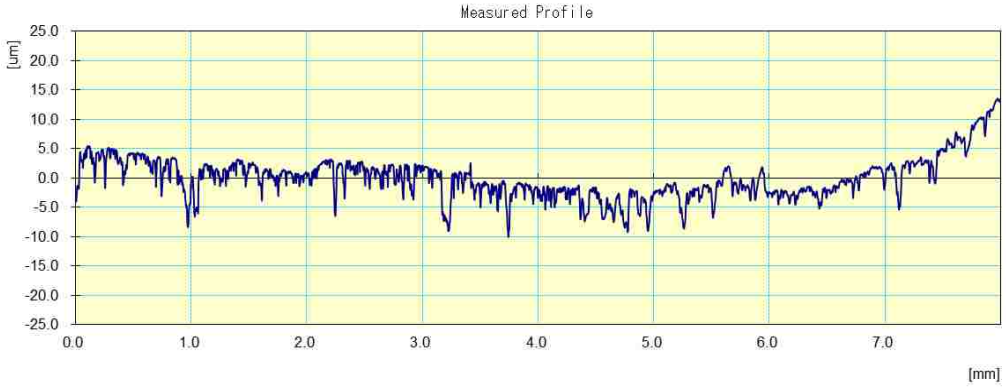

Appendix A - 47: Dynamometer 4 - Engine 2595R - Cylinder 1 – Right

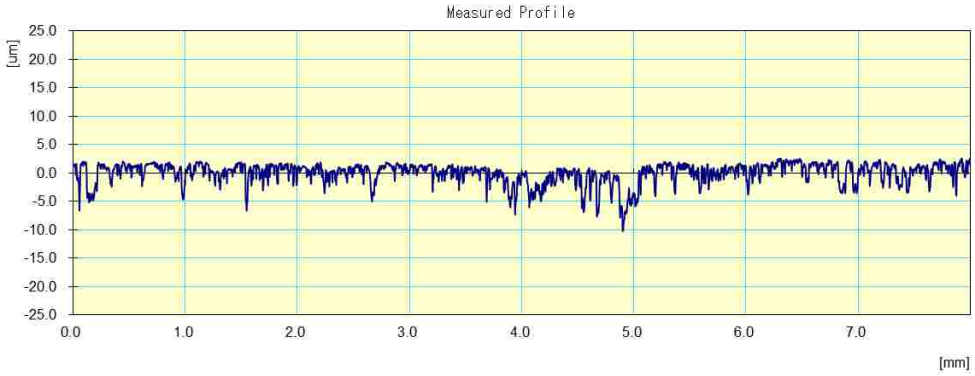

Appendix A - 48: Dynamometer 4 - Engine 2595R - Cylinder 1 – Back

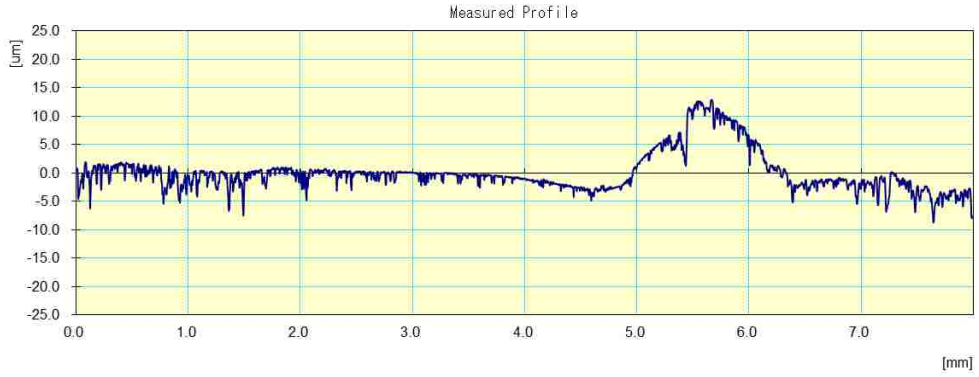

Appendix A - 49: Dynamometer 4 - Engine 2595R - Cylinder 1 – Left

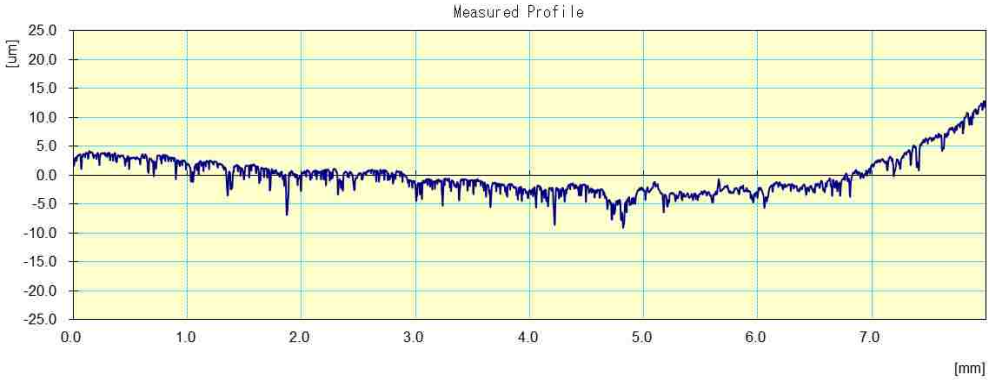

Appendix A - 50: Dynamometer 4 - Engine 2595R - Cylinder 2 - Front

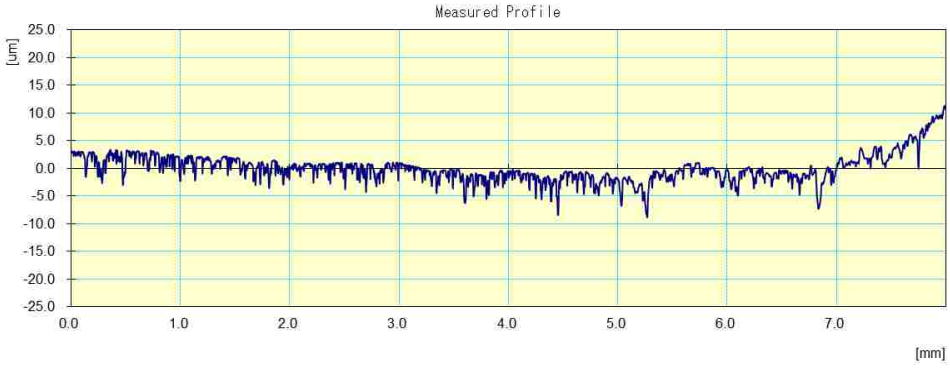

Appendix A - 51: Dynamometer 4 - Engine 2595R - Cylinder 2 - Right

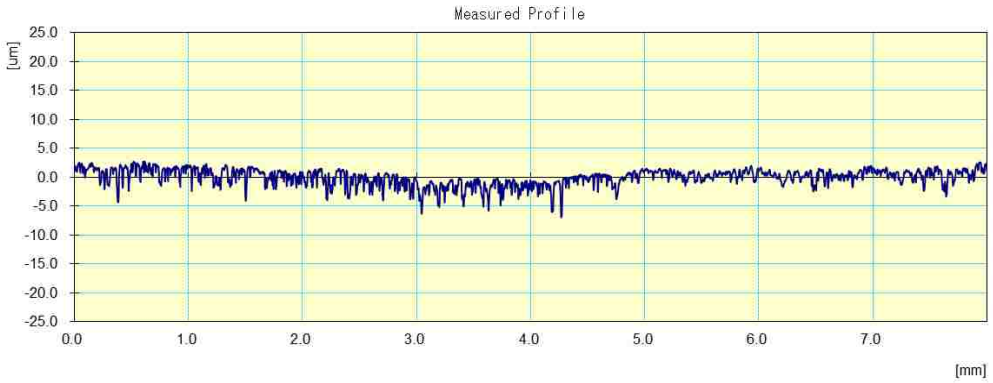

Appendix A - 52: Dynamometer 4 - Engine 2595R - Cylinder 2 - Back

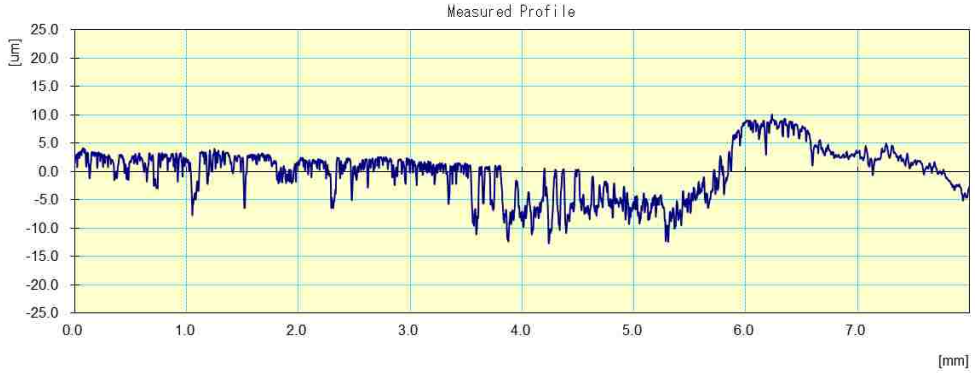

Appendix A - 53: Dynamometer 4 - Engine 2595R - Cylinder 2 – Left

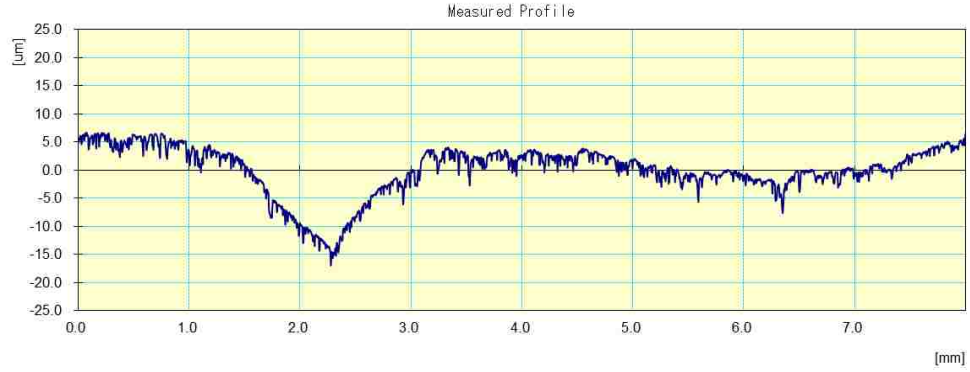

Appendix A - 54: Dynamometer 4 - Engine 2595R - Cylinder 3 - Front

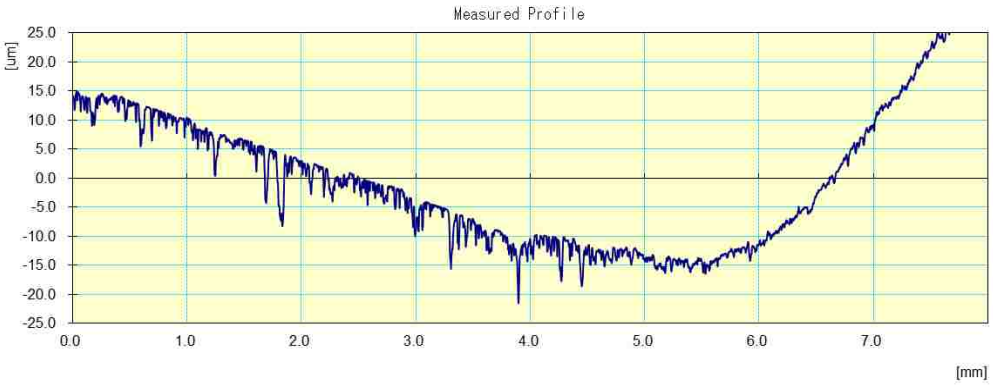

Appendix A - 55: Dynamometer 4 - Engine 2595R - Cylinder 3 - Right

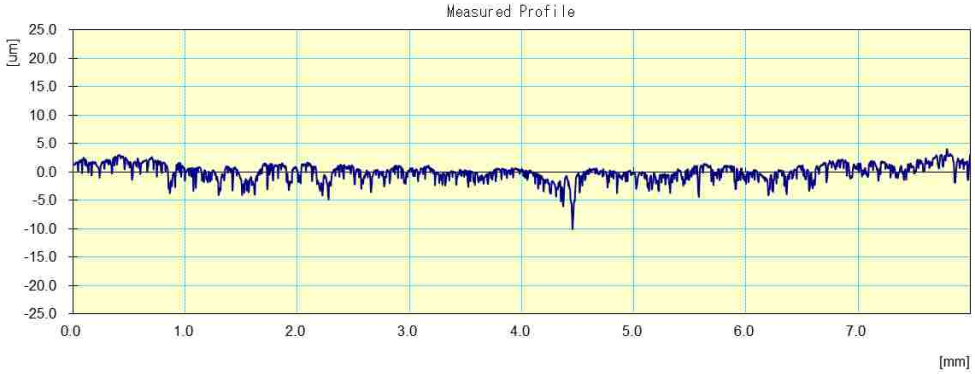

Appendix A - 56: Dynamometer 4 - Engine 2595R - Cylinder 3 - Back

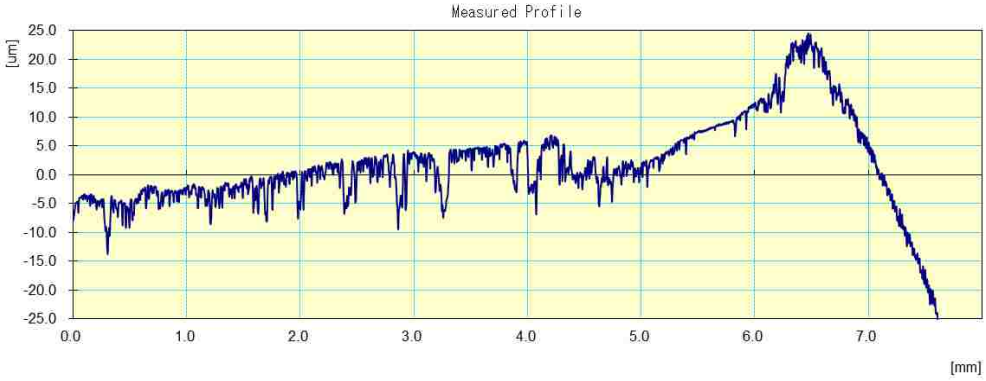

Appendix A - 57: Dynamometer 4 - Engine 2595R - Cylinder 3 – Left

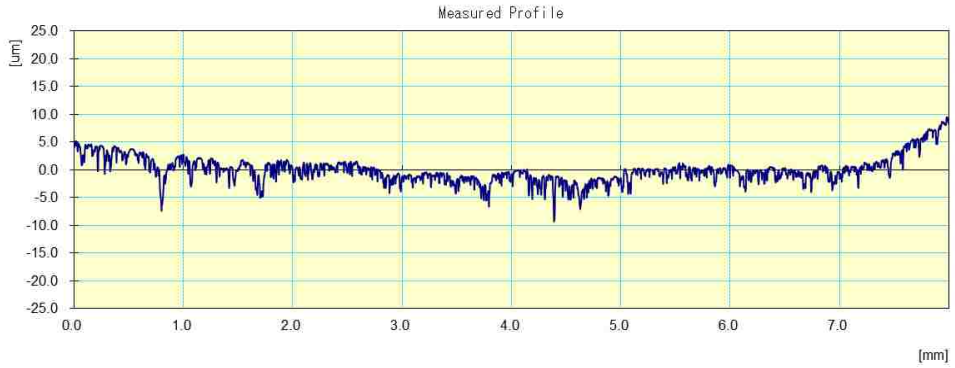

Appendix A - 58: Dynamometer 4 - Engine 2595R - Cylinder 4 - Front

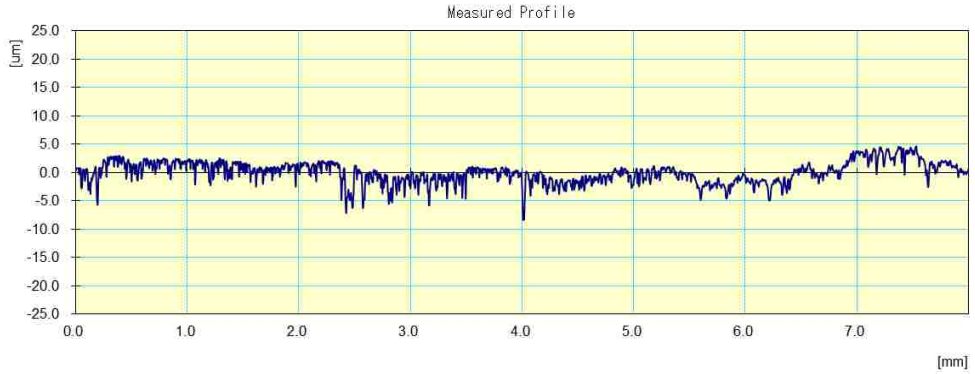

Appendix A - 59: Dynamometer 4 - Engine 2595R - Cylinder 4 - Right

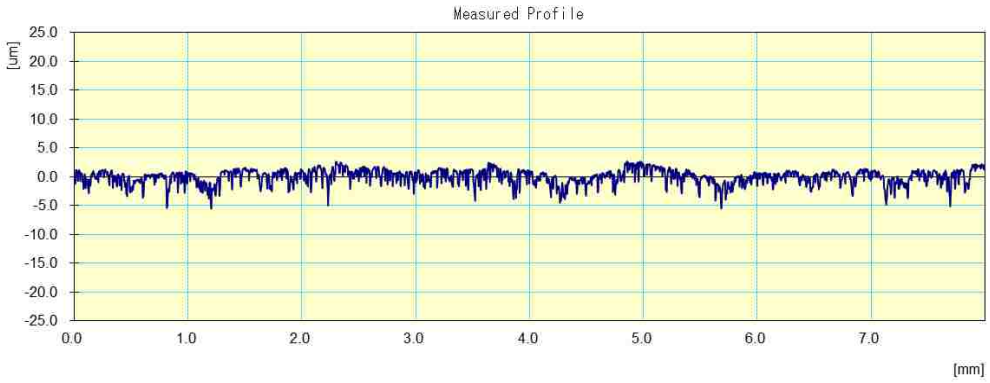

Appendix A - 60: Dynamometer 4 - Engine 2595R - Cylinder 4 - Back

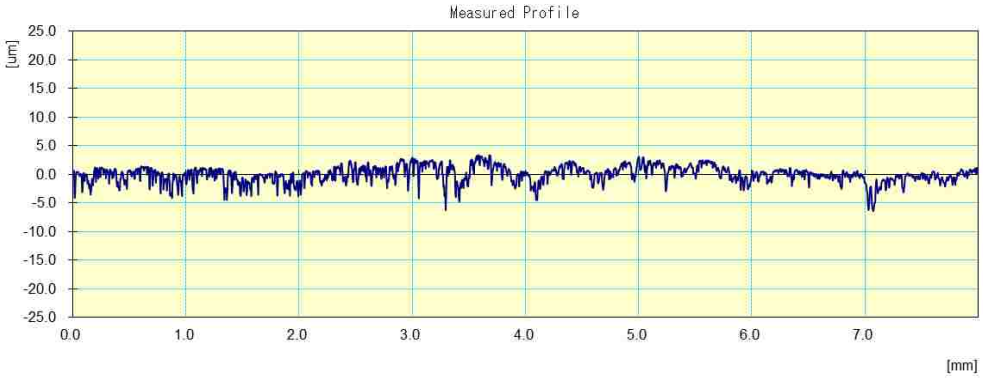

Appendix A - 61: Dynamometer 4 - Engine 2595R - Cylinder 4 – Left

VITA AUCTORIS

NAME:	Vladislav Leshchinsky
PLACE OF BIRTH:	Lugansk, Ukraine
YEAR OF BIRTH:	1992
EDUCATION:	University of Windsor, B.Sc., Windsor, ON, 2014
	University of Windsor, M.A.Sc., Windsor, ON, 2016